STABILITY AND CONTROL ANALYSIS OF SOME PROBLEMS OF CHAOTIC DYNAMICAL SYSTEMS

Thesis submitted for the degree of
Doctor of Philosophy (Sc.)
In Applied Mathematics

by
AMIT MONDAL
DEPARTMENT OF APPLIED MATHEMATICS
UNIVERSITY OF CALCUTTA
2015

Acknowledgement

It gives me great pleasure in expressing my gratitude to all those people who have supported me and had their contributions in making this thesis possible.

I am very grateful to my supervisor Dr. Nurul Islam, Associate Professor of Mathematics, Department of Mathematics, Ramakrishna Mission Residential College, Narendrapur, for his visionary power, inspiration and constructive advices that culminated in the success of this thesis. Without his active guidance it would have not been possible for me to complete the work. I am very fortunate and honored to be able to work with him. I look forward to learning more from him.

I am also very grateful to my joint-supervisor Dr. Sanjay Sen, Professor of Applied Mathematics, University of Calcutta. I highly appreciate his comments and guidance, which have greatly helped to improve the quality of this presentation and increased my knowledge of the subject.

I would like to thank Bipul Islam and Mitul Islam for their fruitful collaborative work which has led to several joint publications.

I would like to thank my colleagues, who laid seeds of enthusiasm and passion in my pursuit of knowledge. Many thanks are due to all my friends who have wholeheartedly supported me and cheered me during my PhD work.

A special thanks to my family. Words cannot express how grateful I am to my father, mother, father-in-law, mother-in-law and sister-in-law, for all of the sacrifices that they have made on my behalf. Your prayers for me is what has sustained me thus far.

At the end I would like to express appreciation to my beloved wife Monalisha Sinha Mondal who spent sleepless nights with me and was always my support in the moments when there was no one to answer my queries. No words can completely describe how grateful I am to my wife, for riding in this roller coaster with me from the beginning till the end. Monalisha, your presence, care and understanding were very vital stabilizing inputs during this highly nonlinear ride. You make everything joyful.

AMIT MONDAL

Dedicated

to

my family

List of Published Papers

1. Amit Mondal , Mitul Islam and Nurul Islam, *Robust anti-synchronization of chaos using sliding mode control strategy*, Pramana -Journal of Physics, Springer, Indian Academy of Sciences, Vol.84, No.1, pp.47-67, 2015 [referred to chapter 6]

2. Amit Mondal , Nurul Islam and Sanjay Sen, *Unidirectional synchronization of chaotic Sprott model L*, Bulletin of Calcutta Mathematical Society, Vol.105, No.2, pp.93-102, 2013 [referred to chapter 7]

3. Amit Mondal , Nurul Islam and Sanjay Sen, *Controlling and stabilizing the dynamical system of Sprott's model B*, Indian Journal of Theoretical Physics, Vol.61, No.2, pp.95-100, 2013 [referred to chapter 2, section 2.1]

4. Amit Mondal and Nurul Islam, *Chaos synchronization of coupled Sprott model L*, International Journal of Pure and Applied Sciences and Technology (IJPAST), Vol.16, No.2, pp.32-38, 2013 [referred to chapter 5]

5. Amit Mondal and Nurul Islam, *Stability and control analysis of the Sprott's model L*, International Journal of Applied Mathematical Sciences (JAMS), Vol.6, No.1, pp.63-68, 2013 [referred to chapter 2, section 2.2]

6. Amit Mondal , Nurul Islam and Sanjay Sen, *Control of chaos in Sprott system B by state space exact linearization method*, Bangmod Int. J. Math. and Comp. Sci. (JMCS), Vol.1, No.1, pp.11-18, 2015 [referred to chapter 3]

7. Amit Mondal and Nurul Islam, *Generalized synchronization of non-linear oscillators via OPCL coupling*, International Journal on Cybernetics and Informatics (IJCI), Vol.3, No.2, pp.21-33, 2014 [referred to chapter 8]

List of communicated papers

- Amit Mondal, Mitul Islam and Nurul Islam, *Linear feedback based control of blood glucose in a modified model for glucose insulin kinetics : A theoretical study*, (communicated) [referred to chapter 4]

- Amit Mondal and Nurul Islam, *Study on dynamical systems with time delay*, (communicated) [referred to chapter 9]

Contents

List of Figures

Chapter 1

Introduction

1.1 Brief Literature Survey

In the literature on dynamical systems, substantial attention has been paid to the problem of control and synchronization for nonlinear dynamical systems. In 1990, E Ott, C Grebogi and JA Yorke [58], published a pioneering work on control of chaos. Their method (now famously known as OGY method) achieves the control objective by making small, carefully chosen time-dependent perturbations of one of the parameters of the system. They crucially used a very important property of the phase space of a chaotic system. Every arbitrary neighbourhood of a chaotic attractor contains periodic attractors. Hence arbitrary small excitations can drive a system from a chaotic attractor to a periodic one. Thus, through proper choice of a sequence of excitations, it is possible to control the chaotic system. In 1992, direct adaptive control process was described by RM Sanner and JE Slotine for Gaussian networks[74]. In 1993, W Gao and JC Hung[21] presented the variable structure control for nonlinear dynamical systems. In 1995, EA Jackson and I Grosu[30] proposed

an open-plus-closed-loop (OPCL) control for complex dynamical systems. EA Misawa (1997)[48] introduced discrete time sliding mode control (SMC) for nonlinear systems with unmatched uncertainties and uncertain control vector. Interestingly, in that year, K Jezernik, M Rodic, R Safaric and B Curk[32] presented a paper on the sliding mode control for neural network. In 1998, C Liqun and L Yanzhu[44], applied state space exact linearization (SSEL) method for controlling non-linear dynamical system. They applied this technique to control the famous Lorenz dynamical system [45]. In the next year(1999), WH Chen, DJ Ballance, PJ Gawthrop and J O'Reilly[15] introduced a useful controller for a nonlinear dynamics, known as PID predictive controller.

A promising tactics for attenuation of chaos is synchronization. In 1990, Pecora and Carroll[65] presented a pioneering work on chaos synchronization which received much attention due to its importance in the theory of non-linear dynamics and its practical applications in electronic circuits, chemical and biological systems and secure communications. They used a common signal to connect two chaotic systems. They also applied this method to construct a real set of chaotic synchronizing circuits. The type of synchronization they had worked on is now known as complete synchronization. Kocarev and Parlitz [38], in 1996, published a paper on general synchronization (GS). LY Cao and YC Lai (1998) [14] discussed antiphase synchronization (AS) in chaotic systems. Long-term anticipatory synchronization of a chaotic dynamical systems was presented by HU Voss (2001)[86]. In that year, HN Agiza and MT Yassen[1] used active control method to synchronize R*ö*ssler and Chen chaotic dynamical

systems. Lag synchronization (LS) in coupled R*össler* oscillators was described in 2002 by M Zhan, GW Wei and CH Lai [94]. L Chen(2002) [16] applied adaptive control method to synchronize uncertain unified chaotic system. Next year, in 2003, Y Yongguang and Z Suachun[92] gave a control technique for uncertain Lu system using backstepping design. In 2004, a number of works had been published on adaptive control method for synchronization of chaotic systems. J Lu, X Wu, X Han and J Lu[46] did the same on unified chaotic system. JH Park[64](2005) discussed the control of chaotic dynamical systems via nonlinear feedback control. In this year, MT Yassen [91] discussed chaos synchronization for two different chaotic systems using active control method. In 2006, DV Senthilkumar, M Lakshmanan and J Kurths [75] demonstrated the phase synchronization (PS) process for a time delayed system. D Ghosh(2009) [23] discussed the stability criteria and projective synchronization for the multiple delay R*össler* system.

The control techniques were not confined only to mathematics. Its effect had been scattered in several areas. In 2005, NM Carusu and V Balan[13], had together presented a paper for controlling a dynamical systems with applications in biology. V Balan and CS Stamin [8] applied the nonlinear feedback control method on a biological system in 2006. They had tried to control neural excitation processes. In 2007, Y Sun and J Cao [81] used adaptive control method to synchronize two different noise-purturbed chaotic systems with fully unknown parameters. In the same year, S Poria and A Tarai[68], published a paper on adaptive synchronization of two coupled chaotic neuronal systems. V Balan and CS Stamin(2007) worked

on a paper on Kaldor's model[6] of macro-economic business cycles. They had chosen the state space exact linearization(SSEL) method to stabilize the Kaldor model. They examined the controllability of the non-linear dynamical system by using the parameter variation and the control duration. In the next year, they applied the state space exact linearization(SSEL) method to construct a scheme for non-linear feedback control law in SODE economic model [7]. A simple adaptive controller was described by R Guo(2008) [26] to obtain chaos and hyperchaos synchronization. In this year (2008), D Ghosh, AR Chowdhury and P Saha [22], chose Rössler dynamical system with multiple delay parameters to analyze the bifurcation behaviour and to control the chaotic nature of the Rössler dynamical system. S Nikolov, JV Gonzalez, V Kotev, O Wolkenhauer and V Petrov(2008) [54] investigated the properties of Jacob-Monob dynamical model in presence of time delays and also described the control of the beta-galactosidase synthesis by the DNA-binding protein in a bacterium which can cause severe food poisoning. Hybrid feedback control scheme had been used by LX Yang, YD Chu, JG Zhang, XF Li and YX Chang (2009)[90] to attain chaos synchronization in autonomous chaotic system. EM Shahverdiev and KA Shore(2009) [76] studied chaos synchronization on laser diodes by introducing multiple optical feedback time delay parameters. In 2010, JZ Li and YN Zhang[43] suggested a force control technique for wheeled inverted pendulum. YF Xu, B Jiang, G Tao and Z Gao(2011)[88] proposed fault tolerant control for a class of nonlinear systems with application to near space vehicle. Tracking control method had been used in 2011 by M Chen, SS Ge and B Ren[17] to control uncertain multi-input

and multi-output (MIMO) nonlinear systems with input saturation. In this year, application of adaptive control method was discussed by ID Landau, R Lozano, M M'Saad and A Karimi [39]. In the following year, S Nikolov, JV Gonzalez, M Nenov and O Wolkenhauer [55], worked with microRNA dynamical model having two delay parameters. This work is very helpful in understanding the correlation between mathematical sciences and biological sciences. Nikolov and his co-workers, discussed the effect of delay parameters on the miRNA dynamical system. In presence of delay parameters, the dynamical system would become unstable. By utilising this fact, they had carried out the bifurcation analysis for the miRNA dynamical model using Hopf-bifurcation theorem. V Balan, C Udriste and I Tevy(2012), published an important work on the study of the sub-Riemannian geometry and optimal control[9] of Lorenz induced distributions. The article contained vital results on single-time optimal control problems and the optimal control problem of non-holonomic geodesics, illustrated for Lorenz system. In 2013, S Vaidyanathan [84] designed a sliding mode controller to attain anti-synchronization in hyperchaotic Lu system. In this year, S Nikolov [56] used three delay parameters on a dynamical system and studied the stability and Andronov-Hopf bifurcation of the system. He also studied the complex behaviour of the miRNA model with three time delay parameters in his paper [57] in 2013.

In engineering and mathematics, controlling the behaviour of dynamical systems is a very active research area nowadays. In our daily life, almost everything needs to be controlled. For example, regulator of a ceiling fan, cooking time controller in microwave, temperature

controller of refrigerator etc. are very simple yet indispensable controllers in our life. For more clarity, consider an electric cloth drier. To dry our wet clothes, we have to schedule or fix a time. Now, without any controller, there is a possibility that the wet cloth may dry before the scheduled time and the drier may burn the cloth if operated for the remaining time. There exists another possibility. The wet cloth may not dry properly within the scheduled time. If the electric cloth drier has a controller, it will increase the temperature when the clothes are too wet and the controller will decrease the temperature when the clothes are nearly dry (otherwise it may burn the clothes!). Hence, this simple example appropriately highlights that controllers play an important role in our daily lives.

In chaotic nonlinear dynamics, controllers perform a very significant function similar to our previously discussed event from daily life. In control theory, it is very essential to establish the appropriate criteria for the effectiveness of the control system. Usually, the control term is added to one of the equations of the dynamical system. Synchronization of two systems is another promising way to control the chaotic nature of non-linear dynamical systems. In this thesis, our aim will be to investigate synchronization of same and different dynamical systems in detail and work towards the concept of generalized synchronization, which is useful for a myriad of practical purposes, like secret communications, cryptography and robotics.

1.2 Non-Linear Dynamics

A physical quantity (position, momentum, phase, electric field etc.) that depends on time represents Dynamical quantity. The set of

dynamical quantities that evolves together under a coupled set of equations or maps defined as Dynamical system. The dynamical system replicas anything that moves in time. Dynamical system has two types, linear and non-linear. Any dynamical system can be written in vector form as

$$\dot{x} = f(x,t) \tag{1.2.1}$$

where $x = (x_1, x_2, x_3, ..., x_n)^T \in \mathbb{R}^n$ and $f : \mathbb{R}^n \to \mathbb{R}^n$ & $t \geq 0$.

In expanded form, the system of equations is :

$$\begin{aligned} \dot{x_1} &= f_1(x_1, x_2, x_3, ..., x_n, t) \\ \dot{x_2} &= f_2(x_1, x_2, x_3, ..., x_n, t) \\ &\vdots \\ \dot{x_n} &= f_n(x_1, x_2, x_3, ..., x_n, t) \end{aligned} \tag{1.2.2}$$

where dots represent the derivative with respect to time.

For example, we consider the differential equation of a simple harmonic oscillator as

$$m\ddot{x} = -kx \tag{1.2.3}$$

Let $x_1 = x$ and $x_2 = \dot{x}$.

Hence, equation (1.2.3) can be written in the form of equation(1.2.1) as,

$$\begin{aligned} \dot{x_1} &= x_2 \\ \dot{x_2} &= -\left(\frac{k}{m}\right) x_1 \end{aligned} \tag{1.2.4}$$

Since the variable terms to the right hand side of (1.2.4) are of degree one, the system of equations (1.2.4) is said to be linear dynamical system. Otherwise, it is said to be non-linear dynamical system.

For example, we consider the velocity $v(t)$ of a skydiver falling to the ground is governed by

$$m\dot{v} = mg - kv^2 \tag{1.2.5}$$

where m is the mass of the skydiver, g is the acceleration due to gravity and $k > 0$ is a constant related to amount of air resistance [80].

By taking $x_1 = x \;\; \& \;\; x_2 = \dot{x}$, equation (1.2.5) can be written as

$$\left.\begin{aligned} \dot{x_1} &= x_2 \\ \dot{x_2} &= g - \left(\frac{k}{m}\right) x_2^2 \end{aligned}\right\} \tag{1.2.6}$$

where $v = \dot{x} = \frac{dx}{dt}$

This is the example of an autonomous non-linear dynamical system. Here, the term autonomous is used as the system (1.2.6) does not depend on the time explicitly.

Now, if we solve the system of equation(1.2.6) with $m = 260, g = 32.2, k = 10 \;\; \& \;\; (x_1, x_2) = (30000, 250)$, we have a point whose coordinates are $(x_1(t), x_2(t))$ and the locus of this point represents a curve in a phase space which is represented by figure (1.1) and the curve ABC is known as a trajectory.

We will now discuss fixed points of a system. For this purpose, we have to understand the flow of a fluid on a line. If we take the line as x-axis with velocity along y-axis, then the following cases may arise :

- the fluid flows to the left if $\dot{x} < 0$
- the fluid flows to the right if $\dot{x} > 0$

- the fluid does not flow if $\dot{x} = 0$

For $\dot{x} = 0$, we get the fixed point or the critical point x^* of the system $\dot{x} = f(x)$, i.e. $f(x^*) = 0$.

There exists two types of fixed point, stable (attractor) and unstable (repeller) [80]. A fixed point is called stable point if the points near it are attracted towards the fixed point and it is called unstable point if the neighbouring points are repelled as the time increases.

For example, we consider a very simple differential equation

$$\dot{x} = x - x^3 \tag{1.2.7}$$

In this example, for $\dot{x} = 0$, we have, $x^* = 0, 1, -1$ which are the fixed points. From figure (1.2), using the flow on a line, we can say that $x^* = 1 \quad \& \quad x^* = -1$ are the stable fixed points and $x^* = 0$ is the unstable fixed point.

From an analytic point of view, the following definitions may be proposed.

Consider $B(x_o, \epsilon) = \{x \in \mathbb{R}^n : \|x - x_o\| < \epsilon\}$ and $\overline{B}(x_o, \epsilon) = \{x \in \mathbb{R}^n : \|x - x_o\| \leq \epsilon\}$. Then, $S(x_o, \epsilon)$ is the boundary of both $B(x_o, \epsilon)$ and $\overline{B}(x_o, \epsilon)$, where $S(x_o, \epsilon) = \{x \in \mathbb{R}^n : \|x - x_o\| = \epsilon\}$.

According to the Lyapunov stability theory[70, 80], a fixed point (sometimes called an equilibrium point) x^* of a non-linear system is said to be stable, if $\forall \ \epsilon > 0$, $\exists \ \delta > 0$ such that

$$x_o \in B(x^*, \delta) \Rightarrow \tau(t) \in B(x^*, \epsilon) \ \ \forall \ \ t \geq 0$$

where $\tau(t)$ is the unique solution to the non-linear system $\dot{x} = f(x(t))$ that corresponds to $x(0) = x_o$.

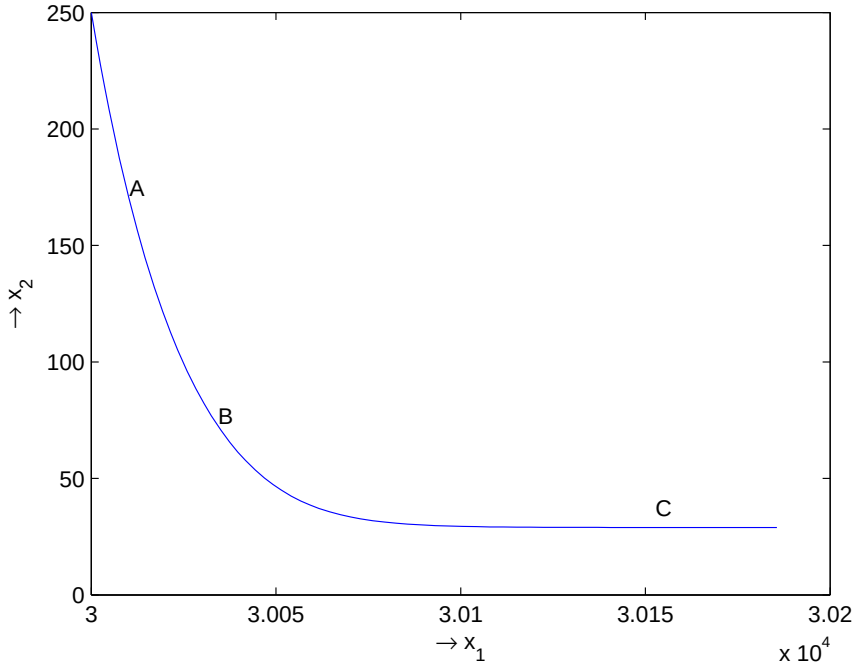

Figure 1.1: Phase space diagram for skydiver

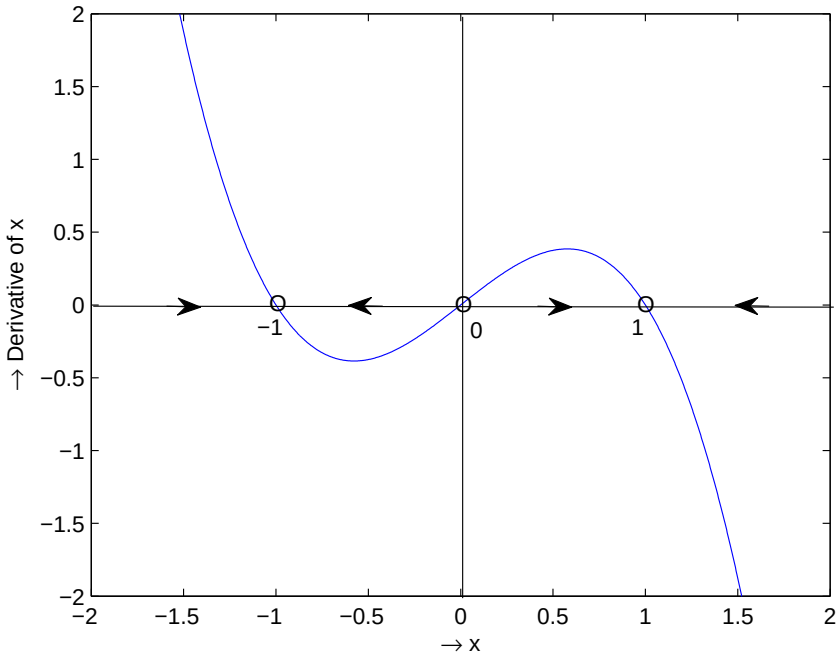

Figure 1.2: Phase portrait of equation (1.2.7)

The fixed point x^* is said to be asymptotically stable, if $\forall\ \epsilon > 0$, $\exists\ \delta > 0$ such that

$$x_o \in B(x^*, \delta) \Rightarrow \begin{cases} \tau(t) \in B(x^*, \epsilon) \ \ \forall \ \ t \geq 0 \\ \lim\limits_{t \to +\infty} \tau(t) = x^* \end{cases}$$

From these definitions, one can easily conclude that asymptotic stability implies stability.

In the phase space, dimension [3] of the attracting set is defined by

$$d = \lim_{\epsilon \to 0} \frac{lnN(\epsilon)}{ln(\frac{1}{\epsilon})}, \quad \text{when the limit exists.}$$

Here, $N(\epsilon)$, which is proportional to $\frac{1}{\epsilon^d}$, represents the number of boxes of edge length ϵ (arbitrarily small) required to cover the attracting set.

If $N(\epsilon) = 1$, then $d = 0$. In this case, the attracting set represents a point attractor, shown by figure (1.3) which is obtained from the system of differential equations as given below:

$$\left.\begin{aligned} \dot{x} &= y \\ \dot{y} &= -2x - 3y \end{aligned}\right\} \tag{1.2.8}$$

If $N(\epsilon) \sim \frac{1}{\epsilon}$, then $d = 1$. In this case, the attracting set represents a limit cycle attractor, shown by figure (1.4) which is obtained from the system of differential equations [80] as given below:

$$\left.\begin{aligned} \dot{x} &= x - y - x(x^2 + 5y^2) \\ \dot{y} &= x + y - y(x^2 + y^2) \end{aligned}\right\} \tag{1.2.9}$$

If $d = 2, 3, \ldots$, the curves represent a tori. But there is a possibility that the dimension d may not always be an integer. It might be

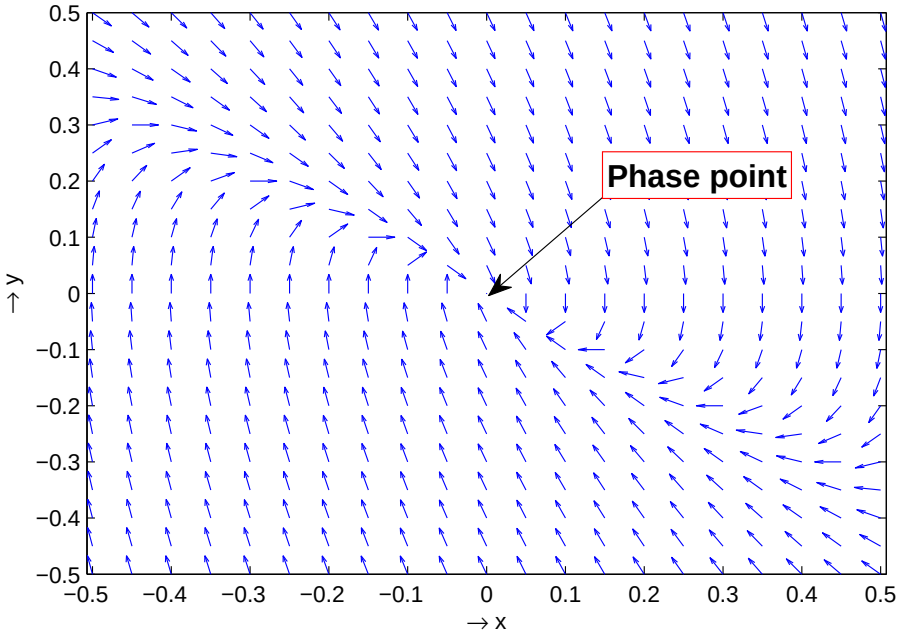

Figure 1.3: Direction field showing phase point of equation (1.2.8)

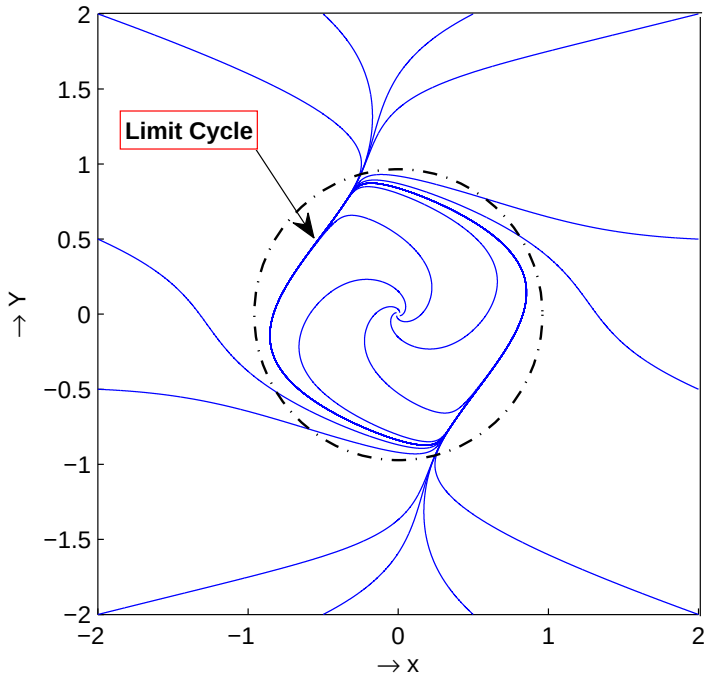

Figure 1.4: State space plot showing limit cycle for equation (1.2.9)

fractional. In that case, the attracting set is said to have fractal dimension and the attractor is called a strange attractor. In physical model, Lorenz first showed the existence of strange attractors.

In particular, if d lies between 2 and 3, the strange attractor behaves like a chaotic nature of a dynamical system with $n(\geq 3)$ variables. Thus, the strange attractors are often called chaotic attractors. Chaos in a dynamical system is generally shown by the complicated and apparently tangled behavior [78] of the attractor. It can't be periodic. It is further characterized by strong dependence on the initial conditions.

1.3 Chaotic Dynamical System

To understand the chaotic dynamics, we have to roll back to the year of 1963, when Lorenz [45] introduced a simple chaotic dynamical system of equations containing three ordinary non-linear differential equations with three state variables that had altogether seven terms with two quadratic non-linear terms. This system displays variety of periodic and chaotic solutions depending on values of one or more system parameters [63]. After this pioneering discovery of Lorenz, much efforts have been applied towards identifying and understanding the chaotic dynamics. R*ö*ssler (1976)[71], 13 years later, described a three dimensional model which had chaotic bounded solution with only one non-linear term. In 1977, oscillations and chaos in a physiological control system was discussed by MC Mackey and L Glass [47]. In 1988, L Glass, A Beuter and D Larocque [24], presented a very deep work on physiological control systems, discussing time-delays, oscillations and chaos theory. They added variable time delays to

the feedback circuit to show the complex rhythms of finger displacement. In investigating problems of nature, often partial differential equations governing physical phenomena are approximated by a set of ordinary differential equations, mostly by truncation method. The truncated system of ordinary differential equations is termed generally as a low-order system. For example, S Panchev (1991)[61] constructed such a low order system from the non-linear boundary layer equations for stratified flows in the atmosphere. In 1992, S Panchev[62] paid attention to the chaotic and deterministic behavior of the non-linear dynamical systems and their applications to practical problems. For this reason, he had chosen the geo-physical fluid dynamics. In 1994, Sprott[79] made a rigorous computer search and discovered a set of nineteen simple distinct chaotic dynamical systems popularly known as Sprott's model A to S.

To illustrate the dynamics of chaos, we have drawn a phase portrait in figure (1.5) of the Sprott D system [79] which is given by

$$\left.\begin{aligned} \dot{x} &= -y \\ \dot{y} &= x + z \\ \dot{z} &= xz + 3y^2 \end{aligned}\right\} \tag{1.3.10}$$

1.4 Control and Synchronization of Chaos

It is generally known that non-linear dynamical systems which are capable of generating chaos are not exactly solvable. Our aim here will be to choose such systems and use analytical tools to extract useful information from them. Stability analysis and study of control

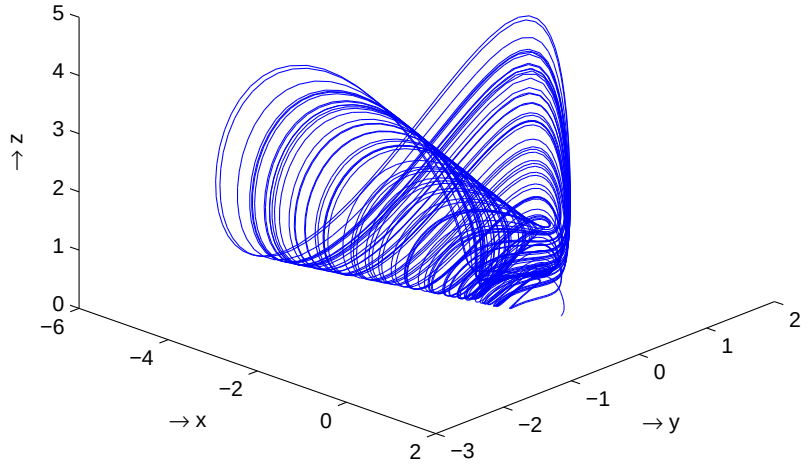

Figure 1.5: Phase portrait showing the chaotic nature of Sprott D system (1.3.10)

are very essential from both mathematical and physical point of view. For stability analysis of the problem, generally, following methods are generally adopted :

(i) Routh-Hurwitz criteria (Local stability)

(ii) Lyapunov's theorem (Global stability)

For any non-linear system $\dot{x} = \phi(x)$, where $x \in \mathbb{R}^n$, $\phi : \mathbb{R}^n \to \mathbb{R}^n$, there exists a linear system $\dot{y} = Ay$, where $y \in \mathbb{R}^n$ and A is Jacobian matrix obtained from $\phi(x)$ at the critical point of the system.
According to Hartman-Grobman theorem[80], the behaviour of the non-linear system near the critical point is qualitatively the same as the behaviour of the corresponding linear system if all the eigen values of A have non-zero real part.

Let λ be an eigen value of the matrix A. Then, the characteristic equation of A in λ can be written as

$$\lambda^n + a_1\lambda^{n-1} + a_2\lambda^{n-2} + a_3\lambda^{n-3} + ... + a_{n-1}\lambda + a_n = 0,$$

where all $a_i \in \mathbb{R}$, $i = \quad 1, 2, 3, ..., n$.

Now, Routh-Hurwitz criteria [19] states that the eigen values of A have negative real parts, which implies the stability of the dynamical system, if and only if

For $n = 2$, $a_i > 0$, $\quad i = 1, 2$.

For $n = 3$, $a_i > 0$, $\quad i = 1, 2, 3$ and $a_1a_2 > a_3$

For $n = 4$, $a_i > 0$, $\quad i = 1, 2, 3, 4$ and $a_1a_2a_3 > a_3^2 + a_1^2a_4$

For $n = 5$, $a_i > 0$, $\quad i = 1, 2, 3, 4, 5$ and $\quad a_1a_2a_3 > a_3^2 + a_1^2a_4$ & $(a_1a_4 - a_5)(a_1a_2a_3 - a_3^2 - a_1^2a_4) > a_5(a_1a_2 - a_3)^2 + a_1a_5^2$

and so on.

Lyapunov's first and second theorems [40] give sufficient conditions for global stability and global asymptotic stability respectively. From the point of view of applications, these theorems concern the construction of a scalar function V(x) (known as Lyapunov function) which in relation to the system have certain properties. Here, x represents the state vector. If $V(0) = 0$ and $V(x) > 0$ for $x \neq 0$, the scalar function $V(x)$ is said to be positive definite and it is negative definite if the negative of this function is positive definite. Lyapunov's theorems state that if $V(x)$ is positive definite and $\dot{V}(x) \leq 0$ for $x \neq 0$, then the equilibrium state is stable. In addition, if $\dot{V}(x) < 0$ for $x \neq 0$ and $\dot{V}(0) = 0$, then the equilibrium state is asymptotically stable. Here, $\dot{V}(x) < 0$ for $x \neq 0$ implies that the system is dissipative. The equilibrium state is globally asymptotically stable at

the origin if $V(x)$ is positive definite, $\dot{V}(x)$ is negative definite and $V(x) \to \infty$ as $||x|| \to \infty$.

Control analysis of the dynamical system is of considerable importance and in particular, it is very essential to establish the appropriate criteria for the effective control of the system. Control analysis of the dynamical systems of some problems of applied interest like those of Biology, Bio-Physics would be of great interest. In this thesis, we will investigate the controller for the non-linear chaotic dynamical systems using different types of control methods. The Routh-Hurwitz criteria and Lyapunov stability theorems will be used for these purpose.

Synchronization is a process of coupling of two or more chaotic dynamical systems, whereby they are found to acquire a tendency to follow closely related motion. Chaos synchronization in dynamical systems is actually a method of controlling chaos. Synchronization between two systems can broadly be classified into the following types:

(i) **Complete Synchronization (CS):** This is the simplest type of synchronization, that happens for two identical diffusively coupled chaotic systems. It is also known as identical synchronization. If we consider $x = (x_1, x_2, x_3, ..., x_n)$ and $y = (y_1, y_2, y_3, ..., y_n)$ as the state variables of the coupled (drive-response) systems, then the error term e is defined as $e_i = x_i - y_i$, $i = 1, 2, 3, .., n$, where $e = (e_1, e_2, e_3, ..., e_n)$. Therefore, Complete Synchronization is achieved when $|x_i - y_i| \to 0$ as the time t tends to infinity. This synchronization can be achieved when the coupling is diffusive, that is, the coupling is a function of $(x - y)$.

The synchronization manifold in CS is $S = \{(x, y) : y = x\}$.

(ii) **Anti Synchronization (AS):** In this case, the error term e is defined as $e = x + y$, where $x(\in \mathbb{R}^n)$ and $y(\in \mathbb{R}^n)$ denote the states of the drive and the response system respectively. As $t \to \infty$, if the error term e goes to zero, then the synchronization state is said to be achieved in the sense of Anti Synchronization. The synchronization manifold in this case is $S = \{(x, y) : y = -x\}$.

(iii) **Generalized Synchronization (GS):** Let us consider the coupled pair of systems

$$\begin{aligned} \dot{x} &= \phi(x) && : \ Drive \ \ system \\ \dot{y} &= \psi(y, \rho(x)) && : \ Response \ \ system \end{aligned}$$

where $x(\in \mathbb{R}^n)$ and $y(\in \mathbb{R}^m)$. Such a coupled pair of systems is said to possess Generalized Synchronization provided there exists a transformation $\eta : \mathbb{R}^n \to \mathbb{R}^m$, a manifold $\Lambda = \{(x, y) : y = \eta(x)\}$ and a set $\Gamma \subseteq \mathbb{R}^n \times \mathbb{R}^m$ with $\Lambda \subseteq \Gamma$ such that all trajectories of the coupled system starting from the basin Γ converges to Λ as $t \to \infty$. The set $\Lambda = \{(x, y) : y = \eta(x)\}$ is known as the synchronization manifold.

If η equals I (I is identity transformation), then the generalized synchronization coincides with Complete Synchronization. If η equals $-I$, then the generalized synchronization coincides with Anti Synchronization.

(iv) **Phase Synchronization (PS):** This type of synchronization occurs when the synchronization manifold is defined by the re-

lation $n\phi_1(t) - m\phi_2(t) =$ constant, where $\phi_1(t)$ and $\phi_2(t)$ are the phases of the two coupled oscillators and $m, n \in \mathbb{N} = \{0, 1, 2, ...\}$. This requires the phases of the oscillators to bear a definite relationship while their amplitudes may be different.

(v) **Lag Synchronization (LS):** This type of synchronization is also known as delay synchronization. If we consider τ as the time delay parameter, then the two coupled chaotic oscillators are in Lag synchronization if the synchronization manifold is defined by $S = \{(x, y) : y(t) = x(t - \tau)\}$, where $x = (x_1, x_2, x_3, ..., x_n)$ and $y = (y_1, y_2, y_3, ..., y_n)$ denotes the drive and the response systems/oscillators. In Lag synchronization, the delay parameter τ may be constant or time dependent.

Depending on the nature of coupling [28] that connects the two systems X and Y with $X \in \mathbb{R}^n$ and $Y \in \mathbb{R}^m$, the synchronization methods can further be classified into three types.

Formally a $(n + m)$ dimensional dynamical system is said to be

(1) **Decoupled** if it can be decomposed into two dynamical system of the form

$$\dot{X} = f(X), \quad \dot{Y} = g(Y)$$

(2) **Unidirectionally coupled** if it can be decomposed into two dynamical system of the form

$$\dot{X} = f(X), \quad \dot{Y} = g(Y) + k(X, Y)$$

(3) **Bidirectionally coupled** if it can be decomposed into two dynamical system of the form

$$\dot{X} = f(X) + k_1(X, Y), \quad \dot{Y} = g(Y) + k_2(X, Y)$$

where f, g, k, k_1, k_2 are all vector valued functions of X and/or Y.

For example, consider the Shimizu-Morioka [29] system as the driver system given below:

$$\left.\begin{aligned} \dot{x} &= y \\ \dot{y} &= x - \alpha_1 y - xz \\ \dot{z} &= -\beta_1 z + x^2 \end{aligned}\right\} \quad \text{where } \alpha_1 = 0.799 \ \ \& \ \ \beta_1 = 0.54 \qquad (1.4.11)$$

We now consider the mismatched Shimizu-Morioka system as the response system given below:

$$\left.\begin{aligned} \dot{x} &= y \\ \dot{y} &= x - \alpha_2 y - xz \\ \dot{z} &= -\beta_2 z + x^2 \end{aligned}\right\} \quad \text{where } \alpha_2 = 0.85 \ \& \ \ \beta_2 = 0.6 \qquad (1.4.12)$$

Here, figure (1.6) represents the graph of the driver system and response system with respect to time. The red vertical line shows the difference between the un-coupled Shimizu-Morioka systems (1.4.11) and (1.4.12). The figures clearly show that the trajectories of the respective systems do not bear any 'regular' relationship with each other. The difference varies erratically. However, it will be observed later in the thesis that such irregular behaviour gives way to extreme regularity and globally stable asymptotic relationship between the two chaotic systems when they are coupled properly. This magical appearance of order from extreme disorder is the beauty of the enigma that we call synchronization.

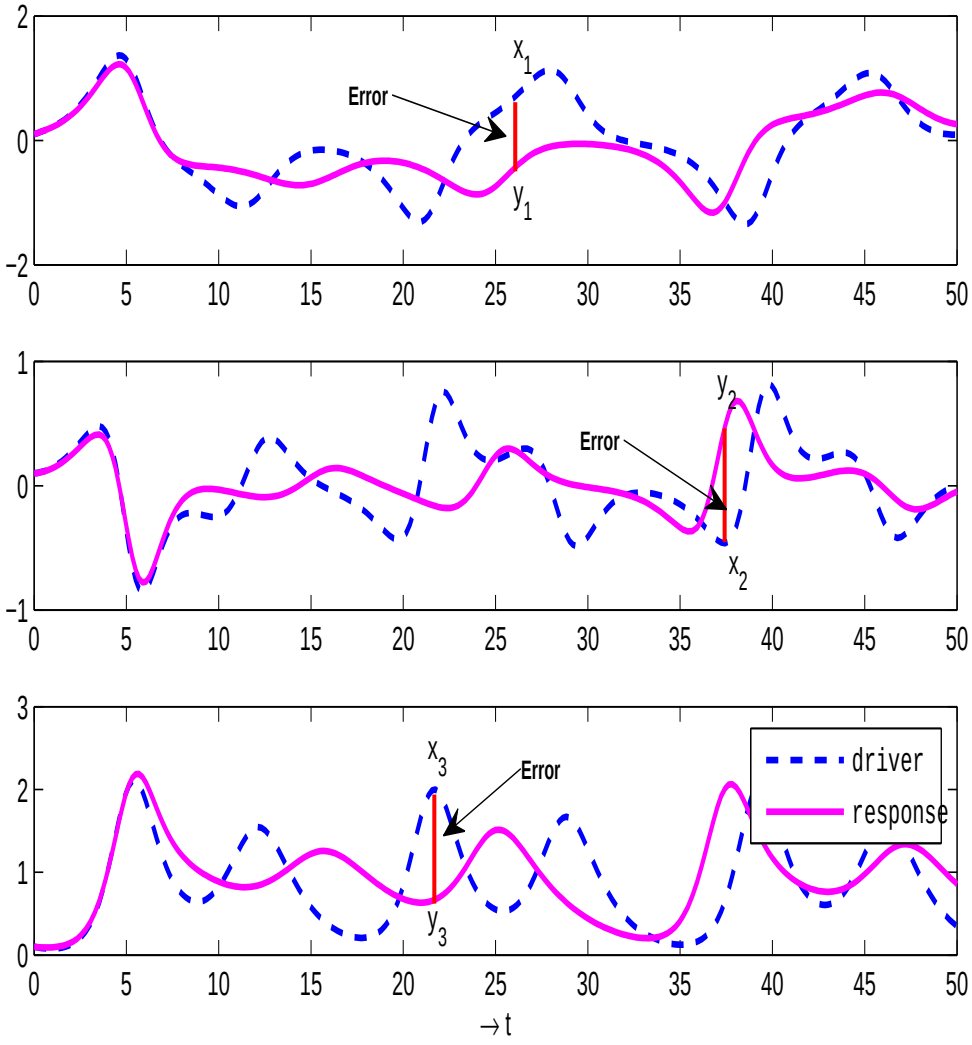

Figure 1.6: Drive and Response system w.r.t time

1.5 Structure of the Thesis

Our aim in this thesis is to analyze the behaviour of chaotic systems and to study the methods of chaos control and chaos synchronization phenomenon.

Chapter 2, presents the stability and control analysis of chaotic dynamical system. Two chaotic models have been considered for the discussion. Linear feedback control strategy is used for stabilizing the unstable critical points and deriving the necessary analytical conditions.

In chapter 3, study of non-linear chaotic dynamical system is performed after converting it into a linear controllable dynamical system using state space exact linearization(SSEL) method.

Chapter 4, presents the control technique as discussed in chapter 2 on a biological system. It is a theoretical study. We have presented a modified minimal model for glucose and insulin kinetics model. The model proposed here is a smooth approximation of the original non-smooth minimal model. The dynamical properties like dissipativity, existence of equilibrium and stability of the system at the equilibrium points are investigated. A linear feedback based control strategy is studied to control the blood glucose level in the situation where the physical system fails to maintain the blood glucose level automatically. A critical control parameter value k_c is determined in terms of the system parameters. Extensive numerical simulation is performed with different sets of parameter values. Assuming different values for the feedback gain parameter, ranges of physiological parameter α are determined where the feedback gain is sufficient to stabilize the system.

Two types of control strategies for complete synchronization have been discussed in chapter 5. For chaos synchronization between two coupled identical chaotic Sprott system L, hybrid and tracking control based strategies are adopted.

Chapter 6, describes a sliding mode control strategy-based scheme for achieving anti-synchronization between two coupled nonlinear chaotic system. A sliding mode control input and a nonlinear coupling function are designed using a linear sliding surface that synchronizes the systems antiphase. Here, we have established finite-time convergence of the method. The controller is also robust to all forms of bounded perturbations and this robustness can be easily achieved by tuning of a single control parameter and introduction of a control vector. The controller is also made chattering-free by producing a continuous analogue of the discontinuous control input. The effectiveness of the method is established by implementing it to antisynchronize chaotic Sprott system and Rössler system.

Chapter 7, is concerned with linear generalized synchronization through unidirectional coupling. In this method only diffusive coupling is required and no external control input is necessary. Transformation matrix in this case of generalized synchronization is determined by a commutation relation.

In chapter 8, we have used open-plus-closed-loop (OPCL) coupling technique to achieve generalized synchronization between two non-linear chaotic dynamical systems. For the asymptotic functional relation between the two systems in generalized synchronization, we have considered a transformation matrix that can be chosen arbitrarily and five different cases have been taken up.

In chapter 9, we have studied the stability properties of a time-delayed non-linear dynamical system. Lag synchronization between coupled chaotic systems has been discussed. The problem considered in this chapter is generalized synchronization where the synchronizing subsystems are asymptotically related by a transformation matrix whose elements are functions of time. OPCL control technique has been suitably modified in this context to construct the controller which serves our purpose. Lag complete and lag anti-synchronization arises as special cases in our study. Another point of importance in our study is the use of system state variables in the transformation matrix.

Chapter 10, addresses the summary of the works and the future possibility of our work is presented in chapter 11.

Chapter 2

Stability and Control of Chaotic Dynamical Systems

2.1 Stabilization and Control of Sprott Model B

2.1.1 Introduction

According to the Poincaré-Bendixson theorem [3], any non-linear dynamical system of equations of dimension less than three have no chaotic solution, but in general, chaotic solution may appear on the system of equations of dimension three or more. Edward Lorenz [45] introduced a three-dimensional non-linear dynamical system from a 12-dimensional system of equations which he made for a miniature atmosphere model. Lorenz's three-dimensional system of equations have three parameters.

Here, we consider a three dimensional non-linear chaotic dynamical system with only one parameter, known as Sprott's model B, one of nineteen different chaotic models discovered by J C Sprott [79].

The Sprott's model B is given by

$$\left.\begin{aligned}\dot{X} &= YZ \\ \dot{Y} &= X - Y \\ \dot{Z} &= a - XY\end{aligned}\right\} \tag{2.1.1}$$

where $a(> 0)$ is the parameter.

In case of $a = 1$, Sprott found that the system (2.1.1) is in chaotic nature.

2.1.2 Stability Analysis

It is obvious that the system (2.1.1) is dissipative,
since $\frac{\partial \dot{X}}{\partial X} + \frac{\partial \dot{Y}}{\partial Y} + \frac{\partial \dot{Z}}{\partial Z} = -1 < 0$.
For critical points, we have,

$$\dot{X} = 0, \quad \dot{Y} = 0 \quad and \quad \dot{Z} = 0.$$

Then, $\dot{Y} = 0$ gives $X = Y$.

$\dot{Z} = 0$ gives $XY = a$ which yields $X = Y = \pm\sqrt{a}$.

Hence, from $\dot{X} = 0$, we have, $Z = 0$.

Therefore, the critical points are $(\pm\sqrt{a}, \pm\sqrt{a}, 0)$.

Let us assume that

$$\begin{aligned}X &= x + \sqrt{a} \\ Y &= y + \sqrt{a} \\ Z &= z\end{aligned} \tag{2.1.2}$$

to give a small perturbation on the system (2.1.1) about the critical point $(\sqrt{a}, \sqrt{a}, 0)$, where x, y, z are small quantities.

Then,

$$\begin{aligned}
\dot{x} &= (y + \sqrt{a})z \\
&= yz + \sqrt{a}z \\
&= \sqrt{a}z \\
&\quad (by\ \ neglecting\ \ second\ \ order\ \ small\ \ quantities) \\
\dot{y} &= (x + \sqrt{a}) - (y + \sqrt{a}) \\
&= x - y \\
\dot{z} &= a - (x + \sqrt{a})(y + \sqrt{a}) \\
&= a - xy - \sqrt{a}x - \sqrt{a}y - a \\
&= -\sqrt{a}x - \sqrt{a}y \\
&\quad (by\ \ neglecting\ \ second\ \ order\ \ small\ \ quantities)
\end{aligned}$$

and hence the system of equation (2.1.1) becomes

$$\begin{aligned}
\dot{x} &= \sqrt{a}z \\
\dot{y} &= x - y \\
\dot{z} &= -\sqrt{a}x - \sqrt{a}y
\end{aligned} \tag{2.1.3}$$

Let $x = Ae^{\mu t}$, $y = Be^{\mu t}$ and $z = Ce^{\mu t}$ where A, B, C are all non-zero constants, be a solution of equations (2.1.3).

Then, we have,

$$\begin{aligned}
\mu A &= \sqrt{a}C \\
\mu B &= A - B \\
\mu C &= -\sqrt{a}A - \sqrt{a}B
\end{aligned}$$

Eliminating A, B, C from above, one can easily find that

$$\begin{vmatrix} \mu & 0 & -\sqrt{a} \\ -1 & (\mu+1) & 0 \\ \sqrt{a} & \sqrt{a} & \mu \end{vmatrix} = 0,$$

which yields

$$\mu^3 + \mu^2 + a\mu + 2a = 0 \tag{2.1.4}$$

By applying Routh-Hurwitz criteria [19, 59], the dynamical system (2.1.1) will be stable if

$$a > 0 \quad \text{and} \quad a - 2a > 0$$
$$i.e. \quad a > 0 \quad \text{and} \quad -a > 0 \quad - \quad \textit{but it is a contradiction.}$$

Therefore, the system is not stable about the critical point $(\sqrt{a}, \sqrt{a}, 0)$.

2.1.3 Control Analysis

Here, we consider a control variable u and the dynamical system (2.1.1) can be written as

$$\left.\begin{aligned} \dot{X} &= YZ \\ \dot{Y} &= X - Y + u \\ \dot{Z} &= a - XY \end{aligned}\right\} \tag{2.1.5}$$

So, in this case, equations (2.1.3) reduce to

$$\begin{aligned} \dot{x} &= \sqrt{a}z \\ \dot{y} &= x - y + u \\ \dot{z} &= -\sqrt{a}x - \sqrt{a}y \end{aligned} \tag{2.1.6}$$

where x, y, z are small quantities.

The system of equations (2.1.6), in matrix form, is given by

$$\dot{W} = \acute{A}W + \acute{B}u,$$

where

$$W = \begin{pmatrix} x \\ y \\ z \end{pmatrix} \in R^3, \quad \acute{B} = \begin{pmatrix} 0 \\ 1 \\ 0 \end{pmatrix}, \quad u \in R,$$

$$and \quad \acute{A} = \begin{pmatrix} 0 & 0 & \sqrt{a} \\ 1 & -1 & 0 \\ -\sqrt{a} & -\sqrt{a} & 0 \end{pmatrix}$$

Then,

$$\acute{A}^2 = \begin{pmatrix} -a & -a & 0 \\ -1 & 1 & \sqrt{a} \\ -\sqrt{a} & \sqrt{a} & -a \end{pmatrix}$$

Hence, by Balachandran and Dauer[5], we can get a controllable system, since $Rank(\acute{B}, \acute{A}\acute{B}, \acute{A}^2\acute{B}) = 3$.
Let us take $u = -kx$, where k is an appropriate gain (Vincent and Yu [85]).
Then, the system of equations (2.1.6) becomes

$$\left.\begin{aligned} \dot{x} &= \sqrt{a}z \\ \dot{y} &= (1-k)x - y \\ \dot{z} &= -\sqrt{a}x - \sqrt{a}y \end{aligned}\right\} \tag{2.1.7}$$

Let $x = A_1e^{\alpha t}$, $y = B_1e^{\alpha t}$ and $z = C_1e^{\alpha t}$, where A_1, B_1 and C_1 are non-zero scalars.

Eliminating A_1, B_1, C_1, we have from (2.1.7)

$$\begin{vmatrix} \alpha & 0 & -\sqrt{a} \\ (k-1) & (\alpha+1) & 0 \\ \sqrt{a} & \sqrt{a} & \alpha \end{vmatrix} = 0,$$

which gives

$$\alpha^3 + \alpha^2 + a\alpha + a(2-k) = 0 \tag{2.1.8}$$

Now, α will have negative real parts if

$$1 < k < 2 \tag{2.1.9}$$

By Routh-Hurwitz criteria, the system (2.1.1) is stable with control if $1 < k < 2$.

2.1.4 Results and Discussions

We have got two critical points $(\sqrt{a}, \sqrt{a}, 0)$ and $(-\sqrt{a}, -\sqrt{a}, 0)$ of the system (2.1.1). For the first point, we have got the stability condition. In case of the another critical point $(-\sqrt{a}, -\sqrt{a}, 0)$, in a similar way, one can easily find that the dynamical system (2.1.1) is stable if $1 < k < 2$.

Hence, we conclude that the system (2.1.1) is stable about its both of the critical points with same condition (2.1.9).

If the condition (2.1.9) fails, the system is not stable.

We will now give some attention on the figures attached. There are two types of figures, controlled figures and uncontrolled figures.

Let us take, at $t = 0$, $(x(0), y(0), z(0)) = (1.05, 1.05, 0)$.

The components of x, y and z depending on time of the uncontrolled system are shown, respectively in figure (2.1), figure (2.3) and figure (2.5).

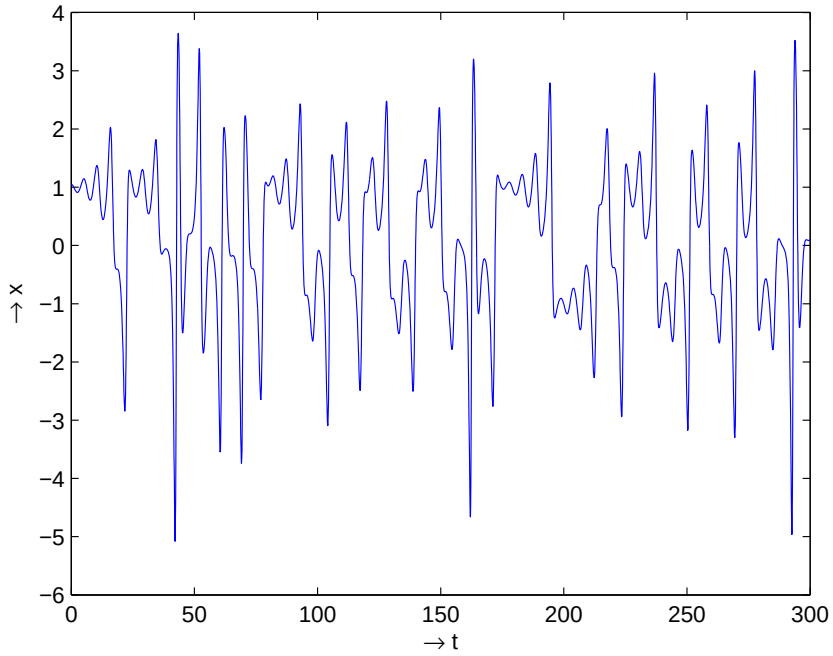

Figure 2.1: Evolution of x in time (without control)

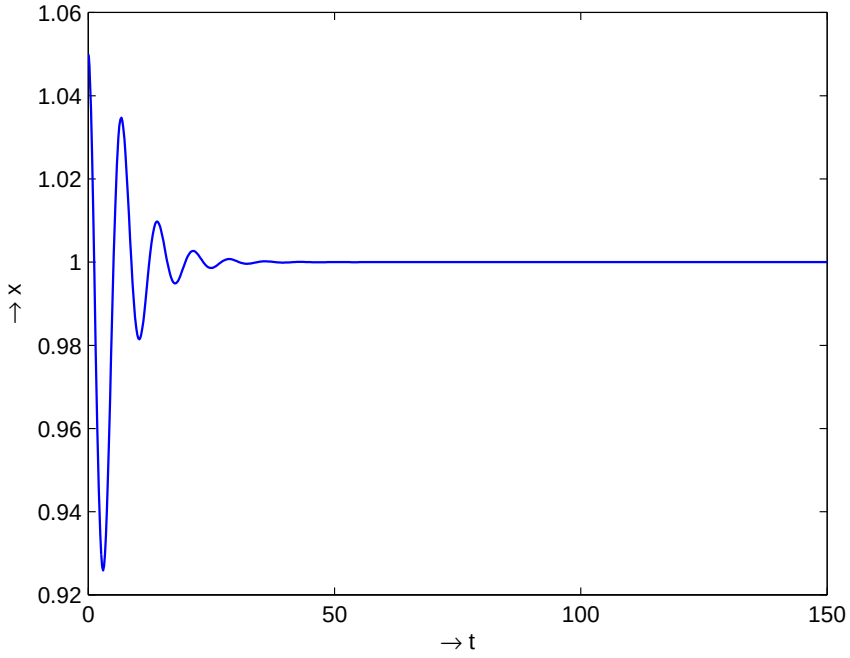

Figure 2.2: Evolution of x in time (with control)

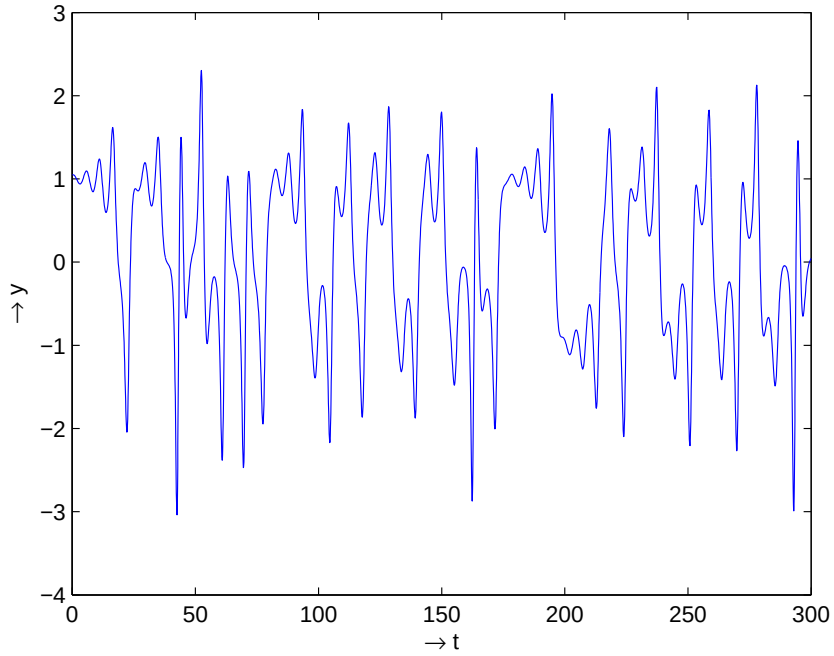

Figure 2.3: Evolution of y in time (without control)

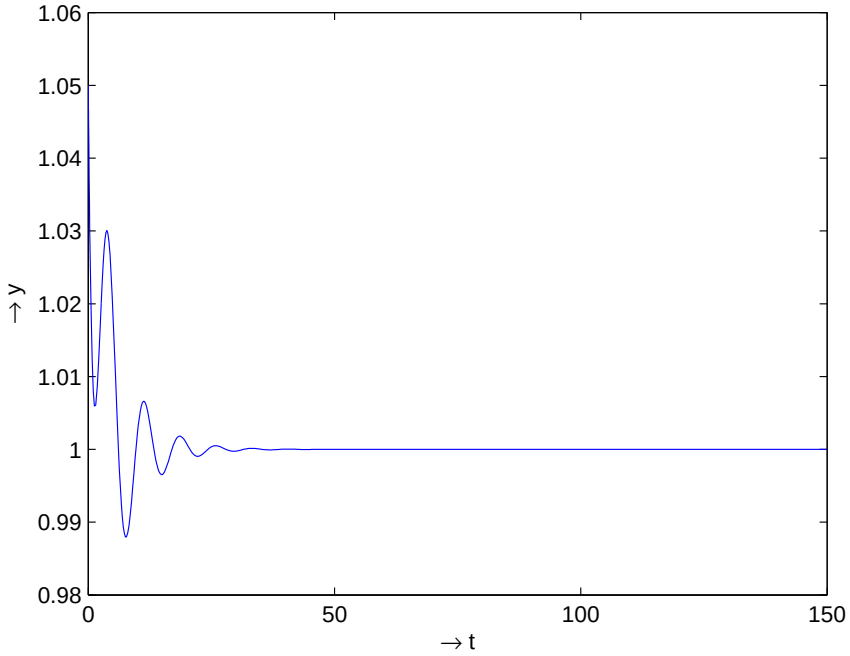

Figure 2.4: Evolution of y in time (with control)

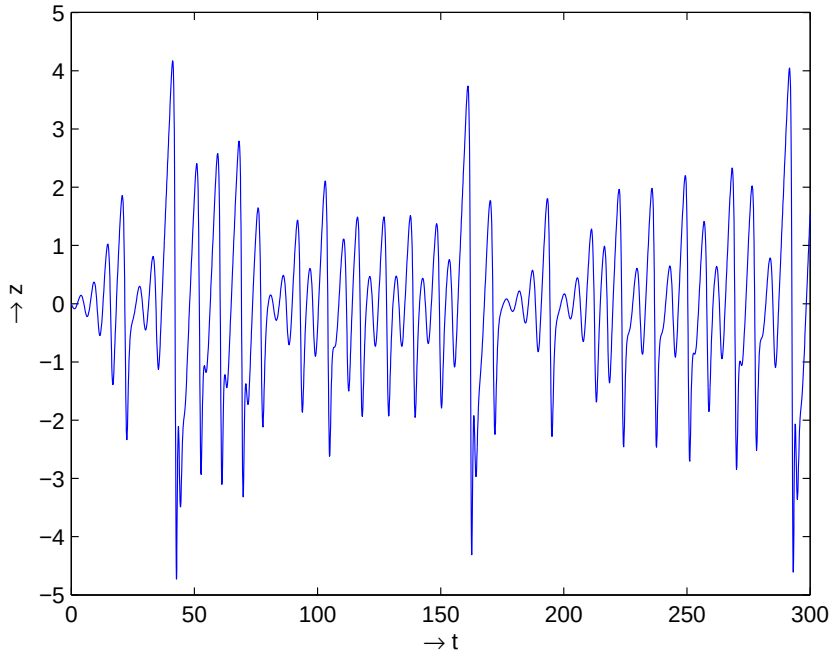

Figure 2.5: Evolution of z in time (without control)

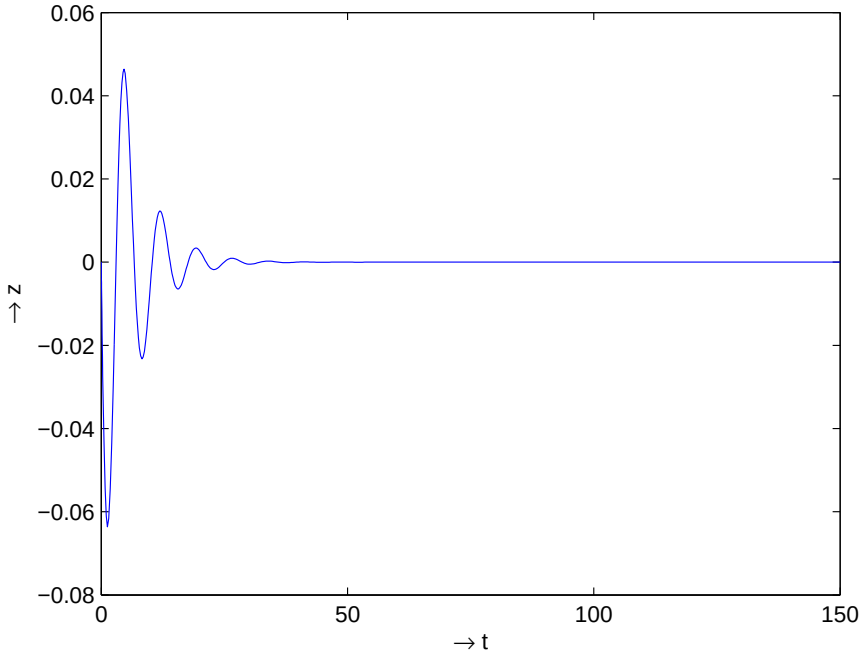

Figure 2.6: Evolution of z in time (with control)

For the controlled system by taking $k = 1.5$, time depending components of x, y and z are shown in figure (2.2), figure (2.4) and figure (2.6) respectively.

In figure (2.7), figure (2.9) and figure (2.11), we represent the phase portrait in the (x,y), (y,z) and (x,z) planes respectively with uncontrolled version.

The controlled figures of the phase portrait in the (x,y), (y,z) and (x,z) planes represented by figure (2.8), figure (2.10) and figure (2.12) respectively.

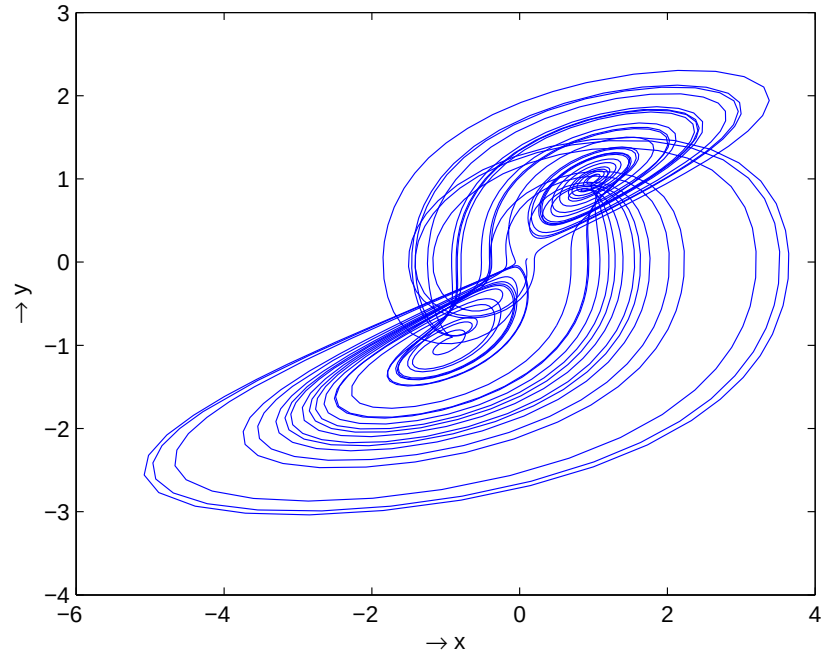

Figure 2.7: Phase portrait in the (x,y) plane (without control)

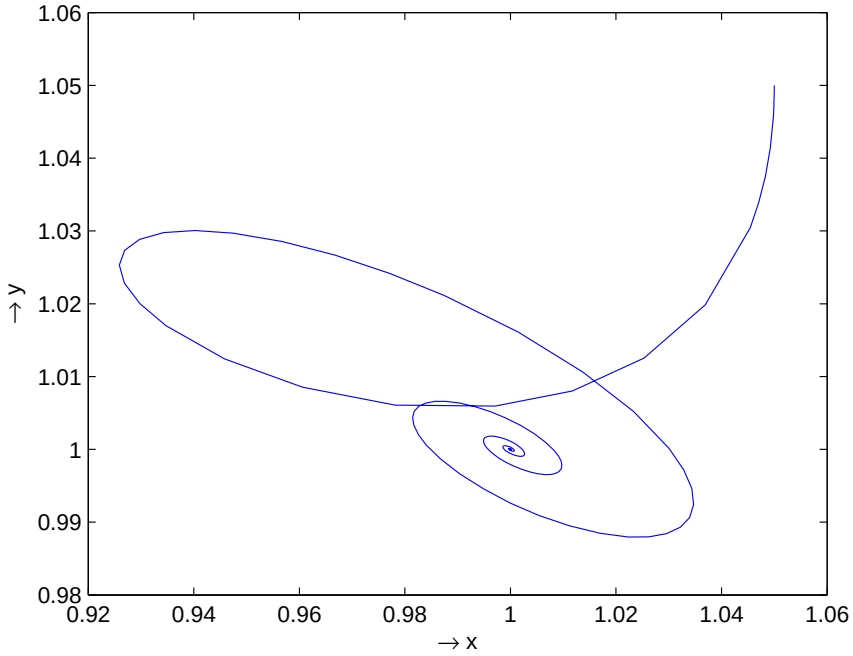

Figure 2.8: Phase portrait in the (x,y) plane (with control)

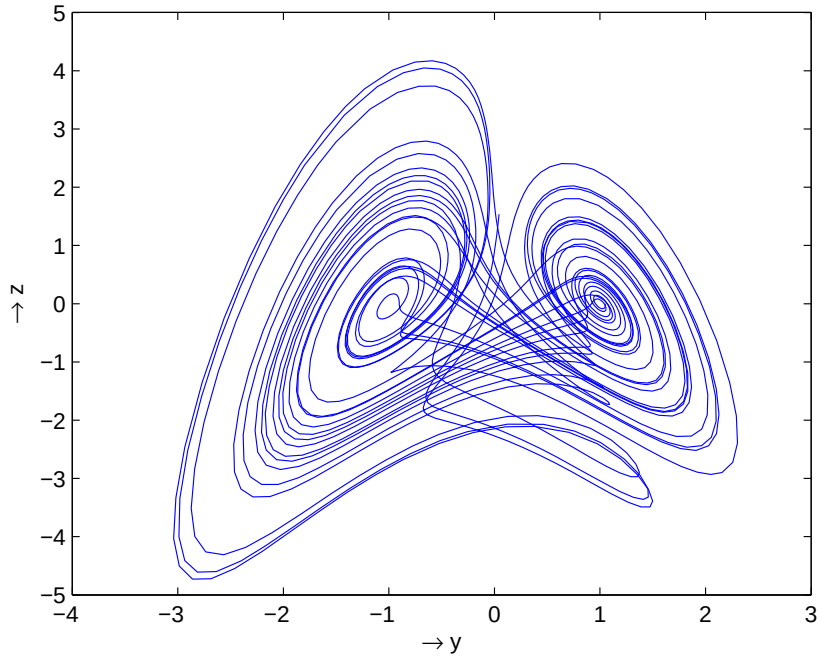

Figure 2.9: Phase portrait in the (y,z) plane (without control)

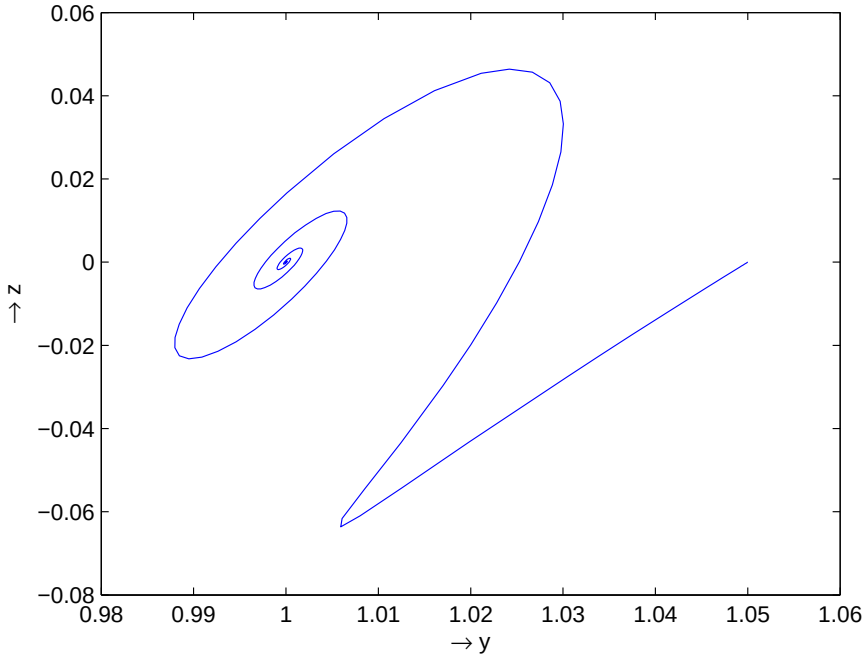

Figure 2.10: Phase portrait in the (y,z) plane (with control)

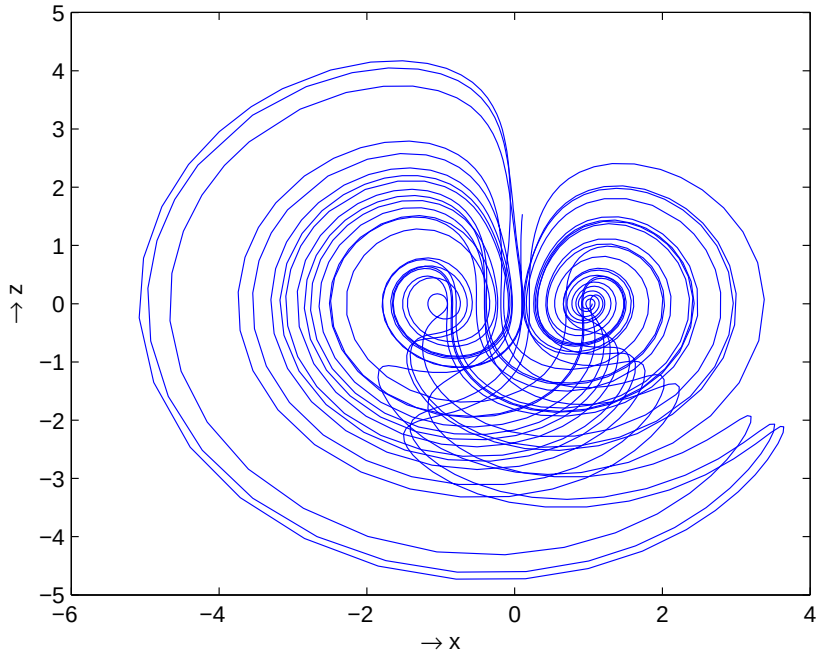

Figure 2.11: Phase portrait in the (x,z) plane (without control)

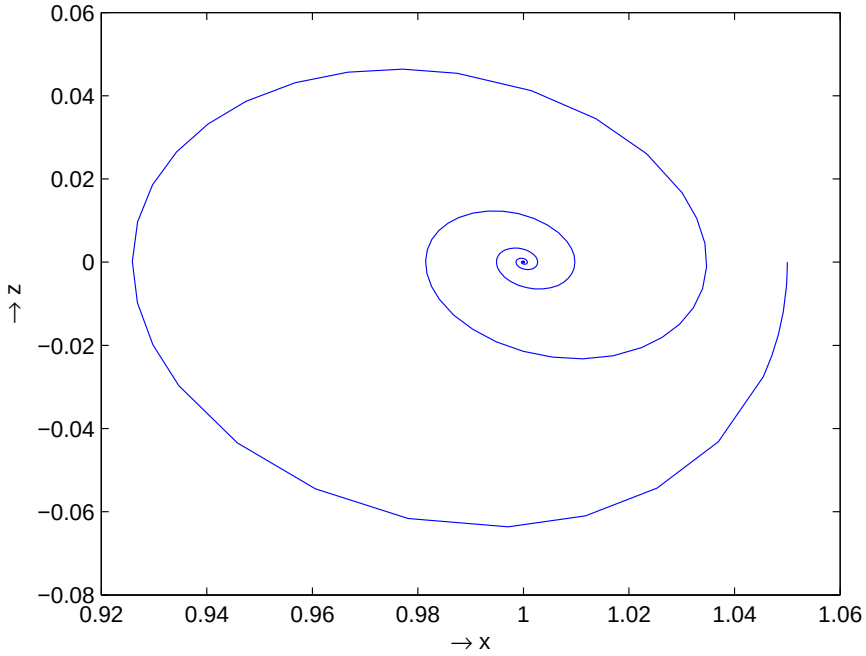

Figure 2.12: Phase portrait in the (x,z) plane (with control)

2.2 Stability and Control Analysis of the Sprott's Model L

2.2.1 Introduction

In 1963, Lorenz [45] was involved with the model of convection rolls in the atmosphere. From this model, he derived a ordinary non-linear three dimensional dynamical system. This system is bounded with chaotic nature. He also introduced a term fractal. It is a fractional dimension between 2 and 3, also known as strange attractor. Rössler(1976) [80] found the simplest possible strange attractor and derived a three dimensional non-linear dynamical system of equation. It also has a chaotic nature. In 1994, Sprott [79] discovered some more simple chaotic non-linear three dimensional dynamical systems, known as Sprott's model A to S.

In this communication, we are taking the Sprott's model L which has six terms with one non-linearity, as given below ,

$$\left.\begin{aligned} \dot{X} &= Y + \alpha Z \\ \dot{Y} &= \beta X^2 - Y \\ \dot{Z} &= \gamma - X \end{aligned}\right\} \tag{2.2.10}$$

where α, β, γ are all positive parameters.

Sprott found that the above system is chaotic when $\alpha = 3.9$, $\beta = 0.9, \quad \gamma = 1.$

Since $\frac{\partial \dot{X}}{\partial X} + \frac{\partial \dot{Y}}{\partial Y} + \frac{\partial \dot{Z}}{\partial Z} = -1 < 0,$
therefore, the dynamical system (2.2.10) is dissipative.

2.2.2 Stability Analysis

One can easily find that the critical point of the dynamical system (2.2.10) is given by $(\gamma, \beta\gamma^2, -\frac{\beta\gamma^2}{\alpha})$.
We now give some small perturbations on the non-linear dynamical system (2.2.10) about the critical point as :

$$X = \gamma + x; \quad Y = \beta\gamma^2 + y; \quad Z = -\frac{\beta\gamma^2}{\alpha} + z \tag{2.2.11}$$

where x, y, z are small quantities.
Then,

$$\begin{aligned}
\dot{x} &= \beta\gamma^2 + y + \alpha(-\frac{\beta\gamma^2}{\alpha} + z) \\
&= y + \alpha z \\
\dot{y} &= \beta(\gamma + x)^2 - (\beta\gamma^2 + y) \\
&= \beta(\gamma^2 + 2\gamma x + x^2) - \beta\gamma^2 - y \\
&= 2\beta\gamma x - y \\
&\quad (\textit{neglecting second degree term as } x, y, z \textit{ are} \\
&\qquad \textit{very small quantities}) \\
\dot{z} &= \gamma - (\gamma + x) \\
&= -x
\end{aligned}$$

Hence, the dynamical system (2.2.10) reduces to

$$\left.\begin{aligned}
\dot{x} &= y + \alpha z \\
\dot{y} &= 2\beta\gamma x - y \\
\dot{z} &= -x
\end{aligned}\right\} \tag{2.2.12}$$

Let

$$x = Ae^{\lambda t}, \quad y = Be^{\lambda t} \text{ and } z = Ce^{\lambda t} \tag{2.2.13}$$

where A.B.C $\neq 0$, be a solution of (2.2.12).
From (2.2.12) and (2.2.13), we have after eliminating A, B and C,

$$\begin{vmatrix} \lambda & -1 & -\alpha \\ -2\beta\gamma & \lambda+1 & 0 \\ 1 & 0 & \lambda \end{vmatrix} = 0$$

$$or, \quad \lambda^2(\lambda+1) - 2\beta\gamma\lambda + \alpha(\lambda+1) = 0$$

$$or, \quad \lambda^3 + \lambda^2 + (\alpha - 2\beta\gamma)\lambda + \alpha = 0 \tag{2.2.14}$$

According to Lyapunov's stability theory, the system of equation (2.2.10) will be stable if the values of λ have negative real parts.

Now, by Routh-Hurwitz criteria, the necessary and sufficient conditions that the system of equations (2.2.10) will be stable at the critical point $(\gamma, \beta\gamma^2, -\frac{\beta\gamma^2}{\alpha})$ if

$$\alpha - 2\beta\gamma > 0, \quad \alpha > 0 \quad \text{and} \quad -2\beta\gamma > 0$$

$$\text{which yields} \quad \alpha > 0, \quad \alpha > 2\beta\gamma, \quad \beta\gamma < 0 \tag{2.2.15}$$

Last inequality contradicts the fact that $\alpha > 0, \beta > 0, \gamma > 0$.
So, the critical point is not stable.

2.2.3 Control on the Sprott's model L

In this case, we introduce a control term u to the right side of the 2nd equation of (2.2.10) and the system of equations become

$$\left.\begin{aligned} \dot{X} &= Y + \alpha Z \\ \dot{Y} &= \beta X^2 - Y + u \\ \dot{Z} &= \gamma - X \end{aligned}\right\} \tag{2.2.16}$$

In terms of perturbation variables given in (2.2.11), system (2.2.16) takes the form

$$\left.\begin{aligned} \dot{x} &= y + \alpha z \\ \dot{y} &= 2\beta\gamma x - y + u \\ \dot{z} &= -x \end{aligned}\right\} \tag{2.2.17}$$

The system of equations (2.2.17) is of the form

$$\dot{W} = \acute{A}W + \acute{B}u,$$

where

$$W = \begin{pmatrix} x \\ y \\ z \end{pmatrix} \in R^3, \quad \acute{B} = \begin{pmatrix} 0 \\ 1 \\ 0 \end{pmatrix} \in R^3$$

$$and \quad \acute{A} = \begin{pmatrix} 0 & 1 & \alpha \\ 2\beta\gamma & -1 & 0 \\ -1 & 0 & 0 \end{pmatrix}, \quad u \in R$$

Then,

$$\acute{A}^2 = \begin{pmatrix} 2\beta\gamma - \alpha & -1 & 0 \\ -2\beta\gamma & 2\beta\gamma + 1 & 2\alpha\beta\gamma \\ 0 & -1 & -\alpha \end{pmatrix}$$

One can easily obtain that $Rank(\acute{B}, \acute{A}\acute{B}, \acute{A}^2\acute{B}) = 3$.
Therefore, the system is controllable (Balachandran and Dauer[5]).
Let $u = -kx$ (Vincent and Yu [85]), where k is an appropriate gain.
Then, the system of equations (2.2.17) becomes

$$\left.\begin{aligned} \dot{x} &= y + \alpha z \\ \dot{y} &= (2\beta\gamma - k)x - y \\ \dot{z} &= -x \end{aligned}\right\} \tag{2.2.18}$$

Let us consider

$$x = A_1 e^{\mu t}, \quad y = B_1 e^{\mu t} \text{ and } z = C_1 e^{\mu t} \tag{2.2.19}$$

where $A_1.B_1.C_1 \neq 0$. Eliminating A_1, B_1, C_1, we have from (2.2.18)

$$\begin{vmatrix} \mu & -1 & -\alpha \\ -(2\beta\gamma - k) & \mu + 1 & 0 \\ 1 & 0 & \mu \end{vmatrix} = 0$$

$$or, \quad \mu^2(\mu + 1) - (2\beta\gamma - k)\mu + \alpha(1 + \mu) = 0$$

$$or, \quad \mu^3 + \mu^2 + (\alpha + k - 2\beta\gamma)\mu + \alpha = 0 \tag{2.2.20}$$

By Routh-Hurwitz criteria, equations (2.2.20) will have all roots with negative real parts if

$$k > 2\beta\gamma - \alpha, \quad \alpha > 0 \text{ and } k > 2\beta\gamma > 0$$

It yields

$$k > 2\beta\gamma > \alpha \tag{2.2.21}$$

Therefore, if the condition (2.2.21) is satisfied,
then the system (2.2.10) is stable.

2.2.4 Results and Discussions

Sprott found that system (2.2.10) is of chaotic nature when
$\alpha = 3.9, \quad \beta = 0.9, \quad \gamma = 1.$

Let us choose, $(x(0), y(0), z(0)) = (1.8, 1.3, 0.1692)$. Now, if we take $k = 0$ in (2.2.18), we get the uncontrol version of the system (2.2.10).

The phase portrait in the (x,y), (y,z) and (x,z) planes are shown respectively in figure (2.13), figure (2.15) and figure (2.17).

The time developments of the x, y and z components of the uncontrolled system are shown, respectively in figure (2.19), figure (2.21) and figure (2.23). The last three figures represent the oscillatory nature of the transients in the x, y and z components.

If we take the value of k in such way that the condition (2.2.21) is satisfied, then the unstable critical point of the system (2.2.10) becomes stable.

Let us take $\alpha = 0.9, \beta = 0.9$ and $\gamma = 1$ with $k = 2$ satisfying the condition(2.2.21) and have got the stable system with control. In this case, phase portrait in the (x,y), (y,z) and (x,z) planes are shown respectively in figure (2.14), figure (2.16) and figure (2.18). The time developments of the x, y and z components of the controlled system are shown, respectively in figure (2.20), figure (2.22) and figure (2.24).

When the system was unstable, we have already noted that the figures [figure (2.19), figure (2.21) and figure (2.23)] represent the oscillatory nature of the transients in the x, y and z components. But in figure (2.20), figure (2.22) and figure (2.24), we have shown that smoothening of the major portion of the transients occur in all three components x, y and z as the system is now stable with the condition (2.2.21).

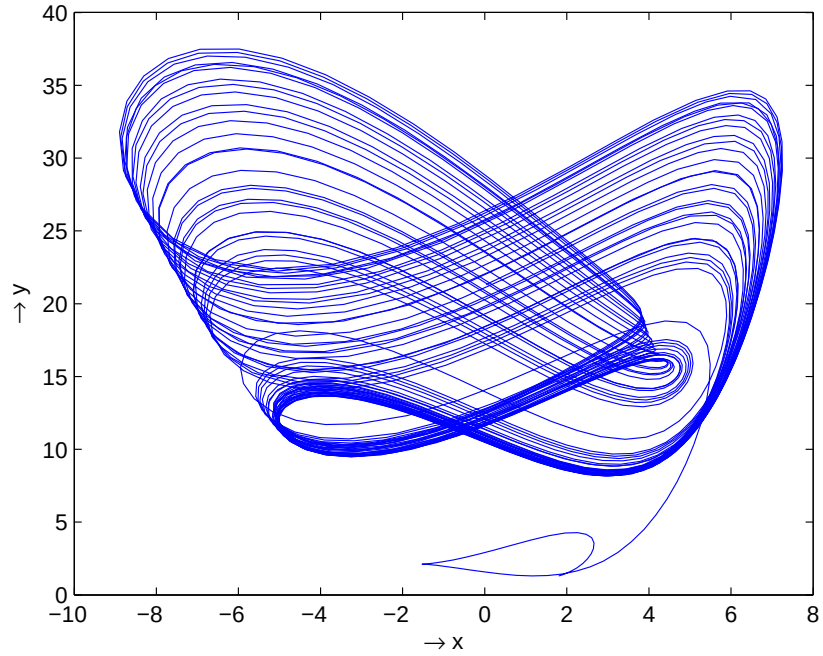

Figure 2.13: Phase portrait in the (x,y) plane (without control)

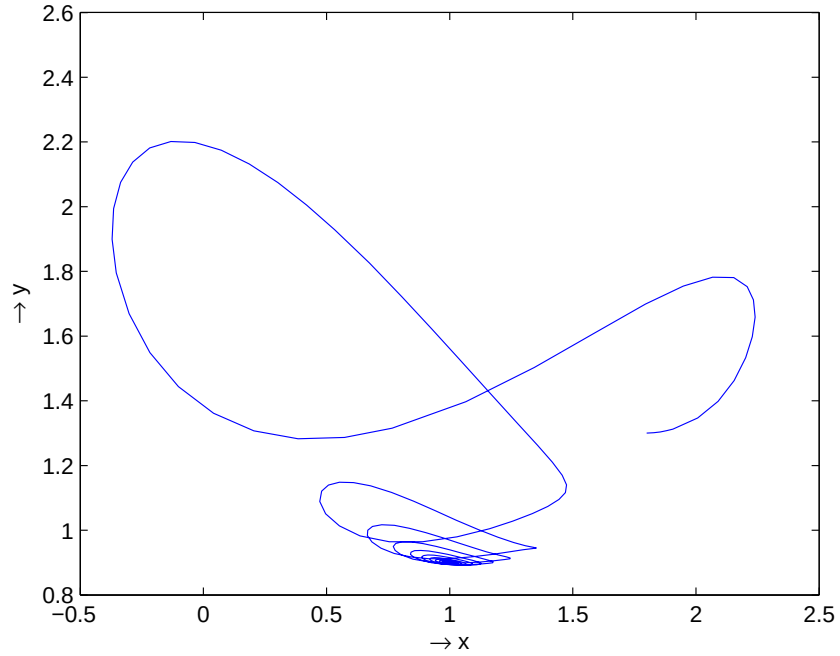

Figure 2.14: Phase portrait in the (x,y) plane (with control)

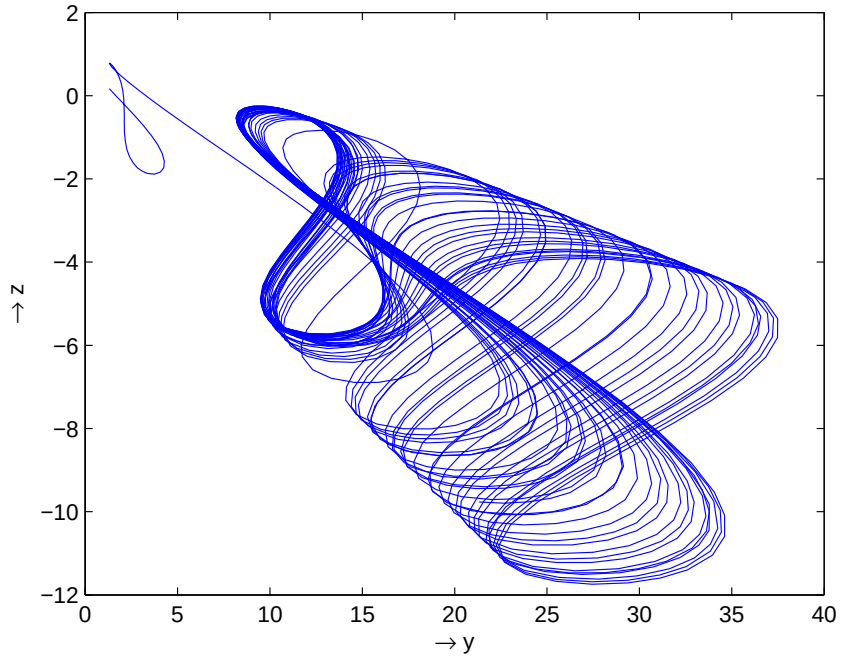

Figure 2.15: Phase portrait in the (y,z) plane (without control)

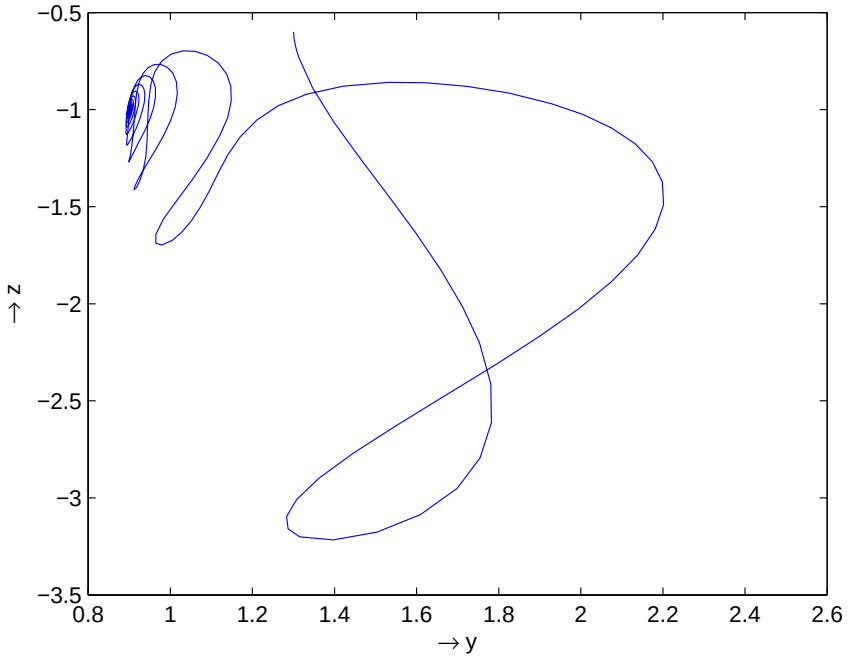

Figure 2.16: Phase portrait in the (y,z) plane (with control)

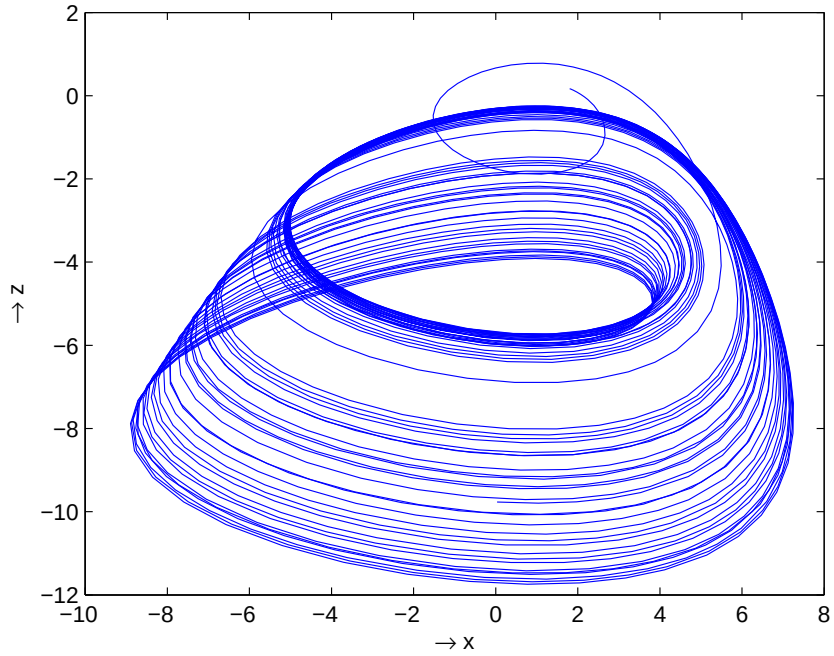

Figure 2.17: Phase portrait in the (x,z) plane (without control)

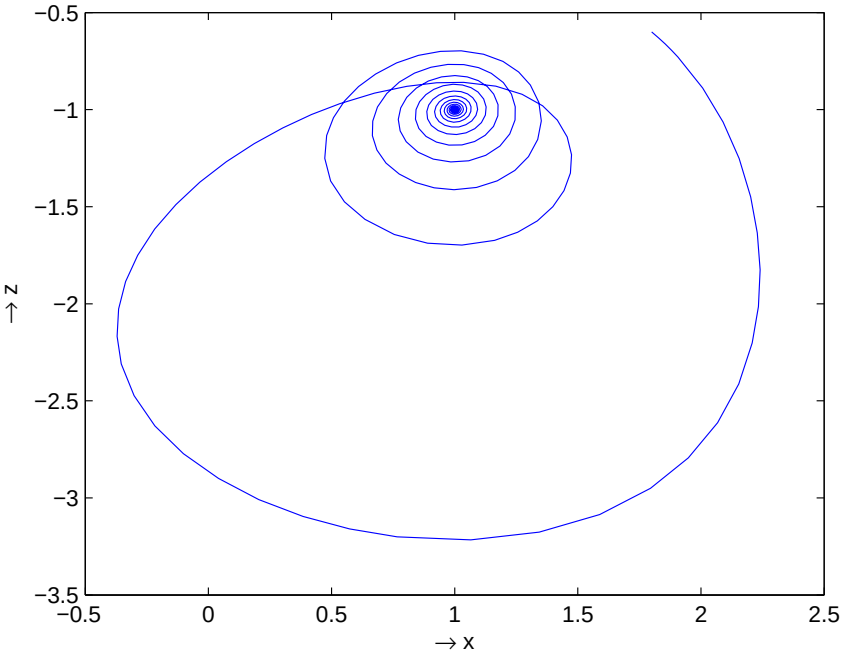

Figure 2.18: Phase portrait in the (x,z) plane (with control)

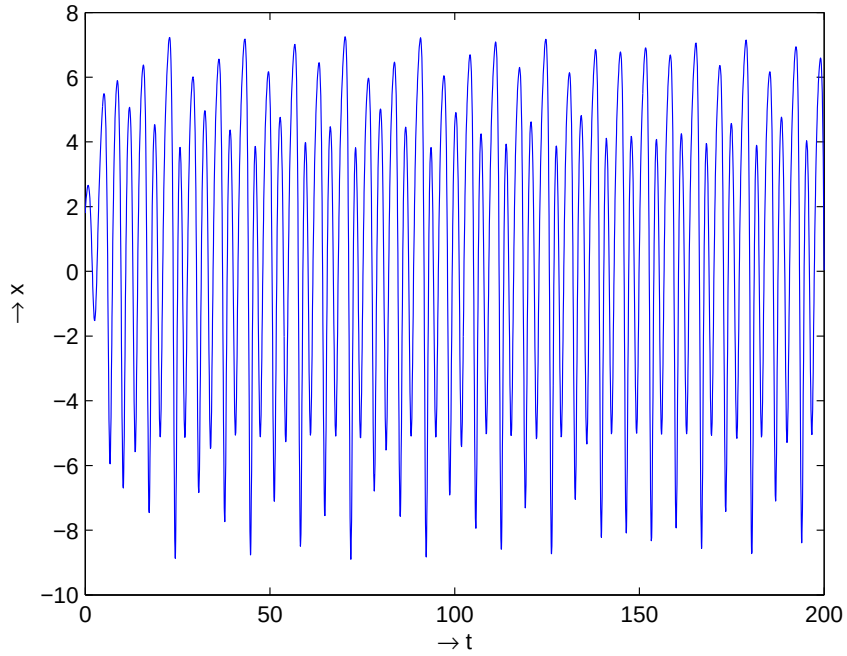

Figure 2.19: Evolution of x in time (without control)

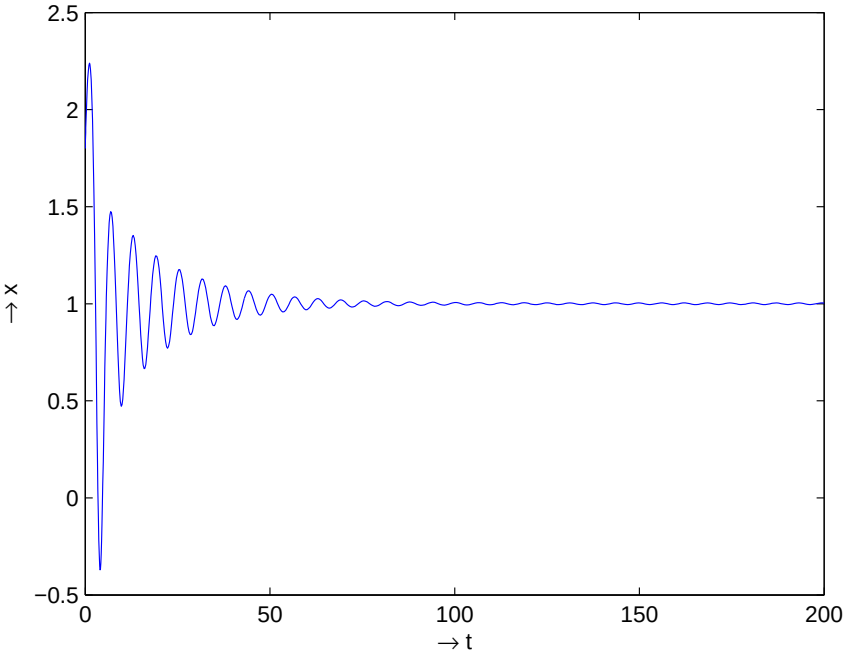

Figure 2.20: Evolution of x in time (with control)

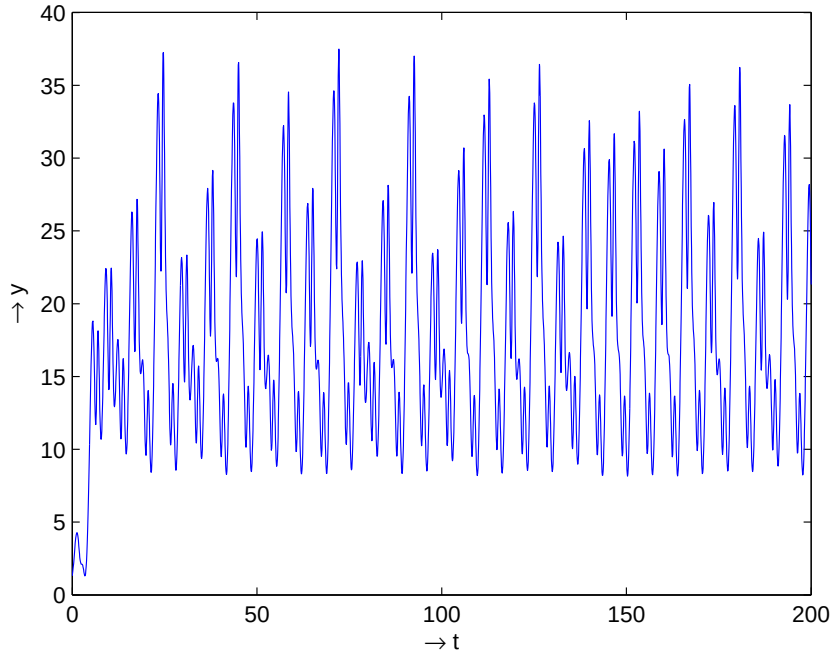

Figure 2.21: Evolution of y in time (without control)

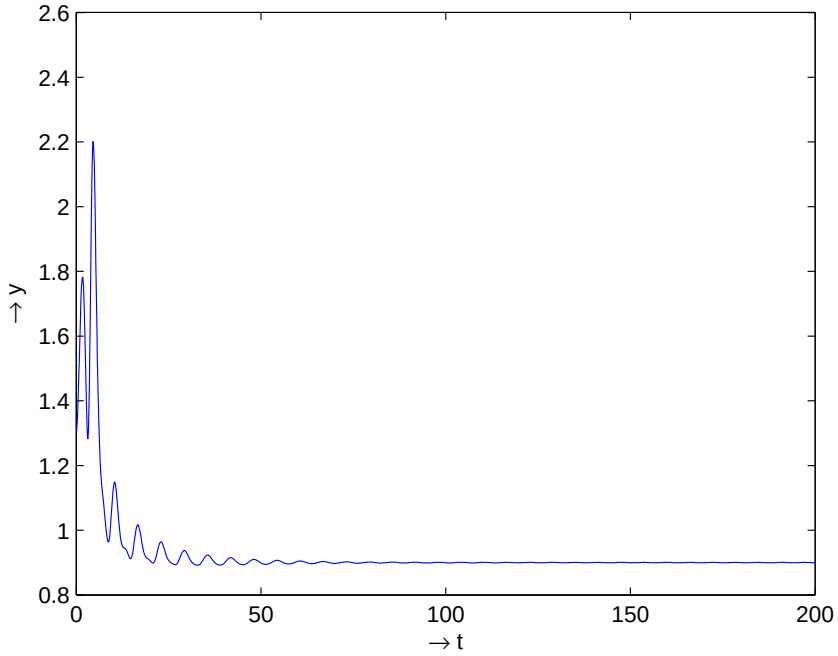

Figure 2.22: Evolution of y in time (with control)

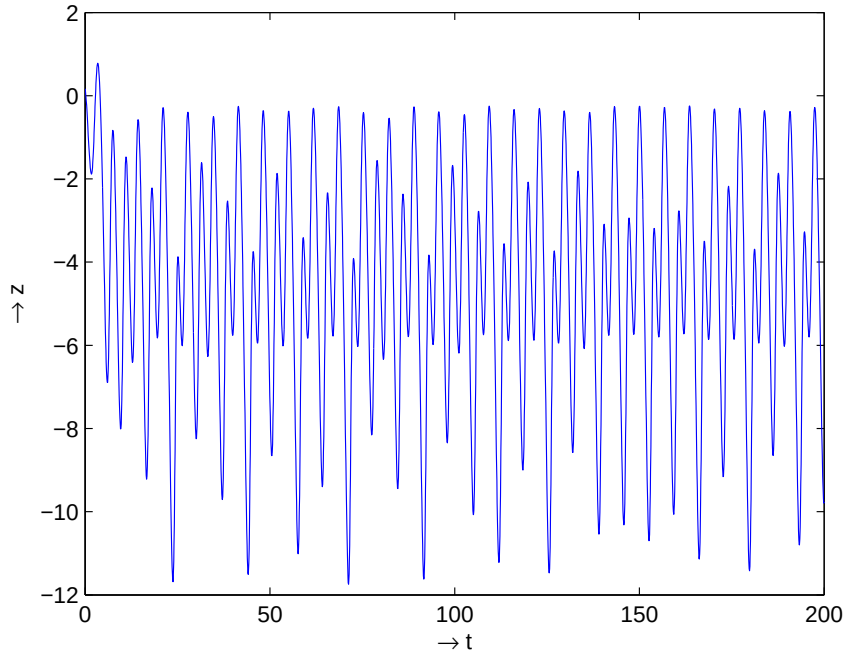

Figure 2.23: Evolution of z in time (without control)

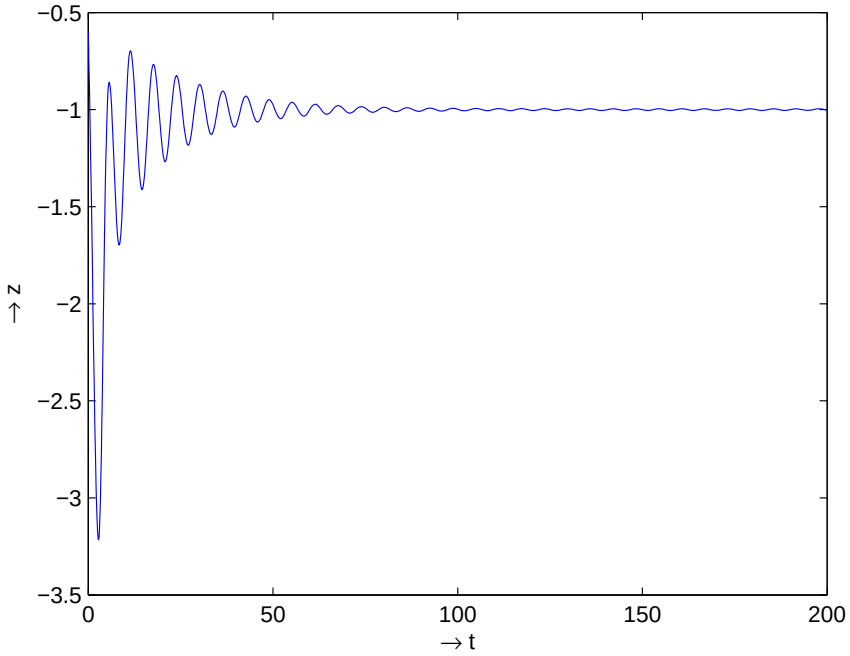

Figure 2.24: Evolution of z in time (with control)

Chapter 3

Control of Chaos using State Space Exact Linearization Control Method

3.1 Introduction

In 1998, the state space exact linearization (SSEL) method for non-linear control system [27] is introduced by Liqun and Yanzhu [44]. They considered the very famous Lorenz dynamical system [45, 77] and applied their method. Here we consider Sprott's chaotic non-linear dynamical system B. This system has two non-linear terms with one non-zero parameter. To control the chaotic Sprott system B, we are applying the previously mentioned SSEL method via lie algebra, which transformed the non-linear dynamical system into a linear controllable system.

3.2 The Exact Linearization Method

Let us consider two smooth functions $f : \mathbb{R}^n \to \mathbb{R}^n$ and $g : \mathbb{R}^n \to \mathbb{R}^n$ which are also smooth vector fields on $\mathbb{R}^n$.

Let $x \in \mathbb{R}^n$ and $u \in \mathbb{R}^1$ be the state variable and control parameter respectively. Then, any single-input non-linear system can be taken as

$$\dot{x} = f(x) + ug(x) \tag{3.2.1}$$

Let [X,Y] be the Lie bracket of vector fields X and Y. Let us denote

$$ad_f^i g(x) = [f, ad_f^{i-1} g](x), \quad i \geq 1 \tag{3.2.2}$$

with $ad_f^0 g(x) = g(x)$.

If $f = [f_1, f_2, f_3, ..., f_n]^T$ and $g = [g_1, g_2, g_3, ..., g_n]^T$,
using Lie-algebra, we may consider

$$ad_f^i g = [(ad_f^i g)_1, (ad_f^i g)_2, (ad_f^i g)_3, ..., (ad_f^i g)_n]^T, \tag{3.2.3}$$

where

$$(ad_f^i g)_j = \sum_{k=1}^{n} \left\{ f_k \frac{\partial (ad_f^{i-1} g)_j}{\partial x_k} - (ad_f^{i-1} g)_k \frac{\partial f_j}{\partial x_k} \right\}, \tag{3.2.4}$$

$j = 1, 2, 3, ..., n \;\; and \;\; i \geq 1$.

Let $L_X \lambda$ denote the Lie derivative of the real-valued function $\lambda(x)$ with respect to the vector field X.
Then, in a neighbourhood $N(x_0)$ of x_0, one can easily obtain the relations

$$L_g \lambda(x) = L_{ad_f^1 g} \lambda(x) = ... = L_{ad_f^{n-2} g} \lambda(x) = 0$$

and

$$L_{ad_f^{n-1}g}\lambda(x_0) \neq 0, \quad x \in N(x_0) \tag{3.2.5}$$

if the following two conditions are satisfied :

(1) Rank of Δ = n,
where $\Delta = [g(x_0), ad_f^1 g(x_0), ..., ad_f^{n-1} g(x_0)]$ and

(2) Γ is involutive ,
where $\Gamma = span\{g, ad_f^1 g, ad_f^2 g, ..., ad_f^{n-2} g\}$, near x_0.

Moreover, in the neighbourhood $N(x_0)$ of x_0, there exists the transformation

$$\begin{aligned} z &= [z_1, z_2, z_3, ..., z_n]^T \\ &= \Psi(x) \\ &= [\Psi_1(x), \Psi_2(x), \Psi_3(x), ..., \Psi_n(x)]^T \\ &= [\lambda(x), L_f\lambda(x), L_f^2\lambda(x), ..., L_f^{n-1}\lambda(x)]^T \end{aligned} \tag{3.2.6}$$

and

$$w = b(x) + ua(x) \tag{3.2.7}$$

where $a(x) = L_g L_f^{n-1}\lambda(x)$ and $b(x) = L_f^n\lambda(x)$.

Hence, we get the linear controllable system [82] from the nonlinear system (3.2.1) by the SSEL method as given below :

$$\dot{z_1} = z_2, \quad \dot{z_2} = z_3, \quad \dot{z_3} = z_4, ..., \quad \dot{z_{n-1}} = z_n, \quad \dot{z_n} = w.$$

3.3 Control of the Sprott Model B

The Sprott's non-linear chaotical dynamical system [79] is given by

$$\left.\begin{aligned} \dot{x_1} &= x_2 x_3 \\ \dot{x_2} &= x_1 - x_2 \\ \dot{x_3} &= \gamma - x_1 x_2 \end{aligned}\right\} \tag{3.3.8}$$

where $\gamma(\neq 0)$ is a parameter.
This system can be written as

$$\dot{x} = f(x) + ug(x)$$

where

$$f(x_1, x_2, x_3) = \begin{pmatrix} x_2 x_3 \\ x_1 - x_2 \\ \gamma - x_1 x_2 \end{pmatrix}$$

and

$$g(x_1, x_2, x_3) = \begin{pmatrix} 0 \\ x_1 \\ 0 \end{pmatrix}, \quad u = u(x_1, x_2, x_3), \quad x \in \mathbb{R}^3$$

To make the linear controllable system using state space exact linearization method, we have to verify the two conditions as discussed earlier :

(1) Rank of $\Delta = 3$, where $\Delta = [g, \quad ad_f^1 g, \quad ad_f^2 g]$ and

(2) Γ is involutive , where $\Gamma = span\{g, \quad ad_f^1 g\}$

Now, using (3.2.2), (3.2.3) and (3.2.4),

$$\begin{aligned}
(ad_f^1 g)_1 &= f_1\frac{\partial g_1}{\partial x_1} - g_1\frac{\partial f_1}{\partial x_1} + f_2\frac{\partial g_1}{\partial x_2} - g_2\frac{\partial f_1}{\partial x_2} + f_3\frac{\partial g_1}{\partial x_3} - g_3\frac{\partial f_1}{\partial x_3} \\
&= -x_1x_3 \\
(ad_f^1 g)_2 &= f_1\frac{\partial g_2}{\partial x_1} - g_1\frac{\partial f_2}{\partial x_1} + f_2\frac{\partial g_2}{\partial x_2} - g_2\frac{\partial f_2}{\partial x_2} + f_3\frac{\partial g_2}{\partial x_3} - g_3\frac{\partial f_2}{\partial x_3} \\
&= x_2x_3 + x_1 \\
(ad_f^1 g)_3 &= f_1\frac{\partial g_3}{\partial x_1} - g_1\frac{\partial f_3}{\partial x_1} + f_2\frac{\partial g_3}{\partial x_2} - g_2\frac{\partial f_3}{\partial x_2} + f_3\frac{\partial g_3}{\partial x_3} - g_3\frac{\partial f_3}{\partial x_3} \\
&= x_1^2
\end{aligned}$$

which yields,

$$[f,g] = ad_f^1 g = \begin{bmatrix} (ad_f^1 g)_1 \\ (ad_f^1 g)_2 \\ (ad_f^1 g)_3 \end{bmatrix}$$

$$or, \quad [f,g] = \begin{bmatrix} -x_1x_3 \\ x_2x_3 + x_1 \\ x_1^2 \end{bmatrix}$$

Again, by similar process, we have,

$$\begin{aligned}
(ad_f^2 g)_1 &= f_1\frac{\partial (ad_f^1 g)_1}{\partial x_1} - (ad_f^1 g)_1\frac{\partial f_1}{\partial x_1} + f_2\frac{\partial (ad_f^1 g)_1}{\partial x_2} \\
&\qquad - (ad_f^1 g)_2\frac{\partial f_1}{\partial x_2} + f_3\frac{\partial (ad_f^1 g)_1}{\partial x_3} - (ad_f^1 g)_3\frac{\partial f_1}{\partial x_3} \\
&= x_2x_3(-x_3) - (x_2x_3 + x_1)x_3 + (\gamma - x_1x_2)(-x_1) - x_1^2x_2 \\
&= -2x_2x_3^2 - x_1x_3 - \gamma x_1
\end{aligned}$$

$$
\begin{aligned}
(ad_f^2 g)_2 &= f_1 \frac{\partial (ad_f^1 g)_2}{\partial x_1} - (ad_f^1 g)_1 \frac{\partial f_2}{\partial x_1} + f_2 \frac{\partial (ad_f^1 g)_2}{\partial x_2} \\
&\quad - (ad_f^1 g)_2 \frac{\partial f_2}{\partial x_2} + f_3 \frac{\partial (ad_f^1 g)_2}{\partial x_3} - (ad_f^1 g)_3 \frac{\partial f_2}{\partial x_3} \\
&= x_2 x_3 .1 - (-x_1 x_3).1 + (x_1 - x_2)x_3 - (x_2 x_3 + x_1)(-1) \\
&\quad + (\gamma - x_1 x_2)x_2 \\
&= x_2 x_3 + 2x_1 x_3 + x_1 + \gamma x_2 - x_1 x_2^2
\end{aligned}
$$

$$
\begin{aligned}
(ad_f^2 g)_3 &= f_1 \frac{\partial (ad_f^1 g)_3}{\partial x_1} - (ad_f^1 g)_1 \frac{\partial f_3}{\partial x_1} + f_2 \frac{\partial (ad_f^1 g)_3}{\partial x_2} \\
&\quad - (ad_f^1 g)_2 \frac{\partial f_3}{\partial x_2} + f_3 \frac{\partial (ad_f^1 g)_3}{\partial x_3} - (ad_f^1 g)_3 \frac{\partial f_3}{\partial x_3} \\
&= x_2 x_3 .2x_1 - (-x_1 x_3)(-x_2) - (x_2 x_3 + x_1)(-x_1) \\
&= 2x_1 x_2 x_3 + x_1^2
\end{aligned}
$$

which yields,

$$
[f, ad_f^1 g] = ad_f^2 g = \begin{bmatrix} -2x_2 x_3^2 - x_1 x_3 - \gamma x_1 \\ x_2 x_3 + 2x_1 x_3 + x_1 + \gamma x_2 - x_1 x_2^2 \\ 2x_1 x_2 x_3 + x_1^2 \end{bmatrix}
$$

So, if $x_1 \neq 0$,

$$
\begin{aligned}
|\Delta| &= \begin{vmatrix} 0 & -x_1 x_3 & -2x_2 x_3^2 - x_1 x_3 - \gamma x_1 \\ x_1 & x_2 x_3 + x_1 & x_2 x_3 + 2x_1 x_3 + x_1 + \gamma x_2 - x_1 x_2^2 \\ 0 & x_1^2 & 2x_1 x_2 x_3 + x_1^2 \end{vmatrix} \\
&= -x_1[-x_1 x_3 (2x_1 x_2 x_3 + x_1^2) - x_1^2(-2x_2 x_3^2 - x_1 x_3 - \gamma x_1)] \\
&= -\gamma x_1^4 \quad \neq 0
\end{aligned}
$$

Therefore, we can say, Rank of $\Delta = 3$.

Now,

$$\begin{aligned}
(g, ad_f^1 g)_1 &= g_1 \frac{\partial (ad_f^1 g)_1}{\partial x_1} - (ad_f^1 g)_1 \frac{\partial g_1}{\partial x_1} + g_2 \frac{\partial (ad_f^1 g)_1}{\partial x_2} \\
&\quad - (ad_f^1 g)_2 \frac{\partial g_1}{\partial x_2} + g_3 \frac{\partial (ad_f^1 g)_1}{\partial x_3} - (ad_f^1 g)_3 \frac{\partial g_1}{\partial x_3} \\
&= 0 \\
(g, ad_f^1 g)_2 &= g_1 \frac{\partial (ad_f^1 g)_2}{\partial x_1} - (ad_f^1 g)_1 \frac{\partial g_2}{\partial x_1} + g_2 \frac{\partial (ad_f^1 g)_2}{\partial x_2} \\
&\quad - (ad_f^1 g)_2 \frac{\partial g_2}{\partial x_2} + g_3 \frac{\partial (ad_f^1 g)_2}{\partial x_3} - (ad_f^1 g)_3 \frac{\partial g_2}{\partial x_3} \\
&= -(-x_1 x_3).1 + x_1 x_3 \\
&= 2x_1 x_3 \\
(g, ad_f^1 g)_3 &= g_1 \frac{\partial (ad_f^1 g)_3}{\partial x_1} - (ad_f^1 g)_1 \frac{\partial g_3}{\partial x_1} + g_2 \frac{\partial (ad_f^1 g)_3}{\partial x_2} \\
&\quad - (ad_f^1 g)_2 \frac{\partial g_3}{\partial x_2} + g_3 \frac{\partial (ad_f^1 g)_3}{\partial x_3} - (ad_f^1 g)_3 \frac{\partial g_3}{\partial x_3} \\
&= 0
\end{aligned}$$

which yields,

$$[g, ad_f^1 g] = \begin{bmatrix} (g, ad_f^1 g)_1 \\ (g, ad_f^1 g)_2 \\ (g, ad_f^1 g)_3 \end{bmatrix} = \begin{bmatrix} 0 \\ 2x_1 x_3 \\ 0 \end{bmatrix}$$

Therefore, it is similar like g as $[g, ad_f^1 g]$ is along the y-axis.

Thus, $\Gamma = span\{g, ad_f^1 g\}$ which is involutive, where $x_i \in \mathbb{R}, \quad i = 1, 2, 3$.

Hence, the required two conditions for the relation (3.2.5) have been satisfied for $n = 3$.

Now, $L_g \lambda(x) = 0$ gives $x_1 \frac{\partial \lambda}{\partial x_2} = 0$.

This implies that

$$\frac{\partial \lambda}{\partial x_2} = 0 \quad as \quad x_1 \neq 0. \tag{3.3.9}$$

$L_{ad_f^1 g}\lambda(x) = 0$ gives

$$-x_1 x_3 \frac{\partial \lambda}{\partial x_1} + x_1^2 \frac{\partial \lambda}{\partial x_3} = 0.$$

$$or, \quad x_3 \frac{\partial \lambda}{\partial x_1} - x_1 \frac{\partial \lambda}{\partial x_3} = 0 \quad as \quad x_1 \neq 0 \tag{3.3.10}$$

Then, solution of the equation (3.3.10) is given by,

$$\lambda = x_1^2 + x_3^2 + \sigma \tag{3.3.11}$$

where σ is a numerical constant chosen in such way that the goal of the control can be attained.

Since $\frac{\partial \lambda}{\partial x_2} = 0$, using (3.3.10), we can write $L_{ad_f^2 g}\lambda(x)$ as

$$\begin{aligned} L_{ad_f^2 g}\lambda(x) &= (ad_f^2 g)_1 \frac{\partial \lambda}{\partial x_1} + (ad_f^2 g)_3 \frac{\partial \lambda}{\partial x_3} \\ &= (-2x_2 x_3^2 - x_1 x_3 - \gamma x_1)\frac{\partial \lambda}{\partial x_1} + (2x_1 x_2 x_3 + x_1^2)\frac{\partial \lambda}{\partial x_3} \\ &= [(-2x_2 x_3^2 - x_1 x_3 - \gamma x_1).\frac{x_1}{x_3} + (2x_1 x_2 x_3 + x_1^2)]\frac{\partial \lambda}{\partial x_3} \\ &= -\frac{\gamma x_1^2}{x_3}\frac{\partial \lambda}{\partial x_3} \\ &= -2\gamma x_1^2 \\ &\neq 0, \quad since \quad x_1 \neq 0 \quad and \quad \gamma \neq 0 \end{aligned} \tag{3.3.12}$$

Using (3.3.11), we have,

$$\begin{aligned} L_f \lambda(x) &= x_2 x_3 \frac{\partial}{\partial x_1}(x_1^2 + x_3^2 + \sigma) + (\gamma - x_1 x_2)\frac{\partial}{\partial x_3}(x_1^2 + x_3^2 + \sigma) \\ &= 2\gamma x_3 \end{aligned} \tag{3.3.13}$$

and

$$\begin{aligned} L_f^2\lambda(x) &= L_f(L_f\lambda(x)) \\ &= x_2x_3\frac{\partial}{\partial x_1}(L_f\lambda(x)) + (x_1 - x_2)\frac{\partial}{\partial x_2}(L_f\lambda(x)) \\ &\quad + (\gamma - x_1x_2)\frac{\partial}{\partial x_3}(L_f\lambda(x)) \\ &= 2\gamma(\gamma - x_1x_2) \end{aligned} \tag{3.3.14}$$

According to the state space exact linearization method, using (3.2.6) we can construct the transformation process as given below:

$$\begin{aligned} z &= [z_1, z_2, z_3]^T \\ &= \Psi(x) \\ &= [\Psi_1(x), \Psi_2(x), \Psi_3(x)]^T \\ &= [\lambda(x), L_f^1\lambda(x), L_f^2\lambda(x)]^T \end{aligned}$$

and

$$w = b(x) + ua(x) \tag{3.3.15}$$

where

$$a(x) = L_gL_f^2\lambda(x) \quad and \quad b(x) = L_f^3\lambda(x) \tag{3.3.16}$$

Hence,

$$\begin{bmatrix} z_1 \\ z_2 \\ z_3 \end{bmatrix} = z = \Psi(x) = \begin{bmatrix} x_1^2 + x_3^2 + \sigma \\ 2\gamma x_3 \\ 2\gamma(\gamma - x_1x_2) \end{bmatrix} \tag{3.3.17}$$

From (3.3.17), we can construct the inverse transformation as

$$\begin{bmatrix} x_1 \\ x_2 \\ x_3 \end{bmatrix} = x = \Psi^{-1}(z) = \begin{bmatrix} \frac{\sqrt{4\gamma^2z_1 - 4\gamma^2\sigma - z_2^2}}{2\gamma} \\ \frac{2\gamma^2 - z_3}{\sqrt{4\gamma^2z_1 - 4\gamma^2\sigma - z_2^2}} \\ \frac{z_2}{2\gamma} \end{bmatrix} \tag{3.3.18}$$

From (3.3.16), we have,

$$\begin{aligned} a(x) &= L_g L_f^2 \lambda(x) \\ &= x_1 \frac{\partial}{\partial x_2}(L_f^2 \lambda(x)) \\ &= x_1 \frac{\partial}{\partial x_2}[2\gamma(\gamma - x_1 x_2)] \\ &= -2\gamma x_1^2 \end{aligned} \tag{3.3.19}$$

and

$$\begin{aligned} b(x) &= L_f^3 \lambda(x) \\ &= L_f(L_f^2 \lambda(x)) \\ &= x_2 x_3 \frac{\partial}{\partial x_1}(L_f^2 \lambda(x)) + (x_1 - x_2)\frac{\partial}{\partial x_2}(L_f^2 \lambda(x)) \\ &\quad + (\gamma - x_1 x_2)\frac{\partial}{\partial x_3}(L_f^2 \lambda(x)) \\ &= x_2 x_3(-2\gamma x_2) + (x_1 - x_2)(-2\gamma x_1) \\ &= -2\gamma x_2^2 x_3 - 2\gamma x_1^2 + 2\gamma x_1 x_2 \end{aligned} \tag{3.3.20}$$

Therefore, from (3.3.15), u can be obtained as

$$u = \frac{w}{a(x)} - \frac{b(x)}{a(x)}$$

$$or, u = -\frac{w}{2\gamma x_1^2} - \frac{x_2^2 x_3 + x_1^2 - x_1 x_2}{x_1^2} \tag{3.3.21}$$

Using (3.3.15) and [(3.3.17) - (3.3.20)], we have got the linear controllable system from the system of equation (3.3.8) as given below:

$$\dot{z_1} = z_2, \quad \dot{z_2} = z_3 \quad \text{and} \quad \dot{z_3} = w, \tag{3.3.22}$$

where w can be taken as

$$w = c_1 z_1 + c_2 z_2 + c_3 z_3 \tag{3.3.23}$$

in such way that by changing the value of σ, we can control the variable x_1 to the goal x_g.

Let us consider,

$$z_1 = P_1 e^{\mu t}, \quad z_2 = Q_1 e^{\mu t} \quad \text{and} \quad z_3 = R_1 e^{\mu t},$$

where $P_1.Q_1.R_1 \neq 0$.

Now, eliminating P_1, Q_1 and R_1, one may easily obtain,

$$\begin{vmatrix} \mu & -1 & 0 \\ 0 & \mu & -1 \\ -c_1 & -c_2 & (\mu - c_3) \end{vmatrix} = 0$$

After simplifying, one gets,

$$\mu^3 + (-c_3)\mu^2 + (-c_2)\mu + (-c_1) = 0$$

Hence, for the controlled system (3.3.22), by Routh-Hurwitz criteria, the values of the parameters c_1, c_2, c_3 are chosen[50] in such way that $c_1 + c_2 c_3 > 0$ with $c_1 < 0, c_2 < 0$ & $c_3 < 0$ are satisfied.

Using (3.3.17) and (3.3.23) in (3.3.21), one gets,

$$u = -\frac{c_1(x_1^2 + x_3^2 + \sigma) + 2c_2\gamma x_3 + 2c_3\gamma(\gamma - x_1 x_2)}{2\gamma x_1^2} - \frac{x_2^2 x_3 + x_1^2 - x_1 x_2}{x_1^2} \tag{3.3.24}$$

which gives the linear feedback control parameter u.

With the help of (3.3.18), we may consider the term σ as given below :

$$\sigma = -x_g^2 \tag{3.3.25}$$

where x_g is the control goal.

3.4 Results and Discussions

For $\gamma = 1$, Sprott found that the system (3.3.8) is chaotic.
Numerical simulation is done with the initial values of the state variables $x_1(0) = 1, \quad x_2(0) = 1 \quad \& \quad x_3(0) = 1$.

Here, we have taken, $c_1 = -0.5, \quad c_2 = -2.5 \quad \& \quad c_3 = -0.75$ and the control is started at $t = 200$ with $x_g = 1.25$. At time $t = 500$, the control goal is changed from $x_g = 1.25$ to $x_g = 1.75$.

Using Runge-Kutta method, time evolution of x_1, x_2, x_3 are shown in the figure (3.1), figure (3.3) and figure (3.5) respectively with $u = 0$ whereas figure (3.2), figure (3.4) and figure (3.6) depict the time evolution of x_1, x_2, x_3 respectively in presence of control u.
Finally, we conclude that the SSEL method has been applied successfully to control the Sprott system B.

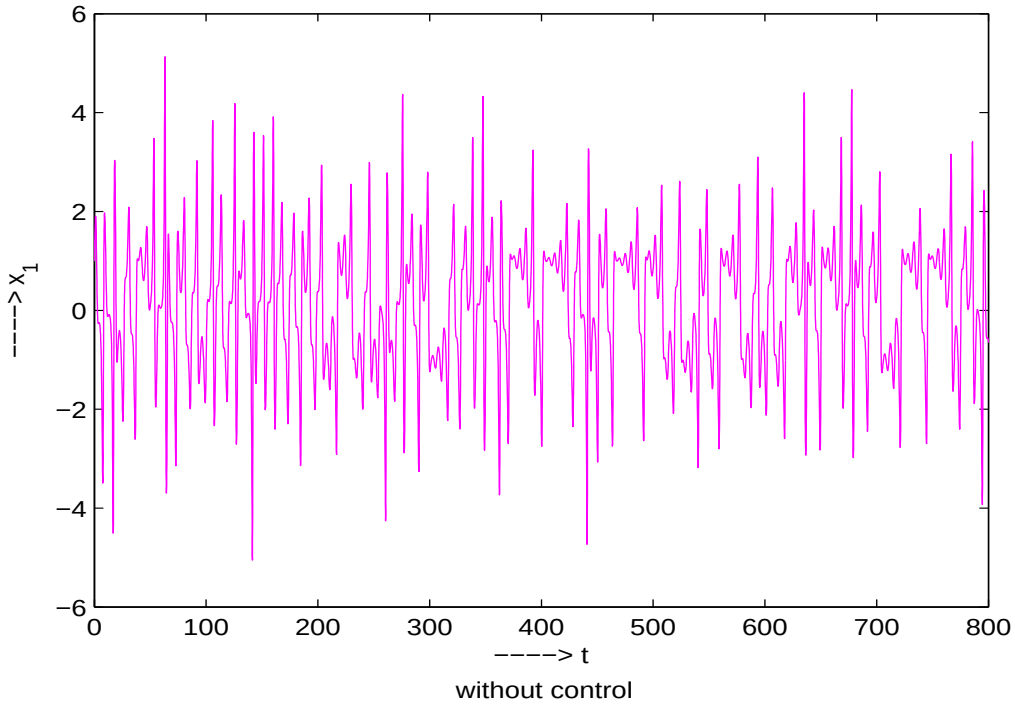

Figure 3.1: The time evolution of x_1 in uncontrolled system

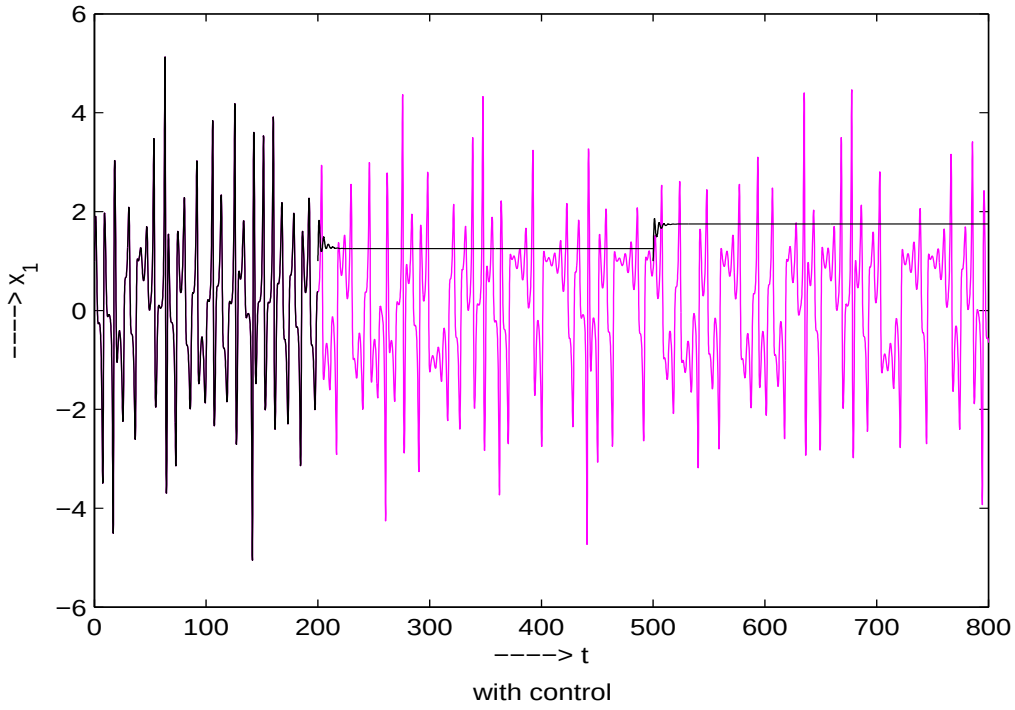

Figure 3.2: The time evolution of x_1 in controlled system

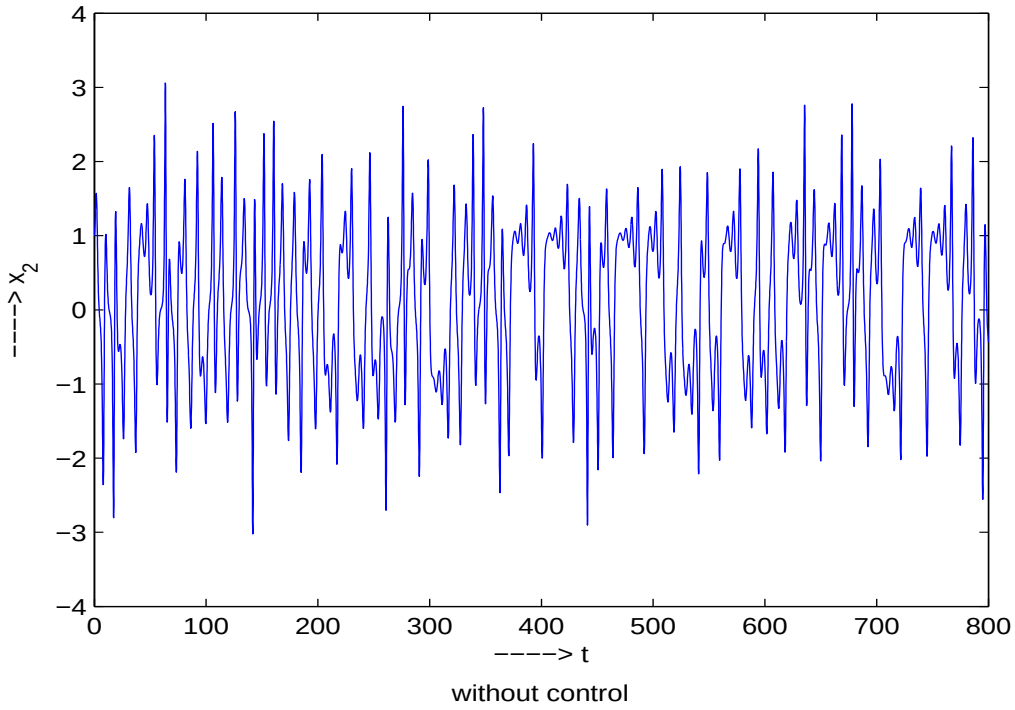

Figure 3.3: The time evolution of x_2 in uncontrolled system

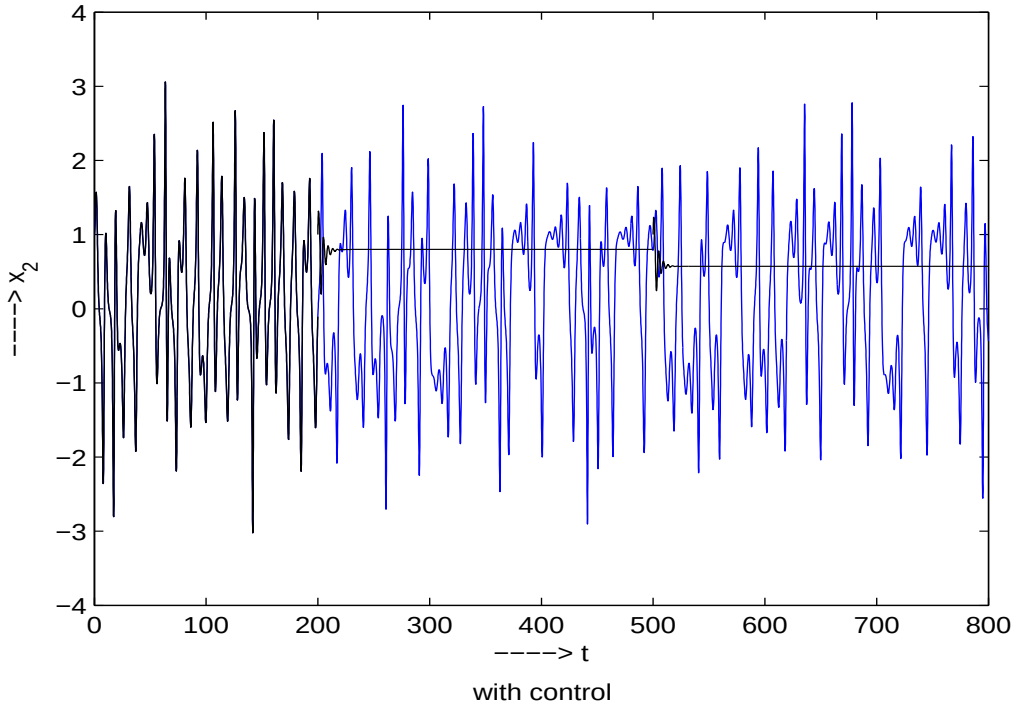

Figure 3.4: The time evolution of x_2 in controlled system

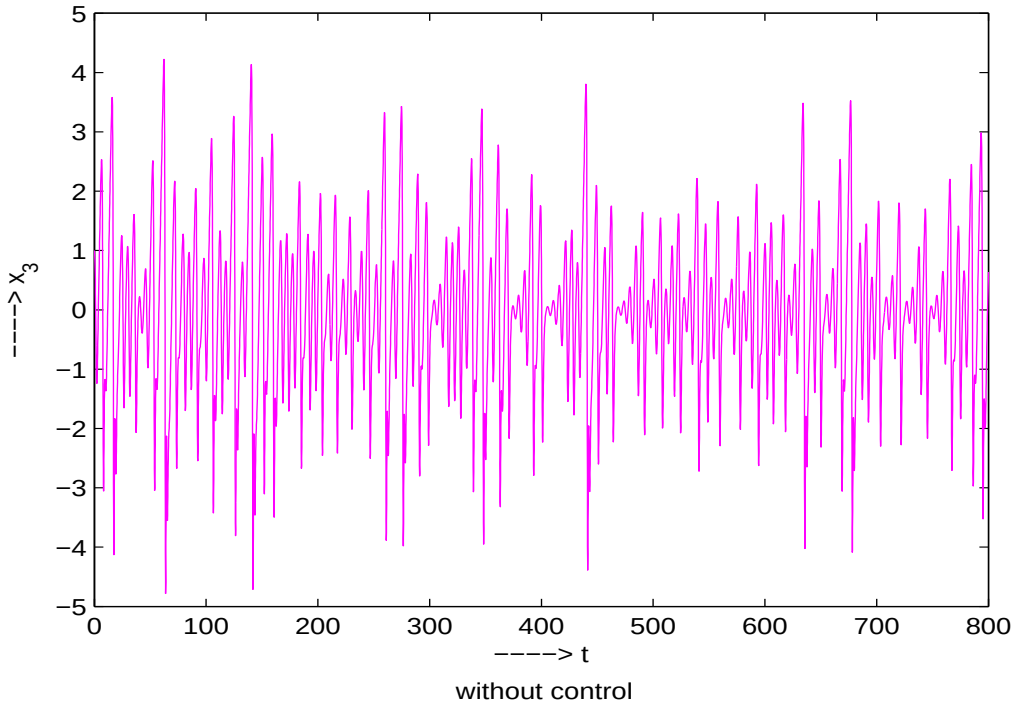

Figure 3.5: The time evolution of x_3 in uncontrolled system

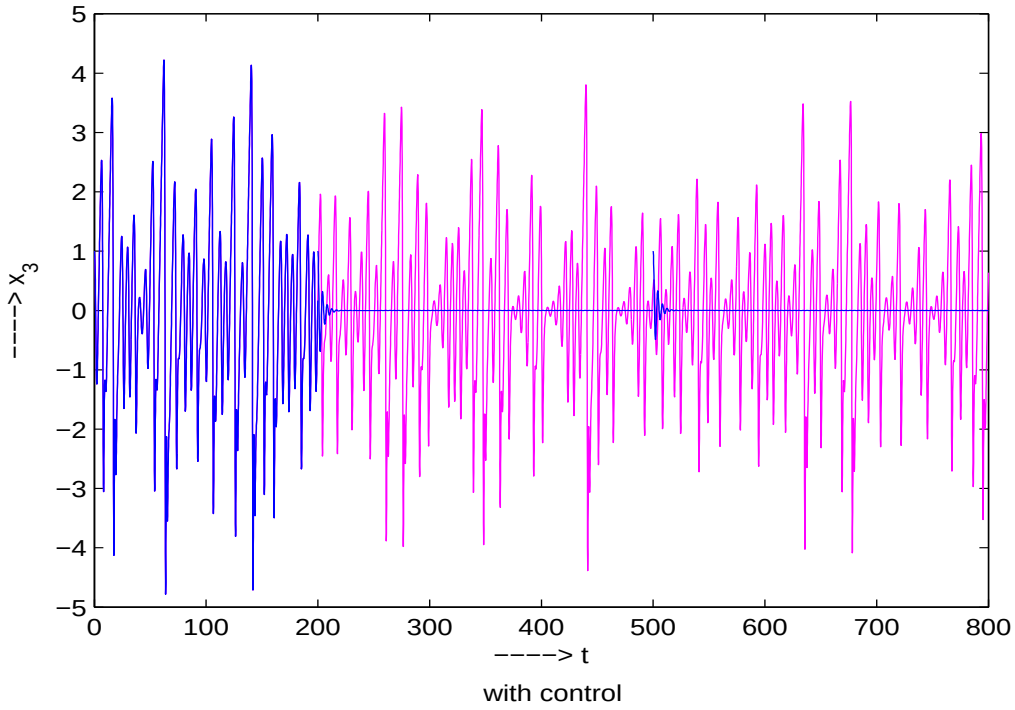

Figure 3.6: The time evolution of x_3 in controlled system

Chapter 4

Linear feedback based control of blood glucose in a modified model for glucose insulin kinetics : A theoretical study

4.1 Introduction

One of the most serious diseases that the world faces today is diabetes. Diabetes results from malfunctions in the blood glucose-insulin kinetics in the human body. Hence, a thorough understanding of the physiological process that controls the glucose insulin kinetics is necessary to devise a treatment for diabetes. It is this motivation that led to investigation of mathematical models guiding this physiological process. Thus, theoretical investigation of such mathematical models is of both theoretical and practical importance. The insight gained through theoretical investigation or numerical computation on such models might prove to be enlightening for the medical researchers working in the same field.

This field of vigorous interdisciplinary research came into being with the pioneering works of Dr. R. N.Bergman and his colleagues[11]. In biological science, frequently-sampled intravenous glucose tolerance (FSIGT) tests [35] are very popular. The test is done by injecting a single intravenous injection of glucose into a fasting human body or dog. Following this, the blood sample containing plasma glucose and plasma insulin is collected. This FSIGT test studies the behaviour of the glucose level against the insulin level in plasma. These tests were introduced by Dr. Bergman and his team in early eighties. Evaluation of the the FSIGT test data guided them to produce a mathematical model for glucose and insulin kinetics, which later came to be known as Bergman's minimal model. A version of this model is given by,

$$\begin{aligned} \dot{X} &= -p_2 X + p_3(I - I_b) \\ \dot{G} &= -XG + p_1(G_b - G) \\ \dot{I} &= \begin{cases} -n_0 I + g(G - h), & \text{if } G \geq h \\ -n_0 I, & \text{otherwise} \end{cases} \end{aligned} \tag{4.1.1}$$

subject to the initial conditions $X(0) = 0, G(0) = G_0(> 0), I(0) = I_0(> 0)$.

The variables involved have the following physical interpretation :

X is the interstitial insulin activity at time t,

G is the plasma glucose concentration at time t,

I is the plasma insulin concentration at time t,

G_b is the basal plasma glucose concentration ,

I_b is the basal plasma insulin concentration,

h is approximately the basal glucose plasma level,

n_0 is the insulin clearance fraction, p_1, p_2, p_3 and G_0 are parameters.

Recently, much complicated models incorporating a large number of variables and factoring in many more parameters have been produced and investigated. But due to their complexity, a proper theoretical study is either rendered impossible or not too enlightening. Though these models are much more accurate, they are mainly useful in the domain of computational studies. Minimal models, on the other hand, try to capture much of the major features of the dynamics within a very simple framework. Thus, minimal models are best suited for theoretical studies. According to Bergman[11] himself, this is probably the reason why so many years after their genesis, the minimal models are still being studied thoroughly.

4.2 The Modified Model for Glucose Insulin Kinetics

The model in (4.1.1) is a non-smooth dynamical system, owing to the discontinuity in the evolution equation of plasma insulin. One possible approach to study such a system is to resort to the theory of non-smooth dynamical systems. In this chapter, however, we adopt a different approach. We generate a smooth approximation of the corresponding non-smooth system by replacing the non-smooth functions with suitable smooth functions. The dynamics of I can be

written as

$$\dot{I} = -n_0 I + f(G)$$

where

$$f(G) = g\ (G - h) sgn(G - h)$$

and sgn is the signum function defined by

$$\begin{aligned} sgn(x) &= 1, \qquad x \geq 0 \\ &= 0, \qquad x < 0 \end{aligned}$$

We contend that the functional response that is widely accepted in ecological studies is an acceptable smooth approximation of the non-smooth function $f(G)$. Let us consider the function

$$f_s(G) = p\frac{G^\alpha}{h^\alpha + G^\alpha},$$

where $0 < \alpha < 1$, p is a constant. The subscript 's' in f_s stands for smooth. $f(G)$ has a discontinuous switching behaviour at h. $f_s(G)$ also displays a switching behaviour at a value h_* that is determined by α. The value of α is restricted to the open unit interval to ensure a very sharp, but smooth nonetheless, switching. $f(G)$ is 0 when $G < h$ and in keeping with this behaviour, $f_s(G)$ maintains a very negligible value when $G < h_*$. The only important modification introduced is that the function $f_s(G)$ saturates at high values of G and approaches 1 as $G \to \infty$. But the behaviour of G is linear when $G > h$. We introduce this modification with the realisation that glucose level G cannot become extremely high in a real world glucose-kinetics system. If we assume that this maximum allowable level is G_M, then we will choose

$$p = \sup_{0 \leq G \leq G_M} f(G).$$

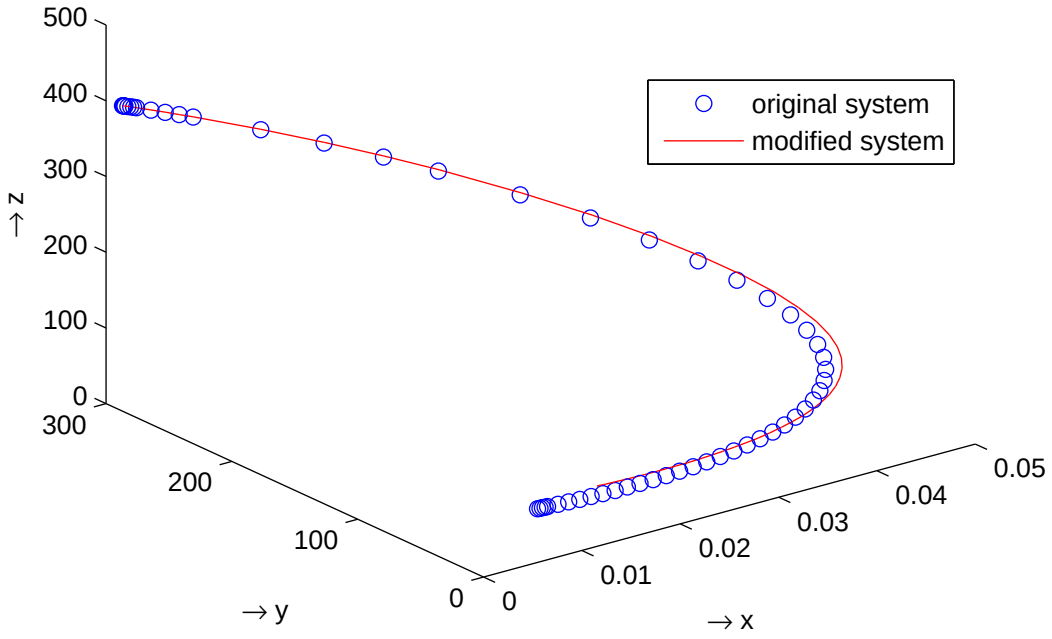

Figure 4.1: Here, $\alpha = 0.15$, $p = 1.5$, $I_b = 11$, $G_b = 92$, $h = 89.5$, $n_0 = 0.3$, $g = 0.003349$, $p_1 = 0.03082$, $p_2 = 0.02093$, $p_3 = 0.00001062$, $X = 0$, $G = Y = 287$, $I = Z = 403.4$

Along with these observations, we also present the figure (4.1) to establish that the modification of the model is justified. From the figure (4.1), we can see that the behaviour of the original dynamical system (4.1.1) is almost same as the modified dynamical system (4.2.2).

Replacing G by Y and I by Z, the modified smooth dynamical

system (4.1.1) is given by

$$\left.\begin{aligned}\dot{X} &= -p_2X + p_3(Z - I_b)\\ \dot{Y} &= -XY + p_1(G_b - Y)\\ \dot{Z} &= -n_0Z + p\frac{Y^\alpha}{h^\alpha + Y^\alpha}\end{aligned}\right\} \tag{4.2.2}$$

where $0 < \alpha < 1$, subject to the initial conditions $X(0) = 0, Y(0) = Y_0(> 0), Z(0) = Z_0(> 0)$.

To make dimensionless system, following transformations are applied:

$$\begin{gathered} x = \frac{X}{X_0}, \quad y = \frac{Y}{Y_0}, \quad z = \frac{Z}{pT_0}, \quad t = \frac{T}{T_0},\\ b = p_2T_0, \quad a = p_1T_0, \quad c = \frac{pp_3T_0^2}{X_0}, \quad d = \frac{I_b}{pT_0},\\ \mu = X_0T_0, \quad m = \frac{G_b}{Y_0}, \quad n = n_0T_0, \quad H = \frac{h}{Y_0}\end{gathered} \tag{4.2.3}$$

and system (4.2.2) takes the final form as

$$\left.\begin{aligned}\dot{x} &= -bx + c(z - d)\\ \dot{y} &= -\mu xy + a(m - y)\\ \dot{z} &= -nz + \frac{y^\alpha}{H^\alpha + y^\alpha}\end{aligned}\right\} \tag{4.2.4}$$

where $0 < \alpha < 1$

4.3 Dynamical Analysis of the Modified Model

4.3.1 Dissipativity

To study the stability of the system (4.2.4), we will first check the dissipativeness of the system (4.2.4).

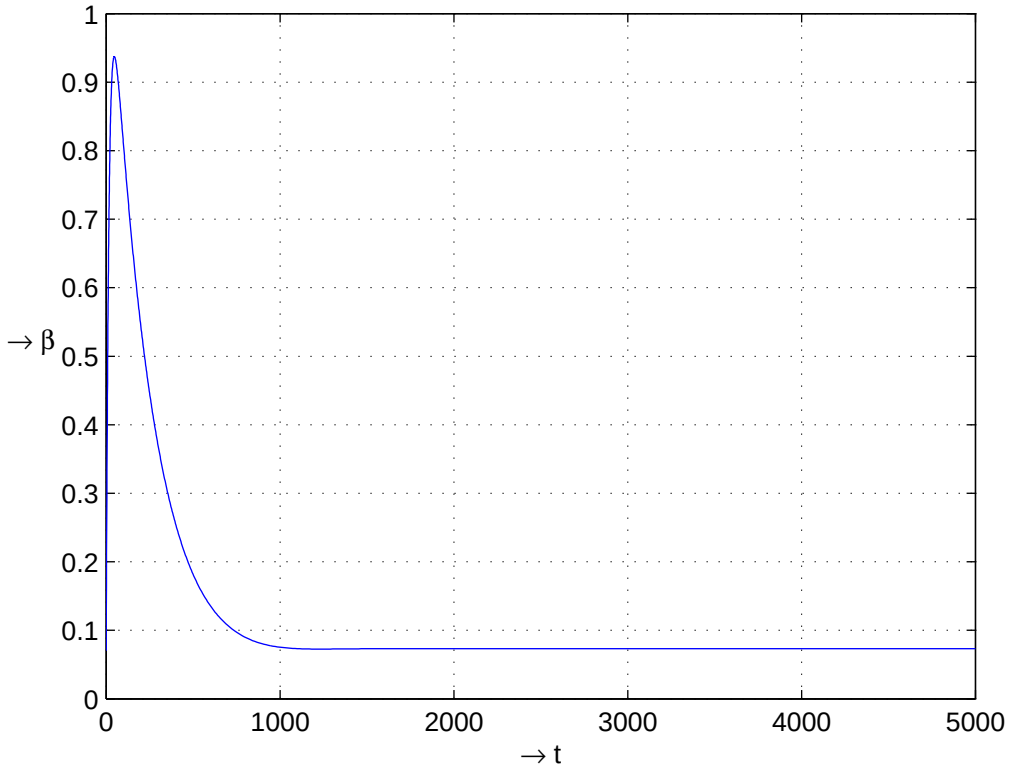

Figure 4.2: $\beta = a + b + n + \mu x, \quad p = 6.7, \quad I_b = 11, \quad G_b = 92,$ $h = 89.5, \quad n_0 = 0.3, \quad g = 0.003349, \quad \alpha = 0.05, \quad p_1 = 0.03082,$ $p_2 = 0.02093, \quad p_3 = 0.004062, \quad X = 0, \quad Y = 287, \quad Z = 403.4,$ $X_0 = 205, \quad Y_0 = 0.69, \quad Z_0 = 0.17, \quad T_0 = 0.2.$

If we set $(a + b + n + \mu x) > 0$, then system (4.2.4) is dissipative since $\frac{\partial \dot{x}}{\partial x} + \frac{\partial \dot{y}}{\partial y} + \frac{\partial \dot{z}}{\partial z} < 0$.
From the figure (4.2), one may claim that $\beta > 0$ as the time t increases where $\beta = a + b + n + \mu x$. Hence, it shows the existence of dissipativeness.

4.3.2 Equilibrium Points

Let the critical point be $E(x_*, y_*, z_*)$.

Then, $\dot{x} = 0$ gives

$$-bx_* + c(z_* - d) = 0$$

$$x_* = \frac{c(z_* - d)}{b} \tag{4.3.5}$$

Now, $\dot{y} = 0$ gives

$$-\mu x_* y_* + a(m - y_*) = 0$$

$$y_*(\mu x_* + a) = am$$

$$y_* = \frac{am}{\mu x_* + a} \tag{4.3.6}$$

From $\dot{z} = 0$, we have,

$$-nz_* + \frac{y_*^\alpha}{H^\alpha + y_*^\alpha} = 0$$

$$z_* = \frac{1}{n} . \frac{y_*^\alpha}{H^\alpha + y_*^\alpha} \tag{4.3.7}$$

Since $x_* > 0$, one gets from (4.3.5), $z_* > d$.
Also, from (4.3.7), it is easy to note that $z_* < \frac{1}{n}$.
Thus,

$$d < z_* < \frac{1}{n} \tag{4.3.8}$$

and hence

$$nd < 1. \tag{4.3.9}$$

The equation (4.3.7) also gives

$$\frac{1}{n}.\frac{y_*^\alpha}{H^\alpha + y_*^\alpha} > d$$

which implies,

$$y_*^\alpha > \frac{ndH^\alpha}{1-nd} \tag{4.3.10}$$

Again, (4.3.5) and (4.3.6) yield

$$\begin{aligned} y_* &= \frac{am}{\mu x_* + a} \\ &= \frac{am}{\mu.\frac{c(z_*-d)}{b} + a} \end{aligned}$$

Hence,

$$y_* = \frac{abm}{\mu c z_* + ab - \mu cd} \tag{4.3.11}$$

and (4.3.6) gives

$$x_* = \frac{a(m-y_*)}{\mu y_*}$$

Substituting this value of x_* in (4.3.5), one may obtain,

$$\begin{aligned} z_* &= d + \frac{bx_*}{c} \\ or, \quad z_* &= d + \frac{b}{c}.\frac{a(m-y_*)}{\mu y_*} \\ or, \quad \frac{1}{n}.\frac{y_*^\alpha}{H^\alpha + y_*^\alpha} &= \frac{(cd\mu - ab)y_* + abm}{c\mu y_*} \\ or, \quad c\mu y_*^{\alpha+1} &= (H^\alpha + y_*^\alpha)\{(cd\mu - ab)y_* + abm\}n \end{aligned} \tag{4.3.12}$$

From the equation (4.3.12), we can find out the value of y_* and hence x_* and z_*.

4.3.3 Analysis of Stability of the Equilibrium Point

In order to investigate stability of the system at $E(x_*, y_*, z_*)$, small perturbations are introduced to the system (4.2.4) by the substitution,

$$x = x' + x_*, \quad y = y' + y_*, \quad z = z' + z_*$$

where x', y', z' are very small.

Then, the system of equation(4.2.4) reduces to

$$\begin{aligned}
\dot{x'} &= -b(x' + x_*) + c\{(z' + z_*) - d\} \\
&= -bx' + cz' + [-bx_* + cz_* - cd] \\
&= -bx' + cz' + \left[-b.\frac{c(z_* - d)}{b} + cz_* - cd\right] \\
&= -bx' + cz'
\end{aligned}$$

$$\begin{aligned}
\dot{y'} &= -\mu(x' + x_*)(y' + y_*) + a\{m - (y' + y_*)\} \\
&= -\mu y_* x' - \mu x_* y' - ay' + [-\mu x_* y_* + am - ay_*] \\
&\quad (neglecting \ \ higher \ \ degree \ \ terms \ \ as \\
&\qquad x', \ \ y', \ \ z' \ \ are \ \ very \ \ small \ \ quantities) \\
&= -\mu y_* x' - (\mu x_* + a)y', \ \ using \ \ (4.3.6)
\end{aligned}$$

$$\begin{aligned}
\dot{z'} &= -n(z' + z_*) + \frac{(y' + y_*)^\alpha}{H^\alpha + (y' + y_*)^\alpha} \\
&= -nz' - nz_* + \frac{1}{1 + H^\alpha (y' + y_*)^{-\alpha}} \\
&= -nz' - nz_* + \frac{1}{1 + y_*^{-\alpha} H^\alpha \left(1 + \frac{y'}{y_*}\right)^{-\alpha}} \\
&= -nz' - nz_* + \frac{1}{1 + y_*^{-\alpha} H^\alpha \left(1 - \alpha \frac{y'}{y_*}\right)}, \quad where \quad \left|\frac{y'}{y_*}\right| < 1 \\
&\qquad\qquad and \quad neglecting \quad higher \quad order \quad terms \\
&= -nz' - nz_* + \frac{1}{(1 + y_*^{-\alpha} H^\alpha) - \alpha H^\alpha y_*^{-(\alpha+1)} y'} \\
&= -nz' - nz_* + \frac{1}{1 + y_*^{-\alpha} H^\alpha} \left[1 - \frac{y'}{\frac{1 + y_*^{-\alpha} H^\alpha}{\alpha H^\alpha y_*^{-(\alpha+1)}}}\right]^{-1} \\
&= -nz' - nz_* + \frac{1}{1 + y_*^{-\alpha} H^\alpha} \left[1 + \frac{y'}{\frac{1 + y_*^{-\alpha} H^\alpha}{\alpha H^\alpha y_*^{-(\alpha+1)}}}\right], \\
&\qquad where \quad \left|\frac{\alpha H^\alpha y_*^{-(\alpha+1)} y'}{1 + y_*^{-\alpha} H^\alpha}\right| < 1 \\
&\qquad\qquad and \quad neglecting \quad higher \quad order \quad terms \\
&= -nz' - nz_* + \frac{1}{(1 + y_*^{-\alpha} H^\alpha)^2} \left[(1 + y_*^{-\alpha} H^\alpha) + \alpha H^\alpha y_*^{-(\alpha+1)} y'\right] \\
&= -nz' + \frac{\alpha H^\alpha y_*^{-(\alpha+1)} y'}{(1 + y_*^{-\alpha} H^\alpha)^2} + \left[-nz_* + \frac{1}{1 + y_*^{-\alpha} H^\alpha}\right] \\
&= \frac{\alpha H^\alpha y_*^{-(\alpha+1)}}{(1 + y_*^{-\alpha} H^\alpha)^2} y' - nz', \quad using (4.3.7)
\end{aligned}$$

Hence, the system of equation (4.2.4) becomes

$$\left.\begin{aligned} \dot{x'} &= -bx' + cz' \\ \dot{y'} &= -\mu y_* x' - (\mu x_* + a)y' \\ \dot{z'} &= \frac{\alpha H^\alpha y_*^{-\alpha-1}}{(1 + y_*^{-\alpha} H^\alpha)^2} y' - nz' \end{aligned}\right\} \tag{4.3.13}$$

where $\alpha \in (0, 1)$

Let

$$x' = A_1 e^{\lambda t}, \quad y' = B_1 e^{\lambda t} \text{ and } z' = C_1 e^{\lambda t} \tag{4.3.14}$$

where $A_1.B_1.C_1 \neq 0$, be a solution of (4.3.13). Substituting (4.3.14), in equation (4.3.13) and eliminating A_1, B_1 and C_1, we obtain,

$$\begin{vmatrix} (\lambda + b) & 0 & -c \\ \mu y_* & (\lambda + a + \mu x_*) & 0 \\ 0 & -\frac{\alpha H^\alpha y_*^{-\alpha-1}}{(1+y_*^{-\alpha} H^\alpha)^2} & (\lambda + n) \end{vmatrix} = 0$$

or,

$$\begin{aligned} \lambda^3 + (\mu x_* + a + b + n)\lambda^2 + [(\mu x_* + a)(b + n) + bn]\lambda \\ + \left[bn(\mu x_* + a) + c\mu y_* \frac{\alpha H^\alpha y_*^{-\alpha-1}}{(1 + y_*^{-\alpha} H^\alpha)^2} \right] = 0 \end{aligned} \tag{4.3.15}$$

According to Lyapunov's fundamental theory [70, 80], the system of equations (4.2.4) will be stable if the values of λ have negative real parts. This condition on eigen values of (4.3.15) leads us to the following theorem.

Theorem 1. *The equilibrium point $E(x_*, y_*, z_*)$ of system (4.2.4) will be locally asymptotically stable if and only if*

$$\begin{aligned} n\alpha H^\alpha A\{(cd\mu - ab)A + abm\} \\ < m^2(H^\alpha + m^\alpha)(a + b)(b + n)(a + n), \end{aligned}$$

where $A^{\alpha} = \frac{ndH^{\alpha}}{1-nd}$.

Proof. By Routh-Hurwitz criteria [50], the equilibrium point $E(x_*, y_*, z_*)$ of (4.2.4) will be stable if and only if

$$\begin{aligned} \mu x_* + a + b + n &> 0, \\ (\mu x_* + a)(b + n) + bn &> 0, \\ bn(\mu x_* + a) + c\mu y_* \frac{\alpha H^{\alpha} y_*^{-\alpha-1}}{(1 + y_*^{-\alpha} H^{\alpha})^2} &> 0 \end{aligned}$$

and

$$\begin{aligned} (\mu x_* + a + b + n)\{(\mu x_* + a)(b + n) + bn\} \\ > bn(\mu x_* + a) + c\mu y_* \frac{\alpha H^{\alpha} y_*^{-\alpha-1}}{(1 + y_*^{-\alpha} H^{\alpha})^2} \end{aligned} \tag{4.3.16}$$

The first three conditions are obviously satisfied. It is the fourth condition that determines the stability criterion.

From (4.3.6),

$$\mu x_* + a = \frac{am}{y_*} \tag{4.3.17}$$

Equations (4.3.16) and (4.3.17) together will give

$$\left(\frac{am}{y_*} + b + n\right)\left\{\frac{am}{y_*}(b + n) + bn\right\} > bn.\frac{am}{y_*} + \frac{\alpha c\mu H^{\alpha} y_*^{-\alpha}}{(1 + y_*^{-\alpha} H^{\alpha})^2}$$

Simple mathematical calculation yields

$$\begin{aligned} (H^{\alpha} + y_*^{\alpha})[a^2 m^2 (b + n) + am(b + n)^2 y_* + bn(b + n)y_*^2] \\ > n\alpha H^{\alpha} y_* \{(cd\mu - ab)y_* + abm\} \end{aligned} \tag{4.3.18}$$

For $x_* > 0$, one may write from equation(4.3.5),

$$z_* > d$$

which gives

$$\mu c z_* + ab - \mu c d > ab \tag{4.3.19}$$

Then, (4.3.11) becomes,

$$y_* < m \quad \text{which gives} \quad y_*^\alpha < m^\alpha$$

Using (4.3.10), we have,

$$A^\alpha = \frac{ndH^\alpha}{1-nd} < y_*^\alpha < m^\alpha \tag{4.3.20}$$

Now, using (4.3.20), the inequality (4.3.18) reduces to

$$\begin{aligned} n\alpha H^\alpha y_*\{(cd\mu - ab)y_* + abm\} < (H^\alpha + m^\alpha)[a^2m^2(b+n) \\ + am(b+n)^2m + bn(b+n)m^2] \end{aligned}$$

or,

$$\begin{aligned} n\alpha H^\alpha A\{(cd\mu - ab)A + abm\} \\ < m^2(H^\alpha + m^\alpha)(b+n)[a^2 + a(b+n) + bn] \end{aligned}$$

or,

$$\begin{aligned} n\alpha H^\alpha A\{(cd\mu - ab)A + abm\} \\ < m^2(H^\alpha + m^\alpha)(a+b)(b+n)(a+n) \end{aligned} \tag{4.3.21}$$

The above inequality (4.3.21) gives the condition for stable situation of the dynamical system (4.2.4).

□

4.4 Control of Blood Glucose : A linear feedback based approach

The system of equation(4.2.4) becomes unstable when

$$\begin{aligned} n\alpha H^{\alpha} A\{(cd\mu - ab)A + abm\} \\ \geq m^2(H^{\alpha} + m^{\alpha})(a+b)(b+n)(a+n) \end{aligned} \tag{4.4.22}$$

Introducing the control term 'u' on the right hand side of second equation of the system (4.2.4), one may obtain,

$$\left.\begin{aligned} \dot{x} &= -bx + c(z-d) \\ \dot{y} &= -\mu xy + a(m-y) + u \\ \dot{z} &= -nz + \frac{y^{\alpha}}{H^{\alpha} + y^{\alpha}}, \quad 0 < \alpha < 1 \end{aligned}\right\} \tag{4.4.23}$$

Under small perturbations to the system(4.4.23) at $E(x_*, y_*, z_*)$ given by the transformation

$$x = \tilde{x} + x_*, \quad y = \tilde{y} + y_*, \quad z = \tilde{z} + z_*$$

the equation(4.4.23) reduces to

$$\left.\begin{aligned} \dot{\tilde{x}} &= -b\tilde{x} + c\tilde{z} \\ \dot{\tilde{y}} &= -\mu y_* \tilde{x} - (\mu x_* + a)\tilde{y} + u \\ \dot{\tilde{z}} &= \frac{\alpha H^{\alpha} y_*^{-\alpha-1}}{(1 + y_*^{-\alpha} H^{\alpha})^2}\tilde{y} - n\tilde{z}, \quad 0 < \alpha < 1 \end{aligned}\right\} \tag{4.4.24}$$

Lemma 1. *The system* (4.4.24) *is controllable.*

Proof. The system(4.4.24) can be represented in the form

$$\dot{W} = \acute{A}W + \acute{B}u \quad ,$$

where

$$\acute{A} = \begin{pmatrix} -b & 0 & c \\ -\mu y_* & -(a+\mu x_*) & 0 \\ 0 & -\frac{\alpha H^\alpha y_*^{-\alpha-1}}{(1+y_*^{-\alpha}H^\alpha)^2} & -n \end{pmatrix},$$

$$W = \begin{pmatrix} \tilde{x} \\ \tilde{y} \\ \tilde{z} \end{pmatrix} \in R^3, \quad \acute{B} = \begin{pmatrix} 0 \\ 1 \\ 0 \end{pmatrix}, \quad u \in R$$

With this choice of $\acute{A}$ and $\acute{B}$, it is easy to check that

$$\text{Rank } (\acute{B}, \acute{A}\acute{B}, \acute{A}^2\acute{B}) = 3.$$

Hence, the system (4.4.23) is controllable[5], as it satisfies the Kalman rank condition. □

Since feedback is the most natural and easily implemented control scheme, we seek a feedback control mechanism [85] to control the given system. Hence, we choose a linear feedback with x_* as control goal, which is mathematically represented by

$$u = k(x - x_*) = k\tilde{x}$$

where the feedback gain k has to be chosen properly.

Then, the system(4.4.24) becomes

$$\left.\begin{aligned} \dot{\tilde{x}} &= -b\tilde{x} + c\tilde{z} \\ \dot{\tilde{y}} &= -(\mu y_* - k)\tilde{x} - \frac{am}{y_*}\tilde{y} \\ \dot{\tilde{z}} &= \frac{\alpha H^\alpha y_*^{-\alpha-1}}{(1+y_*^{-\alpha}H^\alpha)^2}\tilde{y} - n\tilde{z}, \quad 0 < \alpha < 1 \end{aligned}\right\} \tag{4.4.25}$$

Theorem 2. *The controlled system* (4.4.25) *is locally asymptotically stable at the target equilibrium point* $E(x_*, y_*, z_*)$ *if and only if the feedback control gain* k *is chosen such that the inequality*

$$n\alpha H^\alpha \left(A - \frac{k}{\mu}\right)\{(cd\mu - ab)A + abm\} < m^2(H^\alpha + m^\alpha)(a+b)(b+n)(a+n)$$

is satisfied.

Moreover, there exists

$$k_c = \mu\left[A - \frac{m^2(H^\alpha + m^\alpha)(a+b)(b+n)(a+n)}{n\alpha H^\alpha\{(cd\mu - ab)A + abm\}}\right]$$

such that for all $k > k_c$, *the system is stable at* E.

Proof. Let $\tilde{x} = A_2 e^{\lambda_1 t}$, $\tilde{y} = B_2 e^{\lambda_1 t}$, $\tilde{z} = C_2 e^{\lambda_1 t}$.

Eliminating A_2, B_2, C_2 from (4.4.25), one gets,

$$\begin{vmatrix} (\lambda_1 + b) & 0 & -c \\ (\mu y_* - k) & \left(\lambda_1 + \frac{am}{y_*}\right) & 0 \\ 0 & -\frac{\alpha H^\alpha y_*^{-\alpha-1}}{(1+y_*^{-\alpha}H^\alpha)^2} & (\lambda_1 + n) \end{vmatrix} = 0$$

or,

$$\lambda_1^3 + \left\{\frac{am}{y_*} + b + n\right\}\lambda_1^2 + \left\{\frac{am}{y_*}(b+n) + bn\right\}\lambda_1 + \frac{abmn}{y_*} + c(\mu y_* - k)\frac{\alpha H^\alpha y_*^{-\alpha-1}}{(1+y_*^{-\alpha}H^\alpha)^2} = 0 \tag{4.4.26}$$

Therefore, the system(4.4.23) will be stable at $(x_*, \quad y_*, \quad z_*)$ if

$$\begin{aligned} \frac{am}{y_*} + b + n &> 0, \\ \frac{am}{y_*}(b+n) + bn &> 0, \\ \frac{abmn}{y_*} + c(\mu y_* - k)\frac{\alpha H^\alpha y_*^{-\alpha-1}}{(1+y_*^{-\alpha}H^\alpha)^2} &> 0 \end{aligned}$$

and

$$\begin{aligned} &\left(\frac{am}{y_*} + b + n\right)\left\{\frac{am}{y_*}(b+n) + bn\right\} \\ &\qquad > \frac{abmn}{y_*} + c(\mu y_* - k)\frac{\alpha H^\alpha y_*^{-\alpha-1}}{(1+y_*^{-\alpha}H^\alpha)^2} \end{aligned} \tag{4.4.27}$$

Using (4.3.5), (4.3.10), (4.3.11) and (4.3.12), inequality (4.4.27) reduces to

$$\begin{aligned} &n\alpha H^\alpha\left(A - \frac{k}{\mu}\right)\{(cd\mu - ab)A + abm\} \\ &\qquad < m^2(H^\alpha + m^\alpha)(a+b)(b+n)(a+n) \\ \textit{or,} \quad &n\alpha H^\alpha \Gamma < m^2 \Upsilon \end{aligned} \tag{4.4.28}$$

where $\Gamma = \left(A - \frac{k}{\mu}\right)\{(cd\mu - ab)A + abm\}$
and $\Upsilon = (H^\alpha + m^\alpha)(a+b)(b+n)(a+n)$

The inequility(4.4.28) gives the required condition for stable situation. The existence of k_c follows by an easy manipulation of the above inequality. □

4.5 Numerical Analysis and Discussions

Here, we will make three cases to discuss the stability of the dynamical system for the glucose and insulin kinetics. Using matlab

software, stability analysis of the problem is made by observing the numerical data for the respective cases.
Initially, we assume that, $p = 7.7, \quad I_b = 11, \quad G_b = 92, \quad h = 89.5,$
$n_0 = 0.3, \quad g = 0.003349, \quad X = 0, \quad Y = 287, \quad Z = 403.4,$
$X_0 = 355, \quad Y_0 = 0.97, \quad Z_0 = 0.17, \quad T_0 = 0.13.$

Case-I : Let us take, $p_1 = 0.02032, \quad p_2 = 0.01093, \quad p_3 = 0.01341.$ Then, with the help of (4.2.3), one may find the parameters value of the system (4.4.23).

From Table-1, one may observe that the dynamical system (4.4.25) is stable for $\alpha \in (0, 0.48]$. In this interval, the stability of the system is independent of the control variable u (i.e., $k = 0$). But if we take, $\alpha \geq 0.49$, the system without control becomes unstable. In this situation, control is to be activated.

Table-1

k_0	α	$n\alpha H^\alpha \Gamma$	$m^2\Upsilon$	Status
0.000	0.48	1.0528	1.0867	stable
0.000	0.49	1.1523	1.1371	unstable
0.032	0.49	1.1367	1.1371	stable
0.032	0.50	1.2426	1.1899	unstable
0.133	0.50	1.1895	1.1899	stable
0.133	0.51	1.2992	1.2452	unstable
0.229	0.51	1.2447	1.2452	stable
0.229	0.52	1.3585	1.3030	unstable
0.320	0.52	1.3028	1.3030	stable
0.320	0.53	1.4208	1.3635	unstable
0.407	0.53	1.3634	1.3635	stable
0.407	0.54	1.4858	1.4268	unstable
0.491	0.54	1.4262	1.4268	stable

continued on next page

Table-1 (continued)

k_0	α	$n\alpha H^{\alpha}\Gamma$	$m^2\Upsilon$	Status
0.491	0.55	1.5532	1.4930	unstable
0.570	0.55	1.4928	1.4930	stable
0.570	0.56	1.6246	1.5624	unstable
0.646	0.56	1.5622	1.5624	stable
0.646	0.57	1.6991	1.6349	unstable
0.719	0.57	1.6346	1.6349	stable
...	...	...	...	...
...	...	...	...	...
...	...	...	...	...
2.277	0.97	10.0358	10.0445	stable
2.277	0.98	10.7555	10.5109	unstable
2.298	0.98	10.5040	10.5109	stable
2.298	0.99	11.2549	10.9990	unstable
2.319	0.99	10.9883	10.9990	stable

To set up the dynamical system in a stable form for $\alpha = 0.49$, we have to consider $k_0 = 0.032$, where $k_0 = k \times 10^{-3}$. But when α reaches the value 0.50, the system becomes unstable with $k_0 = 0.032$. In this case, the stability of the system is made by choosing $k_0 = 0.133$.

It is interesting to see that the system is unstable again with $k_0 = 0.133$ if we take $\alpha = 0.51$. In this situation, from Table-1, we can say that the system is stable if $k_0 = 0.229$.

In case of $\alpha = 0.52$, we have got the stable system if $k_0 = 0.32$ and so on.

By choosing $k_0 = 2.319$, the system is always stable when $0 < \alpha < 1$.

Figure (4.3) and figure (4.4) represent the evolution curve of x and z with respect to time respectively.

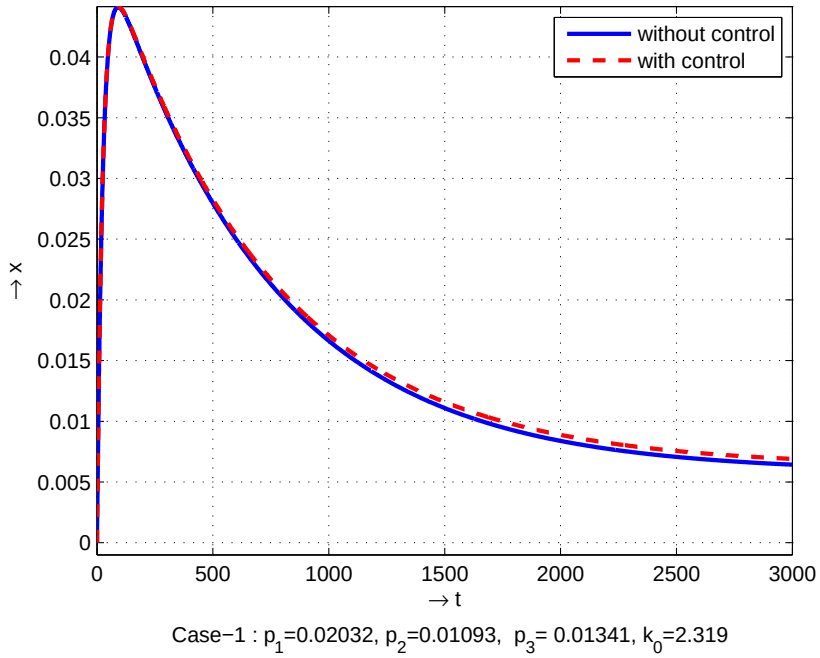

Figure 4.3: Evolution of x in time

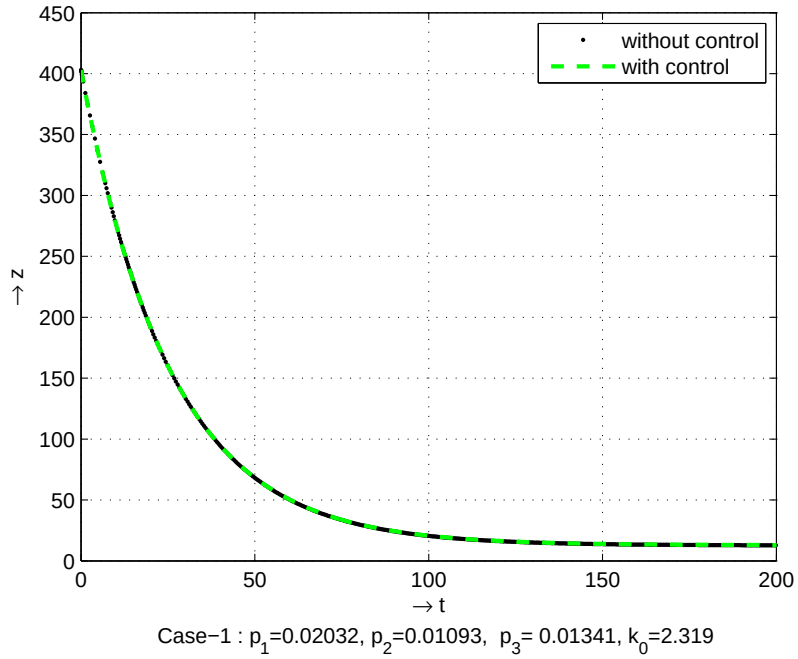

Figure 4.4: Evolution of z in time

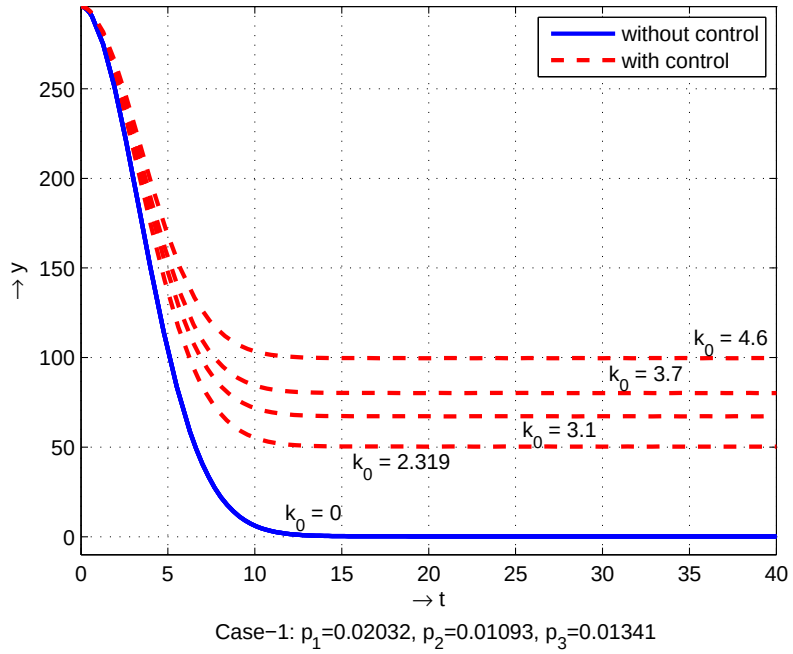

Figure 4.5: Evolution of y in time

To show the controlled glucose level, we have drawn the figure (4.5). This figure gives us a brief idea for making a control dynamical system from an unstable situation. One may set the glucose level by increasing or decreasing the control parameter k_0 as per requirement.

Case-II : We now consider, $p_1 = 0.02032$, $p_2 = 0.01093$, $p_3 = 0.05405$.

Here, the system is stable without control variable when $0 < \alpha \leq 0.28$. If we consider $\alpha = 0.29$, we have to activate the control variable. But in the previous case, we have considered the control term for $\alpha = 0.49$.

In this case, for $\alpha = 0.29$, the stability of the system can be attained with $k_0 = 0.115$.

When $\alpha = 0.30$, we have to consider $k_0 = 0.262$. In case of $k_0 \leq 0.261$, the stability condition (4.4.28) is not satisfied for $\alpha = 0.30$.

Table-2 shows that the system is stable always for any values of $\alpha(\in (0,1))$ if one may assume $k_0 = 2.970$.

Table-2

k_0	α	$n\alpha H^{\alpha}\Gamma$	$m^2\Upsilon$	Status
0.000	0.28	0.4251	0.4384	stable
0.000	0.29	0.4945	0.4588	unstable
0.115	0.29	0.4585	0.4588	stable
0.115	0.30	0.5315	0.4801	unstable
0.262	0.30	0.4800	0.4801	stable
0.262	0.31	0.5553	0.5024	unstable
0.398	0.31	0.5021	0.5024	stable
0.398	0.32	0.5798	0.5257	unstable
0.523	0.32	0.5255	0.5257	stable
0.523	0.33	0.6057	0.5501	unstable
0.639	0.33	0.5498	0.5501	stable
0.639	0.34	0.6327	0.5756	unstable
0.747	0.34	0.5752	0.5756	stable
0.747	0.35	0.6610	0.6024	unstable
0.847	0.35	0.6022	0.6024	stable
0.847	0.36	0.6910	0.6303	unstable
0.941	0.36	0.6302	0.6303	stable
0.941	0.37	0.7222	0.6596	unstable
1.030	0.37	0.6589	0.6596	stable
1.030	0.38	0.7542	0.6902	unstable
1.113	0.38	0.6895	0.6902	stable
1.113	0.39	0.7883	0.7223	unstable
1.191	0.39	0.7217	0.7223	stable
1.191	0.40	0.8242	0.7558	unstable
1.265	0.40	0.7552	0.7558	stable
1.265	0.41	0.8616	0.7909	unstable

continued on next page

Table-2 (**continued**)

k_0	α	$n\alpha H^{\alpha}\Gamma$	$m^2\Upsilon$	Status
1.335	0.41	0.7903	0.7909	stable
1.335	0.42	0.9008	0.8276	unstable
1.401	0.42	0.8275	0.8276	stable
1.401	0.43	0.9423	0.8660	unstable
1.465	0.43	0.8650	0.8660	stable
1.465	0.44	0.9841	0.9063	unstable
1.525	0.44	0.9054	0.9063	stable
1.525	0.45	1.0292	0.9483	unstable
1.582	0.45	0.9479	0.9483	stable
1.582	0.46	1.0766	0.9924	unstable
1.637	0.46	0.9916	0.9924	stable
1.637	0.47	1.1253	1.0384	unstable
1.689	0.47	1.0382	1.0384	stable
1.689	0.48	1.1773	1.0867	unstable
1.740	0.48	1.0849	1.0867	stable
1.740	0.49	1.2294	1.1371	unstable
1.788	0.49	1.1353	1.1371	stable
...	...	...	...	...
...	...	...	...	...
...	...	...	...	...
2.919	0.95	9.1711	9.1729	stable
2.919	0.96	10.1538	9.5989	unstable
2.932	0.96	9.5958	9.5989	stable
2.932	0.97	10.6203	10.0445	unstable
2.945	0.97	10.0286	10.0445	stable
2.945	0.98	11.0961	10.5109	unstable
2.958	0.98	10.4687	10.5109	stable
2.958	0.99	11.5802	10.9990	unstable
2.970	0.99	10.9663	10.9990	stable

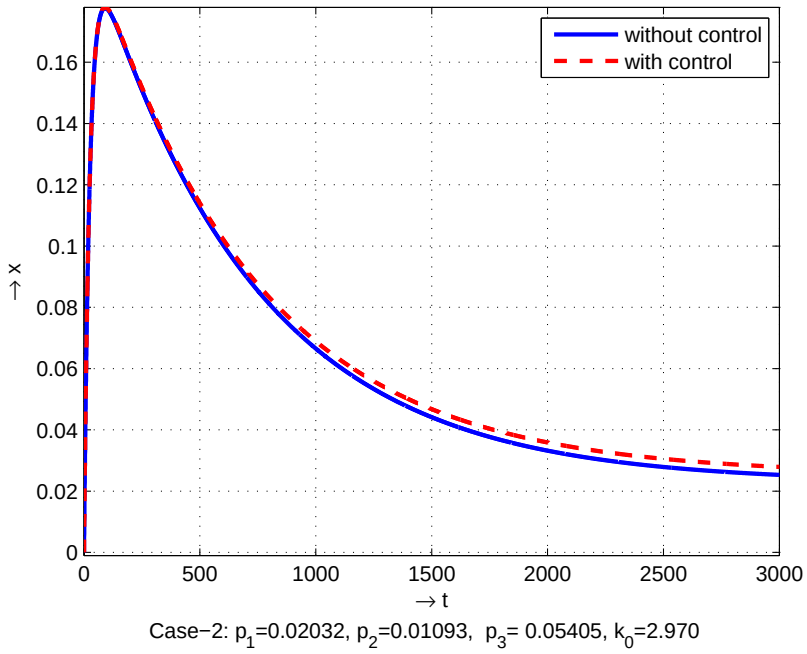

Figure 4.6: Evolution of x in time

We have shown the graph of x and z with respect to time in figure (4.6) and figure (4.7) respectively. Figure (4.8) represents the behaviour of glucose level as the time increases.

Here, different values of k_0 have been taken to show the necessity of the control term. It is clear from the figure (4.8) that one may control the behaviour of glucose level by adjusting the control parameter.

Case-III : Let us take, $p_1 = 0.02032$, $p_2 = 0.01093$, $p_3 = 0.7967$.

In the earlier two cases, we have observed that the system becomes stable for any value of $\alpha(\in (0, 1))$ if $k_0 = 2.319$ and $k_0 = 2.97$ respectively.

At the present case, by choosing $k_0 = 2.970$, the system becomes unstable if $\alpha \geq 0.82$.

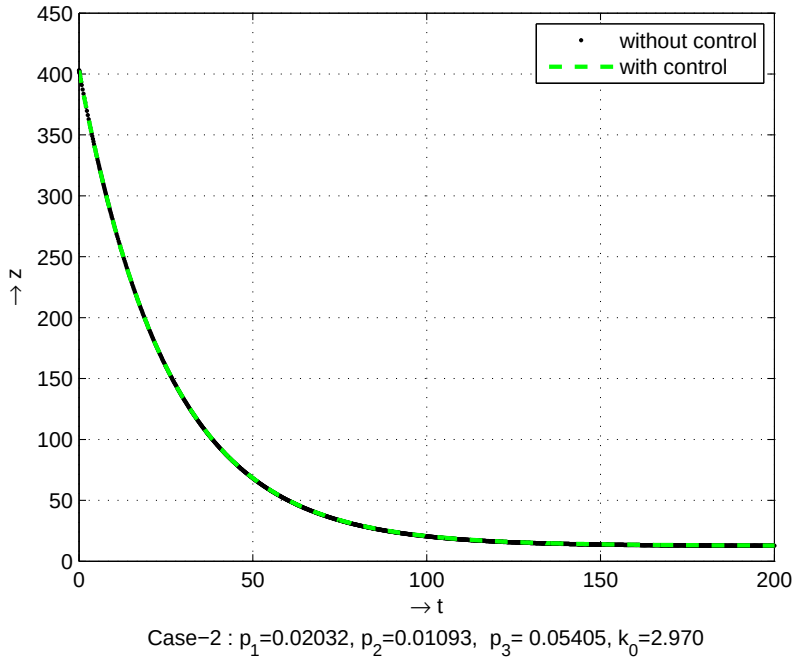

Figure 4.7: Evolution of z in time

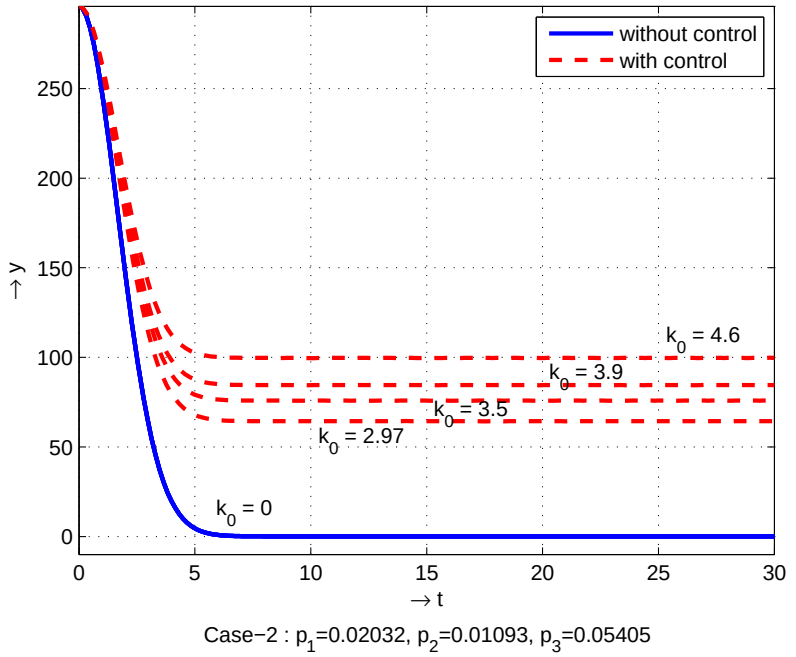

Figure 4.8: Evolution of y in time

To obtain the stable dynamical system again, one may have to satisfy the stability condition (4.4.28) for $\alpha = 0.82$ by taking $k_0 = 2.98$. If we assume $k_0 = 3.17$, the dynamical system remains stable for $0 < \alpha < 1$ which have shown in Table-3.

Table-3

k_0	α	$n\alpha H^{\alpha}\Gamma$	$m^2\Upsilon$	Status
0.000	0.14	0.2129	0.2322	stable
0.000	0.15	0.3139	0.2430	unstable
0.142	0.15	0.2427	0.2430	stable
0.142	0.16	0.3556	0.2543	unstable
0.303	0.16	0.2540	0.2543	stable
0.303	0.17	0.3752	0.2661	unstable
0.443	0.17	0.2660	0.2661	stable
0.443	0.18	0.3971	0.2785	unstable
0.568	0.18	0.2784	0.2785	stable
0.568	0.19	0.4206	0.2914	unstable
0.682	0.19	0.2906	0.2914	stable
0.682	0.20	0.4451	0.3049	unstable
0.786	0.20	0.3041	0.3049	stable
0.786	0.21	0.4720	0.3191	unstable
0.882	0.21	0.3190	0.3191	stable
0.882	0.22	0.5014	0.3339	unstable
0.973	0.22	0.3322	0.3339	stable
0.973	0.23	0.5297	0.3494	unstable
1.057	0.23	0.3488	0.3494	stable
1.057	0.24	0.5627	0.3656	unstable
1.137	0.24	0.3646	0.3656	stable
1.137	0.25	0.5955	0.3826	unstable
1.213	0.25	0.3803	0.3826	stable
1.213	0.26	0.6289	0.4004	unstable
1.284	0.26	0.4002	0.4004	stable
1.284	0.27	0.6678	0.4190	unstable

continued on next page

Table-3 (continued)

k_0	α	$n\alpha H^{\alpha}\Gamma$	$m^2\Upsilon$	Status
1.353	0.27	0.4163	0.4190	stable
...	...	...	...	...
...	...	...	...	...
...	...	...	...	...
2.967	0.81	4.6689	4.8591	stable
2.967	0.82	8.4974	5.0847	unstable
2.980	0.82	4.9553	5.0847	stable
2.980	0.83	8.9503	5.3208	unstable
2.993	0.83	5.1832	5.3208	stable
...	...	...	...	...
...	...	...	...	...
...	...	...	...	...
3.131	0.95	8.7291	9.1729	stable
3.131	0.96	15.5450	9.5989	unstable
3.141	0.96	9.2194	9.5989	stable
3.141	0.97	16.3263	10.0445	unstable
3.151	0.97	9.6183	10.0445	stable
3.151	0.98	17.0215	10.5109	unstable
3.161	0.98	9.9092	10.5109	stable
3.161	0.99	17.6135	10.9990	unstable
3.170	0.99	10.8277	10.9990	stable

Similar to the previous cases, we have drawn the evolution of x, y and z in time in figure (4.9), figure (4.10) and figure (4.11) respectively. The dotted line means the system is under controlled.

Hence, from the above work out, we may conclude that the stable system is obtained for a specific range of α with appropriate value of the control term. As we increase the value of α, we have to fix the value of k_0 for which the expression (4.4.28) is satisfied and the

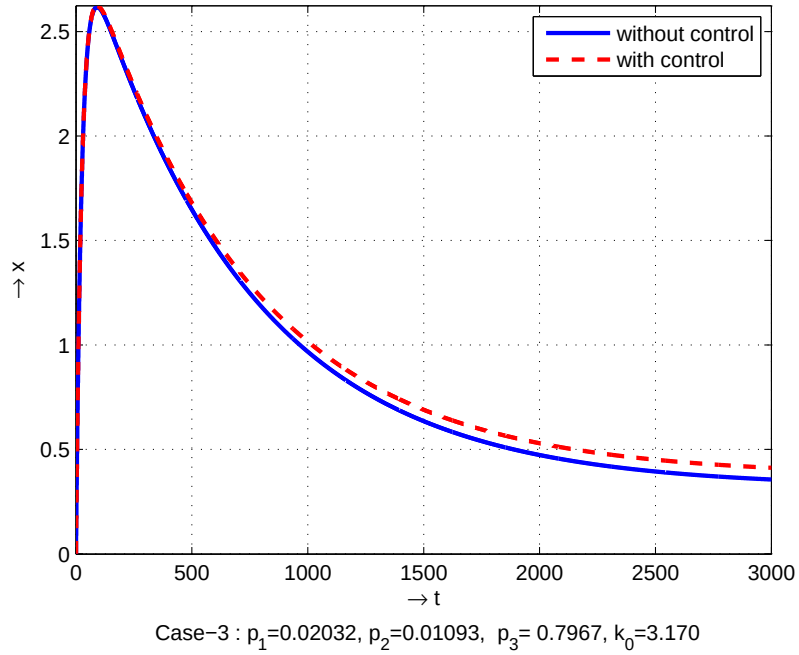

Figure 4.9: Evolution of x in time

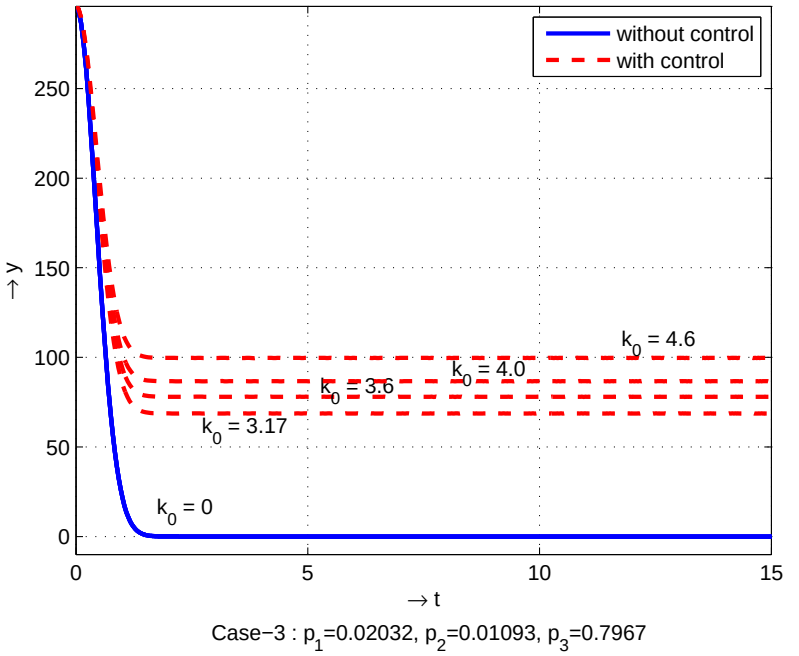

Figure 4.10: Evolution of y in time

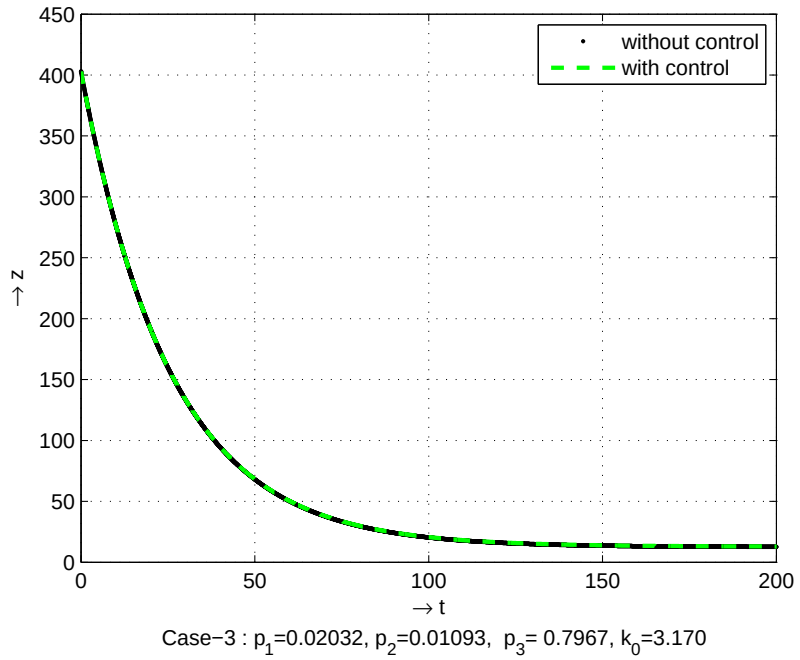

Figure 4.11: Evolution of z in time

system becomes stable from unstable situation.

From the above three cases, we have also seen that the stability of the system depends on the parameters α as well as c in terms of p_3 which have been shown by figure(4.12). In the first case, when we have chosen $p_3 = 0.01341$, the stability of the system is attained if $k_0 = 2.319$. But in case-II, we have taken $k_0 = 2.970$ to meet the stability condition (4.4.28) with $p_3 = 0.05405$. For the last case, by choosing $p_3 = 0.7967$, we have reached the stable situation if $k_0 = 3.17$ for $\alpha \in (0, 1)$.

Hence, it is observed that the newly remodelled dynamical system for glucose and insulin kinetics may be controlled with the addition of a control term on the right hand side of the second equation of the system (4.2.4).

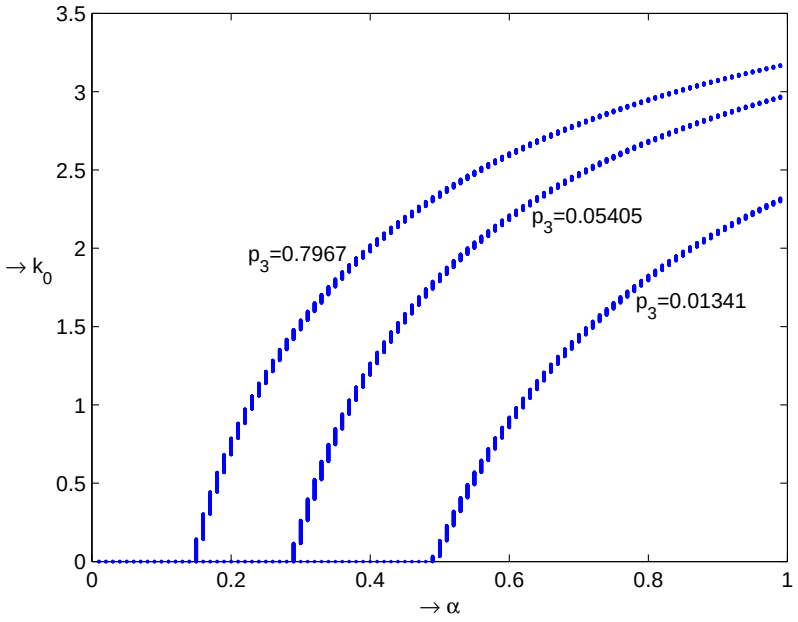

Figure 4.12: α vs k_0

4.6 Conclusion

In this chapter, we have studied a minimal model for glucose-insulin kinetics model theoretically and proposed a blood glucose control mechanism. The study is of interest to both practical and theoretical fields as diabetes is rapidly becoming a serious disease world wide and hence, investigation of the physiological process involving blood glucose and insulin is gaining interest. The original minimal model (4.1.1), which is a non-smooth dynamical system, has been modified by replacing the non-smooth function with a smooth approximation of the same. The resulting smooth system has been investigated for its steady states and the stability properties of the system in the neighbourhood of the steady states. In the event where the auto-regulatory mechanism for blood glucose control fails, we consider a

simple but elegant linear feedback based scheme for blood glucose control. The critical value of the control parameter is determined. For feedback gain beyond this value, it is guaranteed that the blood glucose level will remain under control even if the self regulatory system of the body fails. In the numerical simulation, we test the model under different parameter sets. Assuming different values for the feedback gain, we determine ranges for the physiological parameter α (introduced while smoothing the non-smooth system) over which the particular value of feedback gain will work. Such information is of value to medical practitioners and pharmacists. Finally, it is also shown that beyond the critical value, the system always remains controlled. The scope of future work lies in better approximation of the non-smooth system with smooth systems and investigation of advanced and robust control methods for controlling blood glucose.

Chapter 5

Complete Synchronization of Chaos via Hybrid Feedback and Tracking Control Algorithm

5.1 Introduction

At present, there are so many methods to control chaos, for example, non-linear feedback control method [64], adaptive control method [46, 81, 68, 16], active control method [1], backstepping design method [92] etc. Last twenty years, the ideas of chaos synchronization have been developed by many scientists, namely, Pecora and Carroll [65], Sun and Cao [81], Poria and Tarai [68], Lu and Chen [16] et. al. and so on. In a mathematical sense, if $\lim_{t\to\infty} |x_i(t) - y_i(t)| = 0$ for $i = 1, 2, 3, ..., n$ with the initial conditions $(x_1(0), x_2(0), ..., x_n(0))$ and $(y_1(0), y_2(0), ..., y_n(0))$ where $(x_1, x_2, ..., x_n)$ and $(y_1, y_2, ..., y_n)$ are the state variables of the first (drive) and second (response) systems respectively, then we can say, the two systems are synchronized.

In this communication, we study the synchronization of coupled Sprott model L via hybrid feedback control method [60] and also via

tracking control method [60]. The study is supported by numerical simulation.

5.2 Description of the Hybrid Feedback Controller

Any non-linear dynamical system can be written as

$$\dot{x} = Ax + B[\phi(x)] \tag{5.2.1}$$

where $x \in \mathbb{R}^n, A \in \mathbb{R}^{n\times n}, B \in \mathbb{R}^{n\times n}, \phi : \mathbb{R}^n \to \mathbb{R}^n$ is non-linear vector function.
We consider a new dynamical system which is coupled with the system (5.2.1) as given below :

$$\dot{y} = Ay + B[\phi(y) + u] \tag{5.2.2}$$

where u is the controller which controls the motion of the system (5.2.2).
We also consider a error term e defined as

$$\begin{aligned} e &= (e_1, e_2, e_3, ..., e_n)^T \\ &= (x_1 - y_1, x_2 - y_2, x_3 - y_3, ..., x_n - y_n)^T, \end{aligned}$$

where $x = (x_1, x_2, x_3, ..., x_n)^T$,
$y = (y_1, y_2, y_3, ..., y_n)^T$.

Subtracting (5.2.2) from (5.2.1), one easily gets the dynamical systems of synchronization error as

$$\dot{e} = (A - BK)e \tag{5.2.3}$$

where K is a scalar matrix.

In case of identical synchronization of the two systems (5.2.1) and (5.2.2), the feedback controller u must be chosen appropriately.
Let us take, $u = u_1 + u_2$ such that

$$\left.\begin{aligned} u_1 &= \phi(x) - \phi(y) \\ u_2 &= K(x - y) \end{aligned}\right\} \tag{5.2.4}$$

where $K = \begin{pmatrix} k_1 & 0... & 0 \\ 0 & k_2... & 0 \\ ... & ... & ... \\ ... & ... & ... \\ 0 & 0... & k_n \end{pmatrix}$ is the feedback matrix.

Clearly, u_1 is a non-linear controller and u_2 is a linear controller, so u is the hybrid controller.

Hence, by Yang. et. al [90], the error system (5.2.3) is asymptotically stable at origin if all the eigen values of the matrix $(A - BK)$ has negative real parts.

Then, the two systems (5.2.1) and (5.2.2) are identically synchronized.

5.3 Chaos Synchronization of Sprott Model L via Hybrid Feedback Control

The Sprott Model L [49] is a given by

$$\left.\begin{aligned} \dot{x_1} &= x_2 + \alpha x_3 \\ \dot{x_2} &= \beta x_1^2 - x_2 \\ \dot{x_3} &= \gamma - x_1 \end{aligned}\right\} \tag{5.3.5}$$

where α, β, γ are positive constants.
Sprott found that the system (5.3.5) is chaotic if $\alpha = 3.9, \quad \beta = 0.9, \quad \gamma = 1$.

The system (5.3.5) can be written as

$$\dot{x} = Ax + B[\phi(x)]$$

where

$$x = \begin{pmatrix} x_1 \\ x_2 \\ x_3 \end{pmatrix}, \quad A = \begin{pmatrix} 0 & 1 & \alpha \\ 0 & -1 & 0 \\ -1 & 0 & 0 \end{pmatrix},$$

$$B = \begin{pmatrix} 1 & 0 & 1 \\ 0 & \beta & 0 \\ \gamma & 0 & 0 \end{pmatrix}, \quad \phi(x) = \begin{pmatrix} 1 \\ x_1^2 \\ -1 \end{pmatrix}$$

Therefore,

$$A - BK = \begin{pmatrix} -k_1 & 1 & \alpha - k_3 \\ 0 & -(1 + \beta k_2) & 0 \\ -(1 + \gamma k_1) & 0 & 0 \end{pmatrix},$$

where

$$k = \begin{pmatrix} k_1 & 0 & 0 \\ 0 & k_2 & 0 \\ 0 & 0 & k_3 \end{pmatrix}$$

To make all the eigen values of $(A - BK)$ are negative,
we consider $k_1 = 15, k_2 = 5, k_3 = 3$.

Now, using(5.2.4), we get,

$$u_1 = \begin{pmatrix} 0 \\ x_1^2 - y_1^2 \\ 0 \end{pmatrix},$$

and

$$u_2 = \begin{pmatrix} k_1(x_1 - y_1) \\ k_2(x_2 - y_2) \\ k_3(x_3 - y_3) \end{pmatrix}$$

Therefore,

$$u = \begin{pmatrix} k_1(x_1 - y_1) \\ x_1^2 - y_1^2 + k_2(x_2 - y_2) \\ k_3(x_3 - y_3) \end{pmatrix}$$

Then,

$$u + \phi(y) = \begin{pmatrix} k_1(x_1 - y_1) + 1 \\ x_1^2 + k_2(x_2 - y_2) \\ k_3(x_3 - y_3) - 1 \end{pmatrix}$$

Therefore, the response system(5.2.2) is given by,

$$\dot{y} = Ay + B[\phi(y) + u]$$

$$\begin{pmatrix} \dot{y_1} \\ \dot{y_2} \\ \dot{y_3} \end{pmatrix} = \begin{pmatrix} 0 & 1 & \alpha \\ 0 & -1 & 0 \\ -1 & 0 & 0 \end{pmatrix} \begin{pmatrix} y_1 \\ y_2 \\ y_3 \end{pmatrix} + \begin{pmatrix} k_1(x_1 - y_1) + k_3(x_3 - y_3) \\ \beta[x_1^2 + k_2(x_2 - y_2)] \\ \gamma[k_1(x_1 - y_1) + 1] \end{pmatrix}$$

It yields

$$\left.\begin{aligned} \dot{y_1} &= y_2 + \alpha y_3 + k_1(x_1 - y_1) + k_3(x_3 - y_3) \\ \dot{y_2} &= -y_2 + \beta x_1^2 + k_2\beta(x_2 - y_2) \\ \dot{y_3} &= -y_1 + \gamma + k_1\gamma(x_1 - y_1) \end{aligned}\right\} \tag{5.3.6}$$

5.3.1 Numerical Simulation

Let us take $x(0) = (1, 1.1, -0.231)$ and $y(0) = (1, 0, 1)$ as the initial conditions for the system (5.3.5) and (5.3.6) respectively.

We consider also the initial condition for the synchronization error as $e(0) = (1, 1, 0)$.

Figure (5.1), figure (5.2) and figure (5.3) represent the trajectories of the driving system and the responding system.

Figure (5.4) represents the synchronization error with respect to time. From figure (5.4), we can easily say that the synchronization error goes to zero after some time. Hence, we achieved the identical synchronization between the system (5.3.5) and system (5.3.6).

5.4 Chaos Synchronization of Sprott Model L via Tracking Control

We consider the non-linear dynamical system (5.3.5) as the driving system to apply tracking control method.
Then, the system (5.3.5) can be written as

$$\dot{x} = Ax + B[\phi(x)] \tag{5.4.7}$$

where

$$x = \begin{pmatrix} x_1 \\ x_2 \\ x_3 \end{pmatrix}, \quad A = \begin{pmatrix} 0 & 1 & \alpha \\ 0 & -1 & 0 \\ -1 & 0 & 0 \end{pmatrix},$$

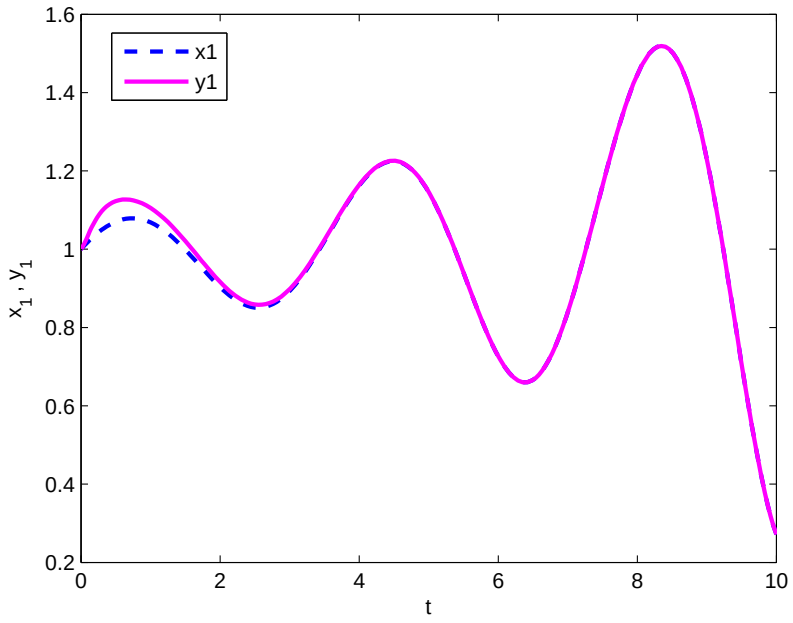

Figure 5.1: Time history of x_1 and y_1

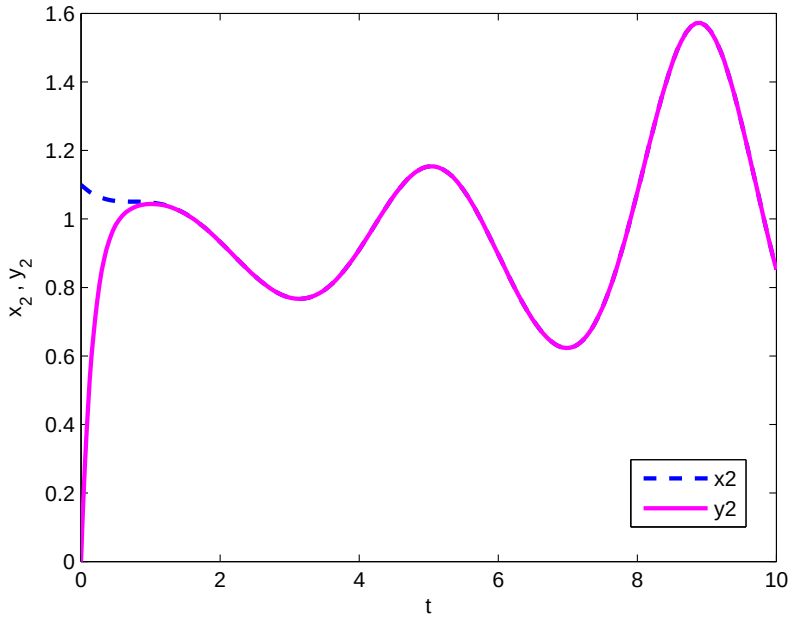

Figure 5.2: Time history of x_2 and y_2

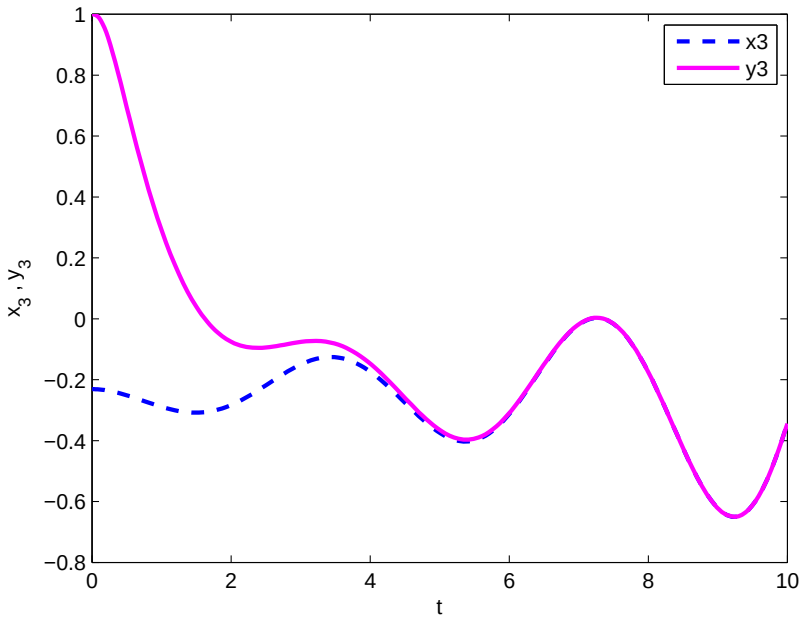

Figure 5.3: Time history of x_3 and y_3

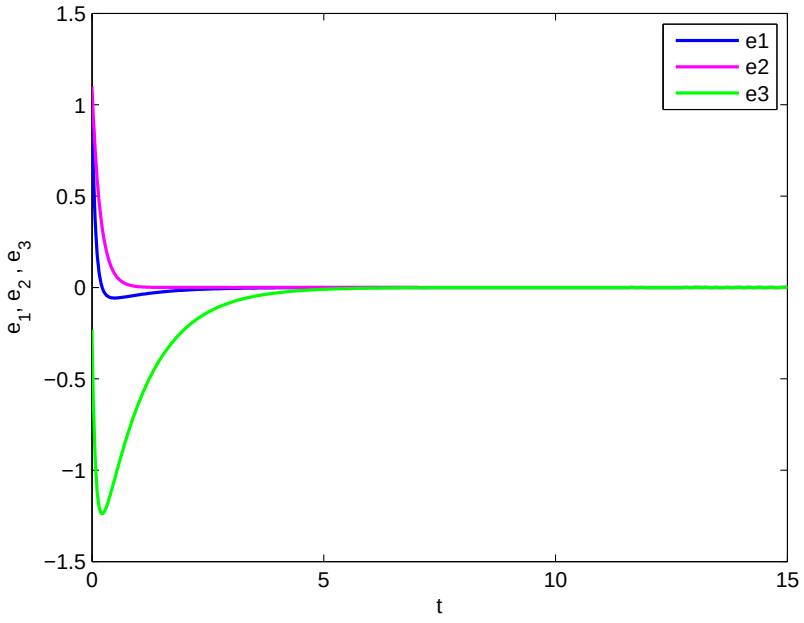

Figure 5.4: Time evolution of synchronization error e

$$B = \begin{pmatrix} 1 & 0 & 1 \\ 0 & \beta & 0 \\ \gamma & 0 & 0 \end{pmatrix}, \quad \phi(x) = \begin{pmatrix} 1 \\ x_1^2 \\ -1 \end{pmatrix}$$

Let us consider the response system as given below

$$\dot{y} = Ay + B[\phi(y)] + U' \tag{5.4.8}$$

where $U' = (u_1', u_2', u_3')^T \in \mathbb{R}^3$ is the control variable and $y \in \mathbb{R}^3$ denote the state variables of the response system.

Hence, the response system can be written as

$$\left.\begin{aligned} \dot{y_1} &= y_2 + \alpha y_3 + u_1' \\ \dot{y_2} &= \beta y_1^2 - y_2 + u_2' \\ \dot{y_3} &= \gamma - y_1 + u_3' \end{aligned}\right\} \tag{5.4.9}$$

Let us take the synchronization error e as

$$e_i = y_i - x_i, \quad i = 1, 2, 3.$$

Therefore, the error system is given by,

$$\left.\begin{aligned} \dot{e_1} &= e_2 + \alpha e_3 + u_1' \\ \dot{e_2} &= \beta y_1^2 - \beta x_1^2 - e_2 + u_2' \\ \dot{e_3} &= -e_1 + u_3' \end{aligned}\right\} \tag{5.4.10}$$

Let us consider Lyapunov function $V(e) = \frac{1}{2}e^T e$, where V(e) is a positive definite function.

If the controllers are chosen in the following way

$$\left.\begin{aligned} u_1' &= -e_1 - e_2 - \alpha e_3 \\ u_2' &= -\beta y_1^2 + \beta x_1^2 \\ u_3' &= e_1 - e_3 \end{aligned}\right\} \tag{5.4.11}$$

then, the error dynamical system (5.4.10) reduces to

$$\dot{e} = He, \qquad \text{where} \quad e = (e_1, e_2, e_3)^T$$

and

$$H = \begin{pmatrix} -1 & 0 & 0 \\ 0 & -1 & 0 \\ 0 & 0 & -1 \end{pmatrix}$$

Therefore, $\dot{V}(e) < 0$. Hence, $||e(t)|| \to 0$ as $t \to \infty$. Thus the synchronization is achieved globally and asymptotically.

5.4.1 Numerical Simulation

Here, we consider the initial conditions of the system (5.4.7) and (5.4.9) as x(0)= (1, 1.1, -0.231) and y(0) = (1, 0, 1). We choose the value of parameters as $\alpha = 3.9, \beta = 0.9, \gamma = 1$. The error system initializes as e(0) = (1, 1, 0). Figure (5.5), figure (5.6) and figure (5.7) represent the trajectories of the x_i, state variable of driving system and y_i, state variable of the responding system, for $i = 1, 2, 3$. We plot the time evolution of the synchronization errors in Figure (5.8). In this figure, it is observed that all the errors go to zero after certain time.

Therefore, the synchronization is established between the systems.

5.5 Conclusions

The two methods, hybrid feedback control and the tracking control are successfully applied to chaotic Sprott Model L and we have found

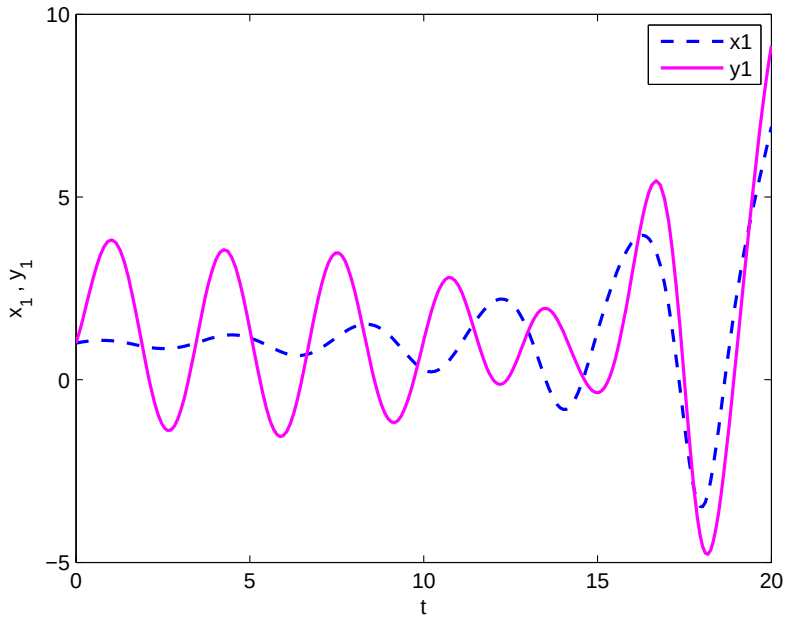

Figure 5.5: Time history of x_1 and y_1

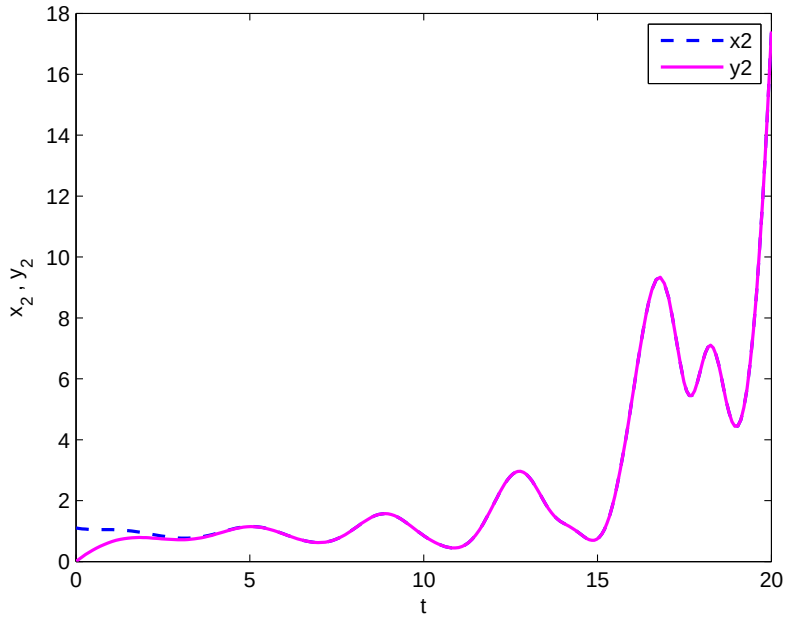

Figure 5.6: Time history of x_2 and y_2

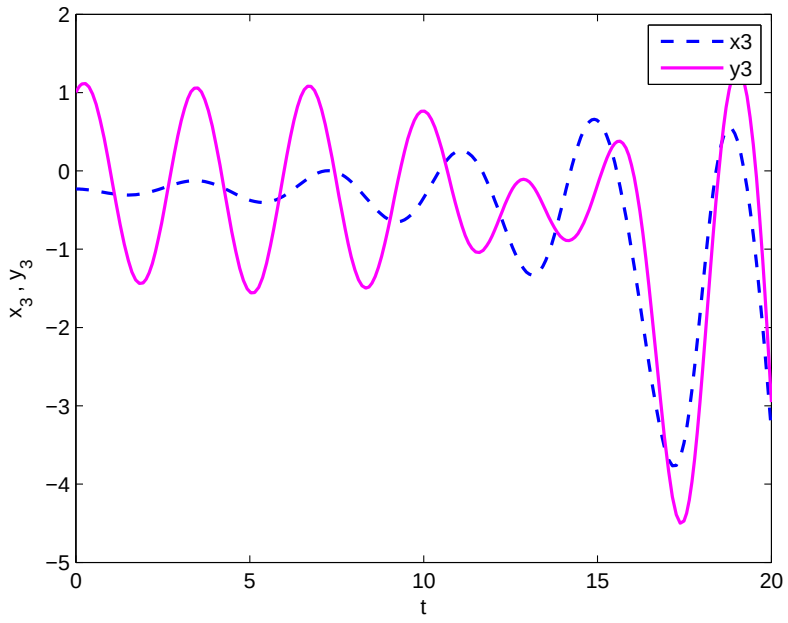

Figure 5.7: Time history of x_3 and y_3

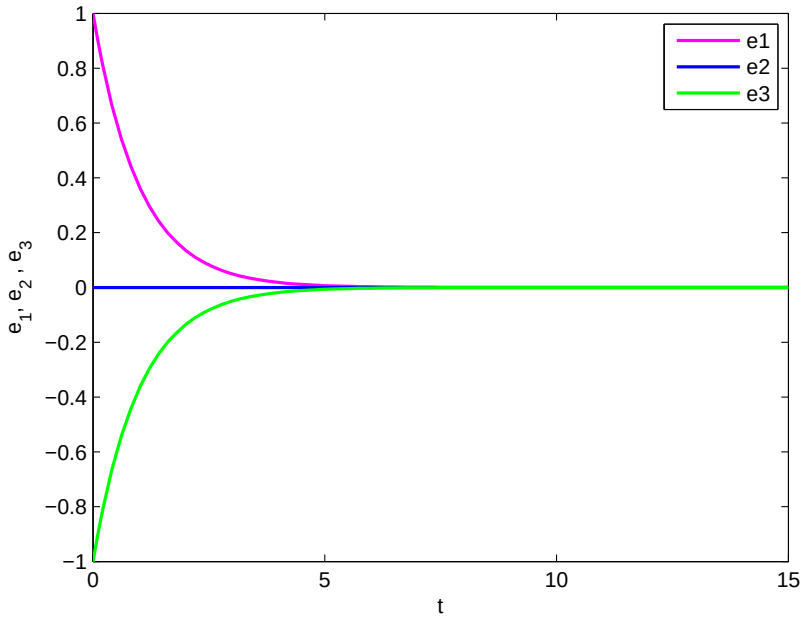

Figure 5.8: History of synchronization error e w.r.t. time

the coupled synchronization Sprott model L for the both cases. This synchronization schemes are based on Lyapunov stability theorem. These results can be used in many areas such as chemical reactions, neural networks, electrical engineering and secure communication etc.

Chapter 6

Robust Antisynchronization of Chaos using Sliding Mode Control Strategy

6.1 Introduction

Synchronization of non-linear chaotic dynamical system has been a hotbed of active research in the field of Physics, Mathematics and Engineering Sciences. Its application in fields ranging from robotics and secure communication to cognitive sciences and social network makes these investigations extremely contemporary and essential. The concept of anti-synchronization dates back to the time of Huygens when he reported anti-phase locking of two different pendulums[36]. The study of synchronization in chaotic systems was a natural extension of this problem, that cuts across the fields of mathematics, engineering and mechanics. In this vast body of research on synchronization, analysis of anti-synchronization occupies a very important place - partly due to its historical roots and partly due to its natural presence in different systems as observed in different experiments.

In coupled oscillators possessing inverse symmetry, the inverse being taken in additive sense, anti-synchronization (AS) sets in quite naturally with the induction of a simple diffusive coupling. While simple coupling is generally sufficient to synchronize such systems possessing high degree of symmetry, synchronization of asymmetric and non-identical systems poses a major challenge. In chaotic systems like the Lorenz or R*ö*ssler systems which lack such special kind of symmetry, anti-synchronization becomes a highly non-trivial problem. Li and Zhou had applied an active control method[42] to anti-synchronize two non-identical systems. Zhang and Zu [95] had considered active and adaptive control methods for this purpose while Ahn had used the H_∞ approach[2]. Fairly recently, Jackson and Grosu introduced open plus closed loop control(OPCL) [30] method for the control of chaos. In [25] and [18], the OPCL method was employed as an effective tool for mixed synchronization and the papers discussed anti-synchronization as a special case of the results obtained therein. To sum up, the techniques of Lyapunov function stability (LFS) and Open-plus-closed loop control (OPCL) and their variants have been the standard tools for achieving AS in chaotic systems for quite some time. These methods do not impose any symmetry restrictions on the systems. The additional advantage of OPCL technique is its ability to accommodate mismatches and small amplitude disturbances. In this chapter, we propose a sliding mode control based mechanism[84] for achieving the same goal.

The benefits of using sliding mode control action has widely been discussed in journals of engineering science [10, 83, 93]. Its inherent advantages of easy realization, fast response and insensitivity to vari-

ation in plant parameters or external disturbances are instrumental in its choice as a viable alternative to OPCL and LFS techniques. Our method considers a pair of coupled non-linear systems in all generality with no restrictions, except the smoothness requirements that are necessary for the existence of solutions to the dynamical equations of the system[33]. Thus, the proposed scheme works for a general class of non-linear systems. Like the OPCL and LFS techniques, no symmetry restrictions are imposed on the class of systems being considered. In this respect, our approach is highly generalized. A planar sliding surface is designed (Section 6.2.1) across which the control action varies discontinuously, with the signum function characterizing the discontinuity. The basic advantage of sliding mode control action is its finite time convergence[69] onto the synchronization manifold, proved in Section 6.2.4. This is a clear advantage of our scheme over other prevalent techniques like LFS, OPCL etc. because a finite time bound is available for at least some portion of the anti-synchronization process. The results are not just asymptotic. This bound is entirely determined by controller parameters and can be modified at will through the tuning of the controller. Moreover, the existence of upper bound on time also imposes an upper bound on the region of synchronization manifold where the trajectories hit, or enter, the manifold.

In most real-life systems, noise, disturbance, error in measurement of parameters and system states, etc. lead to collapse of the ideal framework on which the synchronization scheme was based. Robustness of the controller [89] guarantees stable synchronization irrespective of such perturbations. Our proposed controller is robust

to all forms of bounded perturbations. It is a strong point of our method and it has been proved in Section 6.2.5. Boundedness of the disturbance or perturbation is the only assumption made to prove the result[69] . Importantly, robustness of the controller can be achieved by the tuning of exactly one controller parameter and introduction of a separate control vector. The control vector tracks the perturbation on the synchronization manifold only. Unlike most of the known methods, constant tracking of the disturbance is not necessary for our controller.

The chapter has been structured as follows. Section 6.2 puts forth all the important results of the chapter. The feasibility of the sliding mode control design is established in Sections 6.2.1, 6.2.2 and 6.2.3. The most important characteristics of finite time convergence and robustness have been proved in Sections 6.2.4 and 6.2.5 respectively. The Sections 6.3 and 6.4 establish our theoretical findings by means of numerical simulation. In Section 6.3, we have chosen Sprott system [52] which is chaotic and lacks inverse symmetry. Our designed controller anti-synchronizes it with another identical Sprott system. In Section 6.4, we choose another famous chaotic system - the Rössler system[71] which also lacks inverse symmetry and anti-synchronize it with identical Rössler system. These sections also verify the robustness of the scheme under different bounded perturbations. Section 6.5 discusses the simulation results and Section 6.6 contains our concluding remarks.

6.2 Sliding Mode Control Strategy for Anti-Synchronization

Unidirectional synchronization necessitates the introduction of a master-slave(or, drive-response) configuration in a system of coupled dynamical systems. Without any loss of generality, a system of two coupled non-linear systems may be written as

$$\begin{aligned} \dot{X} &= AX + \phi(X) \qquad \leftarrow \quad \text{Drive system} \\ \dot{Y} &= BY + \psi(Y) + U \leftarrow \quad \text{Response system} \end{aligned} \tag{6.2.1}$$

where $X, Y \in \mathbb{R}^n, \quad A, B \in \mathbb{R}^{n\times n}$ and $\phi, \psi, U : \mathbb{R}^n \to \mathbb{R}^n$ are vector functions on $\mathbb{R}^n$. U represents the external forcing terms which bring about synchronization. In general, $U = u_c + u_s$ where u_c is the coupling function that constitutes the driving mechanism and u_s is the external control input that ensures synchrony between the two systems. In the following section, we propose our method for designing of these components, and hence, U. The suffix $'s'$ in u_s is indicative of our goal of designing the control input through sliding mode control strategy.

To this end, let us define

$$e = Y + X$$

as the vector representing anti-synchronization error, where

$$\begin{aligned} e &= (e_1, e_2, ..., e_n)^T, \\ X &= (x_1, x_2, ..., x_n)^T, \\ and \quad Y &= (y_1, y_2, ..., y_n)^T. \end{aligned}$$

The evolution equation of error is then given by

$$\dot{e} = Ae + F(X, Y) + u_c + u_s, \tag{6.2.2}$$

where $F(X, Y) = \phi(X) + \psi(Y) + (B - A)Y$.

Considering the non-linear coupling function

$$u_c = -F(X, Y)$$

and the control term

$$u_s = Ku$$

where $K \in \mathbb{R}^{n\times 1}$ is a constant vector and $u \in \mathbb{R}$ is the scalar control input to be designed, the system (6.2.2) reduces to

$$\dot{e} = Ae + Ku \tag{6.2.3}$$

Here, K is chosen such that the pair (A, K) is controllable.

6.2.1 Design of the Sliding Surface

The sliding surface is chosen as a linear function of the error states e_i giving a hyperplane $s(e) = Ce$ which contains the targeted state $e = 0$. Here $C \in \mathbb{R}^{1\times n}$ is a constant row vector.
The synchronization manifold is chosen as

$$\Gamma = \{e \in \mathbb{R}^n : s(e) = 0\}$$

This manifold is required to be invariant under the flow of the error dynamics (6.2.3).

According to sliding mode control strategy, the control input

$$u = u_{eq} + u_0$$

where u_{eq} is the equivalent controller that ensures invariance of the manifold Γ and u_0 is discontinuous component of the control law designed such that :

$$\begin{aligned} u &= u_+, \qquad s > 0 \\ u &= u_-, \qquad s < 0 \\ u &= u_{eq}, \qquad s = 0 \end{aligned} \tag{6.2.4}$$

The condition of invariance of Γ is $\dot{s} = 0$ when $s = 0$, dot representing differentiation with respect to time. Imposing this condition on equation (6.2.3),

$$u_{eq} = -(CK)^{-1}CAe \tag{6.2.5}$$

This places the condition that $CK \neq 0$ for the existence of its inverse.

6.2.2 Stability on the Synchronization Manifold

On the synchronization manifold Γ, the evolution equation of error system becomes

$$\begin{aligned} \dot{e} &= (I - (CK)^{-1}KC)Ae \\ or, \quad \dot{e} &= He \end{aligned} \tag{6.2.6}$$

where $H = (I - (CK)^{-1}KC)A$ and I is the identity matrix of order n.

Let us define the Lyapunov function $L = \frac{1}{2}e^T e$, which is clearly positive definite on $\mathbb{R}^n$.
Then,

$$\begin{aligned} \dot{L} &= e^T Ae + u_{eq}e^T K \\ &= e^T[I - (CK)^{-1}KC]Ae \end{aligned}$$

is negative definite if and only if, the matrix

$$H = [I - (CK)^{-1}KC]A$$

is negative definite. Thus, the vectors K and C should be chosen such that

1. $CK \neq 0$
2. $H = [I - (CK)^{-1}KC]A$ is negative definite.

6.2.3 Reachability Condition

In order to ensure global synchronization, it is necessary to establish that the synchronization manifold Γ is reachable for any initial condition $s(0)$. To this end, let us define $V : \mathbb{R} \to \mathbb{R}$ as

$$V(t) = \frac{1}{2}s^2$$

which is a positive definite function on $\mathbb{R}$.

If $\dot{V} < 0$ for all $s \neq 0$, it would imply convergence of system's trajectories onto the manifold Γ. For computing $\dot{V}$, it is necessary to find $\dot{s}$.

The control input u_0 will now arise from the law of evolution of $s(t)$, which we choose as a constant plus proportional rate reaching law

$$\dot{s} = -\delta sgn(s) - \omega s, \tag{6.2.7}$$

where δ, ω are positive real constants and sgn is the signum function. Then, clearly

$$\dot{V} = s\dot{s} = -\omega s^2 - \delta \ s \ sgn(s) < 0, \text{ for all } s \neq 0$$

Eliminating $\dot{s}$ from (6.2.3) and (6.2.7),

$$\begin{aligned} & \dot{s} = C\dot{e} \\ or, \quad & -\delta sgn(s) - \omega s = C(Ae + Ku) \\ or, \quad & (CK)u = -[CAe + \omega s + \delta sgn(s)] \\ or, \quad & (CK)u = -[C(\omega I + A)e + \delta sgn(s)] \end{aligned}$$

which yields

$$u = -(CK)^{-1}[C(\omega I + A)e + \delta sgn(s)]. \tag{6.2.8}$$

Hence, we are now in a position to conclude that the two systems X and Y attain stable anti-synchronization globally. The sliding mode control input which brings about anti-synchrony is

$$\begin{aligned} u = -(CK)^{-1}[C(\omega I + A)e + \delta sgn(s)] \\ \leftarrow \text{Control Input } u \end{aligned} \tag{6.2.9}$$

Having designed the sliding mode controller, we now establish two of the most important characteristics of our synchronization scheme: Finite time convergence onto the synchronization manifold and robustness of the controller towards bounded disturbances and noises.

6.2.4 Finite Time Convergence

Before starting the proof, we define $||s(t)|| = \sqrt{s(t).s(t)}$. Then, $\frac{d}{dt}||s|| = \frac{s\dot{s}}{||s||} \leq -\omega||s|| - \delta$.

Integrating over $[0, t]$,

$$||s(t)|| \leq ||s(0)||exp(-\omega t) - \frac{\delta}{\omega}[1 - exp(-\omega t)] \tag{6.2.10}$$

From here, it is now easy to observe that if

$$t_c = \frac{1}{\omega} ln(1 + \frac{\omega}{\delta}||s(0)||),$$

then $||s(t)||$ attains the value zero for some $t \leq t_c$.

From the invariance of manifold Γ, we can guarantee $||s(t)|| = 0$ for all $t > t_c$. Hence, we ensure finite time convergence onto the synchronization manifold. Tuning of controller parameters δ and ω allows us to adjust the time of reaching Γ. Moreover, the boundedness of $||s||$ additionally restricts the region where trajectories hit Γ. This ensures quick convergence to the desired target $e = 0$. In contrast to other prevalent control methods, here an estimated time of convergence for at least some part of the synchronization process is explicitly available.

6.2.5 Robustness Analysis

In order to analyze the robustness, we consider a coupled non-linear system of the form (6.2.1) along with unmeasured disturbances $d_1(X, t, P)$ and $d_2(Y, t, Q)$, where P and Q represent the hidden variables. They account for any factors that have not been accounted for in the system models or in the controller but can disturb the functioning of the system, e.g.- mechanical vibrations, environmental factors, noise, parameter uncertainties, etc. Other factors like error in system state measurement or due to mismatches are determined by X, Y, t. The only assumptions regarding d_1 and d_2 are their boundedness restrictions : $||d_1||_\infty < \infty$, $||d_2||_\infty < \infty$ where $||.||_\infty$ indicates uniform norm over $\mathbb{R}^n$. It will be seen that the robustness of the controller comes about through simple tuning of the controller parameter (δ

is increased to $\delta + 2M$) and introduction of a control vector. The control vector tracks the external perturbation. But in contrast to most of the other methods in the literature, constant tracking of noise is not necessary. The control vector comes into action only on the sliding manifold.

As outlined before, choosing coupling function

$$v_c = -F(X, Y)$$

and the control vector Z, the system reduces to

$$\dot{e} = Ae + Kv + d_1 + d_2 + Z, \tag{6.2.11}$$

where $K \in \mathbb{R}^{n\times 1}$ is a constant vector, v is the scalar input function and Z is the control vector, a vector-valued function.

Consider the situation when the system has reached the synchronization manifold. Then, $v = v_{eq}$ and $Z \neq 0$.

Writing $v = v_{eq} + v_0$, again we choose

$$v_{eq} = -(CK)^{-1}CAe,$$

where :

1. $CK \neq 0$
2. $H = [I - (CK)^{-1}KC]A$ is negative definite

and Z is chosen as $-[d_1 + d_2]$.
Then, on the synchronization manifold Γ,

$$\dot{e} = He$$

and hence $e(t)$ satisfies $\lim_{t\to\infty} e(t) = 0$ [33]. Hence, the stability of the manifold has been established.

In order to ensure reachability, we modify the reaching law as

$$\dot{s} = -\omega s - (\delta + 2M)sgn(s),$$

where ω and δ are positive and

$$M = max\{|Cd_1|, |Cd_2|\} > 0.$$

The control input then takes the form

$$v = -(CK)^{-1}[CAe + \omega s + (\delta + 2M)sgn(s)].$$

When $s \neq 0$, Z is chosen to be 0. Thus, Z forms another component of the discontinuous control.

Using this control input in (6.2.11), if we now define Lyapunov function $V = \frac{1}{2}s^2$ and compute its time derivative,

$$\begin{aligned}\dot{V} = -\omega s^2 - \delta\ s\ sgn(s) + s(Cd_1 - M\ sgn(s)) \\ + s(Cd_2 - M\ sgn(s))\end{aligned}$$

which is clearly negative if $s \neq 0$.

Thus, the modified sliding mode control input is :

$$\begin{aligned} v &= -(CK)^{-1}[C(A + \omega I)e + (\delta + 2M)sgn(s)] \\ &\qquad \leftarrow \text{Control Input } v, \\ Z &= -[d_1 + d_2]\delta_0(s) \\ &\qquad \leftarrow \text{Control Vector } Z, \end{aligned} \tag{6.2.12}$$

where $\delta_0(s)$ is the Dirac delta function which takes value 1 when $s = 0$ and value 0 elsewhere.

The proposed scheme thus ensures global anti synchronization between X and Y in the presence of bounded disturbance and noise. Notably, the control doesn't require tracking of the noise all through the control action. Tracking of the noise activates only on the synchronization manifold because $\delta_0(s) = 0$ outside Γ.

6.2.6 Chattering-free Controller

Due to the discontinuity in control action, the error keeps oscillating about the synchronization manifold at a very high frequency with small amplitude producing an effect called chattering. Such an effect is undesirable, specially when noise is present in the system, as the chattering gets in the way of elimination of noise by tuning the controller. In order to get rid of this high-frequency chatter of the error about the sliding manifold instead of settling down to the zero equilibrium state, the discontinuous portions of the controllers are replaced by their continuous analogues. Thus, the chattering-free controller (in absence of any disturbance/noise), takes the form :

$$\begin{aligned} u = -(CK)^{-1}[C(\omega I + A)e + \delta tanh(s)] \\ \leftarrow \text{Control Input } u \end{aligned} \tag{6.2.13}$$

The robust chattering-free controller in presence of disturbances has the form:

$$\begin{aligned} v = -(CK)^{-1}[C(A + \omega I)e + (\delta + 2M)tanh(s)] \\ \leftarrow \text{Control Input } v, \\ Z = -[d_1 + d_2](1 - tanh^2(s)) \\ \leftarrow \text{Control Vector } Z. \end{aligned} \tag{6.2.14}$$

6.3 Anti-synchronization of identical Sprott system

We first consider the non-linear chaotic dynamical Sprott system [52] as a drive system, which is given by

$$\left.\begin{aligned} \dot{x_1} &= x_2 + \alpha x_3 \\ \dot{x_2} &= \beta x_1^2 - x_2 \\ \dot{x_3} &= \gamma - x_1 \end{aligned}\right\} \tag{6.3.15}$$

where α, β, γ are all positive parameters.
In matrix form, system of equation (6.3.15) can be written as

$$\dot{x} = Ax + \phi(x)$$

where

$$x = \begin{pmatrix} x_1 \\ x_2 \\ x_3 \end{pmatrix} \in \mathbb{R}^3, \quad \phi(x) = \begin{pmatrix} 0 \\ \beta x_1^2 \\ \gamma \end{pmatrix} \in \mathbb{R}^3$$

and

$$A = \begin{pmatrix} 0 & 1 & \alpha \\ 0 & -1 & 0 \\ -1 & 0 & 0 \end{pmatrix}$$

Then, the response system coupled with the drive system (6.3.15) can be taken as

$$\dot{y} = By + \psi(y) + U,$$

where

$$y = \begin{pmatrix} y_1 \\ y_2 \\ y_3 \end{pmatrix} \in \mathbb{R}^3, \text{is the state vector of the response system,}$$

$$U = \begin{pmatrix} U_1 \\ U_2 \\ U_3 \end{pmatrix} \in \mathbb{R}^3, \text{is the control parameter and}$$

$$\psi(y) = \phi(y) = \begin{pmatrix} 0 \\ \beta y_1^2 \\ \gamma \end{pmatrix} \in \mathbb{R}^3,$$

and $B = A$.
Thus, the response system is

$$\left.\begin{aligned} \dot{y_1} &= y_2 + \alpha y_3 + U_1 \\ \dot{y_2} &= \beta y_1^2 - y_2 + U_2 \\ \dot{y_3} &= \gamma - y_1 + U_3 \end{aligned}\right\} \tag{6.3.16}$$

Now, we construct the anti-synchronization error $e = (e_1, e_2, e_3)^T$ as

$$e_i = y_i + x_i, \quad i = 1, 2, 3.$$

Using (6.2.2), the dynamical system of anti-synchronization error is

$$\left.\begin{aligned} \dot{e_1} &= e_2 + \alpha e_3 + U_1 \\ \dot{e_2} &= -e_2 + \beta y_1^2 + \beta x_1^2 + U_2 \\ \dot{e_3} &= -e_1 + 2\gamma + U_3 \end{aligned}\right\} \tag{6.3.17}$$

Let us take

$$U = u_c + u_s = Ku - F(x, y) \tag{6.3.18}$$

where

$$F(x,y) = \phi(x) + \psi(y) + (B - A)y$$
$$= \begin{pmatrix} 0 \\ \beta(x_1^2 + y_1^2) \\ 2\gamma \end{pmatrix} \tag{6.3.19}$$

To make (A, K) controllable, we take K as

$$K = (1 \quad 2 \quad 1)^T \tag{6.3.20}$$

Following the Section 6.2.1, the sliding manifold s is taken as

$$s(e) = Ce = \sum_{i=1}^{3} C_i e_i,$$

where C_i are to be calculated.

To make the coupled Sprott system (6.3.15) and (6.3.16) globally asymptotically anti-synchronized, we choose,

$$C = (-3 \quad -24 \quad 2)$$

To perform robustness analysis for the coupled Sprott system, we take,

$$d_1 = (0.01sin(t), 0, 0.02cos(t))^T$$
$$\text{and} \quad d_2 = (0.02sin(t), 0, 0.01cos(t))^T.$$

Now, by taking $\omega = 2.5$ and $\delta = 0.01$, we have,

$$\begin{aligned} u &= -0.1939e_1 - 0.7959e_2 - 0.1367e_3 - 2.0408 \times 10^{-04} sgn(s) \\ &\leftarrow \text{Control Input } u, \\ u &= -0.1939e_1 - 0.7959e_2 - 0.1367e_3 - 2.0408 \times 10^{-04} tanh(s) \\ &\leftarrow \text{Chattering-free controller}, \\ v &= -0.1939e_1 - 0.7959e_2 - 0.1367e_3 - 0.0818 tanh(s) \\ &\leftarrow \text{Robust Chattering-free controller}. \end{aligned} \tag{6.3.21}$$

Hence, using (6.3.19), (6.3.20) and (6.3.21), one can evaluate U from (6.3.18) which is the required controller for anti-synchronization of the systems (6.3.15) and (6.3.16).

6.4 Anti-synchronization of identical Rössler system

We now consider the famous Rössler system [71] as a drive system, which is given by

$$\left.\begin{aligned} \dot{x_1} &= -x_2 - x_3 \\ \dot{x_2} &= x_1 + ax_2 \\ \dot{x_3} &= b + x_3(x_1 - c) \end{aligned}\right\} \tag{6.4.22}$$

where a, b, c are all positive parameters.

Then, the system of equation (6.4.22) can be written as

$$\dot{x} = Ax + \phi(x)$$

where

$$x = \begin{pmatrix} x_1 \\ x_2 \\ x_3 \end{pmatrix} \in \mathbb{R}^3, \quad \phi(x) = \begin{pmatrix} 0 \\ 0 \\ b + x_1 x_3 \end{pmatrix} \in \mathbb{R}^3$$

and

$$A = \begin{pmatrix} 0 & -1 & -1 \\ 1 & a & 0 \\ 0 & 0 & -c \end{pmatrix}$$

Then, the response system coupled with the drive system (6.4.22) can be taken as

$$\dot{y} = By + \psi(y) + U,$$

where

$$y = \begin{pmatrix} y_1 \\ y_2 \\ y_3 \end{pmatrix} \in \mathbb{R}^3, \text{is the state vector of the response system,}$$

$$U = \begin{pmatrix} U_1 \\ U_2 \\ U_3 \end{pmatrix} \in \mathbb{R}^3, \text{is the control parameter and}$$

$$\psi(y) = \phi(y) = \begin{pmatrix} 0 \\ 0 \\ b + y_1 y_3 \end{pmatrix} \in \mathbb{R}^3 \quad \textit{and} \quad B = A.$$

Thus, the response system is

$$\left.\begin{aligned} \dot{y_1} &= -y_2 - y_3 + U_1 \\ \dot{y_2} &= y_1 + a y_2 + U_2 \\ \dot{y_3} &= b - c y_3 + y_1 y_3 + U_3 \end{aligned}\right\} \tag{6.4.23}$$

Now, we construct the anti-synchronization error $e = (e_1, e_2, e_3)^T$ as

$$e_i = y_i + x_i, \quad i = 1, 2, 3.$$

Using (6.2.2), the dynamical system of anti-synchronization error is

$$\left.\begin{aligned} \dot{e_1} &= -e_2 - e_3 + U_1 \\ \dot{e_2} &= e_1 + ae_2 + U_2 \\ \dot{e_3} &= -ce_3 + 2b + x_1x_3 + y_1y_3 + U_3 \end{aligned}\right\} \tag{6.4.24}$$

In this case,

$$U = u_c + u_s = Ku - F(x, y) \tag{6.4.25}$$

where

$$\begin{aligned} F(x, y) &= \phi(x) + \psi(y) + (B - A)y \\ &= \begin{pmatrix} 0 \\ 0 \\ 2b + x_1x_3 + y_1y_3 \end{pmatrix} \end{aligned} \tag{6.4.26}$$

To make (A, K) controllable, let us take K as

$$K = (-4 \quad 11 \quad 5)^T \tag{6.4.27}$$

To make the coupled Rössler System (6.4.22) and (6.4.23) globally asymptotically anti-synchronized, we choose,

$$C = (16 \quad -12 \quad -1)$$

In case of robust controller for the coupled Rössler system, we take,

$$\begin{aligned} & d_1 = (0.01sin(t), 0, 0.02cos(t))^T \\ \& \quad & d_2 = (0.02sin(t), 0, 0.01cos(t))^T. \end{aligned}$$

By taking $\omega = 3$ and $\delta = 0.25$, we have,

$$\begin{aligned} u &= 0.1791e_1 - 0.2706e_2 - 0.0662e_3 + 0.0012sgn(s) \\ &\leftarrow \text{Control Input u,} \\ u &= 0.1791e_1 - 0.2706e_2 - 0.0662e_3 + 0.0012tanh(s) \\ &\leftarrow \text{Chattering-free controller,} \\ v &= 0.1791e_1 - 0.2706e_2 - 0.0662e_3 + 0.0361tanh(s) \\ &\leftarrow \text{Robust Chattering-free controller.} \end{aligned} \tag{6.4.28}$$

Hence, using (6.4.26), (6.4.27) and (6.4.28), one can evaluate U from (6.4.25) which is the required controller and the systems (6.4.22) and (6.4.23) are anti-synchronized.

6.5 Numerical Simulation Results

Numerical simulations have been performed using fourth-order Runge-Kutta method in MATLAB.

Chaotic nature of the Sprott system is seen for $\alpha = 3.9$, $\beta = 0.9$, $\gamma = 1$. These values have been used in Section 6.3.

The initial conditions of the systems (6.3.15) and (6.3.16) are selected as $x(0) = (1, 0.1, 0.5)$ and $y(0) = (2, 0.1, 0.5)$ respectively. At $t = 0$, $e(0) = (3, 0.2, 1)$.

In Section 6.4, we have chosen Rössler system with $a = b = 0.2$ & $c = 5.7$. For numerical simulation, we have considered $x(0) = (2, -1, 2)$ and $y(0) = (-8, 6, -5)$ for the systems (6.4.22) and (6.4.23) respectively. At $t = 0$, $e(0) = (-6, 5, -3)$.

In figure (6.1) and figure (6.2), we observe anti-synchronization between the states of the drive system and the states of the response

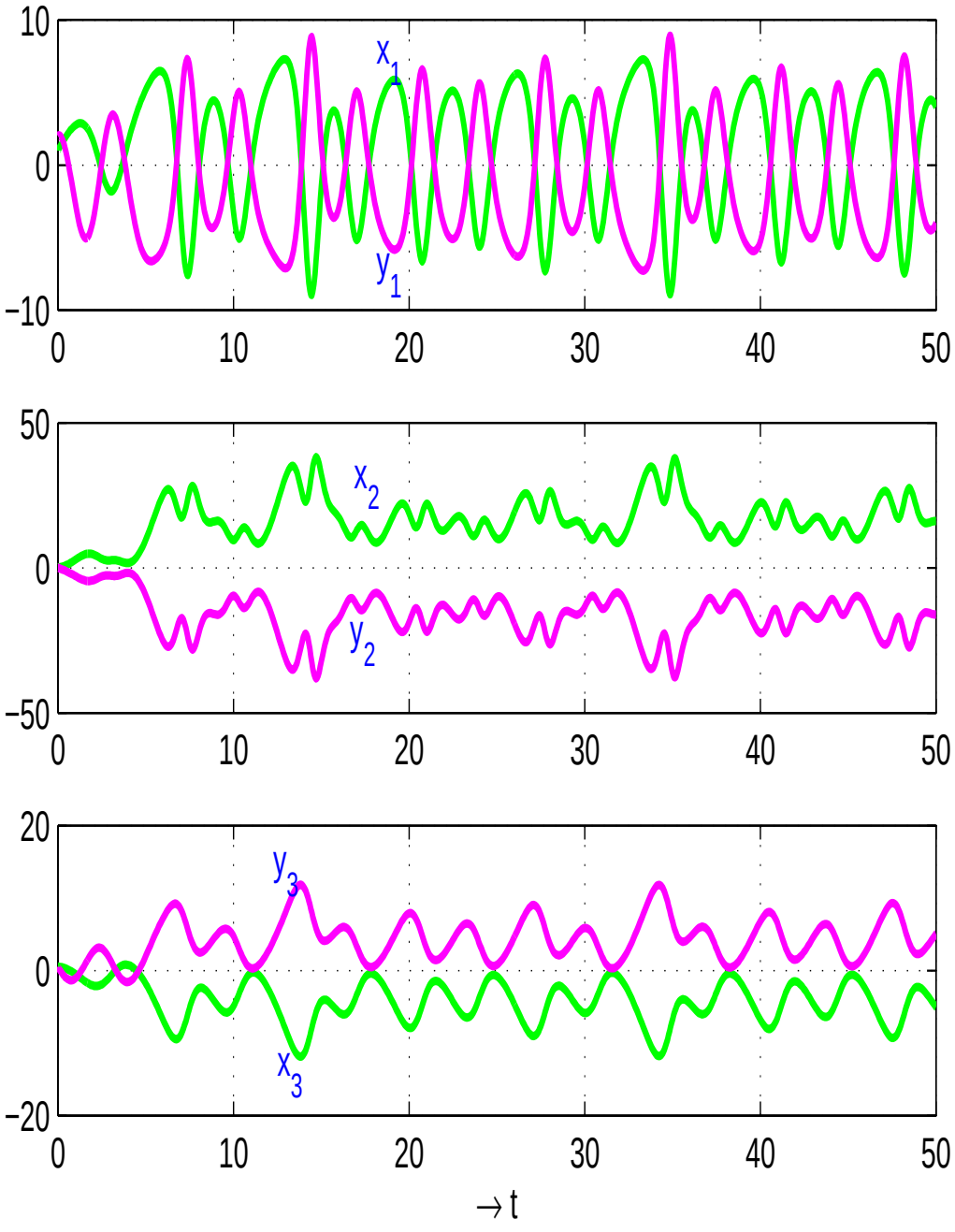

Figure 6.1: Anti-synchronization of coupled Sprott system

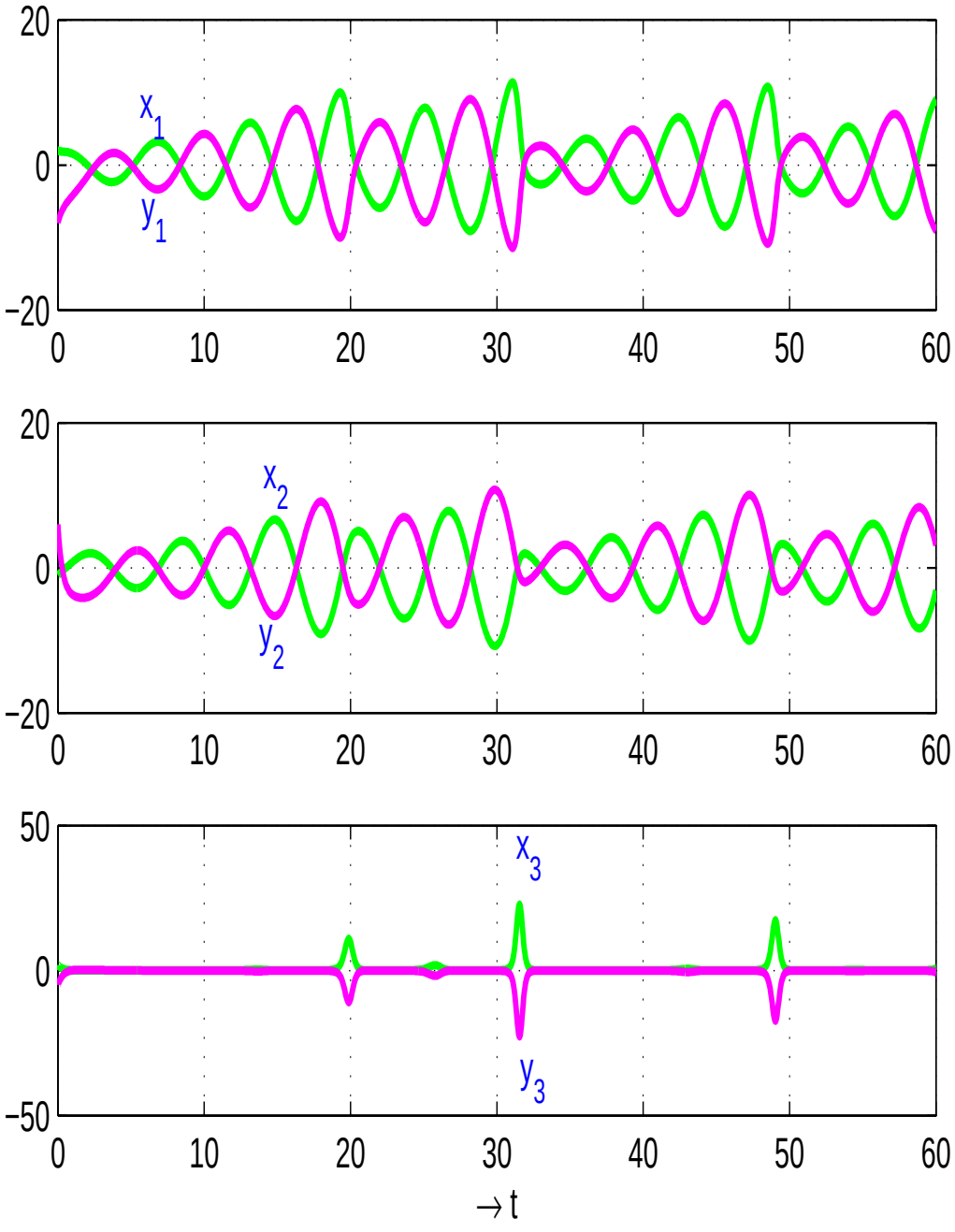

Figure 6.2: Anti-synchronization of coupled Rössler system

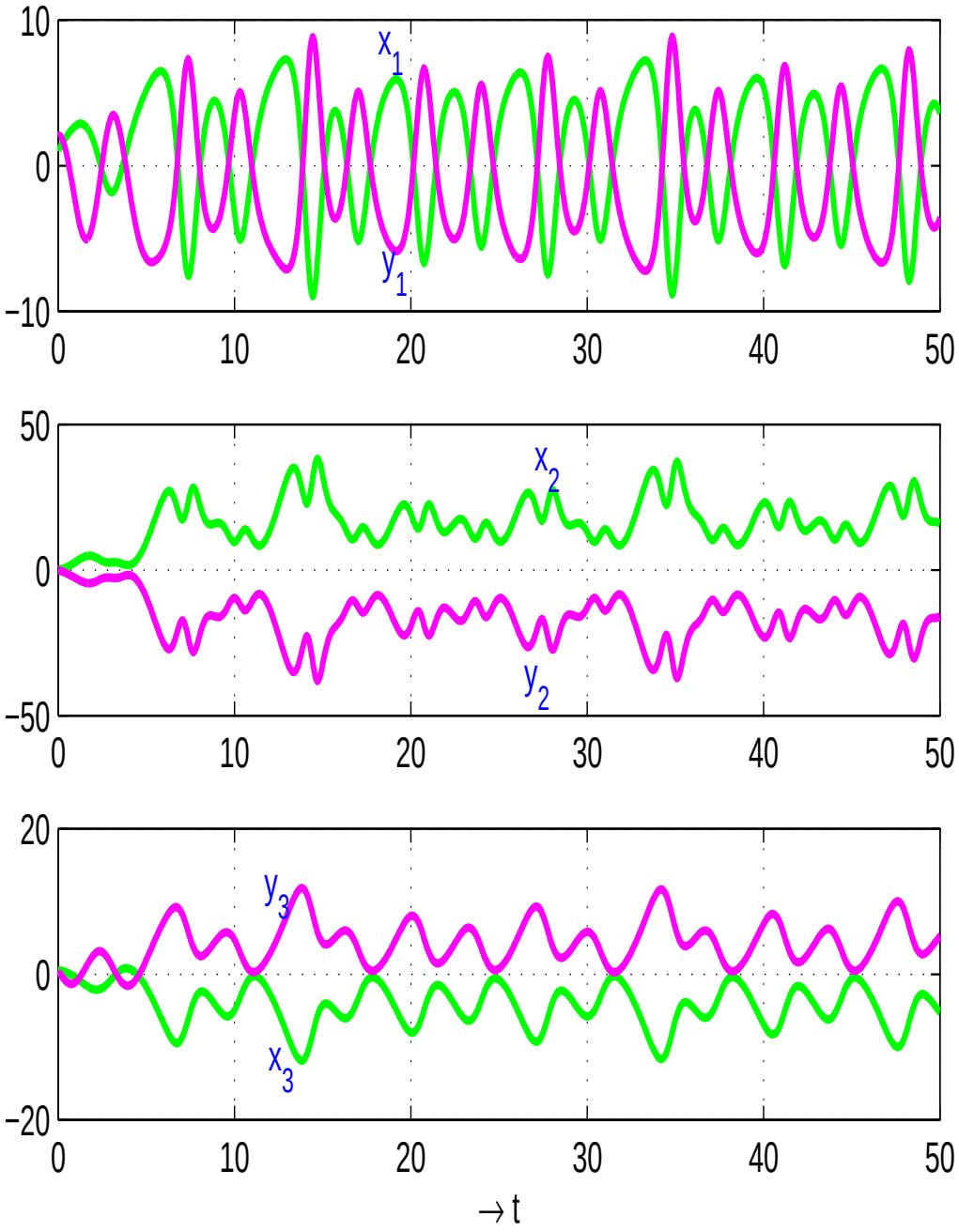

Figure 6.3: Anti-synchronization of coupled Sprott system for chattering free controller

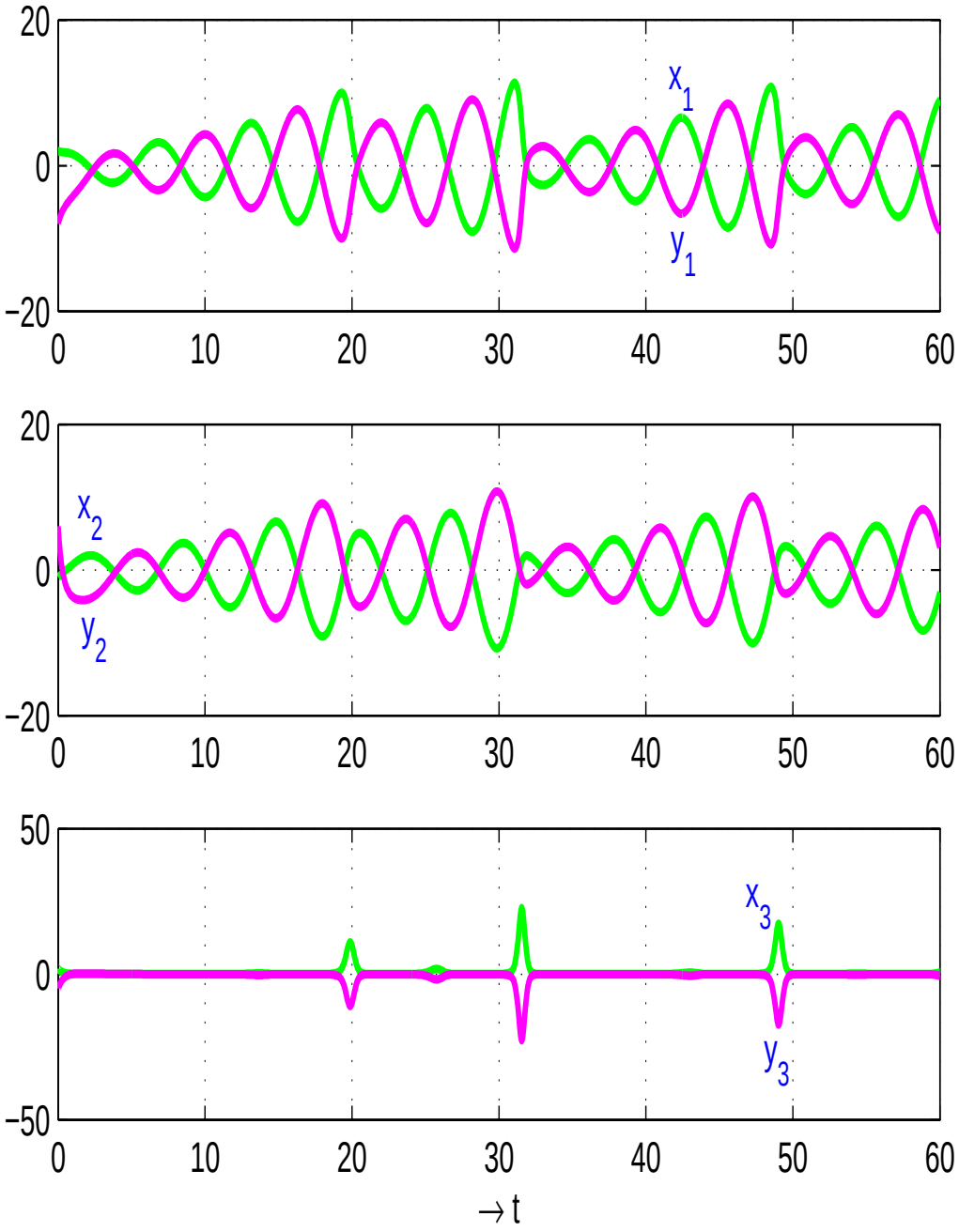

Figure 6.4: Anti-synchronization of coupled Rössler system for chattering free controller

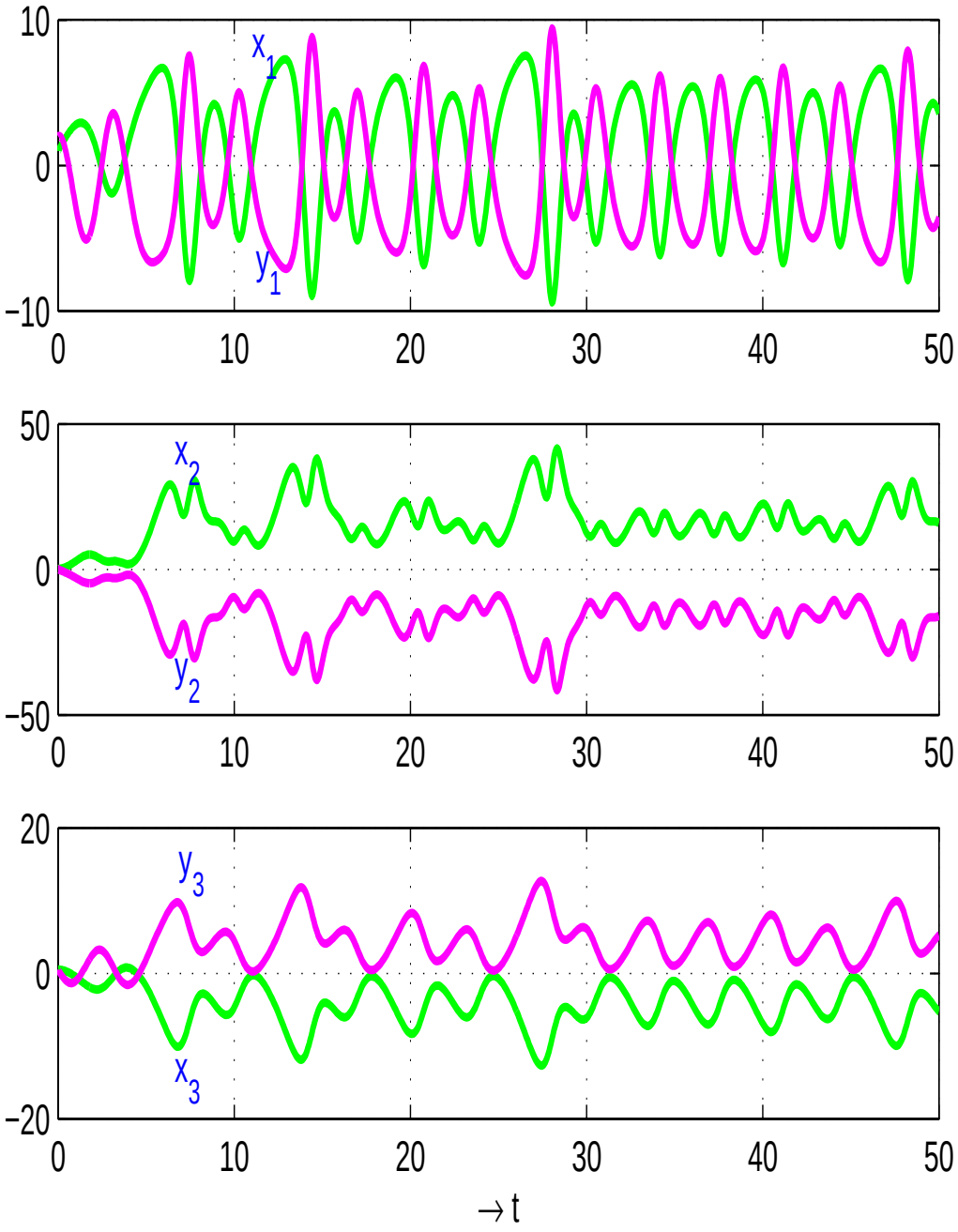

Figure 6.5: Anti-synchronization of coupled Sprott system for chattering free controller in presence of disturbance with M=2

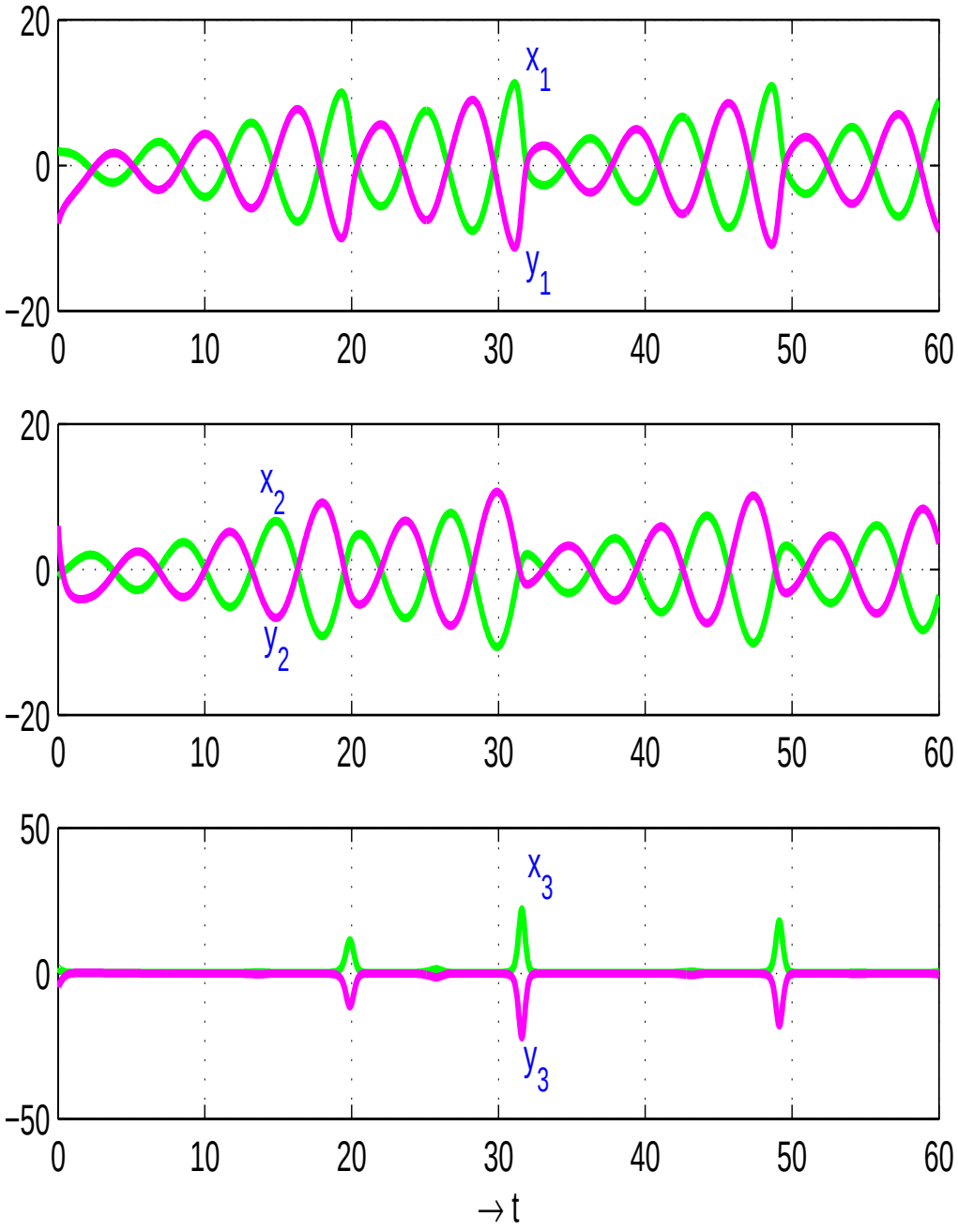

Figure 6.6: Anti-synchronization of coupled Rössler system for chattering free controller in presence of disturbance with M=3.5

system. These have been obtained by using the discontinuous control input u. Using the chattering-free controller, we have figure (6.3) and figure (6.4). For systems having bounded disturbance, the robust chattering-free controller is applied to get figure (6.5) and figure (6.6) represents the anti -synchronization between the states of the drive system and the states of the response system.

The anti-synchronization error with respect to time is shown in figure (6.7) and figure (6.8) for coupled Sprott system and coupled Rössler system respectively. It is seen that the anti-synchronization errors reduce rapidly to zero (after 30 units of time approximately in the figure (6.7) for coupled Sprott system, after 12 units of time approximately in the figure (6.8) for coupled Rössler system). The corresponding diagrams with chattering-free controller are given in figure (6.9) and figure (6.10). Finally, applying the robust chattering-free controller to systems with bounded disturbance, we obtain figure (6.11) and figure (6.12).

As per theory, the sliding variable s should go to zero as $t \to \infty$. This is investigated in figure (6.13) and figure (6.14) respectively. But due to the discontinuity in control action, s does not exactly reach zero - it keeps oscillating about the sliding manifold with high frequency and small amplitude producing an effect called chattering of the controller. This can be avoided by using the chattering-free controller, as observed in figure (6.15) and figure (6.16) respectively. Lastly, figure (6.17) and figure (6.18) show the sliding variable with respect to time for robust chattering-free controller with the tuning factor $M = 2$ and $M = 3.5$ respectively.

All of the figures derive a common statement, that is, finite time

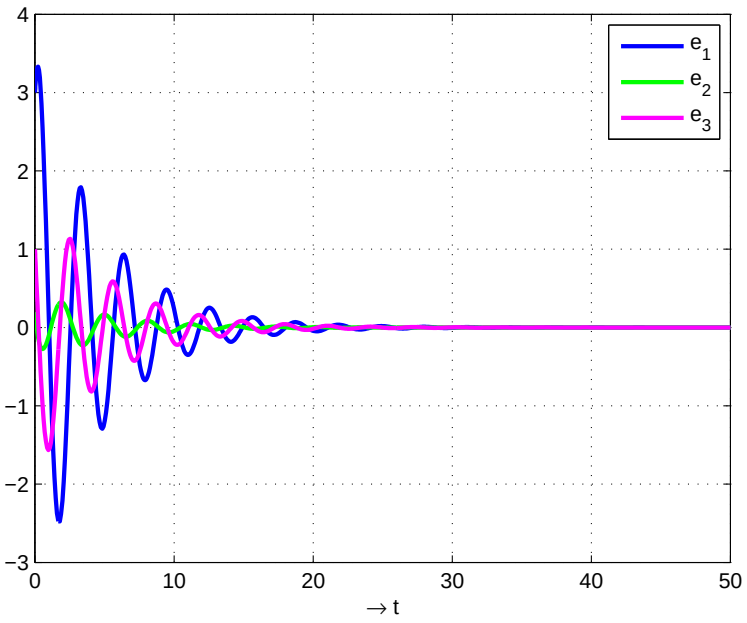

Figure 6.7: Anti-synchronization error w.r.t. time for Sprott system

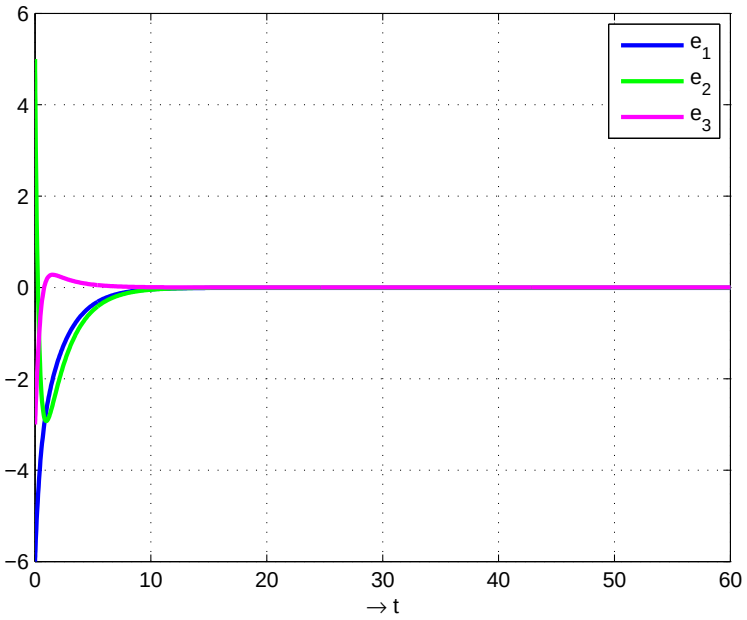

Figure 6.8: Anti-synchronization error w.r.t. time for Rössler system

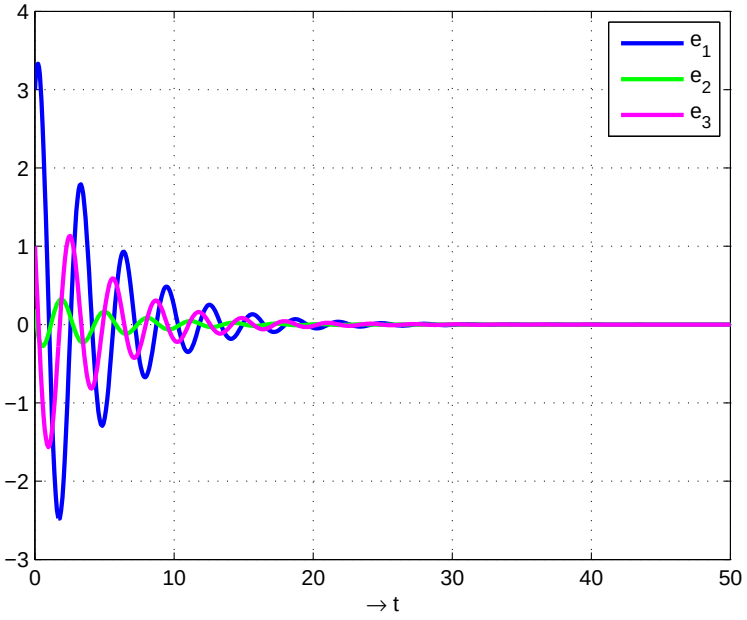

Figure 6.9: Anti-synchronization error w.r.t. time for Sprott system with chattering free controller

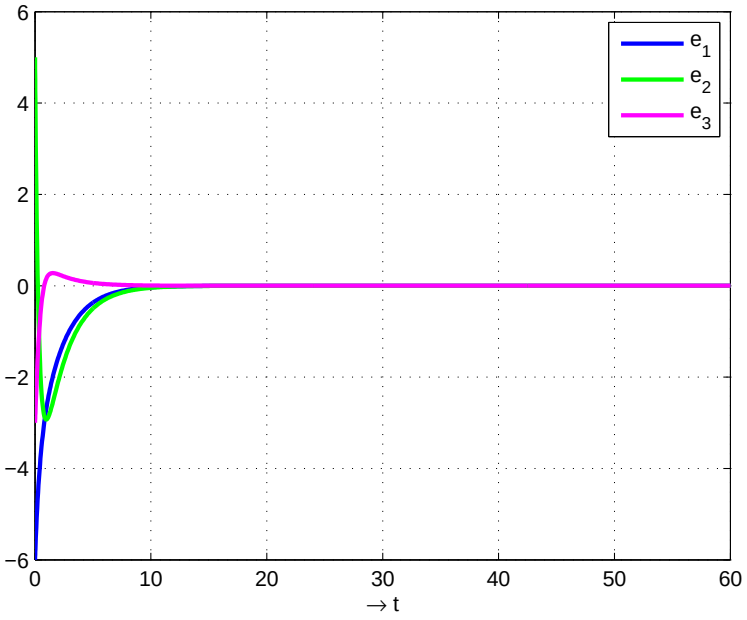

Figure 6.10: Anti-synchronization error w.r.t. time for Rössler system with chattering free controller

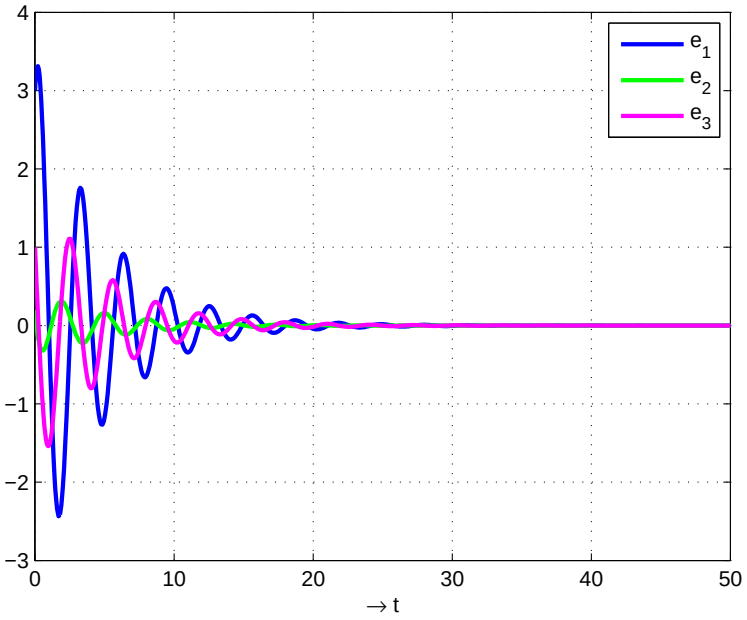

Figure 6.11: Anti-synchronization error w.r.t. time with M=2 for Sprott system

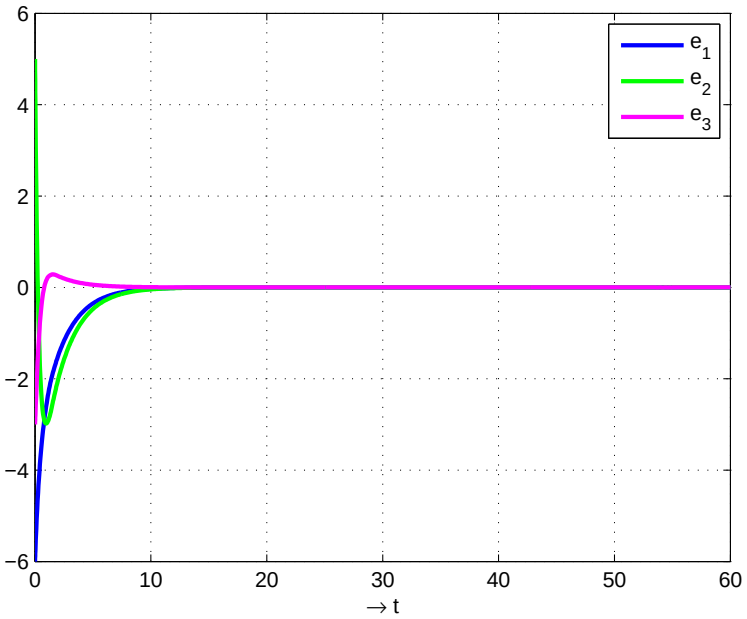

Figure 6.12: Anti-synchronization error w.r.t. time with M=3.5 for Rössler system

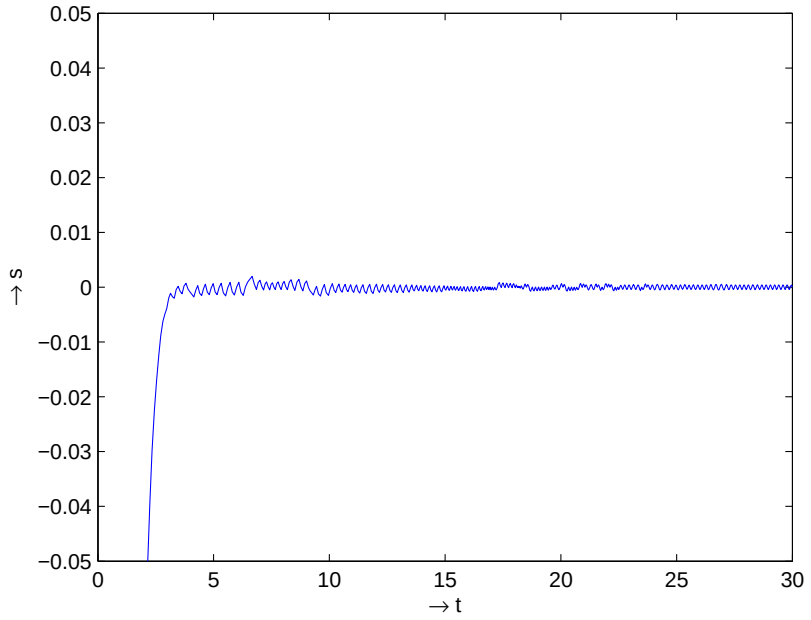

Figure 6.13: Time evolution of the sliding variable for Sprott system

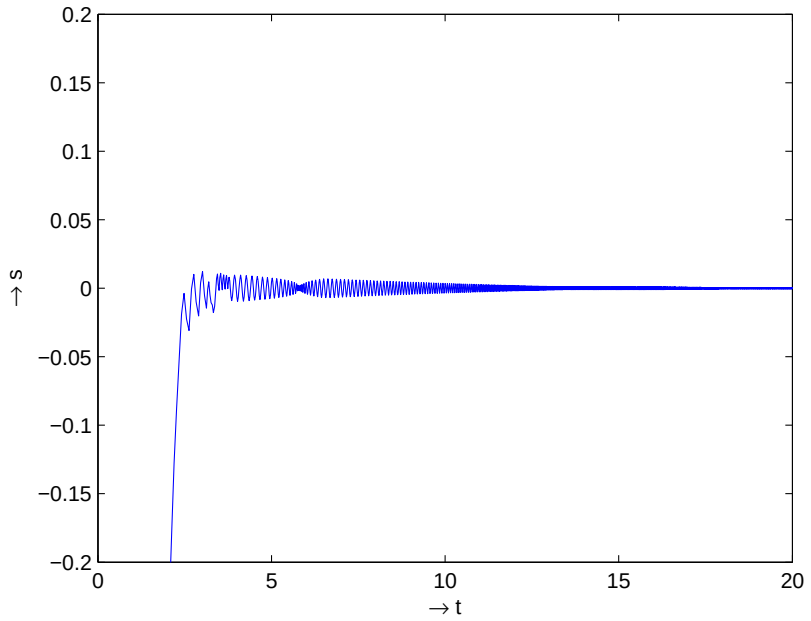

Figure 6.14: Time evolution of the sliding variable for Rössler system

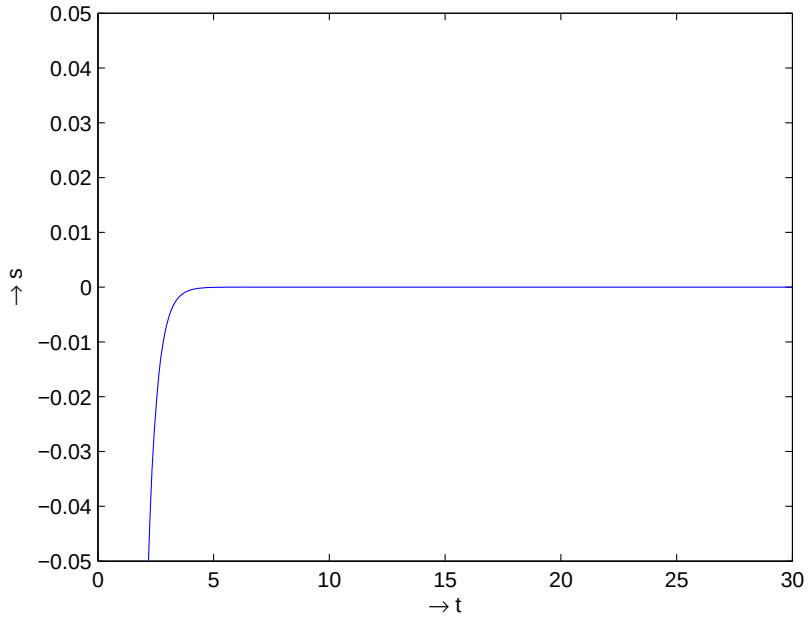

Figure 6.15: Time evolution of the sliding variable for Sprott system with chattering free controller

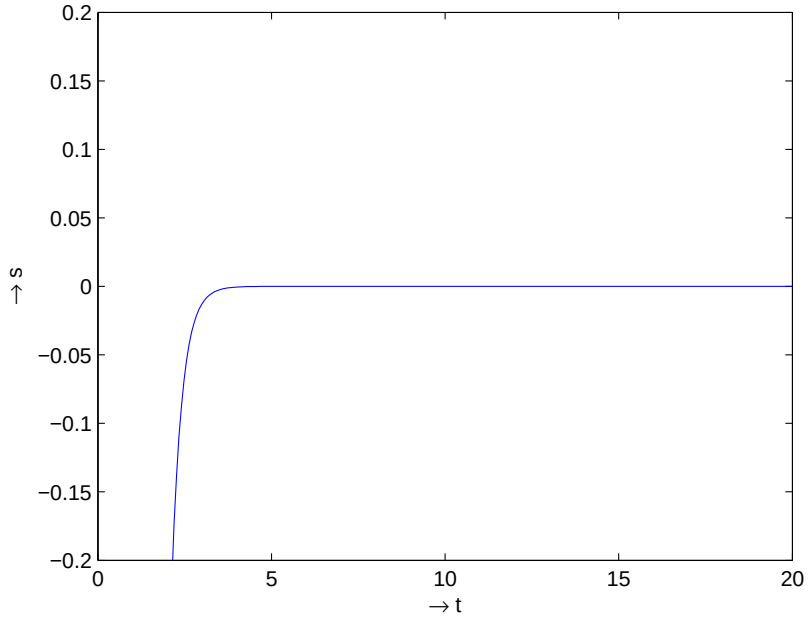

Figure 6.16: Time evolution of the sliding variable for Rössler system with chattering free controller

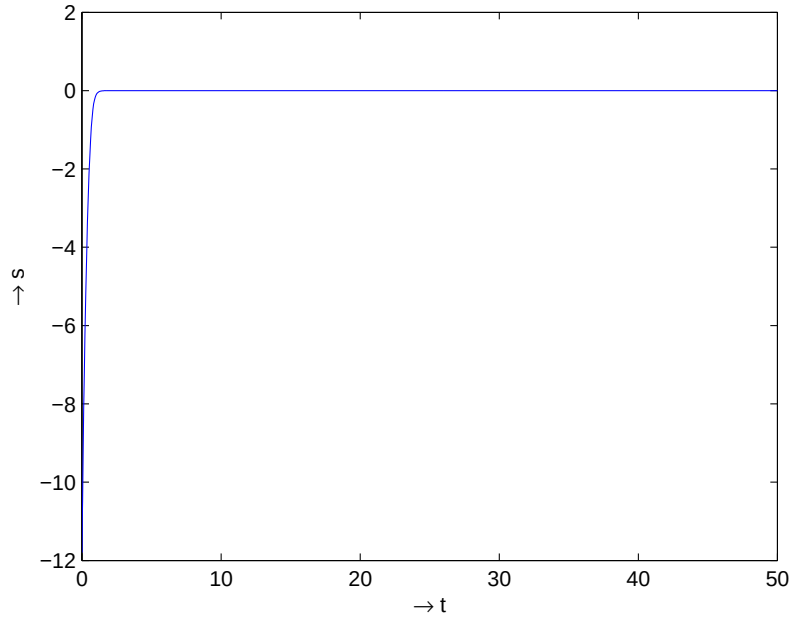

Figure 6.17: Time evolution of the sliding variable with M=2 for Sprott system

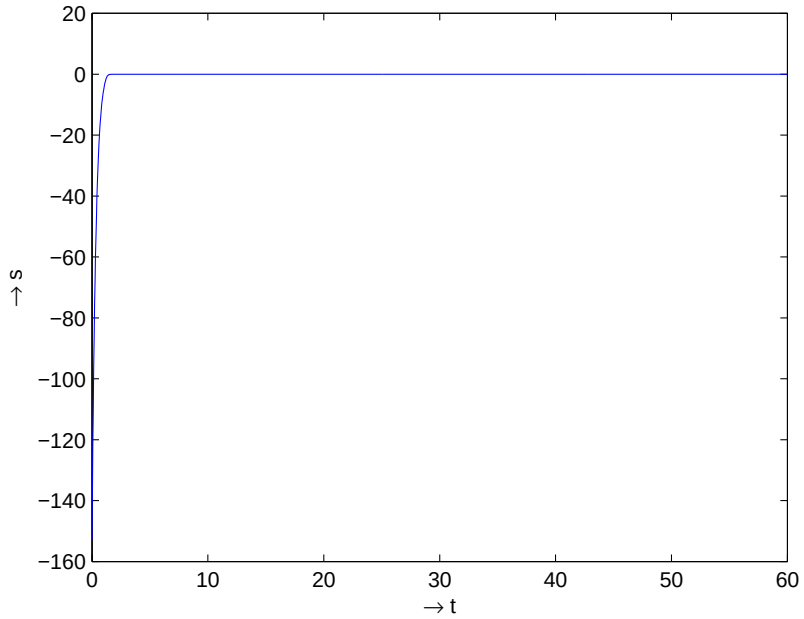

Figure 6.18: Time evolution of the sliding variable with M=3.5 for Rössler system

convergence onto synchronization manifold and stable asymptotic convergence to the zero error state. Hence, we can conclude that the anti-synchronization between the states of drive system and the states of response system is achieved.

6.6 Conclusion :

In this chapter, we propose a sliding mode control-based strategy to anti-synchronize a general class of chaotic systems. Unlike the conventional diffusive coupling approach, our method accommodates all kinds of systems without imposing any symmetry restrictions. In fact, symmetry of the systems is not even a determining factor in the method as it is also applicable for systems having widely different dynamical behaviour. In this respect, our controller is comparable to other well-known techniques like the OPCL and LFS that are currently used to attain AS. In addition, the scheme we propose has two additional benefits of finite time convergence and robustness. Finite time convergence produces a clearly defined upper bound for the time taken to reach the synchronization manifold. Thus, the results are global and exact; not just asymptotic. Robustness to bounded perturbations comes about through the tuning of a controller parameter and introduction of a control vector based on partial tracking of the disturbances. To sum up, the proposed controller requires a nonlinear coupling function to couple the two systems and a sliding mode control input. A control vector is required in case of perturbations in the system. As a result, we have a very elegant and concise controller that is quite easy to implement, as has been widely discussed

in engineering science journals over quite a few years. The controller easily accommodates bounded disturbance. The discontinuous control may also be replaced by a continuous equivalent which gets rid of the chattering phenomenon observed in many discontinuous control input systems.

In order to support our findings, we have applied our method to anti-synchronize two identical coupled Sprott systems and two identical coupled R*ö*ssler systems. The results indicate successful realization of the proposed method. In both the above situations, one can easily observe that the error term reduces to zero after a short time interval which is the benefit of sliding mode controller design. Our method guarantees globally stable anti-synchronization which has been established theoretically and through simulation. As practical implementation of sliding mode methods has become quite commonplace nowadays, we believe that our proposed method would prove to be useful in various disciplines like neural networks, information processing, chemical reactions, biological systems and quantum physics etc.

Chapter 7

Linear Generalized Unidirectional Synchronization

7.1 Introduction

Sprott model L [79] is a very simple chaotic dynamical system. It is bounded. This system has three parameters and one non-linear term. At present time, there are so many synchronization method to obtain a chaotic synchronized system, for example, feedback control [64], active control [91], adaptive control [81], open plus closed loop coupling method [72] etc. In this chapter, we will make a new chaotic system whose behavior is closely related to the behavior of the Sprott model L and we call the new chaotic system as synchronized system. This synchronization idea for a chaotic system was introduced by Pecora and Carroll [65] in 1990. After five years, Rulkov et.al. [73] generalized the concept of identical synchronization for unidirectionally coupled dynamical systems. Unidirectionally coupled systems

are given by

$$\left.\begin{aligned}\dot{\overrightarrow{X}} &= F(\overrightarrow{X}) \\ \dot{\overrightarrow{Y}} &= G(\overrightarrow{X}, \overrightarrow{Y})\end{aligned}\right\}$$

In this chapter, we are studying the unidirectionally coupled Sprott model L through linear transformation. Here, we will analyze the behavior of the synchronized system using numerical simulation.

7.2 Discussions of Linear Generalized Synchronization

In matrix form, any dynamical system can be written as

$$\dot{\overrightarrow{X}} = A\overrightarrow{X} + \phi(\overrightarrow{X}) \tag{7.2.1}$$

where A is a constant matrix of order $n \times n$, $\overrightarrow{X} \in \mathbb{R}^n$ and $\phi : \mathbb{R}^n \to \mathbb{R}^n$.

This system (7.2.1) is known as driving system. The response system is obtained by changing the term $\phi(\overrightarrow{X})$ and the unidirectional synchronization scheme is given by

$$\begin{aligned}\dot{\overrightarrow{X}} &= A\overrightarrow{X} + \phi(\overrightarrow{X}) \quad &: \text{Driving System} \\ \dot{\overrightarrow{Y}} &= A\overrightarrow{Y} + B\phi(\overrightarrow{X}) \quad &: \text{Response System}\end{aligned} \tag{7.2.2}$$

where B is a matrix of order $n \times n$.

The two dynamical systems in (7.2.2) are in a state of generalized synchronization through linear transformation

$$\overrightarrow{Y} = B\overrightarrow{X} \tag{7.2.3}$$

if and only if $AB = BA$ and all the eigen values of A have negative real parts [29].

For a given matrix A, we can evaluate the matrix B in many ways such that they commute each other. Hence, there is possibility to make several forms of linear generalized synchronization [67] between two chaotic systems.

In this chapter, we choose three types of B, such that $AB = BA$ holds, as follows :

1. B is a scalar matrix of the same order as A
2. $B =$ inverse of A
3. $B = A^n$, where n is a positive integer.

7.3 Generalized Synchronization of Sprott Model L

Here, we will construct the linear generalized synchronized system for the Sprott model L [50]. The dynamical system of Sprott model L is given by

$$\left.\begin{aligned} \dot{x_1} &= x_2 + \alpha x_3 \\ \dot{x_2} &= \beta x_1^2 - x_2 \\ \dot{x_3} &= \gamma - x_1 \end{aligned}\right\} \tag{7.3.4}$$

where α, β, γ are three positive parameters.

The system(7.3.4) can be written in the form of (7.2.1) as

$$\dot{\overrightarrow{X}} = A\overrightarrow{X} + \phi(\overrightarrow{X}) \tag{7.3.5}$$

where

$$A = \begin{pmatrix} -1 & 1 & 0 \\ 0 & -1 & 0 \\ 0 & 0 & -1 \end{pmatrix}, \quad \overrightarrow{X} = \begin{pmatrix} x_1 \\ x_2 \\ x_3 \end{pmatrix},$$

and

$$\phi(\overrightarrow{X}) = \begin{pmatrix} x_1 + \alpha x_3 \\ \beta x_1^2 \\ \gamma - x_1 + x_3 \end{pmatrix}$$

Obviously, A is negative definite matrix.
Therefore, all the eigen values of A are negative.
We consider the response system as

$$\dot{\overrightarrow{Y}} = A\overrightarrow{Y} + B\phi(\overrightarrow{X}) \tag{7.3.6}$$

The driving system of Sprott model L (7.3.5) and the response system of Sprott model L (7.3.6) are in a state of generalized synchronization if $AB = BA$.

7.4 Results and Discussions

In this section, we will get simulation results for different forms of B. Sprott found that the system (7.3.4) is chaotic when $\alpha = 3.9$, $\beta = 0.9$ and $\gamma = 1$.
To solve the coupled driving and response Sprott model L, we will use Runge-Kutta method of fourth order.
$(0.25, 0, -0.25)$ and $(0, 0.25, -0.25)$ are the initial conditions for the driving system and the response system respectively.

Case-I : Let us consider

$$B = \begin{pmatrix} k & 0 & 0 \\ 0 & k & 0 \\ 0 & 0 & k \end{pmatrix},$$

where k($\neq 0$) is a real number.

Therefore, all the conditions for synchronization are satisfied since $AB = BA$.

In this case, the driving system is of the form (7.3.4) and the response system of Sprott model L is given by

$$\begin{pmatrix} \dot{y_1} \\ \dot{y_2} \\ \dot{y_3} \end{pmatrix} = \begin{pmatrix} -1 & 1 & 0 \\ 0 & -1 & 0 \\ 0 & 0 & -1 \end{pmatrix} \begin{pmatrix} y_1 \\ y_2 \\ y_3 \end{pmatrix} + \begin{pmatrix} k & 0 & 0 \\ 0 & k & 0 \\ 0 & 0 & k \end{pmatrix} \begin{pmatrix} x_1 + \alpha x_3 \\ \beta x_1^2 \\ \gamma - x_1 + x_3 \end{pmatrix}$$

It gives,

$$\left.\begin{aligned} \dot{y_1} &= -y_1 + y_2 + k(x_1 + \alpha x_3) \\ \dot{y_2} &= -y_2 + k\beta x_1^2 \\ \dot{y_3} &= -y_3 + k(\gamma - x_1 + x_3) \end{aligned}\right\} \tag{7.4.7}$$

where $\overrightarrow{Y} = (y_1, y_2, y_3)^t$.

The simulation results are shown in figure (7.1), figure (7.2) and figure (7.3).

The state variables of the driving system and the response system

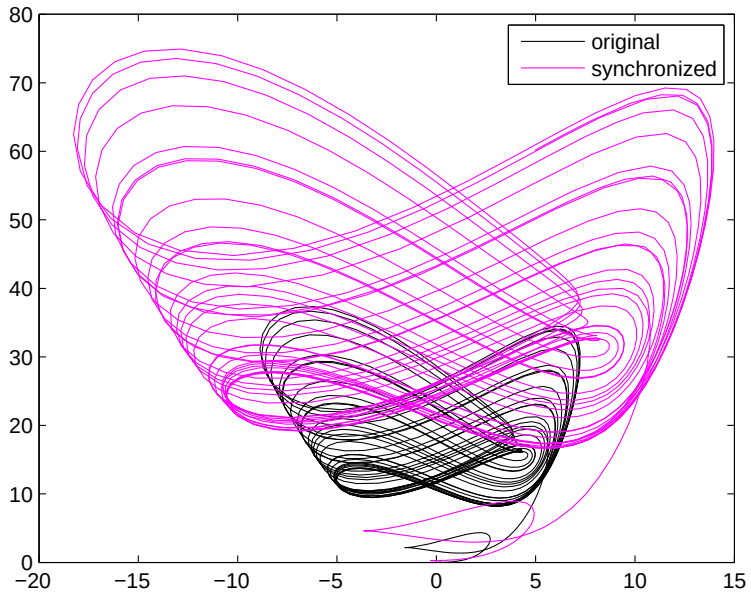

Figure 7.1: Simulation 1: $x_1 \ \ vs \ \ x_2 \ \ \& \ \ y_1 \ \ vs \ \ y_2$

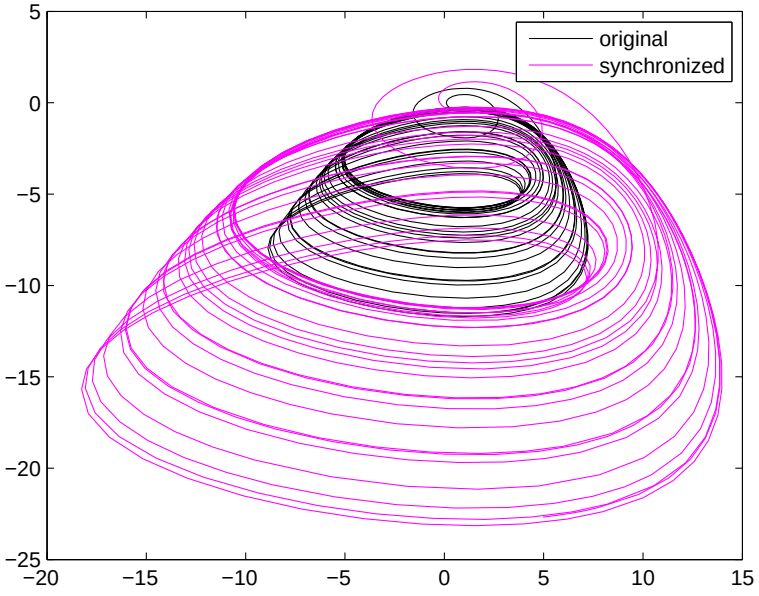

Figure 7.2: Simulation 1: $x_1 \ \ vs \ \ x_3 \ \ \& \ \ y_1 \ \ vs \ \ y_3$

are connected by the linear transformation as

$$\left.\begin{aligned} y_1 &= kx_1 \\ y_2 &= kx_2 \\ y_3 &= kx_3 \end{aligned}\right\} \quad \text{with k=2} \tag{7.4.8}$$

Case-II : In this case, we consider,

$$B = A^{-1} = \begin{pmatrix} -1 & -1 & 0 \\ 0 & -1 & 0 \\ 0 & 0 & -1 \end{pmatrix},$$

satisfying the condition $AB = BA$.

The response system of Sprott model L is given by

$$\begin{pmatrix} \dot{y_1} \\ \dot{y_2} \\ \dot{y_3} \end{pmatrix} = \begin{pmatrix} -1 & 1 & 0 \\ 0 & -1 & 0 \\ 0 & 0 & -1 \end{pmatrix} \begin{pmatrix} y_1 \\ y_2 \\ y_3 \end{pmatrix} + \begin{pmatrix} -1 & -1 & 0 \\ 0 & -1 & 0 \\ 0 & 0 & -1 \end{pmatrix} \begin{pmatrix} x_1 + \alpha x_3 \\ \beta x_1^2 \\ \gamma - x_1 + x_3 \end{pmatrix}$$

which gives,

$$\left.\begin{aligned} \dot{y_1} &= -y_1 + y_2 - x_1 - \alpha x_3 - \beta x_1^2 \\ \dot{y_2} &= -y_2 - \beta x_1^2 \\ \dot{y_3} &= -y_3 - \gamma + x_1 - x_3 \end{aligned}\right\} \tag{7.4.9}$$

where $\overrightarrow{Y} = (y_1, y_2, y_3)^t$.

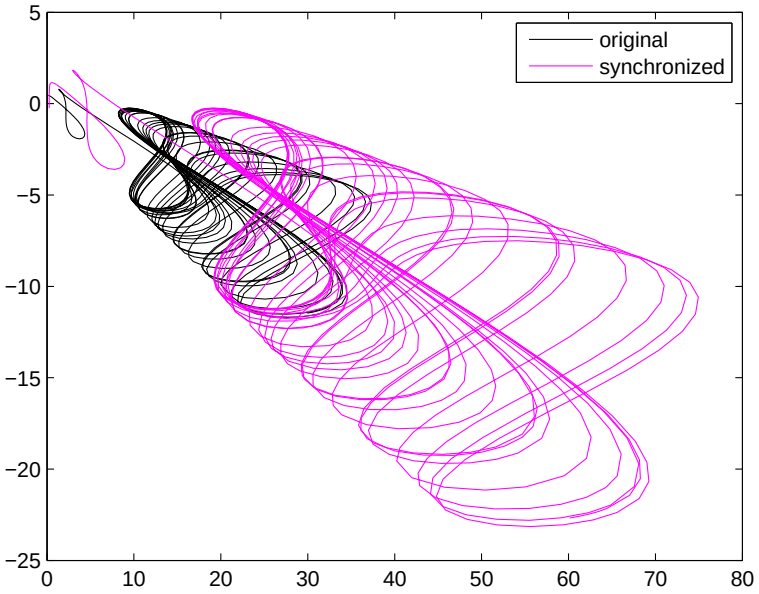

Figure 7.3: Simulation 1: x_2 vs x_3 & y_2 vs y_3

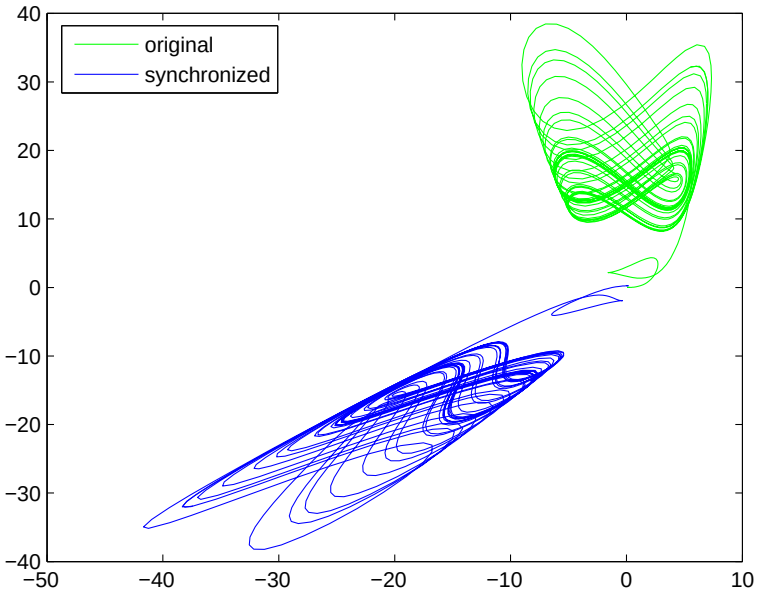

Figure 7.4: Simulation 2: x_1 vs x_2 & y_1 vs y_2

and the corresponding linear transformation is

$$\left.\begin{aligned} y_1 &= -x_1 - x_2 \\ y_2 &= -x_2 \\ y_3 &= -x_3 \end{aligned}\right\} \tag{7.4.10}$$

In this case, figure (7.4), figure (7.5) and figure (7.6) represent the simulation results.

Case-III : Let us take

$$B = A^n = p\begin{pmatrix} 1 & -n & 0 \\ 0 & 1 & 0 \\ 0 & 0 & 1 \end{pmatrix},$$

where $p = (-1)^n$.
Clearly, $AB = BA$.

Hence, the response system of Sprott model L is evaluated as

$$\begin{pmatrix} \dot{y_1} \\ \dot{y_2} \\ \dot{y_3} \end{pmatrix} = \begin{pmatrix} -1 & 1 & 0 \\ 0 & -1 & 0 \\ 0 & 0 & -1 \end{pmatrix}\begin{pmatrix} y_1 \\ y_2 \\ y_3 \end{pmatrix} + \begin{pmatrix} p & -np & 0 \\ 0 & p & 0 \\ 0 & 0 & p \end{pmatrix}\begin{pmatrix} x_1 + \alpha x_3 \\ \beta x_1^2 \\ \gamma - x_1 + x_3 \end{pmatrix}$$

It yields,

$$\left.\begin{aligned} \dot{y_1} &= -y_1 + y_2 + p(x_1 + \alpha x_3 - n\beta x_1^2) \\ \dot{y_2} &= -y_2 + p\beta x_1^2 \\ \dot{y_3} &= -y_3 + p(\gamma - x_1 + x_3) \end{aligned}\right\} \tag{7.4.11}$$

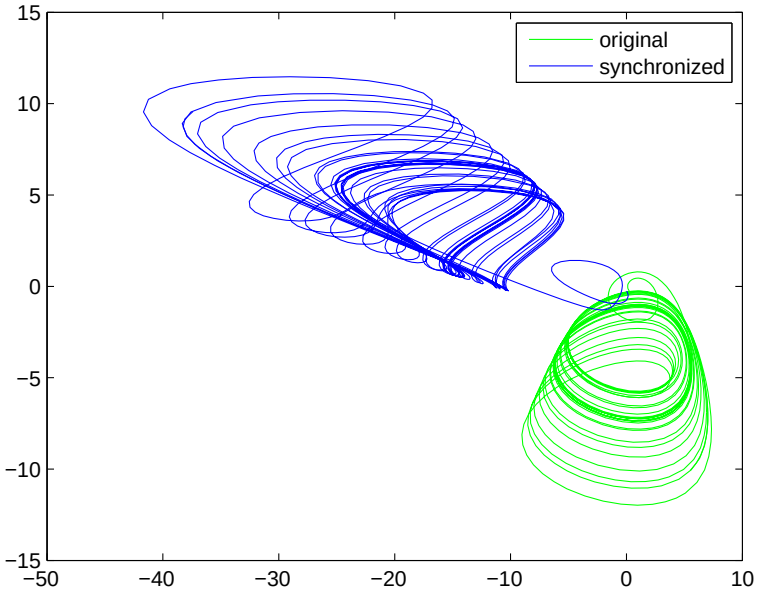

Figure 7.5: Simulation 2: x_1 vs x_3 & y_1 vs y_3

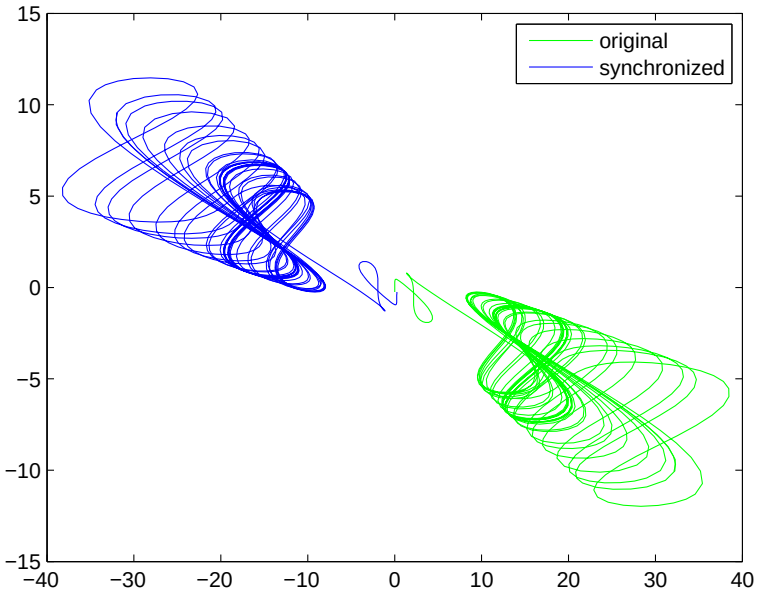

Figure 7.6: Simulation 2: x_2 vs x_3 & y_2 vs y_3

where $\overrightarrow{Y} = (y_1, y_2, y_3)^t$.
and the corresponding linear transformation is

$$\left.\begin{aligned} y_1 &= px_1 - npx_2 \\ y_2 &= px_2 \\ y_3 &= px_3 \end{aligned}\right\} \tag{7.4.12}$$

where, $p = (-1)^n$.

For $n = 1$, the simulation results are shown in figure (7.7), figure (7.8) and figure (7.9).

For $n = 2$, figure (7.10), figure (7.11) and figure (7.12) represent the corresponding simulation results.

In this method, one can easily find the functional relationship between the states of the driving system and the response system. Hence, the behavior of the response system can be obtained in advance by knowing the behavior of the driving system. Again, the matrix associated with linear transformation being invertible, the behavior of the driving system can be determined by knowing the behavior of the response system. This synchronization method is very useful to apply in secure communication, electronic circuits, biological systems, chemical system, information processing, engineering etc. and it is also useful to study in non-linear dynamics.

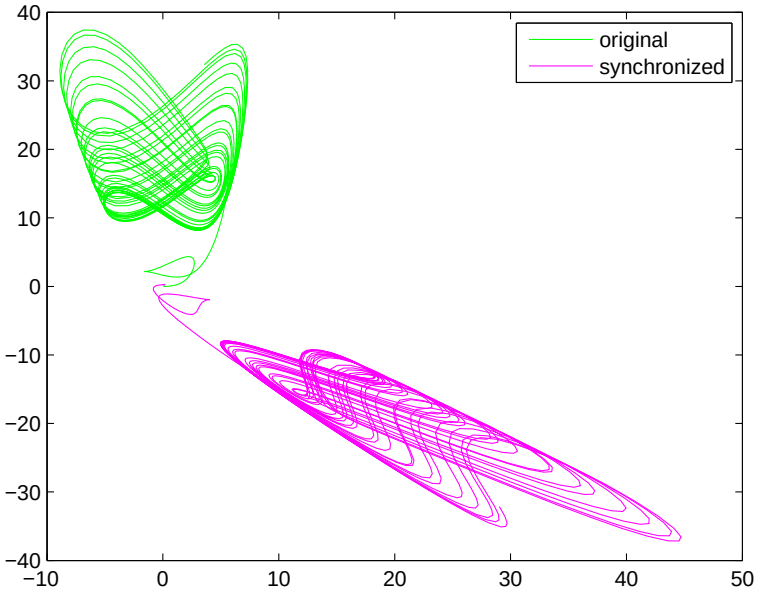

Figure 7.7: Simulation 3: $x_1 \;\; vs \;\; x_2 \;\; \& \;\; y_1 \;\; vs \;\; y_2$

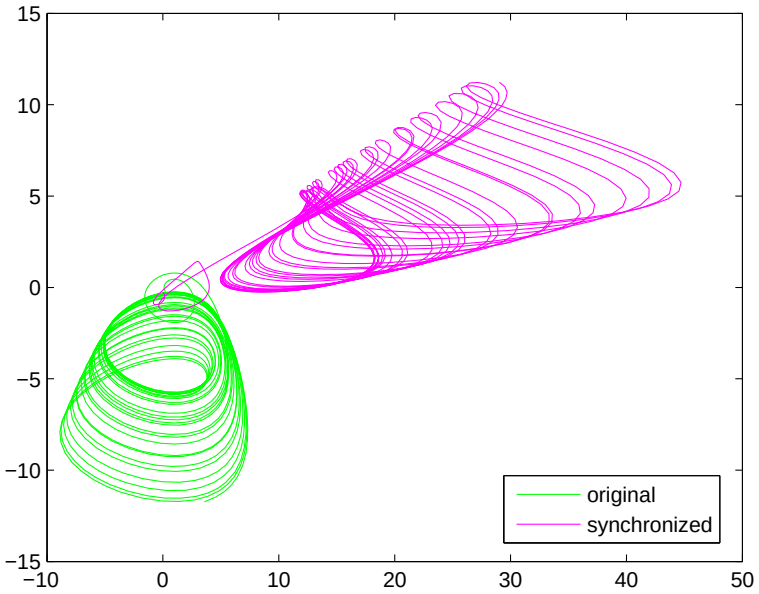

Figure 7.8: Simulation 3: $x_1 \;\; vs \;\; x_3 \;\; \& \;\; y_1 \;\; vs \;\; y_3$

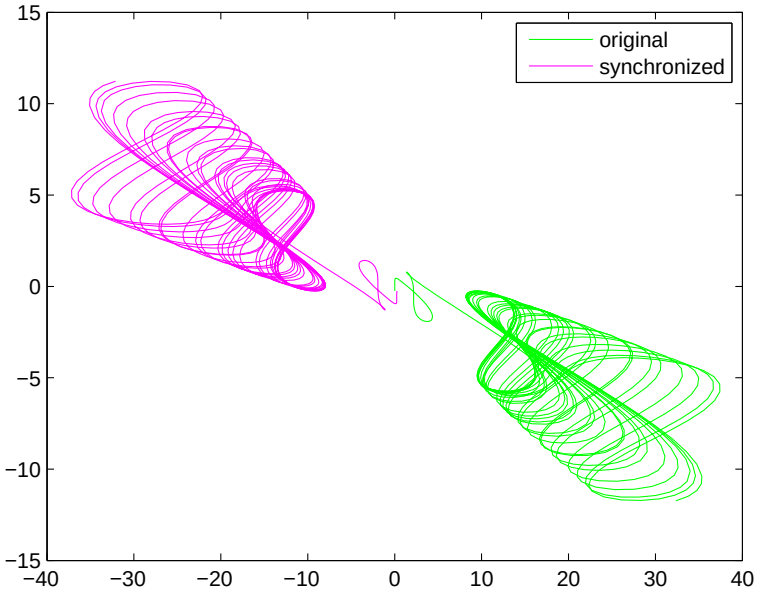

Figure 7.9: Simulation 3: $x_2 \ \ vs \ \ x_3 \ \ \& \ \ y_2 \ \ vs \ \ y_3$

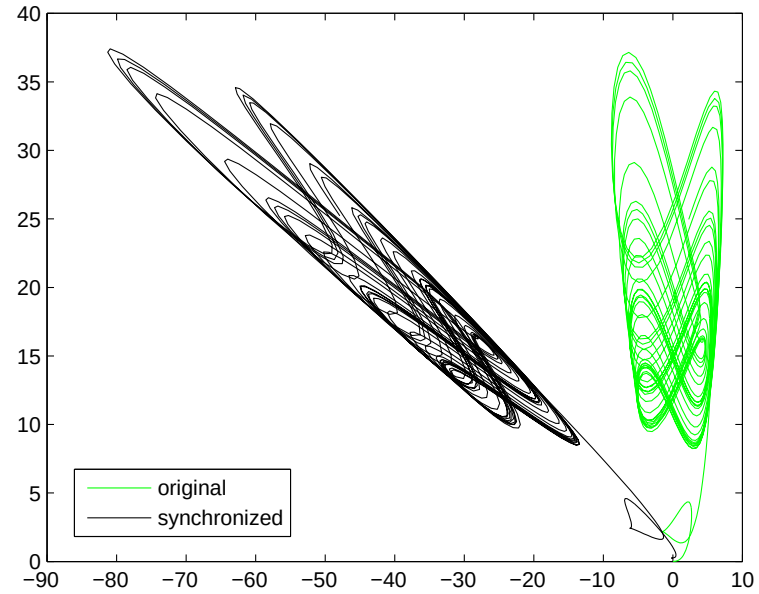

Figure 7.10: Simulation 4: $x_1 \ \ vs \ \ x_2 \ \ \& \ \ y_1 \ \ vs \ \ y_2$

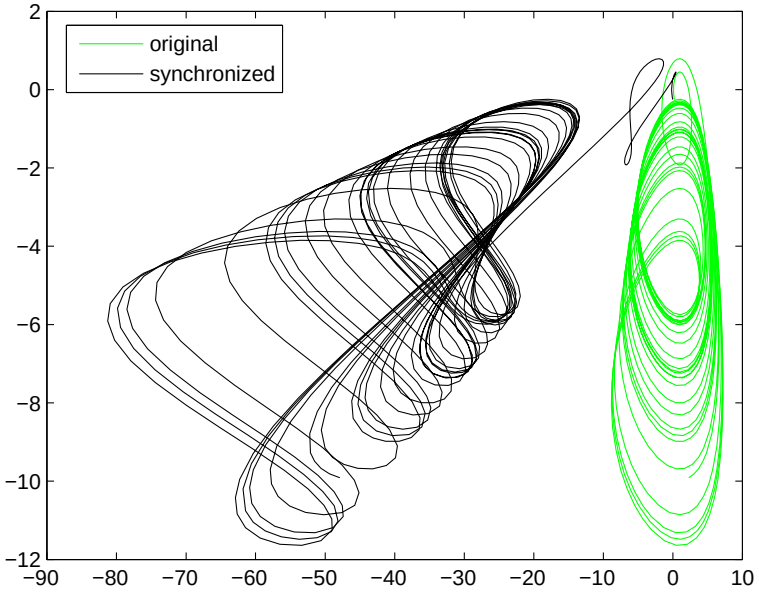

Figure 7.11: Simulation 4: $x_1 \ \ vs \ \ x_3 \ \ \& \ \ y_1 \ \ vs \ \ y_3$

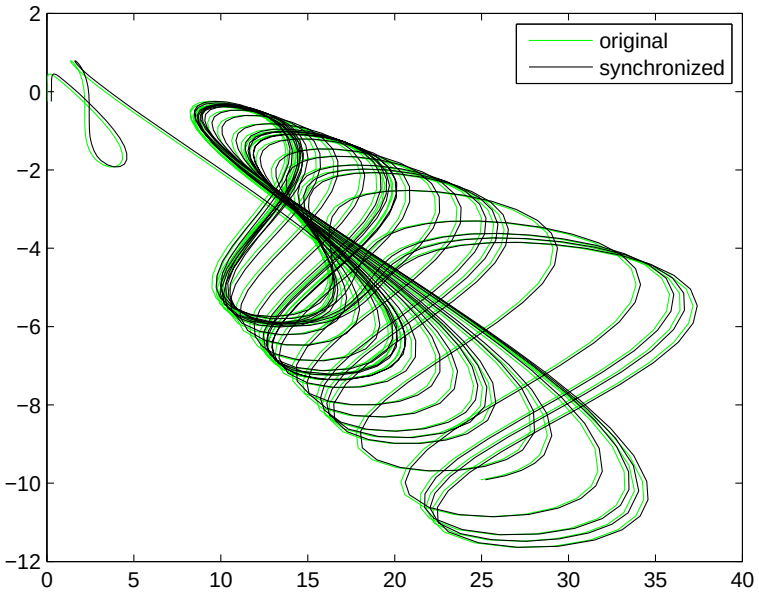

Figure 7.12: Simulation 4: $x_2 \ \ vs \ \ x_3 \ \ \& \ \ y_2 \ \ vs \ \ y_3$

Chapter 8

Generalized Synchronization of Nonlinear Oscillators via OPCL Coupling

8.1 Introduction

Currently, there are many well-known control methods to stabilize non-linear chaotic dynamical systems. Out of all those control methods ([1],[4],[39],[44],[60],[76] and [84]), open-plus-closed-loop control method [72] is the most efficient method to make generalized synchronization (GS) for a coupled dynamical systems. This proposed method is insensitive with respect to system parameters which is one of the advantages of this method. This is a combination of open-loop system and closed-loop system. Open-loop means feed forward and closed-loop means feed backward. This combination gives us more flexibility to control and stabilize the dynamical systems. Using this method, the error term which is the difference between actual output and required output, reduces automatically by adjusting the system inputs. In this method, we are dealing with two systems

known as master (drive) system and slave (response) system. Let $x = (x_1, x_2, x_3, ..., x_n)^T \in \mathbb{R}^n$ be the state variable of the master system and $y = (y_1, y_2, y_3, ..., y_n)^T \in \mathbb{R}^n$ be the state variable of the slave system. There exists another state known as goal state. Our aim is to reduce the difference between the goal system and slave system. Goal system depends on the master system such that $\sigma = Kx$, where $\sigma = (\sigma_1, \sigma_2, \sigma_3, ..., \sigma_n)^T \in \mathbb{R}^n$, the state variable of the goal system and K is a transformation matrix of order n, chosen arbitrarily. Here, in this communication, we will choose five different forms of the matrix K. In section 3, we will study five different cases corresponding to different forms of the matrix K. In the first case, the elements of K are taken constants. In case-II, periodic functions are considered as the elements of K-matrix. The state variables of the master system will be taken as the elements of K-matrix in case-III. For the next case, the elements of K-matrix are taken as the state variables of the other dynamical system. Finally, in case-V, discussion is made where one dynamical system drives another dynamical system which is totally different in nature with the former dynamical system along with the K-matrix whose elements are the state variables of the other dynamical system. This last case is the most interesting part of this chapter. Open-plus-closed-loop coupling method is very useful in engineering science, chemical reactions, quantum physics, lasers, electronic circuits, secure communication, microwave oscillators, electrical cloth drier etc.

8.2 Description of OPCL Controller for GS

To describe this method, let us take a non-linear dynamical system as the master system given below:

$$\dot{x} = \phi(x) \tag{8.2.1}$$

where x ($\in \mathbb{R}^n$) is the state variable of the master system and $\phi : \mathbb{R}^n \to \mathbb{R}^n$.
Next, we consider the slave system given by the following dynamics

$$\dot{y} = \psi(y) + u \tag{8.2.2}$$

where y ($\in \mathbb{R}^n$) is the state variable of the slave system and $\psi : \mathbb{R}^n \to \mathbb{R}^n$ and u is the control input.

Let the generalized synchronization error e be defined as

$$\begin{aligned} e &= y - Kx \\ or, \quad y &= \sigma + e, \quad where \quad \sigma = Kx. \end{aligned} \tag{8.2.3}$$

Now, using Taylor's expansion of a function, we have from equations (8.2.2) & (8.2.3)

$$\begin{aligned} \dot{y} &= \psi(\sigma + e) + u \\ &= \psi(\sigma) + \frac{\partial \psi(\sigma)}{\partial \sigma} e + u, \end{aligned}$$

neglecting second and higher orders of e to be very small.
Therefore,

$$\dot{y} = \psi(\sigma) + J(\sigma)e + u, \tag{8.2.4}$$

where $J(\sigma)$ is the Jacobian of the flow $\psi(\sigma)$.
Let us define ,

$$u = \dot{\sigma} - \psi(\sigma) + \mu e, \quad where \quad \mu = V - J(\sigma) \tag{8.2.5}$$

and V is a matrix of order n.
Using (8.2.4) and (8.2.5), one gets easily

$$\dot{e} = Ve \tag{8.2.6}$$

which gives the error dynamics.

Now, the error dynamics (8.2.6) is globally asymptotically stable if V-matrix is Hurwitz.

Hence, we can conclude that generalized synchronization between the system (8.2.1) and (8.2.2) does not depend on K-matrix, it depends on the V-matrix. In this communication, we are choosing the elements of the V-matrix are similar to the elements of the Jacobian matrix of the slave system except all those elements which carry the state variables of the slave system. In this situation, we take constant value $w_i (i = 1, 2, 3, ...)$ instead of the state variable of the slave system for which V-matrix is Hurwitz, i.e., all the eigen values of V have negative real parts. Accordingly the error dynamics (8.2.6) is globally asymptotically stable. Finally, we claim that the generalized synchronization of the master-slave system is made successfully.

8.3 Examples of GS using OPCL Controller

Case-I : According to previous section 8.2, we first consider a nonlinear chaotic Sprott system L as the master system given by

$$\dot{x} = \phi(x), \quad x \in \mathbb{R}^3 \tag{8.3.7}$$

where

$$\phi(x) = \begin{pmatrix} x_2 + a_1 x_3 \\ b_1 x_1^2 - x_2 \\ c_1 - x_1 \end{pmatrix}, \quad a_1, \ \ b_1 \ \ \& \ \ c_1 \ \ are \ \ the \ \ parameters.$$

The slave system is taken as the mismatch Sprott system L

$$\dot{y} = \psi(y) + u, \quad y \in \mathbb{R}^3 \tag{8.3.8}$$

where

$$\psi(y) = \begin{pmatrix} y_2 + a_2 y_3 \\ b_2 y_1^2 - y_2 \\ c_2 - y_1 \end{pmatrix}, \quad a_2, \quad b_2 \ \& \ c_2 \ \textit{are the parameters}$$

and $u = (u_1, u_2, u_3)^t \in \mathbb{R}^3$ is the controller.
Let

$$K = \begin{pmatrix} 1 & -0.8 & -2.7 \\ 0 & 0.5 & -2.3 \\ 0.5 & 0 & 0.7 \end{pmatrix}$$

Using $\sigma = Kx$, we have the goal dynamics as

$$\begin{pmatrix} \dot{\sigma_1} \\ \dot{\sigma_2} \\ \dot{\sigma_3} \end{pmatrix} = \begin{pmatrix} 1 & -0.8 & -2.7 \\ 0 & 0.5 & -2.3 \\ 0.5 & 0 & 0.7 \end{pmatrix} \begin{pmatrix} \dot{x_1} \\ \dot{x_2} \\ \dot{x_3} \end{pmatrix}$$

which yields,

$$\left.\begin{aligned} \dot{\sigma_1} &= \dot{x_1} - 0.8\dot{x_2} - 2.7\dot{x_3} \\ \dot{\sigma_2} &= 0.5\dot{x_2} - 2.3\dot{x_3} \\ \dot{\sigma_3} &= 0.5\dot{x_1} + 0.7\dot{x_3} \end{aligned}\right\} \tag{8.3.9}$$

The Jacobian matrix of the slave system is given by

$$J(y) = \begin{pmatrix} 0 & 1 & a_2 \\ 2b_2 y_1 & -1 & 0 \\ -1 & 0 & 0 \end{pmatrix}$$

Then, V can be taken as,

$$V = \begin{pmatrix} 0 & 1 & a_2 \\ 2b_2w_1 & -1 & 0 \\ -1 & 0 & 0 \end{pmatrix},$$

where w_1 is chosen arbitrarily so that V is Hurwitz.

Hence, from equation (8.2.6), the error dynamics becomes

$$\left.\begin{aligned} \dot{e_1} &= e_2 + a_2e_3 \\ \dot{e_2} &= 2b_2w_1e_1 - e_2 \\ \dot{e_3} &= -e_1 \end{aligned}\right\} \tag{8.3.10}$$

Then, one can easily obtain,

$$\mu = \begin{pmatrix} 0 & 0 & 0 \\ 2b_2(w_1 - \sigma_1) & 0 & 0 \\ 0 & 0 & 0 \end{pmatrix},$$

where w_1 is chosen arbitrarily so that V is Hurwitz.

Now, using (8.2.5), the control input u is found as

$$\begin{pmatrix} u_1 \\ u_2 \\ u_3 \end{pmatrix} = \begin{pmatrix} \dot{\sigma_1} \\ \dot{\sigma_2} \\ \dot{\sigma_3} \end{pmatrix} - \begin{pmatrix} \sigma_2 + a_2\sigma_3 \\ b_2\sigma_1^2 - \sigma_2 \\ c_2 - \sigma_1 \end{pmatrix} + \begin{pmatrix} 0 & 0 & 0 \\ 2b_2(w_1 - \sigma_1) & 0 & 0 \\ 0 & 0 & 0 \end{pmatrix} \begin{pmatrix} e_1 \\ e_2 \\ e_3 \end{pmatrix}$$

which yields,

$$\left.\begin{aligned} u_1 &= \dot{\sigma_1} - \sigma_2 - a_2\sigma_3 \\ u_2 &= \dot{\sigma_2} - b_2\sigma_1^2 + \sigma_2 + 2b_2(w_1 - \sigma_1)e_1 \\ u_3 &= \dot{\sigma_3} - c_2 + \sigma_1 \end{aligned}\right\} \tag{8.3.11}$$

Case-II : Here, the master system and the slave system are taken to be same as the system (8.3.7) & (8.3.8) respectively.

In this case, K is taken to be a 3×3 matrix with periodic function as its elements given below :

$$K = \begin{pmatrix} 0 & -0.2cos(0.6t) & 3.5 \\ 1 & 1 & 0 \\ -sin(0.1t) & -0.5 & 0 \end{pmatrix}$$

Thus, we have the goal dynamics as

$$\dot{\sigma} = K\dot{x} + \dot{K}x,$$

or,

$$\begin{pmatrix} \dot{\sigma_1} \\ \dot{\sigma_2} \\ \dot{\sigma_3} \end{pmatrix} = \begin{pmatrix} 0 & -0.2cos(0.6t) & 3.5 \\ 1 & 1 & 0 \\ -sin(0.1t) & -0.5 & 0 \end{pmatrix} \begin{pmatrix} \dot{x_1} \\ \dot{x_2} \\ \dot{x_3} \end{pmatrix} + \begin{pmatrix} 0 & 0.12sin(0.6t) & 0 \\ 0 & 0 & 0 \\ -0.1cos(0.1t) & 0 & 0 \end{pmatrix} \begin{pmatrix} x_1 \\ x_2 \\ x_3 \end{pmatrix}$$

which yields

$$\left.\begin{aligned} \dot{\sigma_1} &= -0.2cos(0.6t)\dot{x_2} + 3.5\dot{x_3} + 0.12sin(0.6t)x_2 \\ \dot{\sigma_2} &= \dot{x_1} + \dot{x_2} \\ \dot{\sigma_3} &= -sin(0.1t)\dot{x_1} - 0.5\dot{x_2} - 0.1cos(0.1t)x_1 \end{aligned}\right\} \qquad (8.3.12)$$

The error dynamics is same as the previous case, because the Jacobian matrix of the slave system remains the same.

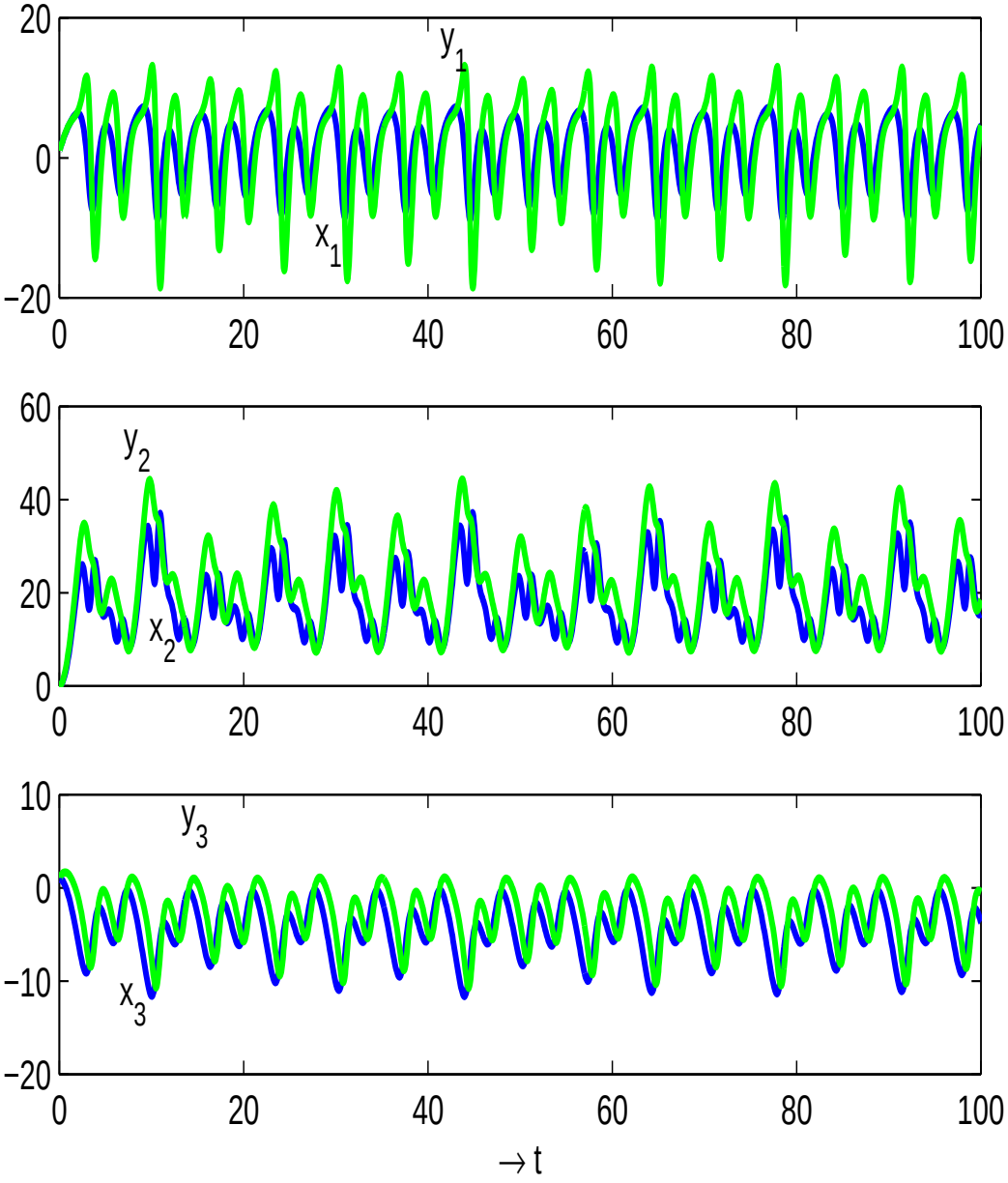

Figure 8.1: Case-I: master system (x) & slave system (y) with respect to time

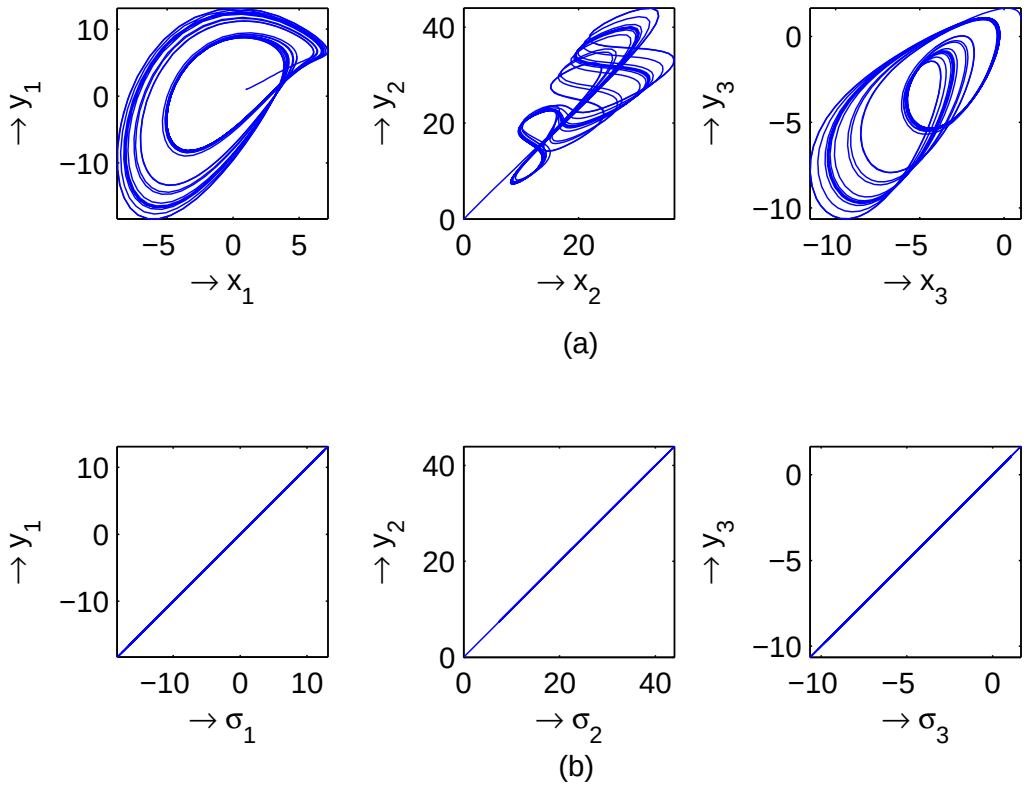

Figure 8.2: Case-I: (a) x vs y plot (b) σ vs y plot

Hence, using (8.2.5), the control input u is given by

$$\left.\begin{aligned} u_1 &= \dot{\sigma_1} - \sigma_2 - a_2\sigma_3 \\ u_2 &= \dot{\sigma_2} - b_2\sigma_1^2 + \sigma_2 + 2b_2(w_1 - \sigma_1)e_1 \\ u_3 &= \dot{\sigma_3} - c_2 + \sigma_1 \end{aligned}\right\} \tag{8.3.13}$$

Case- III : Let K be a 3×3 matrix containing the state variables of the master system (8.3.7) as its elements and the slave system remains unchanged,
where

$$K = \begin{pmatrix} 1 & 0.03x_1 & 0 \\ -0.02x_1 & -0.1x_3 & 0 \\ 0 & 0.01x_2 & 0 \end{pmatrix}$$

Then, the system of goal dynamics is obtained as

$$\begin{pmatrix} \dot{\sigma_1} \\ \dot{\sigma_2} \\ \dot{\sigma_3} \end{pmatrix} = \begin{pmatrix} 1 & 0.03x_1 & 0 \\ -0.02x_1 & -0.1x_3 & 0 \\ 0 & 0.01x_2 & 0 \end{pmatrix} \begin{pmatrix} \dot{x_1} \\ \dot{x_2} \\ \dot{x_3} \end{pmatrix} + \begin{pmatrix} 0 & 0.03\dot{x_1} & 0 \\ -0.02\dot{x_1} & -0.1\dot{x_3} & 0 \\ 0 & 0.01\dot{x_2} & 0 \end{pmatrix} \begin{pmatrix} x_1 \\ x_2 \\ x_3 \end{pmatrix}$$

which yields

$$\left.\begin{aligned} \dot{\sigma_1} &= \dot{x_1} + 0.03(\dot{x_1}x_2 + x_1\dot{x_2}) \\ \dot{\sigma_2} &= -0.04x_1\dot{x_1} - 0.1(\dot{x_3}x_2 + x_3\dot{x_2}) \\ \dot{\sigma_3} &= 0.02\dot{x_2}x_2 \end{aligned}\right\} \tag{8.3.14}$$

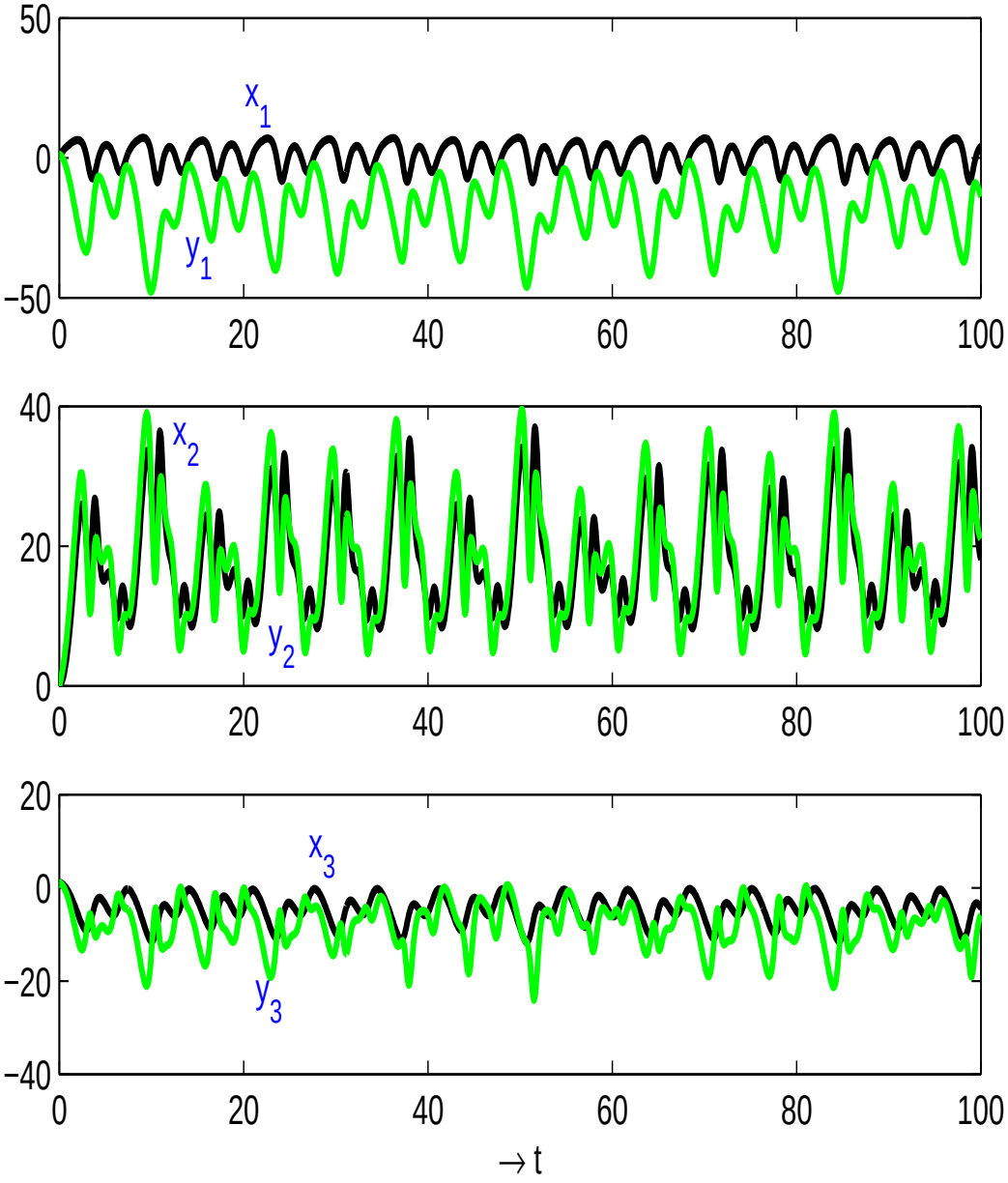

Figure 8.3: Case-II: master system (x) & slave system (y) with respect to time

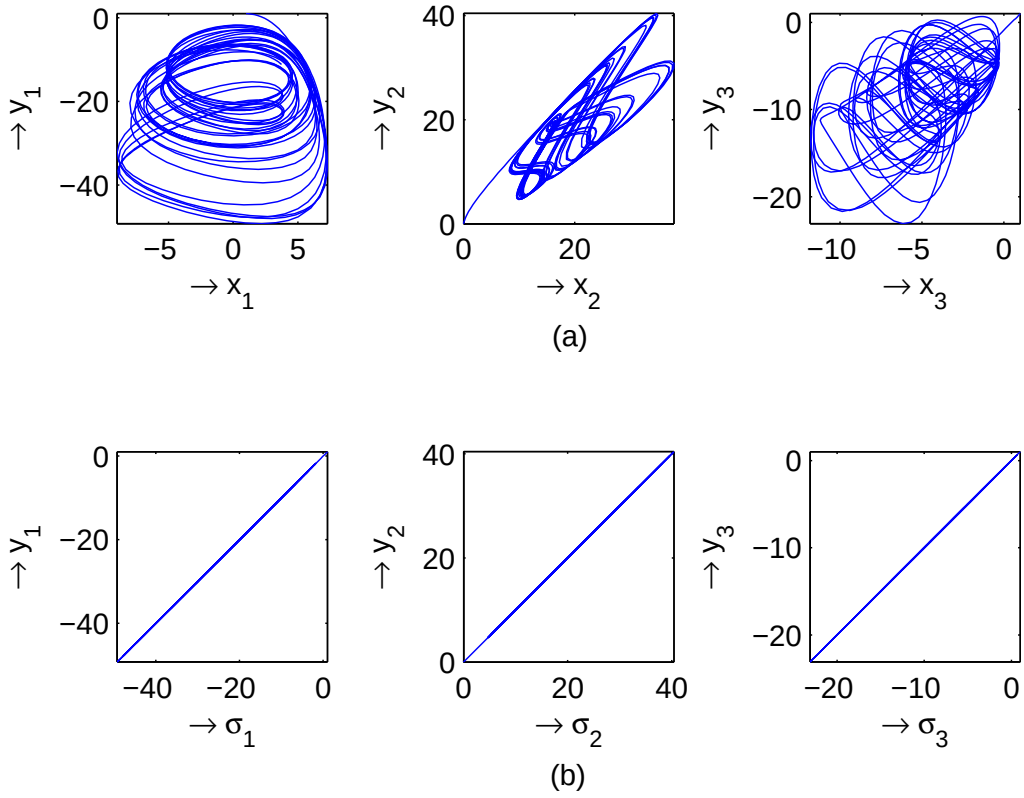

Figure 8.4: Case-II: (a) x vs y plot (b) σ vs y plot

Here, the error dynamics remains similar as the previous case and the controller u as follows :

$$\left.\begin{aligned} u_1 &= \dot{\sigma_1} - \sigma_2 - a_2\sigma_3 \\ u_2 &= \dot{\sigma_2} - b_2\sigma_1^2 + \sigma_2 + 2b_2(w_1 - \sigma_1)e_1 \\ u_3 &= \dot{\sigma_3} - c_2 + \sigma_1 \end{aligned}\right\} \tag{8.3.15}$$

Case- IV : In this case, the elements of K-matrix are chosen so that it contains the state variables of Shimizu-Morioka system whereas the master-slave system are taken to be the mismatched coupled Sprott system L given by the system (8.3.7) & (8.3.8).

The Shimizu-Morioka system [29] is given by

$$\left.\begin{aligned} \dot{z_1} &= \delta z_2 \\ \dot{z_2} &= \delta(z_1 - \lambda z_2 - z_1 z_3) \\ \dot{z_3} &= \delta(-\rho z_3 + z_1^2), \end{aligned}\right\} \tag{8.3.16}$$

where λ & ρ are the positive parameters and $\delta = 0.02$ for which the original system of equation is slightly being changed without loss of generality.

Let

$$K = \begin{pmatrix} -3.5z_2 & 0 & 0 \\ 0 & 0.1z_1 & 3 \\ -1 & 0 & 2.7z_3 \end{pmatrix}$$

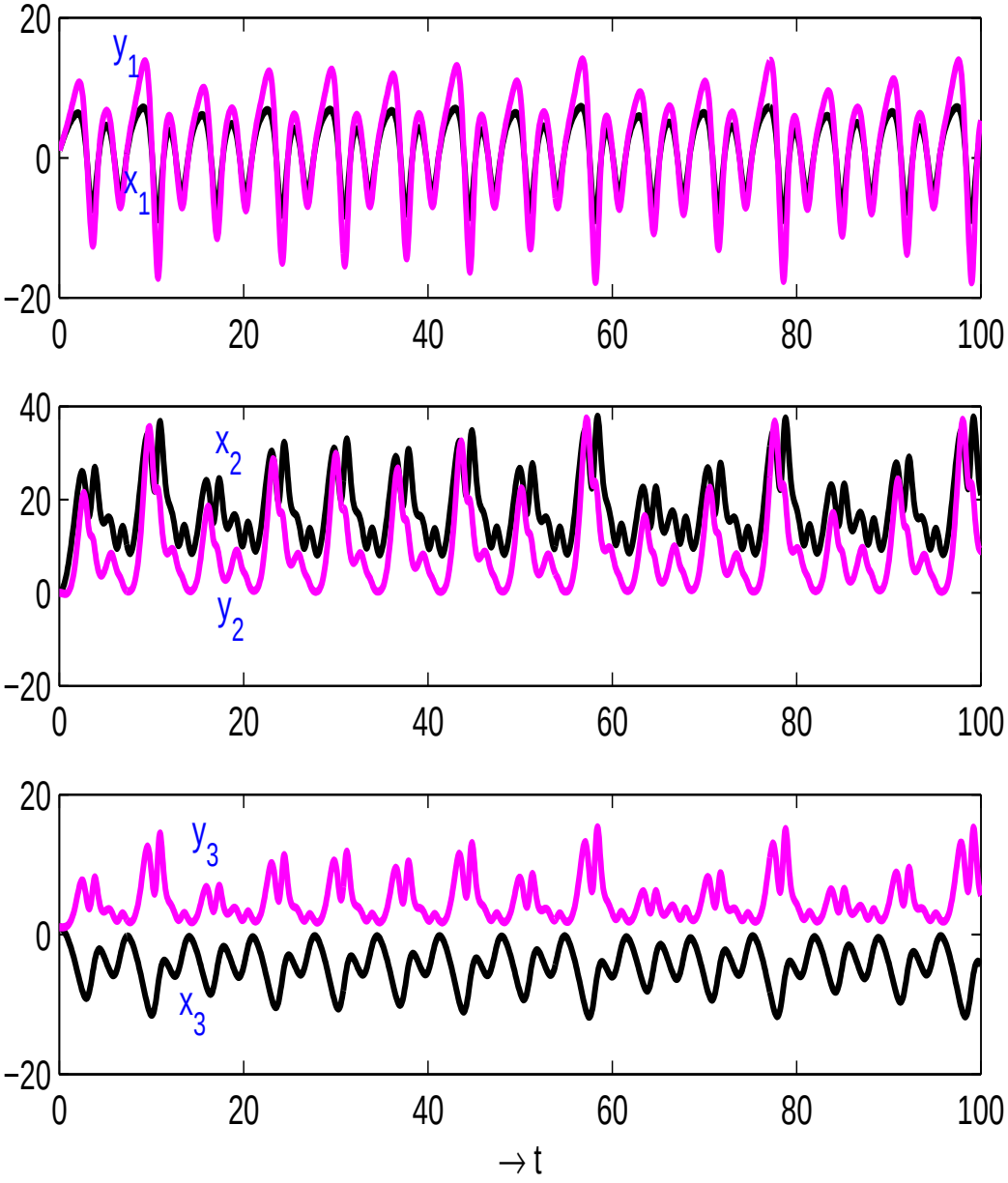

Figure 8.5: Case-III: master system (x) & slave system (y) with respect to time

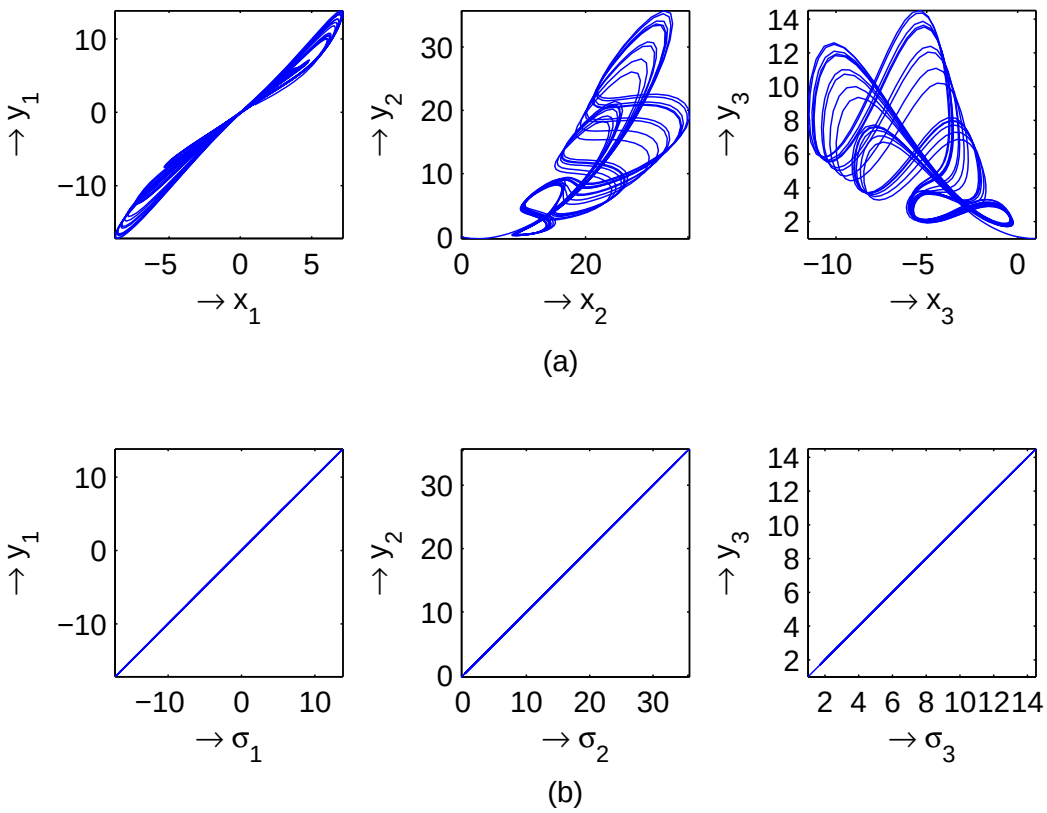

Figure 8.6: Case-III: (a) x vs y plot (b) σ vs y plot

Then, the goal dynamics is found as

$$\begin{pmatrix} \dot{\sigma_1} \\ \dot{\sigma_2} \\ \dot{\sigma_3} \end{pmatrix} = \begin{pmatrix} -3.5z_2 & 0 & 0 \\ 0 & 0.1z_1 & 3 \\ -1 & 0 & 2.7z_3 \end{pmatrix} \begin{pmatrix} \dot{x_1} \\ \dot{x_2} \\ \dot{x_3} \end{pmatrix} + \begin{pmatrix} -3.5\dot{z_2} & 0 & 0 \\ 0 & 0.1\dot{z_1} & 0 \\ 0 & 0 & 2.7\dot{z_3} \end{pmatrix} \begin{pmatrix} x_1 \\ x_2 \\ x_3 \end{pmatrix}$$

which yields

$$\left.\begin{aligned} \dot{\sigma_1} &= -3.5(\dot{x_1}z_2 + x_1\dot{z_2}) \\ \dot{\sigma_2} &= 3\dot{x_3} + 0.1(\dot{z_1}x_2 + z_1\dot{x_2}) \\ \dot{\sigma_3} &= -\dot{x_1} + 2.7(\dot{x_3}z_3 + x_3\dot{z_3}) \end{aligned}\right\} \tag{8.3.17}$$

Using (8.3.17) and (8.2.5), we get the controller u as,

$$\left.\begin{aligned} u_1 &= \dot{\sigma_1} - \sigma_2 - a_2\sigma_3 \\ u_2 &= \dot{\sigma_2} - b_2\sigma_1^2 + \sigma_2 + 2b_2(w_1 - \sigma_1)e_1 \\ u_3 &= \dot{\sigma_3} - c_2 + \sigma_1 \end{aligned}\right\} \tag{8.3.18}$$

where $e = (e_1, e_2, e_3)^t \in \mathbb{R}^3$, the state variables of the error system (8.3.10).

Case- V : Here, Rikitake system drives Sprott L system (8.3.8) with transformation matrix K consisting state variables of Rössler system.

The non-linear Rikitake system [31] considered as the master system given by

$$\left.\begin{aligned} \dot{r_1} &= \alpha r_1 + r_2 r_3 \\ \dot{r_2} &= -\alpha r_2 + (r_3 - \beta)r_1 \\ \dot{r_3} &= 1 - r_1 r_2 \end{aligned}\right\}, \tag{8.3.19}$$

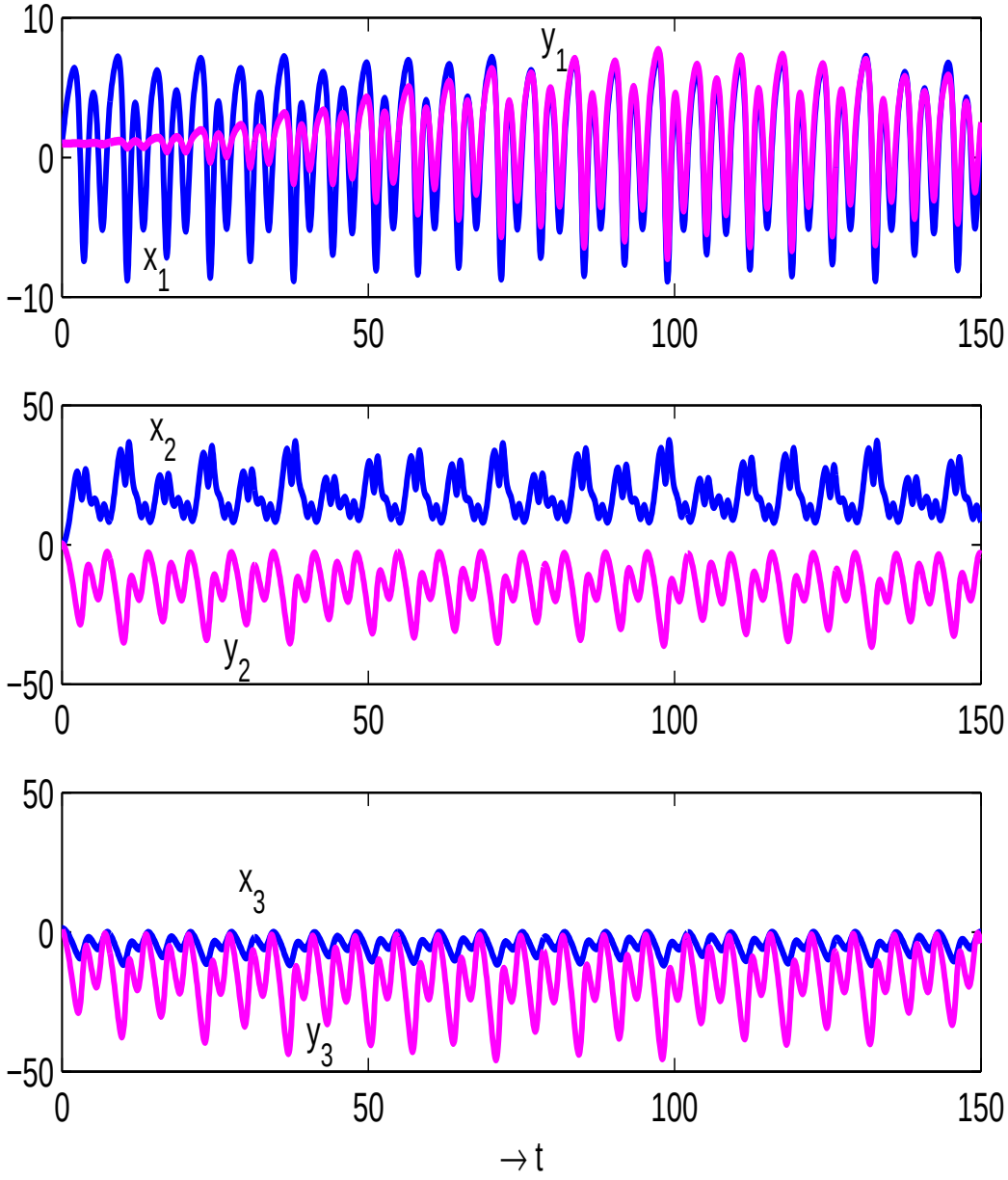

Figure 8.7: Case-IV: master system (x) & slave system (y) with respect to time

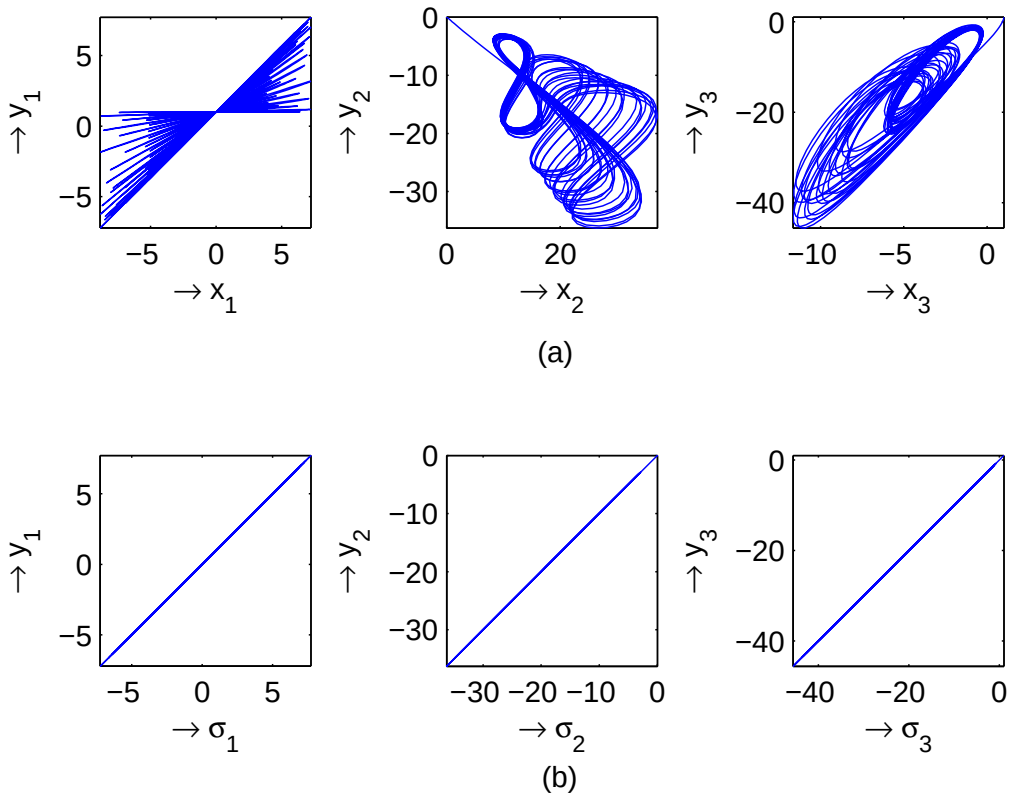

Figure 8.8: Case-IV: (a) x vs y plot (b) σ vs y plot

where α, β are the parameters.

To construct the K-matrix, we consider the Rössler dynamical system [71] as

$$\left.\begin{aligned} \dot{s_1} &= -s_2 - s_3 \\ \dot{s_2} &= s_1 + ls_2 \\ \dot{s_3} &= m + s_3(s_1 - p) \end{aligned}\right\}, \tag{8.3.20}$$

where l, m, p are the parameters.

Let us take,

$$K = \begin{pmatrix} 0.75s_1 & 0.45s_3 & -0.01s_1 \\ 0 & -0.35s_1 & -0.1s_1 \\ -0.01s_3 & 0 & 0.02s_2 \end{pmatrix}$$

In this case, the goal variable can be selected as

$$\sigma = Kr, \quad r = (r_1, r_2, r_3)^t \in \mathbb{R}^3,$$

the state variable of the master system (8.3.19).
Then, the goal dynamics is given by

$$\begin{pmatrix} \dot{\sigma_1} \\ \dot{\sigma_2} \\ \dot{\sigma_3} \end{pmatrix} = \begin{pmatrix} 0.75s_1 & 0.45s_3 & -0.01s_1 \\ 0 & -0.35s_1 & -0.1s_1 \\ -0.01s_3 & 0 & 0.02s_2 \end{pmatrix} \begin{pmatrix} \dot{r_1} \\ \dot{r_2} \\ \dot{r_3} \end{pmatrix} + \begin{pmatrix} 0.75\dot{s_1} & 0.45\dot{s_3} & -0.01\dot{s_1} \\ 0 & -0.35\dot{s_1} & -0.1\dot{s_1} \\ -0.01\dot{s_3} & 0 & 0.02\dot{s_2} \end{pmatrix} \begin{pmatrix} r_1 \\ r_2 \\ r_3 \end{pmatrix}$$

which yields

$$\left.\begin{aligned} \dot{\sigma_1} = \quad & 0.75(s_1\dot{r_1} + \dot{s_1}r_1) + 0.45(s_3\dot{r_2} + \dot{s_3}r_2) \\ & - 0.01(s_1\dot{r_3} + \dot{s_1}r_3) \\ \dot{\sigma_2} = & -0.35(s_1\dot{r_2} + \dot{s_1}r_2) - 0.1(s_1\dot{r_3} + \dot{s_1}r_3) \\ \dot{\sigma_3} = & -0.01(s_3\dot{r_1} + \dot{s_3}r_1) + 0.02(s_2\dot{r_3} + \dot{s_2}r_3) \end{aligned}\right\} \tag{8.3.21}$$

Hence, u, the control input of the slave system (Sprott L system) is calculated as

$$\left.\begin{aligned} u_1 &= \dot{\sigma_1} - \sigma_2 - a_2\sigma_3 \\ u_2 &= \dot{\sigma_2} - b_2\sigma_1^2 + \sigma_2 + 2b_2(w_1 - \sigma_1)e_1 \\ u_3 &= \dot{\sigma_3} - c_2 + \sigma_1 \end{aligned}\right\} \tag{8.3.22}$$

where $e = (e_1, e_2, e_3)^t \in \mathbb{R}^3$, the state variables of the error system which remains same with the previous four cases because V-matrix remains unchanged.

8.4 Numerical Results & Discussions

Here, we will discuss the previous section numerically with the help of matlab software.

Sprott found the chaotic nature for the master system (8.3.7) when $a_1 = 3.9, \quad b_1 = 0.9, \quad c_1 = 1.$

To make non-identical coupled Sprott L system for the slave system (8.3.8), we take $a_2 = 4.4, \quad b_2 = 1.6, \quad c_2 = 1.7.$

V-matrix reduces to Hurwitz if we take $w_1 = -4.5$.

In Shimizu-Morioka system (8.3.16), we consider $\lambda = 0.799$ & $\rho = 0.54$ for showing its chaotic nature.

In the non-linear Rikitake system (8.3.19), there exists two parameters α & β. Let $\alpha = 2, \quad \beta = 5$.

We choose $l = m = 0.2$ & $p = 5.7$ for the Rössler system given by equation(8.3.20).

Let us consider, $x(0) = (1, 0, 1)$, $y(0) = (1, 0, 1)$ and $\sigma(0) = (1, 0, 1)$ for the cases I-IV.

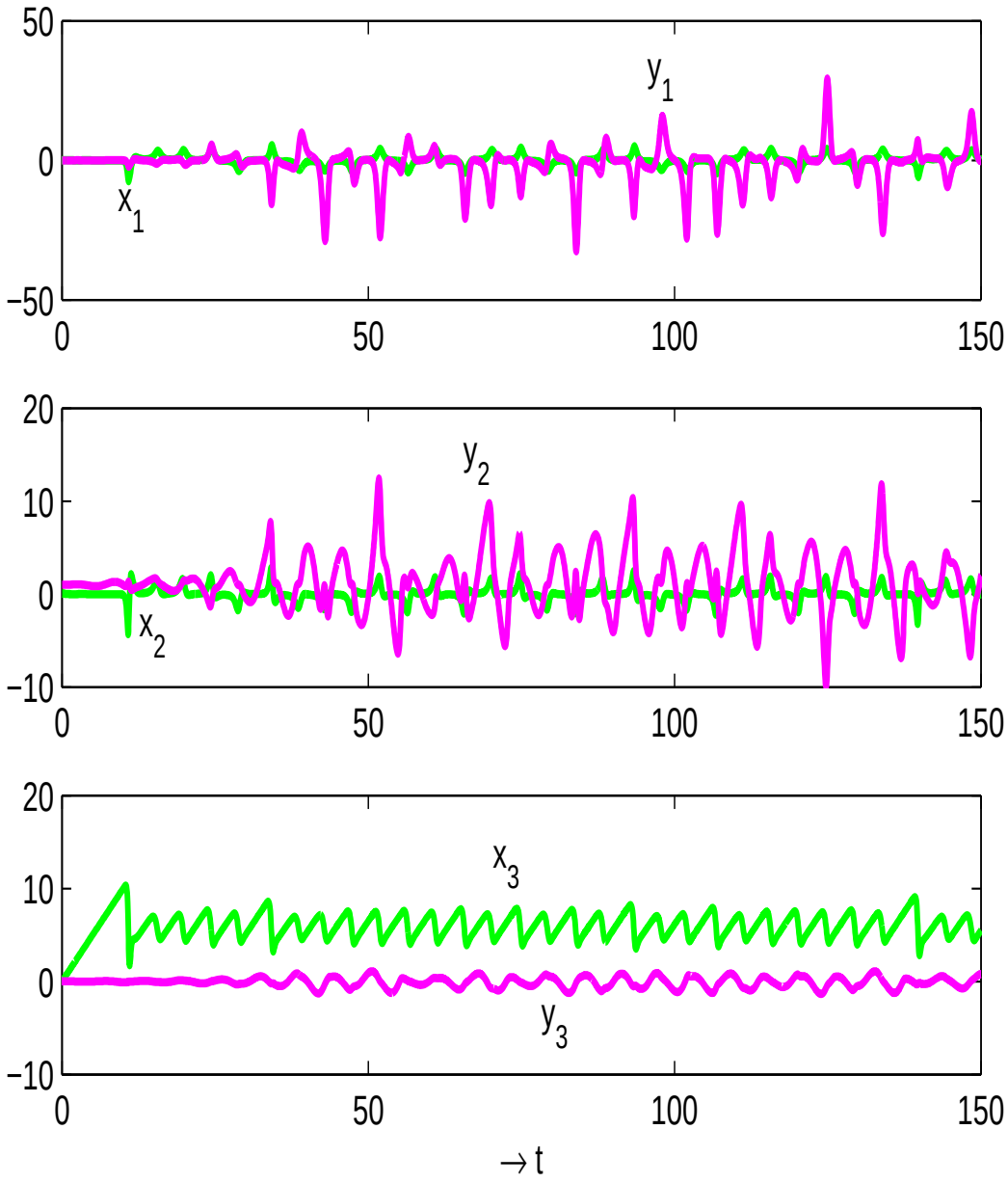

Figure 8.9: Case-V: master system (x) & slave system (y) with respect to time

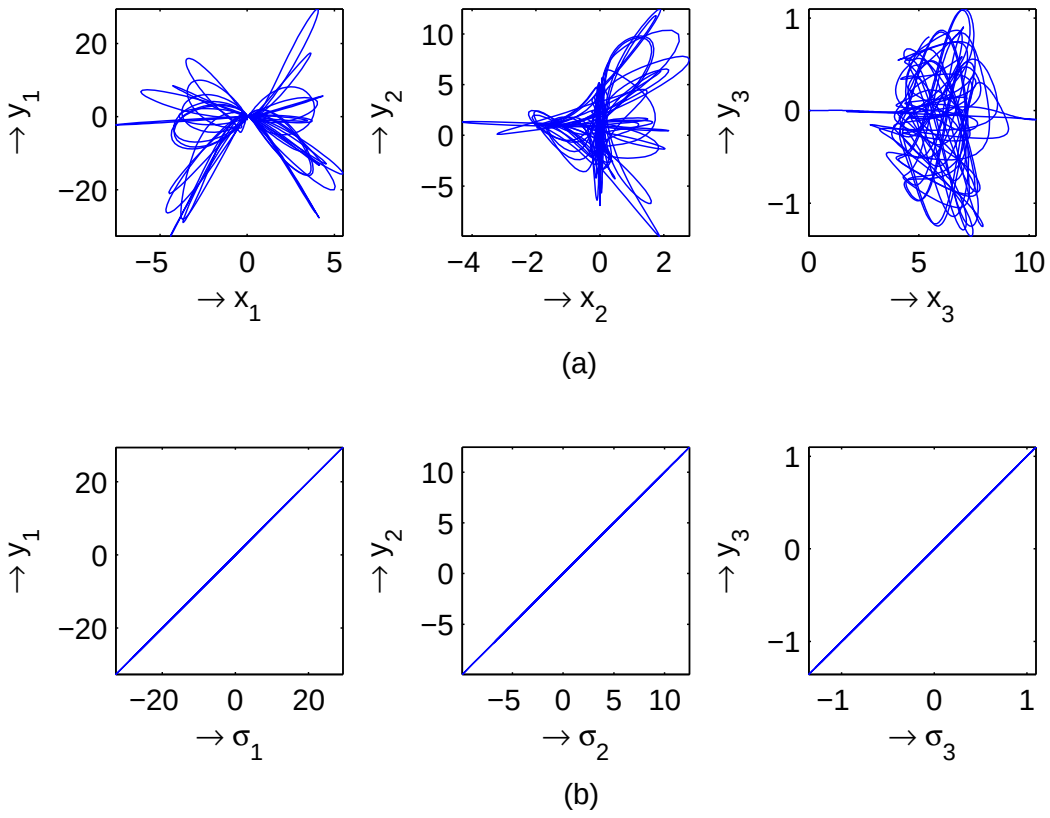

Figure 8.10: Case-V: (a) x vs y plot (b) σ vs y plot

But, for the case-V, the initial condition for the drive system (Rikitake system) and response system (Sprott system) be chosen as (0,0.1,0) and (0,1,0) respectively. In this case, at $t = 0$, we have also considered, $s_1(0) = 0.1, \quad s_2(0) = 0.1, \quad s_3(0) = 0.1, \quad \sigma_1(0) = 0, \quad \sigma_2(0) = 1$ and $\sigma_3(0) = 0$.

Figure (8.1), figure (8.3), figure (8.5), figure (8.7) and figure (8.9) represents the graph of the master and the slave system with respect to time respectively.

In figure (8.2)(a), figure (8.4)(a), figure (8.6)(a), figure (8.8)(a) and figure (8.10)(a), we have plotted $x_i \ \ vs \ \ y_i, \ \ i = 1, 2, 3$ for all the cases I through V.

From the relation (8.2.3), we can claim that the error term goes to zero after some finite time by reducing the difference between goal variables and slave variables. To establish our claim, we have drawn figure (8.2)(b), figure (8.4)(b), figure (8.6)(b), figure (8.8)(b) and figure (8.10)(b).

8.5 Conclusion

In this chapter, we have successfully established the generalized synchronization between the master (drive) system & the slave (response) system via OPCL method. This method is mostly independent of the system parameters. This method has so many applications in practical life, for example, microwave oscillators, electrical cloth drier etc. In engineering sciences, it is also very useful.

Chapter 9

Study on Dynamical Systems with Time-Delay

9.1 Introduction

Interest on chaos based systems is increasing, as the time goes on. The popularity of chaotic system is mainly for its behaviour. It is very much sensitive on initial conditions and system parameters. Lorenz(1963)[45] gives us the opportunity to discover the behaviour of chaos. At present, there exists incalculable number of papers on chaotic dynamical systems. In 1994, J.C.Sprott[52] discovered a set of nineteen dynamical systems, known as Sprott model A to S. Out of those dynamical systems, we consider the Sprott model L which has one non-linear term and three system parameters. Stability of chaos is very important part of chaotic dynamical system. In this chapter, we will make the stability analysis by applying small perturbation near critical points to the time-delayed Sprott model L. In control theory, stability analysis of a dynamical system with multiple time delay is an interesting area because the system be-

comes unstable due to delays. There exists so many control methods, namely, sliding mode control(SMC)[53, 84], open-plus-closed loop(OPCL) control[72], backstepping control method [92], active control[4], adaptive control[26], hybrid and tracking control[90], time-delay method[22] etc.

Next, our aim is to investigate the drive-response synchronization of time-delayed Sprott model L. In the literature, many methods have been developed for the drive-response synchronization of a coupled chaotic non-linear dynamical systems, for example, projective synchronization [23], phase synchronization[75], identical or complete synchronization [65], anti-synchronization[14], lag synchronization[94], anticipatory synchronization [86], generalised synchronization[38] etc.

Here, we will study five distinct cases by choosing five different types of matrix B, where B is the variable matrix of order n, associated with the response system of the time-delayed Sprott system L. To get identical synchronization in case-I, we will consider the matrix B as unit matrix. In second case, the matrix B can be chosen as scalar matrix with diagonal elements (-1) to obtain anti-synchronization between the coupled Sprott system. In the next case, we will take the matrix B as a constant matrix. Periodic functions are chosen as the elements of the matrix B in case-IV. For the last case, the elements of the matrix B are taken as the state variables of the drive system. The time-delayed chaos synchronization of a non-linear dynamical system is useful in secure communication [37], electronic experiments[41], chemical and biological system[67], engineering sciences[72], mathematical system, laser physics[76], ecology, economics and cognitive sciences[47] etc.

In the next section, we will study the stability of a nonlinear chaotic dynamical system with multiple delay parameters. In section 9.3, we will make a delay synchronization scheme and for this purpose, we have chosen Sprott system in section 9.4. Using Runge-Kutta method and matlab software, numerical simulation is done in section 9.5.

9.2 Stability Analysis

To discuss the stability of a non-linear time-delayed dynamical system, we consider a chaotic dynamical system with one non-linear term known as Sprott system L[52], written as

$$\left.\begin{aligned} \dot{x} &= y + az + d_1 x(t-\tau_1) + d_2 x(t-\tau_2) \\ \dot{y} &= bx^2 - y \\ \dot{z} &= c - x \end{aligned}\right\} \tag{9.2.1}$$

where a, b, c are regular parameters, τ_1 and τ_2 are delay parameters and d_1, d_2 are the geometric factors.

In case of critical points,

$$\dot{x} = 0, \quad \dot{y} = 0 \quad \text{and} \quad \dot{z} = 0$$

It gives the critical point of the system (9.2.1) as

$$(x_0, y_0, z_0) \equiv \left(c, bc^2, -\frac{c(d_1 + d_2 + bc)}{a}\right)$$

To perform a small perturbation at the critical point of the system (9.2.1), let us take,

$$x = x_0 + x', \quad y = y_0 + y', \quad z = z_0 + z'$$

Then,

$$\begin{aligned}
\dot{x'} &= y' + az' + d_1x'(t-\tau_1) + d_2x'(t-\tau_2)\\
\dot{y'} &= b(x_0+x')^2 - (y_0+y')\\
&= (bx_0^2 - y_0) + 2bx_0x' - y' + bx'^2\\
&= 2bx_0x' - y', \quad since \quad bx_0^2 - y_0 = 0.\\
&\quad (neglecting \ \ second \ \ order \ \ term \ \ as \ \ x' \ \ is \ \ so \ \ small)\\
\dot{z'} &= (c - x_0) - x'\\
&= -x', \quad since \quad c - x_0 = 0.
\end{aligned}$$

Hence, the time-delayed system (9.2.1) reduces to

$$\left.\begin{aligned}
\dot{x'} &= y' + az' + d_1x'(t-\tau_1) + d_2x'(t-\tau_2)\\
\dot{y'} &= 2bx_0x' - y'\\
\dot{z'} &= -x'
\end{aligned}\right\} \tag{9.2.2}$$

Let $x' = Ae^{\mu t}, \quad y' = Be^{\mu t}, \quad z' = Ce^{\mu t}$ be the solution of (9.2.2). Then, from the system of equation(9.2.2), one may easily find that

$$\left.\begin{aligned}
(\mu - d_1e^{-\mu\tau_1} - d_2e^{-\mu\tau_2})A - B - aC &= 0\\
\text{and} \quad -2bcA + (\mu+1)B &= 0\\
\text{and} \quad A + \mu C &= 0
\end{aligned}\right\} \tag{9.2.3}$$

Eliminating $A, \quad B, \quad C$ from (9.2.3), one gets,

$$\begin{vmatrix}
\mu - d_1e^{-\mu\tau_1} - d_2e^{-\mu\tau_2} & -1 & -a\\
-2bc & (\mu+1) & 0\\
1 & 0 & \mu
\end{vmatrix} = 0$$

which yields,

$$\begin{aligned}
&\mu^3 + (1 - d_1e^{-\mu\tau_1} - d_2e^{-\mu\tau_2})\mu^2\\
&\qquad + (a - 2bc - d_1e^{-\mu\tau_1} - d_2e^{-\mu\tau_2})\mu + a = 0
\end{aligned} \tag{9.2.4}$$

Now, by applying Routh-Hurwitz criterion [59], the above characteristic equation (9.2.4) in μ gives the stability criteria for the dynamical system in absence of delay, i.e., $\tau_1 = 0$ and $\tau_2 = 0$ if and only if,

$$\begin{aligned} 1 - d_1 - d_2 > 0, \quad a - 2bc - d_1 - d_2 > 0, \quad a > 0 \\ \text{and} \quad (1 - d_1 - d_2)(a - 2bc - d_1 - d_2) > a \end{aligned} \tag{9.2.5}$$

From the first two inequality, we have,

$$(d_1 + d_2) < min\{1, (a - 2bc)\}$$

and from the last inequality of (9.2.5), we have,

$$(d_1 + d_2)^2 + (2bc - a - 1)(d_1 + d_2) - 2bc > 0$$

But, in presence of delay parameters, let us take, $\mu = \alpha + i\beta, \quad \beta > 0$. Then, the equation (9.2.4) becomes,

$$\begin{aligned} (\alpha + i\beta)^3 + (1 - d_1 e^{-(\alpha+i\beta)\tau_1} - d_2 e^{-(\alpha+i\beta)\tau_2})(\alpha + i\beta)^2 \\ + (a - 2bc - d_1 e^{-(\alpha+i\beta)\tau_1} - d_2 e^{-(\alpha+i\beta)\tau_2})(\alpha + i\beta) + a = 0. \end{aligned}$$

or,

$$\begin{aligned} &\{(\alpha^3 - 3\alpha\beta^2) + i(3\alpha^2\beta - \beta^3)\} \\ &\quad + \{1 - d_1 e^{-\alpha\tau_1}(cos(\beta\tau_1) - isin(\beta\tau_1)) \\ &\qquad - d_2 e^{-\alpha\tau_2}(cos(\beta\tau_2) - isin(\beta\tau_2))\}\{(\alpha^2 - \beta^2) + i2\alpha\beta\} \\ &\quad + \{a - 2bc - d_1 e^{-\alpha\tau_1}(cos(\beta\tau_1) - isin(\beta\tau_1)) \\ &\qquad - d_2 e^{-\alpha\tau_2}(cos(\beta\tau_2) - isin(\beta\tau_2))\}(\alpha + i\beta) + a = 0. \end{aligned}$$

or,

$$\begin{aligned}
&\{(\alpha^3 - 3\alpha\beta^2) + i(3\alpha^2\beta - \beta^3)\} \\
&\quad + \{(1 - d_1 e^{-\alpha\tau_1} cos(\beta\tau_1) - d_2 e^{-\alpha\tau_2} cos(\beta\tau_2)) \\
&\qquad + i(d_1 e^{-\alpha\tau_1} sin(\beta\tau_1) + d_2 e^{-\alpha\tau_2} sin(\beta\tau_2))\}\{(\alpha^2 - \beta^2) + i2\alpha\beta\} \\
&\quad + \{(a - 2bc - d_1 e^{-\alpha\tau_1} cos(\beta\tau_1) - d_2 e^{-\alpha\tau_2} cos(\beta\tau_2)) \\
&\qquad + i(d_1 e^{-\alpha\tau_1} sin(\beta\tau_1) + d_2 e^{-\alpha\tau_2} sin(\beta\tau_2))\}(\alpha + i\beta) + a = 0.
\end{aligned}$$

or,

$$\begin{aligned}
&\{(\alpha^3 - 3\alpha\beta^2) + i(3\alpha^2\beta - \beta^3)\} \\
&\quad + \{(1 - d_1 e^{-\alpha\tau_1} cos(\beta\tau_1) - d_2 e^{-\alpha\tau_2} cos(\beta\tau_2))(\alpha^2 - \beta^2) \\
&\qquad - 2\alpha\beta(d_1 e^{-\alpha\tau_1} sin(\beta\tau_1) + d_2 e^{-\alpha\tau_2} sin(\beta\tau_2))\} \\
&\quad + i\{2\alpha\beta(1 - d_1 e^{-\alpha\tau_1} cos(\beta\tau_1) - d_2 e^{-\alpha\tau_2} cos(\beta\tau_2)) \\
&\qquad + (\alpha^2 - \beta^2)(d_1 e^{-\alpha\tau_1} sin(\beta\tau_1) + d_2 e^{-\alpha\tau_2} sin(\beta\tau_2))\} \\
&\quad + \{\alpha(a - 2bc - d_1 e^{-\alpha\tau_1} cos(\beta\tau_1) - d_2 e^{-\alpha\tau_2} cos(\beta\tau_2)) \\
&\qquad - \beta(d_1 e^{-\alpha\tau_1} sin(\beta\tau_1) + d_2 e^{-\alpha\tau_2} sin(\beta\tau_2))\} \\
&\quad + i\{\beta(a - 2bc - d_1 e^{-\alpha\tau_1} cos(\beta\tau_1) - d_2 e^{-\alpha\tau_2} cos(\beta\tau_2)) \\
&\qquad + \alpha(d_1 e^{-\alpha\tau_1} sin(\beta\tau_1) + d_2 e^{-\alpha\tau_2} sin(\beta\tau_2))\} + a = 0.
\end{aligned}$$

Now, separating the real and imaginary parts of the above expression, one may find,

$$\begin{aligned}
&(\alpha^3 - 3\alpha\beta^2) \\
&\quad + (\alpha^2 - \beta^2)\{1 - d_1 e^{-\alpha\tau_1} cos(\beta\tau_1) - d_2 e^{-\alpha\tau_2} cos(\beta\tau_2)\} \\
&\quad - 2\alpha\beta\{d_1 e^{-\alpha\tau_1} sin(\beta\tau_1) + d_2 e^{-\alpha\tau_2} sin(\beta\tau_2)\} \\
&\quad + \alpha\{a - 2bc - d_1 e^{-\alpha\tau_1} cos(\beta\tau_1) - d_2 e^{-\alpha\tau_2} cos(\beta\tau_2)\} \\
&\quad - \beta\{d_1 e^{-\alpha\tau_1} sin(\beta\tau_1) + d_2 e^{-\alpha\tau_2} sin(\beta\tau_2)\} + a = 0
\end{aligned} \tag{9.2.6}$$

and,

$$
\begin{aligned}
&(3\alpha^2\beta - \beta^3) \\
&\quad + 2\alpha\beta\{1 - d_1 e^{-\alpha\tau_1} cos(\beta\tau_1) - d_2 e^{-\alpha\tau_2} cos(\beta\tau_2)\} \\
&\quad + (\alpha^2 - \beta^2)(d_1 e^{-\alpha\tau_1} sin(\beta\tau_1) + d_2 e^{-\alpha\tau_2} sin(\beta\tau_2)) \\
&\quad + \beta\{a - 2bc - d_1 e^{-\alpha\tau_1} cos(\beta\tau_1) - d_2 e^{-\alpha\tau_2} cos(\beta\tau_2)\} \\
&\quad + \alpha\{d_1 e^{-\alpha\tau_1} sin(\beta\tau_1) + d_2 e^{-\alpha\tau_2} sin(\beta\tau_2)\} = 0
\end{aligned} \tag{9.2.7}
$$

Let us choose, $\tau_1 = \tau_2 = \tau$, then the expressions (9.2.6) and (9.2.7) reduce to

$$
\begin{aligned}
(\alpha^3 - 3\alpha\beta^2) + (\alpha^2 - \beta^2)\{1 - (d_1 + d_2)e^{-\alpha\tau} cos(\beta\tau)\} \\
- 2\alpha\beta(d_1 + d_2)e^{-\alpha\tau} sin(\beta\tau) \\
+ \alpha\{a - 2bc - (d_1 + d_2)e^{-\alpha\tau} cos(\beta\tau)\} \\
- \beta(d_1 + d_2)e^{-\alpha\tau} sin(\beta\tau) + a = 0
\end{aligned}
$$

and,

$$
\begin{aligned}
(3\alpha^2\beta - \beta^3) + 2\alpha\beta\{1 - (d_1 + d_2)e^{-\alpha\tau} cos(\beta\tau)\} \\
+ (\alpha^2 - \beta^2)(d_1 + d_2)e^{-\alpha\tau} sin(\beta\tau) \\
+ \beta\{a - 2bc - (d_1 + d_2)e^{-\alpha\tau} cos(\beta\tau)\} \\
+ \alpha(d_1 + d_2)e^{-\alpha\tau} sin(\beta\tau) = 0
\end{aligned}
$$

or,

$$
\begin{aligned}
&(d_1{+}d_2)(\beta^2 - \alpha^2 - \alpha)e^{-\alpha\tau} cos(\beta\tau) \\
&\quad - (d_1 + d_2)(2\alpha + 1)\beta e^{-\alpha\tau} sin(\beta\tau) \\
&\quad + \{\alpha^3 + \alpha^2 + (a - 2bc - 3\beta^2)\alpha + (a - \beta^2)\} = 0
\end{aligned} \tag{9.2.8}
$$

and

$$\begin{aligned}(d_1+d_2)(\alpha^2+\alpha-\beta^2)e^{-\alpha\tau}sin(\beta\tau)\\ -(d_1+d_2)(2\alpha+1)\beta e^{-\alpha\tau}cos(\beta\tau)\\ +\{3\alpha^2\beta+2\alpha\beta+(a-2bc-\beta^2)\beta\}=0\end{aligned} \tag{9.2.9}$$

If we set, $\alpha = 0$, we have,

$$(d_1+d_2)\beta^2 cos(\beta\tau)-(d_1+d_2)\beta sin(\beta\tau)+(a-\beta^2)=0$$

and

$$-(d_1+d_2)\beta cos(\beta\tau)-(d_1+d_2)\beta^2 sin(\beta\tau)+(a-2bc-\beta^2)\beta=0$$

or,

$$\left.\begin{aligned}u_1 cos(\beta\tau)+u_2 sin(\beta\tau)+v_1=0\\ \text{and}\quad u_2 cos(\beta\tau)-u_1 sin(\beta\tau)+v_2=0\end{aligned}\right\} \tag{9.2.10}$$

where

$$\begin{aligned}u_1=(d_1+d_2)\beta^2, \quad u_2=-(d_1+d_2)\beta\\ v_1=a-\beta^2, \qquad v_2=(a-2bc-\beta^2)\beta\end{aligned}$$

Eliminating τ from (9.2.10), one gets,

$$u_1^2+u_2^2=v_1^2+v_2^2$$

This implies that,

$$(d_1+d_2)^2\beta^2(\beta^2+1)=(a-\beta^2)^2+(a-2bc-\beta^2)^2\beta^2 \tag{9.2.11}$$

Let $\beta^2=\sigma$. Then, we have,

$$(d_1+d_2)^2\sigma(\sigma+1)=(a-\sigma)^2+(a-2bc-\sigma)^2\sigma$$

$$or, \qquad \sigma^3+h_1\sigma^2+h_2\sigma+h_3=0 \tag{9.2.12}$$

where, $h_1 = 1 - 2(a - 2bc) - (d_1 + d_2)^2$,
$h_2 = (a - 2bc)^2 - 2a - (d_1 + d_2)^2$ and $h_3 = a^2$.

Let us define

$$f(\sigma) = \sigma^3 + h_1\sigma^2 + h_2\sigma + h_3 \tag{9.2.13}$$

The existence of a positive root of $f(\sigma) = 0$ amounts to the existence of a β as discussed above. Hence, the existence of a positive root is equivalent to bifurcation in the time delay system.

Now,

$$\begin{aligned}
\frac{df}{d\sigma} &= 3\sigma^2 + 2h_1\sigma + h_2 \\
&= 3\left[\sigma^2 + 2h_1.\frac{\sigma}{3} + \frac{h_2}{3}\right] \\
&= 3\left[\left(\sigma + \frac{h_1}{3}\right)^2 + \frac{h_2}{3} - \frac{h_1^2}{9}\right] \\
&= 3\left[\left(\sigma + \frac{h_1}{3}\right)^2 + \frac{3h_2 - h_1^2}{9}\right]
\end{aligned}$$

Case I : $3h_2 - h_1^2 \geq 0$.

Then, $\frac{df}{d\sigma} \geq 0$. Therefore, $f(\sigma)$ is non-decreasing
and $f(0) = h_3 = a^2 > 0$.
Hence, there is no possibility of occurrence of a positive root of the equation (9.2.12).

Case II : $3h_2 - h_1^2 < 0$.

Then,

$$\frac{df}{d\sigma} = 3\left[\left(\sigma + \frac{h_1}{3}\right)^2 + \frac{3h_2 - h_1^2}{9}\right]$$

which gives

$$\frac{d^2f}{d\sigma^2} = 6\left(\sigma + \frac{h_1}{3}\right)$$

Therefore, $\frac{d^2f}{d\sigma^2} < 0$, if and only if, $\sigma + \frac{h_1}{3} < 0$, that is, if and only if, $\sigma < \frac{1}{3}\left\{(d_1+d_2)^2 + 2(a-2bc) - 1\right\} = M$ say.

In this case, $\frac{df}{d\sigma}$ is decreasing and

$$\left[\frac{df}{d\sigma}\right]_{\sigma=0} = 3\left[\left(\frac{h_1}{3}\right)^2 + \frac{3h_2 - h_1^2}{9}\right] = h_2$$

Then,

$$\left[\frac{df}{d\sigma}\right]_{\sigma=0} < 0 \quad if \quad (a-2bc)^2 - 2a - (d_1+d_2)^2 < 0.$$

In this case, $\frac{df}{d\sigma} < 0$ for all $\sigma \in (0, M)$ provided $M > 0$.

Therefore, we have the following result :

If d_1 *and* d_2 *are chosen such that* $M = \frac{1}{3}\left\{(d_1+d_2)^2 + 2(a-2bc) - 1\right\} > 0$ *and* $(a-2bc)^2 - 2a - (d_1+d_2)^2 < 0$, *then* $f(\sigma)$ *is decreasing in* $(0, M)$.

As $f(0) > 0$, there may be a positive root of $f(\sigma) = 0$.

In addition, if there exists $\eta > 0$ such that

$$\eta^3 + h_1\eta^2 + h_2\eta + h_3 < 0,$$

then f has a positive root in $(0, \eta)$.

The parameter values for Sprott system L to be chaotic are $a = 3.9, b = 0.9$ and $c = 1.0$.
Choosing $d_1 = 0.2$ and $d_2 = 0.3$, we can check that the required

conditions for f to be decreasing on $(0, M)$ are satisfied.
In addition, simple computations show that for any $\eta \in [2.60, 2.88]$,

$$\eta^3 + h_1\eta^2 + h_2\eta + h_3 < 0.$$

Hence, there indeed exists a positive root of $f(\sigma) = 0$ in $(0, \eta)$ where $\eta \in [2.60, 2.88]$.

As we have shown the existence of positive roots for proper choice of d_1 and d_2, let us consider,

$$\beta_j = \sqrt{\sigma_j}, \qquad j = 1, 2, 3. \tag{9.2.14}$$

Hence, from (9.2.10), one may easily obtain,

$$cos(\beta\tau) = \frac{-2bc}{(d_1 + d_2)(\beta^2 + 1)}$$

It yields,

$$\tau_j^{(m)} = \frac{1}{\sqrt{\sigma_j}} \left[cos^{-1} \left\{ \frac{-2bc}{(d_1 + d_2)(\sigma_j + 1)} \right\} + 2m\pi \right] \tag{9.2.15}$$

where $m = 0, 1, 2, ...$ and $j = 1, 2, 3$.

Define,

$$\tau_0 = \tau_{j_0}^{(0)} = \min_{j \in \{1,2,3\}} \{\tau_j^{(0)}\}, \quad \beta_0 = \beta_{j_0} \tag{9.2.16}$$

Thus, when $\tau = \tau_0$, the characteristic values of the linearized time delay system become completely imaginary. The stability behaviour of the critical point of the system (9.2.1) changes as τ varies across τ_0. At $\tau = \tau_0$, a limit cycle around the critical point is generated and the critical point loses stability. The Sprott system L thus undergoes a Hopf bifurcation. There exists countably infinite values of τ for which such bifurcations occur and the sequences $\tau_j^{(m)}$ enumerates all such values. The smallest one of them, τ_0, has been chosen for discussion above.

9.3 Delay Synchronization Scheme

Any non-linear dynamical system can be written as

$$\dot{x} = Ax + \phi(x(t), x(t-\tau)), \tag{9.3.17}$$

where $x \in \mathbb{R}^n$, $A \in \mathbb{R}^{n\times n}$, $\phi : \mathbb{R}^n \to \mathbb{R}^n$ is non-linear vector function.

We now consider a new dynamical system which is coupled with the system (9.3.17) as given below:

$$\dot{y} = Ay + B(x(t), x(t-\tau), t).\phi(x(t), x(t-\tau)) + u, \tag{9.3.18}$$

where B is a variable matrix of order n and u is the controller which controls the motion of the system (9.3.18).

Let us assume the error term e defined as

$$\begin{aligned} e &= y - Bx \\ &= y - V, \end{aligned} \tag{9.3.19}$$

where $V = Bx$.

Therefore, the error dynamics can be written as

$$\begin{aligned} \dot{e} &= \dot{y} - \dot{B}x - B\dot{x} \\ &= Ay + B\phi + u - \dot{B}x - B(Ax + \phi) \\ &= Ay - BAx + u - \dot{B}x \\ &= A(y - Bx) + u - \dot{B}x + (AB - BA)x \end{aligned}$$

Therefore,

$$\dot{e} = Ae + u - \dot{B}x + (AB - BA)x \tag{9.3.20}$$

Let the controller be chosen as,

$$u = \dot{B}x - (AB - BA)x - pe \tag{9.3.21}$$

where p is a scalar which generates the coupling strength.

Then, the error dynamics (9.3.20) becomes

$$\dot{e} = He, \quad \text{where} \quad H = A - pI \tag{9.3.22}$$

where I is the unit matrix of order n.

Let us take, lyapunov function $V(e) = \frac{1}{2}e^T e$, where V(e) is a positive definite function.

Now, $\dot{V}(e) < 0$ if H is Hurwitz.

Hence, $\|e(t)\| \to 0$ as $t \to \infty$.

Thus, the delay synchronization is achieved globally and asymptotically.

9.4 Application of Delay Synchronization

Let us consider the Sprott model L [50] with time delay as the driver system, given by,

$$\left.\begin{aligned} \dot{x_1} &= x_2 + ax_3 + d_1x_1(t-\tau_1) + d_2x_1(t-\tau_2) \\ \dot{x_2} &= bx_1^2 - x_2 \\ \dot{x_3} &= c - x_1 \end{aligned}\right\} \tag{9.4.23}$$

Now, the system (9.4.23) can be written as in the form (9.3.17) as

$$\dot{x} = Ax + \phi(x, x_\tau), \quad x_\tau = x(t-\tau)$$

where $x = (x_1, x_2, x_3)^T$, and $A = \begin{pmatrix} 0 & 1 & a \\ 0 & -1 & 0 \\ -1 & 0 & 0 \end{pmatrix}$

$$\phi = \begin{pmatrix} d_1x_1(t-\tau_1) + d_2x_1(t-\tau_2) \\ bx_1^2 \\ c \end{pmatrix}$$

Then, the response system can be written as

$$\begin{aligned}\dot{y} &= Ay + B\phi + u \\ &= Ay + B\phi + \dot{B}x - (AB - BA)x - pe \\ &= Ay + B\phi + \dot{B}x - (AB - BA)x - p(y - Bx) \\ &= (A - pI)y + B\phi + \dot{B}x + pBx - (AB - BA)x\end{aligned}$$

which yields,

$$\dot{y} = Hy + B[\phi + px] + \dot{B}x - (AB - BA)x \tag{9.4.24}$$

where $H = A - pI$.

Using (9.3.22), the error dynamics is given by,

$$\left.\begin{aligned}\dot{e_1} &= -pe_1 + e_2 + ae_3 \\ \dot{e_2} &= -(1 + p)e_2 \\ \dot{e_3} &= -e_1 - pe_3\end{aligned}\right\} \tag{9.4.25}$$

9.5 Numerical Discussions and Results

Here, we have considered the values of the system parameters as $a = 3.9, \quad b = 0.9, \quad c = 1.0$ with delay parameters as $\tau_1 = 1.7$ and $\tau_2 = 1.0$.

Let us take $x(0) = (0.01, 0, 0.01)$ and $y(0) = (1, 0, 1)$ as the initial conditions for the coupled system(9.4.23) and (9.4.24). We also consider the initial condition for the synchronization error as $e(0) = (1, 0, -1)$. Let us also assume $d_1 = 0.01$ and $d_2 = 0.03$.

We have chosen $p = 8.5$, so that H is hurwitz.

To establish our claim, we will discuss five different cases.

Case I : B is a unit matrix.

Let $B = \begin{pmatrix} 1 & 0 & 0 \\ 0 & 1 & 0 \\ 0 & 0 & 1 \end{pmatrix}$

Therefore, $AB = BA$

Now, one may easily obtain that

$$H = A - pI = \begin{pmatrix} -p & 1 & a \\ 0 & -(1+p) & 0 \\ -1 & 0 & -p \end{pmatrix}$$

and $\phi + px = \begin{pmatrix} d_1x_1(t-\tau_1) + d_2x_1(t-\tau_2) + px_1 \\ bx_1^2 + px_2 \\ c + px_3 \end{pmatrix}$

Then, the response system (9.4.24) is given by,

$$\begin{aligned} \dot{y_1} &= -py_1 + y_2 + ay_3 + d_1x_1(t-\tau_1) + d_2x_1(t-\tau_2) + px_1 \\ \dot{y_2} &= -(1+p)y_2 + bx_1^2 + px_2 \\ \dot{y_3} &= -y_1 - py_3 + c + px_3 \end{aligned} \tag{9.5.26}$$

From figure (9.1), figure (9.2) and figure (9.3), we can say that the drive system (9.4.23) and the response system (9.5.26) are synchronized identically with time delay.

Case II : B is a scalar matrix.

If we consider $B = \begin{pmatrix} -1 & 0 & 0 \\ 0 & -1 & 0 \\ 0 & 0 & -1 \end{pmatrix}$ then, $AB = BA$.

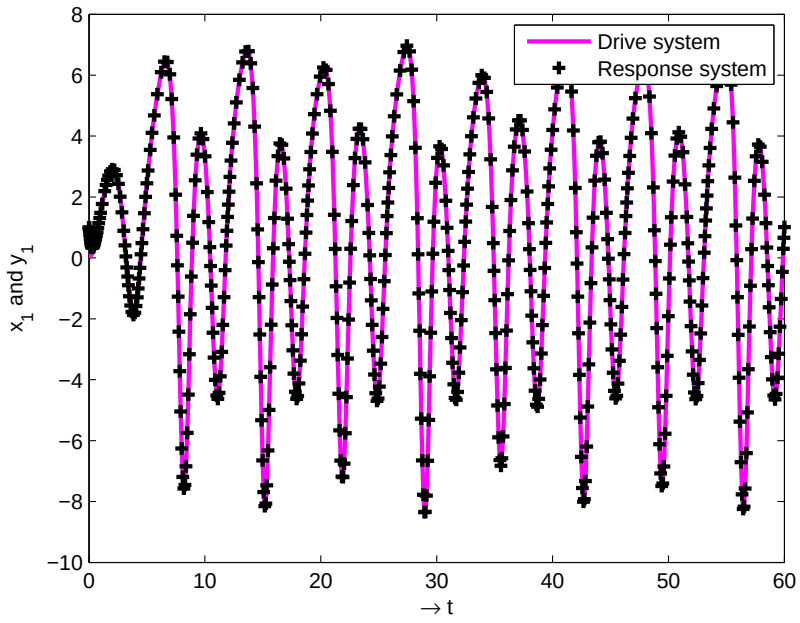

Figure 9.1: Case-I: x_1 *and* y_1 with respect to time

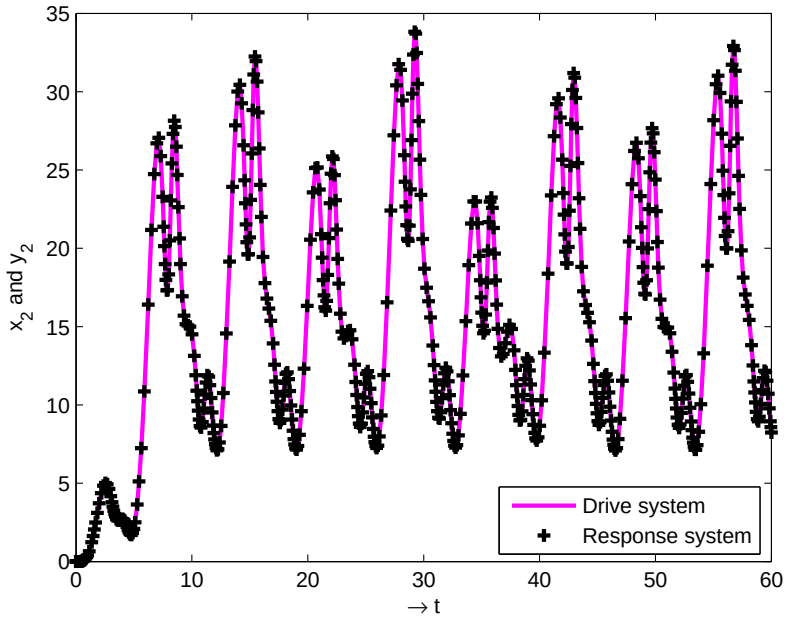

Figure 9.2: Case-I: x_2 *and* y_2 with respect to time

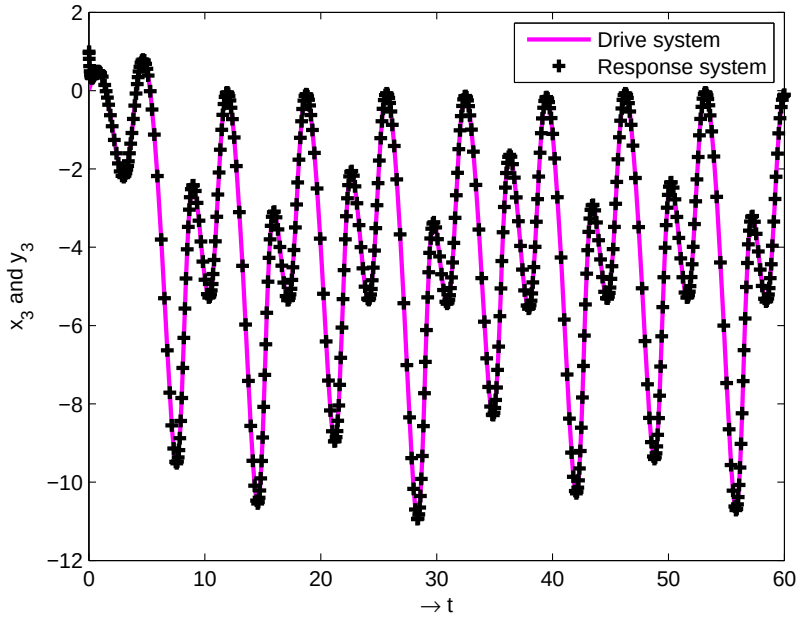

Figure 9.3: Case-I: x_3 *and* y_3 with respect to time

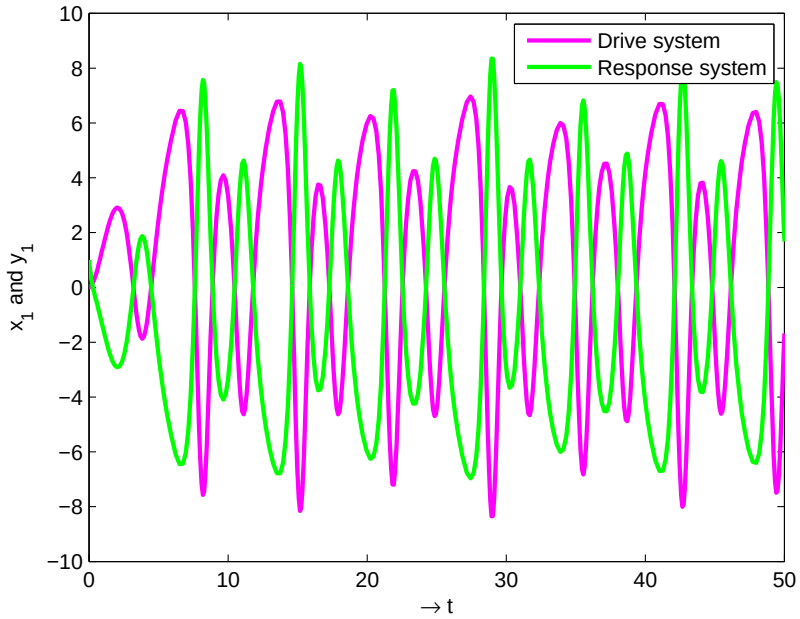

Figure 9.4: Case-II: x_1 *and* y_1 with respect to time

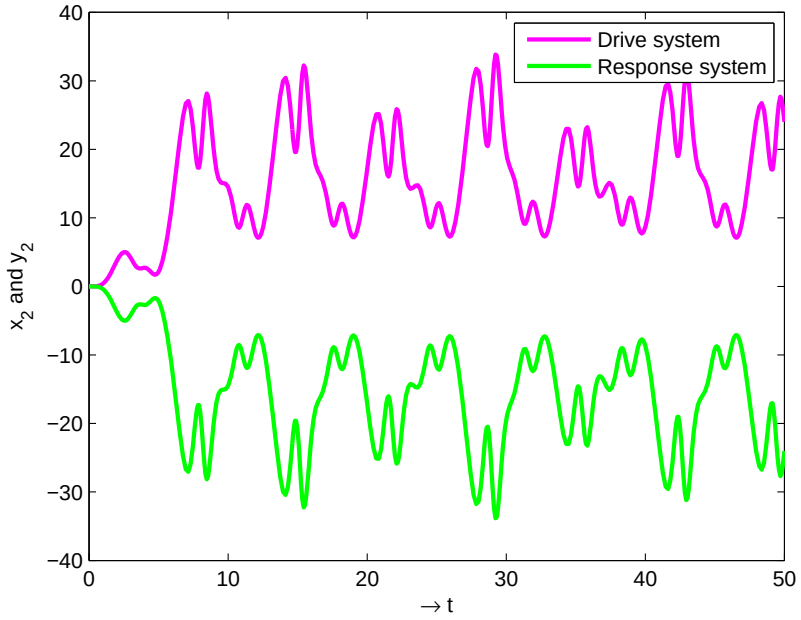

Figure 9.5: Case-II: x_2 *and* y_2 with respect to time

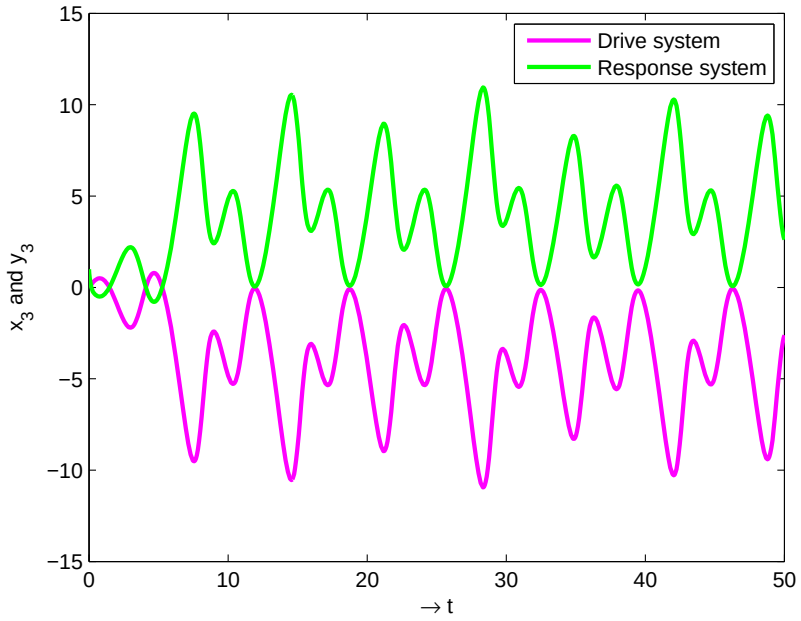

Figure 9.6: Case-II: x_3 *and* y_3 with respect to time

Since the matrices H and $(\phi+px)$ remain unchanged, the response system (9.4.24) becomes,

$$\begin{aligned}
\dot{y_1} &= -py_1 + y_2 + ay_3 - d_1x_1(t-\tau_1) - d_2x_1(t-\tau_2) - px_1 \\
\dot{y_2} &= -(1+p)y_2 - bx_1^2 - px_2 \\
\dot{y_3} &= -y_1 - py_3 - c - px_3
\end{aligned} \tag{9.5.27}$$

The anti-synchronization of the time-delayed coupled Sprott L systems (9.4.23) and (9.5.27) is successfully achieved by figure (9.4) figure (9.5) and figure (9.6).

Case III : B is a constant matrix of order 3.

One may take, $B = \begin{pmatrix} 0.2 & 0 & -1.3 \\ 0 & 2.7 & 1 \\ 0 & 0.5 & 0 \end{pmatrix}$

Then,

$$AB = \begin{pmatrix} 0 & (2.7+0.5a) & 1 \\ 0 & -2.7 & -1 \\ -0.2 & 0 & 1.3 \end{pmatrix}$$

$$\text{and} \quad BA = \begin{pmatrix} 1.3 & 0.2 & 0.2a \\ -1 & -2.7 & 0 \\ 0 & -0.5 & 0 \end{pmatrix}$$

Therefore, $AB - BA = \begin{pmatrix} -1.3 & (2.5+0.5a) & (1-0.2a) \\ 1 & 0 & -1 \\ -0.2 & 0.5 & 1.3 \end{pmatrix}$

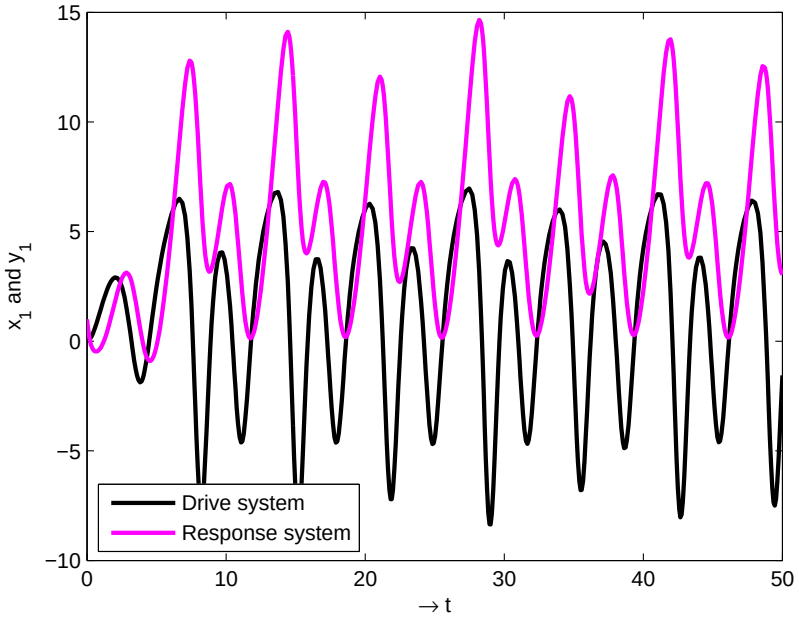

Figure 9.7: Case-III: x_1 *and* y_1 with respect to time

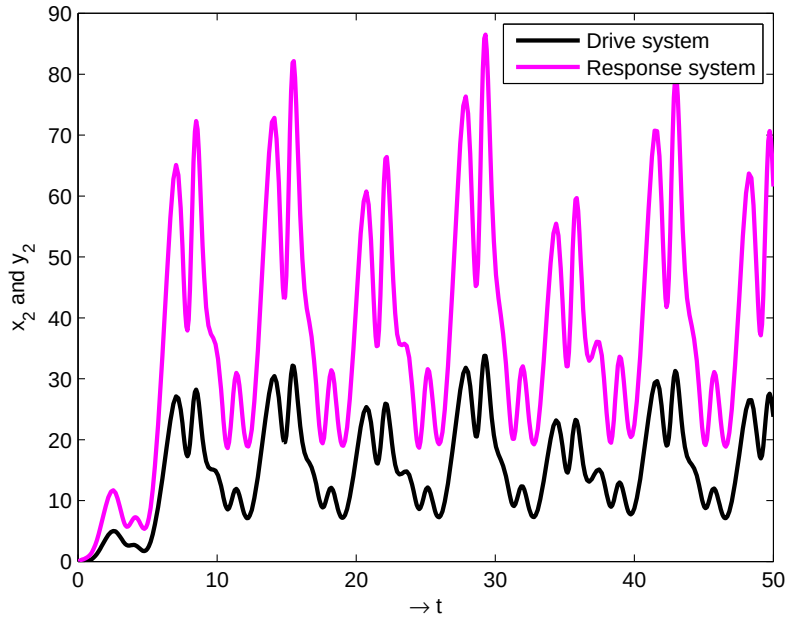

Figure 9.8: Case-III: x_2 *and* y_2 with respect to time

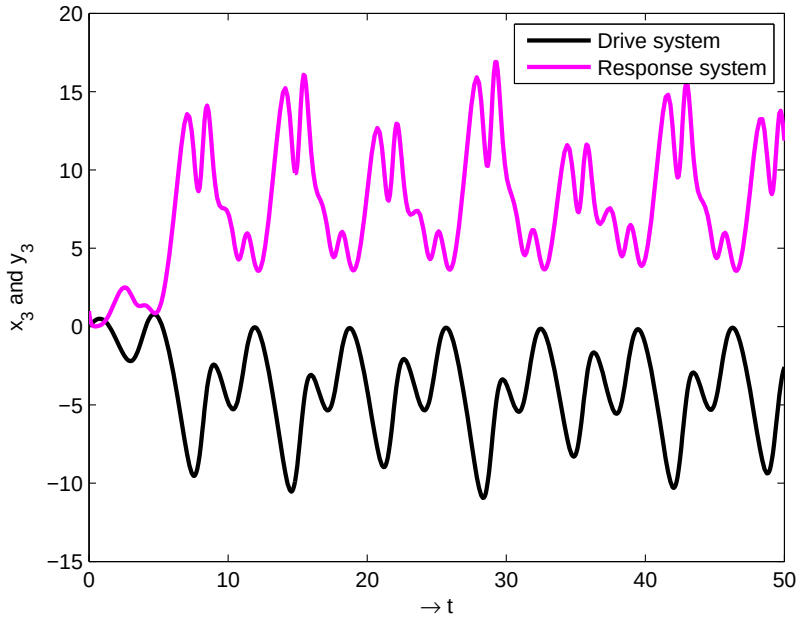

Figure 9.9: Case-III: x_3 *and* y_3 with respect to time

Then, the response system (9.4.24) is given by,

$$\begin{aligned}
\dot{y_1} &= -py_1 + y_2 + ay_3 - 1.3(c + px_3) + 1.3x_1 \\
&\quad + 0.2(d_1x_1(t-\tau_1) + d_2x_1(t-\tau_2) + px_1) \\
&\quad - (2.5 + 0.5a)x_2 - (1 - 0.2a)x_3 \qquad (9.5.28) \\
\dot{y_2} &= -(1+p)y_2 + 2.7(bx_1^2 + px_2) + (c + px_3) - x_1 + x_3 \\
\dot{y_3} &= -y_1 - py_3 + 0.5(bx_1^2 + px_2) + 0.2x_1 - 0.5x_2 - 1.3x_3
\end{aligned}$$

Figure (9.7), figure (9.8) and figure (9.9) shows the time history of the state variable x_i of the drive system (9.4.23) and the state variable y_i of the response system (9.5.28) respectively, where $i = 1, 2, 3$.

Case IV : B is chosen to be a 3×3 matrix with periodic function as its elements given below:

$$B = \begin{pmatrix} 2.3 & 0 & -0.1sin(0.1t) \\ -1 & 1 & 0 \\ 0 & 0.2cos(0.9t) & 0 \end{pmatrix}$$

Therefore, $\dot{B} = \begin{pmatrix} 0 & 0 & -0.01cos(0.1t) \\ 0 & 0 & 0 \\ 0 & -0.18sin(0.9t) & 0 \end{pmatrix}$

In this case,

$$AB = \begin{pmatrix} -1 & 1 + 0.2cos(0.9t)a & 0 \\ 1 & -1 & 0 \\ -2.3 & 0 & 0.1sin(0.1t) \end{pmatrix}$$

$$BA = \begin{pmatrix} 0.1sin(0.1t) & 2.3 & 2.3a \\ 0 & -2 & -a \\ 0 & -0.2cos(0.9t) & 0 \end{pmatrix}$$

Then, $AB - BA$

$$= \begin{pmatrix} -1 - 0.1sin(0.1t) & -1.3 + 0.2cos(0.9t)a & -2.3a \\ 1 & 1 & a \\ -2.3 & 0.2cos(0.9t) & 0.1sin(0.1t) \end{pmatrix}$$

Here, the response system (9.4.24) becomes,

$$\begin{aligned}
\dot{y_1} &= -py_1 + y_2 + ay_3 - 0.1sin(0.1t)(c + px_3) \\
&\quad + 2.3(d_1x_1(t-\tau_1) + d_2x_1(t-\tau_2) + px_1) \\
&\quad - 0.01cos(0.1t)x_3 + (1 + 0.1sin(0.1t))x_1 \\
&\quad - (-1.3 + 0.2cos(0.9t)a)x_2 + 2.3ax_3 \\
\dot{y_2} &= -(1+p)y_2 + (bx_1^2 + px_2) - x_1 - x_2 - ax_3 \\
&\quad - (d_1x_1(t-\tau_1) + d_2x_1(t-\tau_2) + px_1) \\
\dot{y_3} &= -y_1 - py_3 + 0.2cos(0.9t)(bx_1^2 + px_2) \\
&\quad - 0.18sin(0.9t)x_2 + 2.3x_1 \\
&\quad - 0.2cos(0.9t)x_2 - 0.1sin(0.1t)x_3
\end{aligned} \tag{9.5.29}$$

The coupled synchronization is successfully made for this case shown by the figure (9.10), figure (9.11) and figure (9.12).

Case V : B contains the state variables of the Sprott L system (9.4.23).

Therefore, B can be taken as

$$B = \begin{pmatrix} 0 & -1 & 0.01x_2 \\ 1 & -0.2x_1 & -x_3 \\ x_1 & 0 & 0 \end{pmatrix}$$

One can easily find,

$$\dot{B} = \begin{pmatrix} 0 & 0 & 0.01\dot{x_2} \\ 0 & -0.2\dot{x_1} & -\dot{x_3} \\ \dot{x_1} & 0 & 0 \end{pmatrix}$$

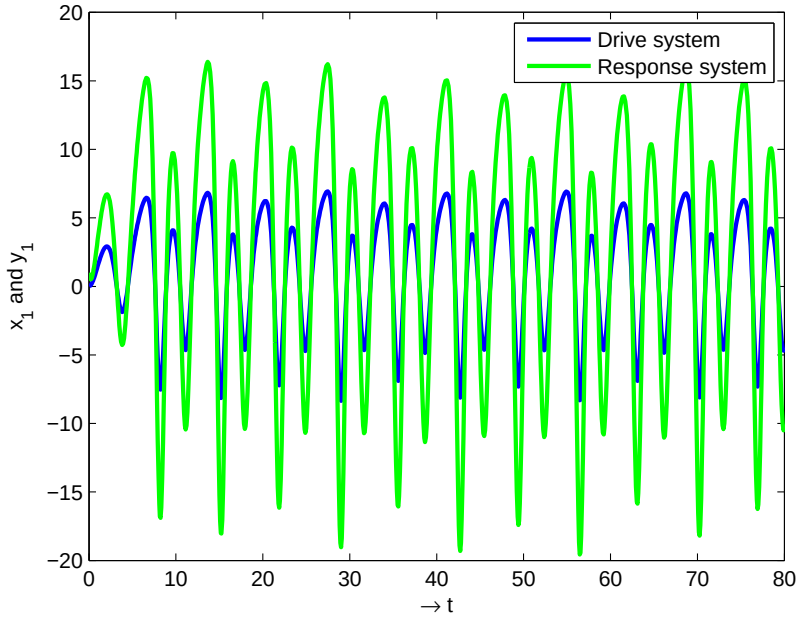

Figure 9.10: Case-IV: x_1 *and* y_1 with respect to time

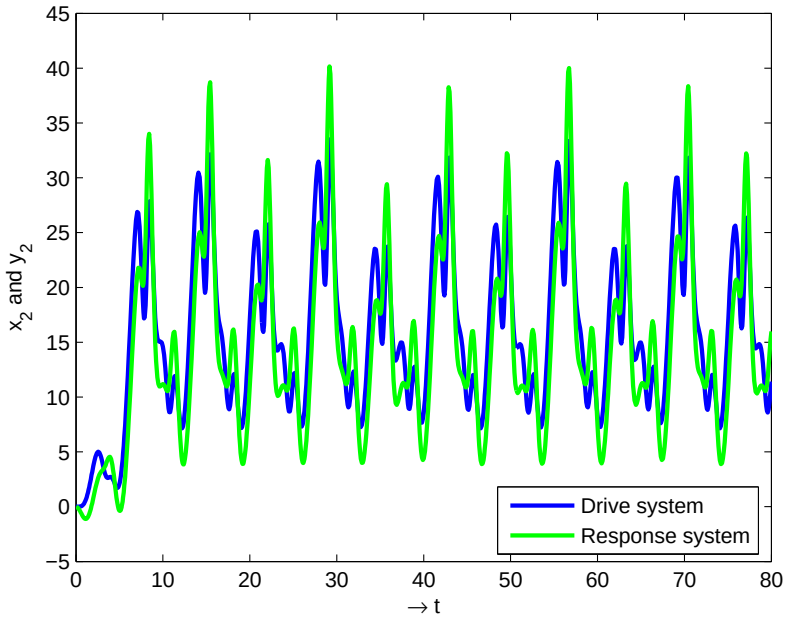

Figure 9.11: Case-IV: x_2 *and* y_2 with respect to time

Now,

$$AB = \begin{pmatrix} 1+ax_1 & -0.2x_1 & -x_3 \\ -1 & 0.2x_1 & x_3 \\ 0 & 1 & -0.01x_2 \end{pmatrix}$$

$$BA = \begin{pmatrix} -0.01x_2 & 1 & 0 \\ x_3 & 1+0.2x_1 & a \\ 0 & x_1 & ax_1 \end{pmatrix}$$

$Then,\ AB - BA$

$$= \begin{pmatrix} 1+ax_1+0.01x_2 & -(0.2x_1+1) & -x_3 \\ -(1+x_3) & -1 & x_3-a \\ 0 & 1-x_1 & -(0.01x_2+ax_1) \end{pmatrix}$$

Therefore, the response system (9.4.24) reduces to,

$$\begin{aligned} \dot{y_1} &= -py_1 + y_2 + ay_3 - (bx_1^2 + px_2) + 0.01x_2(c+px_3) \\ &\quad + 0.01\dot{x_2}x_3 - (1+ax_1+0.01x_2)x_1 \\ &\quad + (0.2x_1+1)x_2 + x_3^2 \\ \dot{y_2} &= -(1+p)y_2 + (d_1x_1(t-\tau_1) + d_2x_1(t-\tau_2) + px_1) \\ &\quad - 0.2x_1(bx_1^2 + px_2) - x_3(c+px_3) - 0.2\dot{x_1}x_2 \\ &\quad - \dot{x_3}x_3 + (1+x_3)x_1 + x_2 - (x_3-a)x_3 \\ \dot{y_3} &= -y_1 - py_3 + x_1(d_1x_1(t-\tau_1) + d_2x_1(t-\tau_2) + px_1) \\ &\quad + \dot{x_1}x_1 - (1-x_1)x_2 + (0.01x_2+ax_1)x_3 \end{aligned} \tag{9.5.30}$$

The drive-response coupled synchronization is again achieved successfully representing by figure (9.13), figure (9.14) and figure (9.15) as we have shown in previous cases.

It is observed that the error dynamics (9.3.22) remain same for

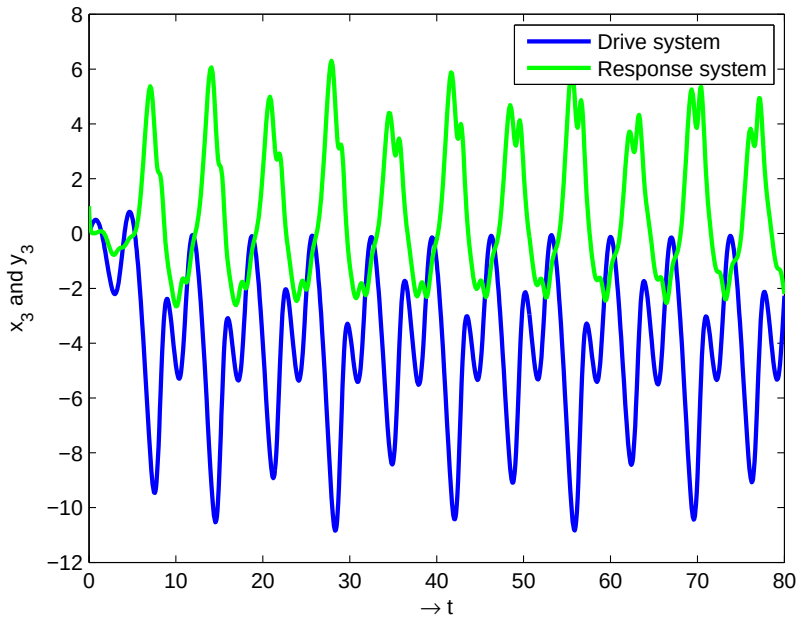

Figure 9.12: Case-IV: x_3 *and* y_3 with respect to time

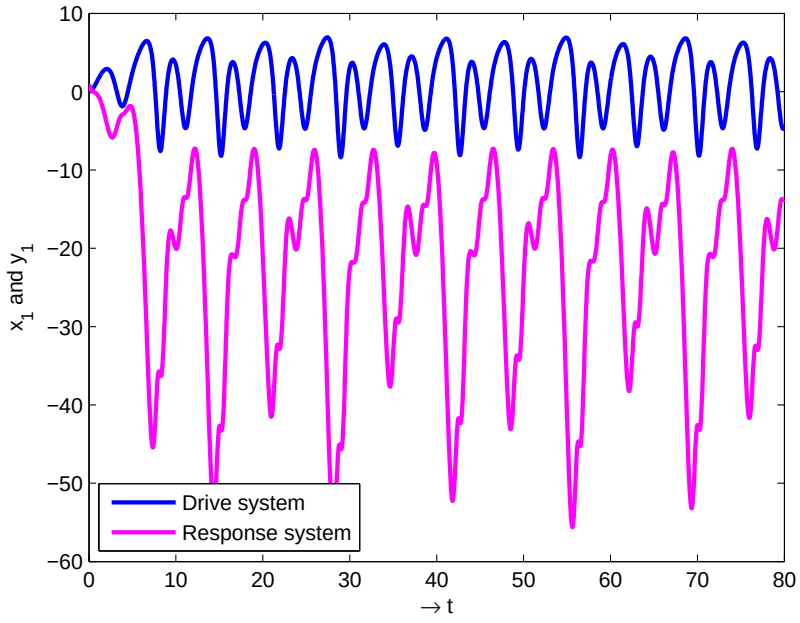

Figure 9.13: Case-V: x_1 *and* y_1 with respect to time

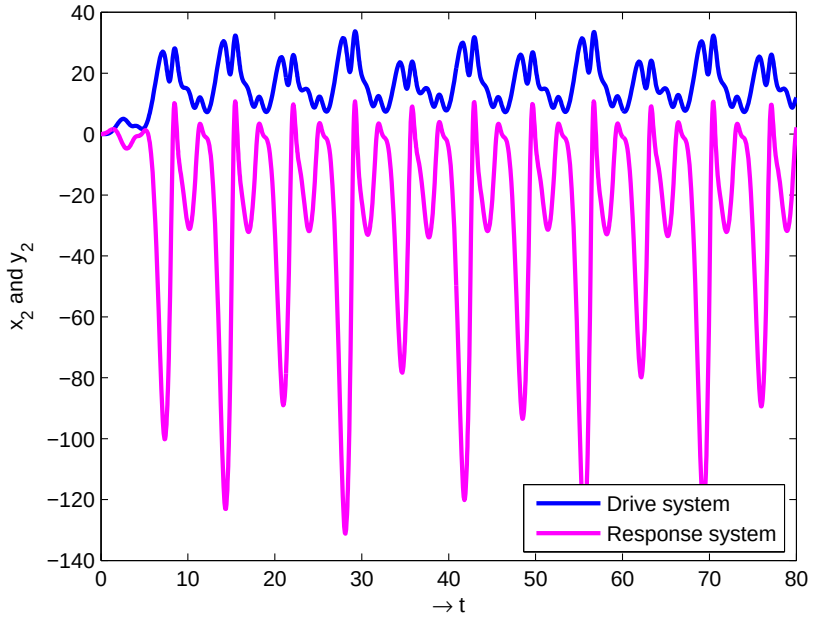

Figure 9.14: Case-V: x_2 *and* y_2 with respect to time

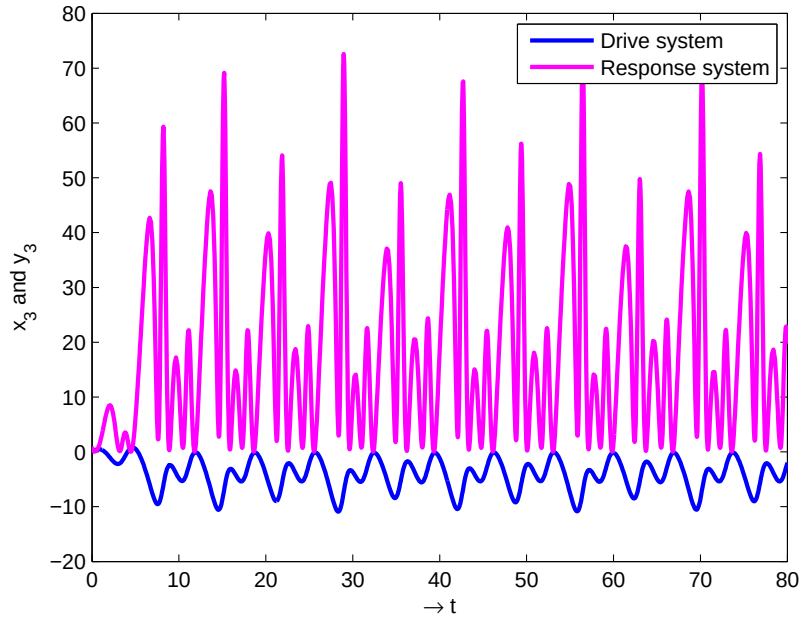

Figure 9.15: Case-V: x_3 *and* y_3 with respect to time

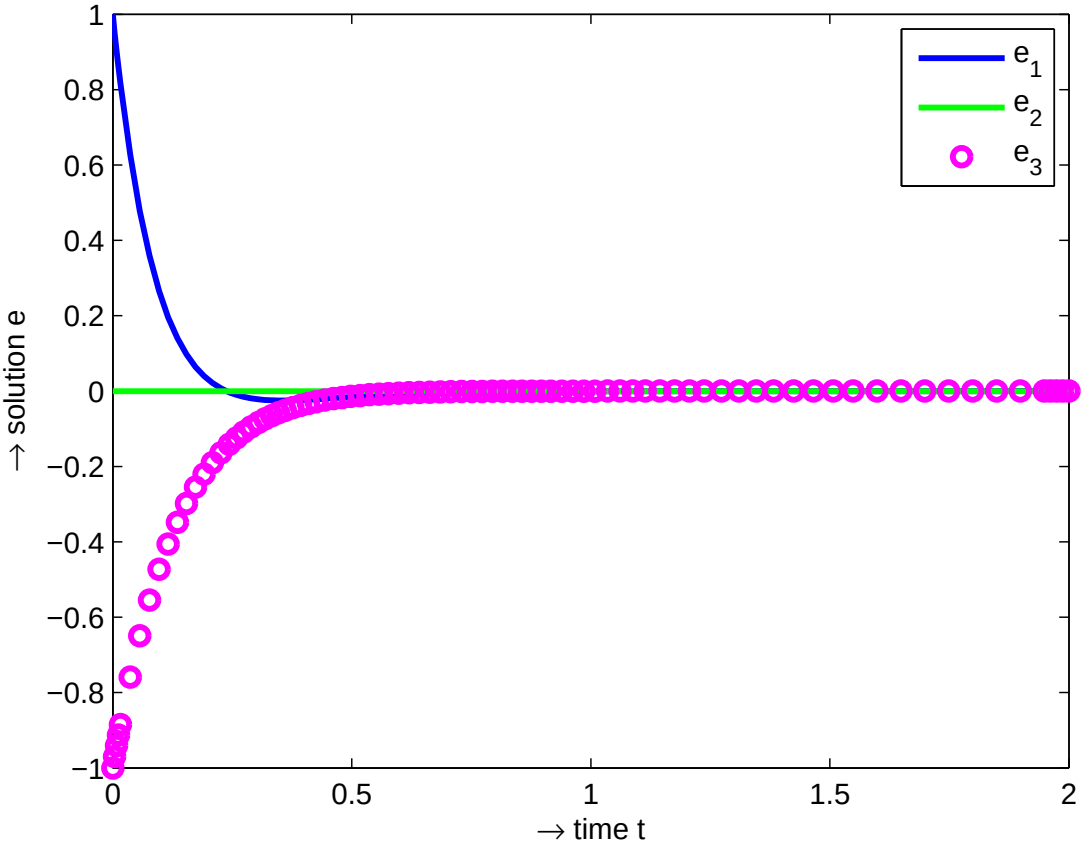

Figure 9.16: Time evolution of the synchronization error e

all the above cases. Figure (9.16) illustrates the time history of the synchronization error.

9.6 Conclusion

Here, we have found the stability condition at the critical points of time delay system in absence of delay using Routh-Hurwitz criterion in section 9.2. In presence of delay, we investigate how the stable critical points of the original system (without delay) undergo Hopf

bifurcation and lose their stability. Interestingly, this transformation of stability behaviour of the critical points with variation of time delay is a cyclic process and it keeps repeating itself. Using Lyapunov stability theory, in section 9.3, we have established the generalized delay synchronization scheme. In this context, OPCL control technique is suitably modified to construct the controller which brings about synchronization. In section 9.4, we have studied lag generalized synchronization for the coupled Sprott system with multiple time delay. Lag complete and lag anti-synchronization arises as special cases in our study in section 9.5. Another point of importance is the use of system state variables in the transformation matrix. The synchronization is global and asymptotically stable. Five different cases are analyzed. To test the analytical findings, numerical simulation is performed. This method is suitable for electronic experiments, laser physics, neural systems, engineering sciences and so on.

Chapter 10

Summary

In chapter 1, we have discussed some important developments in dynamical system over the last few decades which share deep relations with the problems undertaken in this thesis. We have divided this chapter into five parts. In section 1.1, we have presented a short literature survey on control of chaos and synchronization. Some basic concepts on non-linear dynamics is discussed in section 1.2. The next section 1.3 covers the discussion on the phenomenon of chaos in the context of non-linear dynamical system. Section 1.4 contains the discussion on the theoretical tools necessary for studying control and synchronization. It also discusses various types of synchronization in the context of chaotic systems. In the last section of this chapter, we have described the structure of the thesis.

In chapter 2, we have analyzed the control of chaotic dynamical systems by locally stabilizing the unstable critical points of the said systems. For this purpose, two chaotic models have been chosen, namely the Sprott model B and the Sprott model L. We have first verified the dissipativity of the systems. The controllability of the

systems under small perturbations is proved by utilising the Kalman rank condition. Then, in the neighbourhood of the critical points of the systems, we have introduced small perturbations. Applying Routh-Hurwitz criterion, the conditions for stability of the systems under small perturbations is determined. Next, linear feedback control law is used for chaos control. Numerical simulations are presented to depict the efficiency of the method.

In chapter 3, we have investigated the sophisticated state space exact linearization (SSEL) control method which designs non-linear feedback and diffeomorphic coordinate transformation to obtain local exact linearization. The linearized system is controllable and hence a suitable controller is designed that control the original chaotic system. This nonlinear feedback control technique is then used to stabilize the chaotic Sprott model B. Using numerical simulations, we have shown the how the control goal can be changed with time which drives the system to any chosen point (provided the chosen point lies within the reachable set).

In chapter 4, we have studied a non-smooth minimal model for glucose and insulin kinetics system. After producing a smooth approximation of the system, we have checked the dissipativity and existence of the critical points. Here, we have studied the behaviour of the blood glucose level in human body. We have designed a linear feedback based control to regulate the blood glucose level automatically when the physical system fails. Numerical simulation have done to show the stability of the control system by choosing different val-

ues for the feedback gain parameter. A critical control parameter value k_c is determined in terms of the system parameters. Extensive numerical simulation is performed with different sets of parameter values. Assuming different values for the feedback gain parameter, ranges of physiological parameter α are determined where the feedback gain is sufficient to stabilize the system.

In chapter 5, complete synchronization has been achieved by designing controllers using hybrid feedback control and tracking control techniques. Here, we have established the complete synchronization between the two identical Sprott model L using both the methods. These synchronization scheme are based on Lyapunov stability theorem. The error term goes to zero after a very short time for both the cases, as is verified by numerical simulations. The same technique is applicable for any pair of identical coupled systems and can be used in many areas such as chemical reactions, neural networks, electrical engineering and secure communication etc.

In chapter 6, we have studied an anti-synchronization scheme for a general class of chaotic systems using a sliding mode control based strategy. For this reason, a linear sliding surface is designed. The reachability condition for the synchronization manifold for any initial condition is proved to ensure global synchronization. This process guarantees finite time convergence. Robustness of the control system is achieved by tuning a control parameter and introducing a control vector based on partial tracking of the disturbances. A chattering-free continuous analogue of the discontinuous sliding mode controller

is also discussed. In contrast to the usual diffusive coupling approach, our method accommodates all kind of systems without imposing any symmetry restrictions. Easy realization, fast response and insensitivity to variation in plant parameters or external disturbances, are the inherent advantages of this method. In order to support our findings, we have applied our method to anti-synchronize two identical coupled Sprott systems and two identical coupled R*ö*ssler systems. In both the above situations, we have established that the error term reduces to zero after a short time interval which is the benefit of the sliding mode controller design. Numerical simulation results are presented to show the feasibility and effectiveness of the approach. This method would prove to be useful in various disciplines like neural networks, information processing, chemical reactions, biological systems, robotics etc.

In chapter 7, we have analyzed linear generalized synchronization for unidirectionally coupled chaotic systems. In this method, the asymptotic nature of the response system can be predicted in advance by knowing the asymptotic nature of the driving system. This is achieved by using the asymptotic functional relationship between the states of the driving system and the response system. Again, the matrix associated with linear transformation being invertible, the behaviour of the driving system can be determined by knowing the behaviour of the response system in the long run. In order to illustrate the theory, chaotic Sprott model L is considered. Here, we have studied three cases by changing the transformation matrix. The efficiency of this method is verified by numerical simulations. We believe

that this synchronization method will prove to be useful for application in secure communication, electronic circuits, biological systems etc.

In chapter 8, we have studied generalized synchronization of coupled non-linear oscillators using open-plus-closed-loop (OPCL) control method. For a master-slave pair, we generate another dynamical system, commonly known as goal system which depends on master system. Actually, the goal dynamical systems is a function of the master system. This function is, quite appropriately, called the goal function. Five distinct cases are discussed by changing the nature of the goal function. Here, we have shown the synchronization of two different chaotic systems where the asymptotic functional relation between them depends on the states of a third chaotic dynamical system. This example is quite promising and itself demands further study as we can accommodate three chaotic systems within the same framework. Such approaches may have important cryptographic applications. Numerical simulation is done to show how the difference between the goal system and the slave system reduces to zero with time. This method is mostly independent of the system parameters. This framework is expected to have applications in practical life, for example, robotic systems, chemical systems, communication systems etc.

In chapter 9, stability of time delay system has been discussed. Routh-Hurwitz criterion is used to find the stability condition at the critical points of the time-delayed system in absence of delay. In presence of delay, we investigate how the stable critical points of the orig-

inal system(without delay) undergo Hopf bifurcation and lose their stability. Interestingly, this transformation of stability behaviour of the critical points with variation of time delay is a cyclic process and it keeps repeating itself. Lag generalized synchronization is then studied for the coupled Sprott system with multiple time delay. Using Lyapunov stability theory, the generalized delay synchronization criteria is obtained. OPCL control technique is suitably modified in this context to construct the controller which brings about synchronization. Lag complete and lag anti-synchronization arises as special cases in our study. Another point of importance is the use of system state variables in the transformation matrix. The synchronization is global and asymptotically stable. Five different cases are analyzed. To test the analytical findings, numerical simulation is performed. This method is suitable for electronic experiments, laser physics, neural systems, engineering sciences and so on.

Chapter 11

Possible Future Developments

Since the discovery of chaos, it has been a part of the vibrant world of scientific research. It is not limited only to mathematical sciences. It is rapidly approaching towards various other fields, especially biological systems. To elucidate the role of chaos in biological systems, W.J. Freeman gives a very interesting observation regarding chaos. According to him, human brain, in absence of chaotic behaviour, may not work properly [12, 20]. This statement emphasizes the fact that the control methods in chaos theory is going to play a very significant role in development of the artificial neural systems.

At present time, no one can think of a world without electricity. Due to external parameters, mechanical vibration, natural disasters, human creator, insufficient loads, the power systems may fail to fulfil our requirement. It is a big issue for industrial fields, high-speed electrified transportation system [87] etc. In this situation, chaos synchronization has a major role to play. By stabilizing the power systems which function as a network, it may develop the existing power supply schemes and control the possibly erratic behaviour of

the power signals. It is expected that the stability of non-linear chaotic dynamical systems and their control will become a hotbed of research activity, drawing experts from diverse fields like mathematics, physics, engineering sciences, biological and chemical sciences etc.

We may finally conclude that the aim of the thesis is achieved successfully. The research work undertaken so far has opened up some extremely interesting possibilities for future work. Application of the methods of control and synchronization studied in the thesis, specially in the context of biological problems, is one of the possible lines of work. We believe that our proposed methods would prove to be useful in various disciplines like secure communication, neural networks, information processing, chemical reactions, biological system, quantum physics, electronic circuits, secret messaging, engineering sciences, mathematics etc.

Bibliography

[1] Agiza H N and Yassen M T, *Synchronization of Rössler and Chen chaotical dynamical systems using active control*, Phys. Lett. A, Vol.278, No.4, pp.191-197 (2001)

[2] Ahn C K, *An H_∞ approach to anti-synchronization for chaotic systems*, Physics Letters A, Vol.373, No.20, pp.1729-1733 (2009)

[3] Alligood K T, Sauer T D and Yorke J A,*Chaos-an introduction to dynamical systems*, Springer International Edition, (2008)

[4] Bai E W and Lonngren K E, *Synchronization of two Lorenz systems using active control*, Chaos,Solitons and Fractals, 8, 51 (1997)

[5] Balachandran K and Dauer JP, *Elements of Control Theory*, London : Narosa Publishing House, (1999)

[6] Balan V and Stamin C S, *Stabilization with feedback control in the Kaldor economic model*, Mathematics in Engineering and Numerical Physics, Vol.14, pp.19-24 (2007)

[7] Balan V and Stamin C S, *State-space exact linearization and stabilization with feedback control in SODE economic models*, Journalof Appl. Math. Comput. (JAMC), Vol.28, pp.271-281 (2008)

[8] Balan V and Stamin C S, *Applications of the nonlinear feedback control in neural excitation processes*, Mathematics Applied in Biology and Biophysics, Vol.2, pp.119-128 (2006)

[9] Balan V, Udriste C and Tevy I, *Sub-Riemannian geometry and optimal control for Lorenz-induced distributions*, The International Conference on Differential Geometry and Dynamical Systems, 29 August - 2 September 2012, Mangalia, Romania (2012)

[10] Bartoszewicz A and Patton R J, *Sliding mode control*, International Journal of Adaptive Control and Signal Processing, Vol.21, Nos.8-9, pp.635-637 (2007)

[11] Bergman R N, *Minimal model: perspective from 2005. Hormone research*, Vol.64, No.3, pp.8-15 (2005)

[12] Bower B, *"Chaotic Connections"*, Science News, Vol.133, pp.58-59 (1988)

[13] Carusu N M and Balan V, *Second order extensions and controllability for dynamical systems with applications in biology*, Proc. of Symposium - Commemoration of Acad. Gh. Vranceanu (1900-1979), 27 April 2004, University of Bucahrest, Romania, An. Univ. Bucuresti, Vol.54, No.1, pp.43-50 (2005)

[14] Cao L Y and Lai Y C, *Anti-phase synchronization in chaotic systems*, Phys. Rev. E., Vol.58, pp.382-386 (1998)

[15] Chen W H, Ballance D J, Gawthrop P J and O'Reilly J, *Nonlinear pid predictive controller*, IEE Proceedings Control Theory & Applications, Vol. 146, No. 6, pp. 603-611, (1999)

[16] Chen L, *Synchronization of an uncertain unified chaotic system via adaptive control*, Chaos, Solitons and Fractals Vol.14, No.4, pp.643-647 (2002)

[17] Chen M, Ge S S and Ren B, *Adaptive tracking control of uncertain MIMO nonlinear systems with input saturation*, Automatica, Vol. 47, No. 3, pp.452-465, (2011)

[18] Dana S K, Padmanaban E, Banerjee R, Roy P K and Grosu I, *Design of Coupling for Mixed Synchronization in Chaotic Oscillators*, IEEE 9781-4244-3786-3/09 (2009)

[19] ECE 680 Modern Automatic Control, Rouths Stability Criterion, pp.1-6, (2007)

[20] Freeman W J and Yao Y, *Model of Biological Pattern Recognition with Spatially Chaotic Dynamics*, Neural Networks, Vol.3, pp.153-170 (1990)

[21] Gao W and Hung JC, *Variable Structure Control of Nonlinear Systems: A New Approach*, IEEE Trans. on Industrial Electronics, Vol. 40, No. 1, pp.45-55, (1993)

[22] Ghosh D, Chowdhury A R and Saha P, *Multiple delay Rössler system -Bifurcation and chaos control*, Chaos, Solitons and Fractals, Vol.35, pp.472-485 (2008)

[23] Ghosh D, *Stabilty and projective synchronization in multiple delay Rössler system*, International Journal of Nonlinear Science, Vol.7, No.2, pp.207-214 (2009)

[24] Glass L, Beuter A and Larocque D, *Time Delays, Oscillations and Chaos in Physiological Control Systems*, Mathematical Biosciences, Vo.90, pp.111-125 (1988)

[25] Grosu I, Padmanaban E, Roy P K and Dana S K, *Designing Coupling for Synchronization and Amplification of Chaos*, Phy. Rev. Lett., PRL 100, 234102 (2008)

[26] Guo R, *A simple adaptive controller for chaos and hyperchaos synchronization*, Phys. Lett. A, Vol.372, No.4, pp.5593-5597 (2008)

[27] Isidori A, Non-linear Control Systems, Springer-Verlag, pp.156-172 (1989)

[28] Islam M, Islam B and Islam N, *Dynamics of anti-synchronization of two chaotic systems*, Int.J. of Applied Mathematics and Mechanics, Vol.10, No.9, pp.1-13 (2014)

[29] Islam N, Islam B and Mazumdar HP, *Generalized chaos synchronization of unidirectionally coupled Shimizu-Morioka dynamical systems*,Differential Geometry and Dynamical System (DGDS), Vol.13, pp.101-106 (2011)

[30] Jackson EA and Grosu I, *An open-plus-closed-loop (OPCL)control of complex dynamic systems*, Physica D, Vol.85, No.1, pp.1-9, (1995)

[31] Javidi M and Nyamoradi N, *Numerical Chaotic Behavior of the Fractional Rikitake System*, World Journal of Modelling and Simulation, Vol.9, No.2, pp.120-129, (2013)

[32] Jezernik K, Rodic M, Safaric R and Curk B, *Neural Network Sliding Mode Control*, Robotica, Vol. 15, pp. 23-30, (1997)

[33] Jordan D W and Smith P, *Nonlinear Ordinary Differential Equations*, Oxford University Press, USA (2007)

[34] Kaynak O, Harashima F and Hashimoto H, *Variable Structure Systems Theory, as Applied to Sub-time Optimal Position Control with an Invariant Trajectory*, Trans. IEE of Japan, Sec. E, 104 Vol. 3-4, pp. 47-52,(1984)

[35] Kerner D R, *Minimal Models for Glucose and Insulin Kinetics*, PhD, Civilized Software, Inc., 12109 Heritage Park Circle, Silver Spring MD 20906, URL: www.civilized.com

[36] Kitanov P M, Langford W F and Willms A R, *Double Hopf Bifurcation with Huygens Symmetry*, SIAM J. APPLIED DYNAMICAL SYSTEMS, Vol.12, No.1, pp.126-174 (2013)

[37] Kocarev L J, Halle K S, Eckert K, Parlitz U and Chua L O, *Experimental demonstration of secure communications via chaotic synchronization*, Int. J. Bifur. Chaos, Vol.2, pp.709-713 (1992)

[38] Kocarev L and Parlitz U, *Generalized synchronization, predictability and equivalence of unidirectionally coupled dynamical systems*, Phys. Rev. Lett., Vol.76, No.11, pp.1816-1819 (1996)

[39] Landau I D, Lozano R, M'Saad M and Karimi A, *Adaptive control, communication and control engineering*, Springer-Verlag London Limited, 2011

[40] Lasalle J P and Lefschetz S, *Stability by Lyapunov's direct method with applications*, Academic Press, New York (1961)

[41] Lee M W, Larger L and Goedgebuer J-P, *Transmission system using chaotic delays between light waves*, IEEE J Quantum Electron, Vo.39, pp.931-935 (2003)

[42] Li G H and Zhou S P, *Anti-synchronization in different chaotic systems*, Chaos, Solitons and Fractals, Vol.32, No.2, pp.516-520 (2007)

[43] Li J Z and Zhang Y N, *Robust adaptive motion/force control for wheeled inverted pendulums*, Automatica, Vol.46, No.8, pp. 1346-1353, (2010)

[44] Liqun C and Yanzhu L, *Control of the Lorenz Chaos by the Exact Linearization*, Applied Mathematics and Mechanics, Vol.19, No.1, pp.67-73 (1998)

[45] Lorenz E N, *Deterministic non-periodic flow*, J.Atmos.Sci., Vol.20, pp.130-141,(1963).

[46] Lu J, Wu X, Han X and Lu J, *Adaptive feedback synchronization of a unified chaotic system*, Phys. Lett. A, Vol.329, pp. 327-333, (2004)

[47] Mackey M C and Glass L, *Oscillations and chaos in a physiological control systems*, Science, Vo.197, pp.287-289 (1977)

[48] Misawa E A, *Discrete-time sliding mode control for nonlinear systems with unmatched uncertainties and uncertain control vec-*

tor, Transactions of the ASME, Journal of Dynamic Systems, Measurement, and Control, Vol. 119, pp. 503-512, (1997)

[49] Mondal A and Islam N, *A short note on the integrals of motion for Sprott's Model L*, Global Journal of Mathematics and Mathematical Sciences (GJMMS), vol 2, No.1, pp.57-60, (2012)

[50] Mondal A and Islam N, *Stability and Control Analysis of the Sprott's Model L*, International Journal of Applied Mathematical Sciences (JAMS), Vol.6, No.1, pp.63-68 (2013)

[51] Mondal A, Islam N and Sen S, *Controlling and Stabilizing the dynamical system of Sprott's Model B*, Indian Journal of Theoretical Physics, Vol.61, No.2, pp.95-100, (2013)

[52] Mondal A and Islam N, *Chaos synchronization of coupled Sprott model L*, International Journal of Pure and Applied Science and Technology(IJPAST), Vol.16, No.2, pp.32-38, (2013)

[53] Mondal A, Islam M and Islam N, *Robust antisynchronization of chaos using sliding mode control strategy*, Pramana-journal of physics, Indian Academy of Sciences, Vo.84, No.1, pp.47-67 (2015)

[54] Nikolov S, Vera J, Kotev V, Wolkenhauer O and Petrov V, *Dynamic Properties of a delayed protein cross talk model* BioSystems, Vol.91,No.1, pp.51-68, (2008)

[55] Nikolov S, Vera J, Nenov M and Wolkenhauer O, *Dynamics of a miRNA Model with Two Delays*, Biotechnology and Biotechnological Equipment, Vol.26, No.5, pp.3315-3320, (2012)

[56] Nikolov S, *Stabilty and Andronov-Hopf bifurcation of a system with three time delays*, Journal of Mathematics, Vol.2013, art. ID 347071(11 pages), (2013)

[57] Nikolov S, *Complex behaviour of a miRNA model with three delays*, Series on Biomechanics, Vol.28, No.3-4, pp.74-89, (2013)

[58] Ott E, Grebogi C and Yorke J A, *Controlling Chaos*, Physical Review Letters, Vol.64, No.11, pp.1196-1199, (1990)

[59] Pai B, Islam N and Mazumder H P, *On the Stability and Control of Goodwin-Griffith System of Dynamical Equations Governing Tryptophan Operon*, Proc. Indian National Science Academy, Vol.73, No.4, pp.221-225,(2007).

[60] Pal S, *Synchronization of coupled hyper-chaotic systems*, Differential Geometry and Dynamical System (DGDS), Vol.14, pp.117-124, (2012)

[61] Panchev S, *Low order spectral system derived from a nonlinear boundary layer diffusion equation*, Acta Meteorologica Sinica, Vol.5, No.4, pp.489-496, (1991)

[62] Panchev S, *Chaotic and deterministic behavior of non-linear Geo-physical fluid dynamical systems*, Acta Appcandae Mathematicae, Vol.26, pp.271-291 (1992)

[63] Panchev S, *Theory of Chaos*, Bulgarian Acad. Press, (2001)

[64] Park J H, *Controlling chaotic systems via nonlinear feedback control*, Chaos, Solitons and Fractals, Vol.23, No.3, pp.1049-1054, (2005)

[65] Pecora L M and Carroll T L, *Synchronization in chaotic system*, Phys.Rev.Lett., Vol.64, No.8, pp.821-824, (1990)

[66] Phillipson P and Schuster P, *Bifurcation dynamics of three-dimensional system*, Int.J.Bifurcat.Chaos, Vol.10, No.8, pp.1787-1804, (2000)

[67] Poria S, *The linear generalized chaos synchronization and predictability*,Int.J.of App. Mech. and Engg., Vol.12, No.3, pp.879, (2007)

[68] Poria S and Tarai A, *Adaptive synchronization of two coupled chaotic neuronal systems*, Rev. Bull. Calcutta Math. Soc., Vol.15, No.1, pp. 53-60, (2007)

[69] Qiaoping L and Wenlin L, *Anti-synchronization of Chaotic System by Sliding Mode Control and Observer*, Key Engineering Materials, Vols.439-440, pp.1247-1252 (2010)

[70] Ramponi F, *Notes on Lyapunov's theorem*

[71] Rössler O E, *An equation for continuous chaos*, Physics Letters A, Vol.57, No.5, pp.397-398 (1976)

[72] Roy P K, Hens C, Grosu I and Dana S K, *Engineering generalized synchronization in chaotic oscillators*, Chaos 21, 013106 (2011)

[73] Rulkov N F, Suschik M M and Tsimring L S, *Generalized synchronization of unidirectionally coupled chaotic system*, Phys.Rev.E, Vol.51, No.2, pp.980(1995)

[74] Sanner RM and Slotine J-J.E, *Gaussian networks for direct adaptive control*, IEEE Transactions on Neural Networks, Vol.3, No.6, pp.837-863, (1992)

[75] Senthilkumar D V, Lakshmanan M and Kurths J, *Phase synchronization in time-delay systems*, Phys. Rev. E., Vol.74, 035205(R) (2006)

[76] Shahverdiev E M and Shore K A, *Impact of modulated multiple optical feedback time delays on laser diode chaos synchronization*, Optics communication, Vol.282, pp.3568-3572 (2009)

[77] Sparrow C, *The Lorenz Equation: Bifurcations, Chaos and Strange Attractors*, Springer-Verlag (1982)

[78] Sprott J C, *Elegant Chaos, Algebraically simple chaotic flows*, World Scientific Publishing Co.Pte.Ltd, (2010)

[79] Sprott J C, *Some simple chaotic flow*, Phys.Rev.E, Vol.50, No.2, pp.R647-R650 (1994)

[80] Strogatz SH, *Non-linear Dynamics and Chaos*, Levant Books - Kolkata, India, (2007)

[81] Sun Y and Cao J, *Adaptive synchronization between two different noise-purturbed chaotic system with fully unknown parameters*, Physica A, Vol.376, pp. 253-265 (2007)

[82] Tsagas G R and Mazumdar H P, *On the control of a dynamical system by a linearization method via lie algebra*, Review Bull. Cal. Math. Soc., Vol.8, No.1-2, pp.25-32 (2000)

[83] Utkin V I, *Sliding mode control*, in: Variable structure systems: From principles to implementation(IET Control Engineering Series 66, London, UK, 2004), pp.1

[84] Vaidyanathan S, *Sliding Mode Controller design for the anti-synchronization of hyperchaotic Lu systems*, Int.J. on Cybernetics and Informatics (IJCI), Vol.2, No.1, pp.31-38, (2013)

[85] Vincent TL and J Yu, *Control of Chaotic System- Dynamics and Control*, Vol.1, pp.35-52, (1991)

[86] Voss H U, *Dynamic long-term anticipation of chaotic states*, Phys. Rev. Lett., Vol.87, 014102 (2001)

[87] Wang MH and Yau HT, *New Power Quality Analysis Method Based on Chaos Synchronization and Extention Neural Network*, Energies, Vol.7, No.10, pp.6340-6357 (2014)

[88] Xu Y F, Jiang B, Tao G and Gao Z, *Fault tolerant control for a class of nonlinear systems with application to near space vehicle*, Circuits, Systems, and Signal Processing, Vol. 30, No. 3, pp. 655-672, (2011)

[89] Yan J J, Yang Y.-S, Chiang T.-Y and Chen C.-Y, *Robust synchronization of unified chaotic systems via sliding mode control*, Chaos, Solitons & Fractals Vol.34, No.3, pp.947-954 (2007)

[90] Yang LX, Chu Y.-D, Zhang J.-G, Li X.-F, Chang Y.-X, *Chaos synchronization in autonomous chaotic system via hybrid feedback control*, Chaos, Solitons and Fractals, Vol.41, No.1, pp.214-223, (2009)

[91] Yassen M T, *Synchronization of Rössler and Chen dynamical systems using active control*, Chaos, Solitons and fractals, Vol.23, pp.131-140 (2005)

[92] Yongguang Y and Suachun Z, *Controlling uncertain Lu system using backstepping design*, Chaos, Solitons and Fractals, Vol.15, No.5, pp.897-902, (2003)

[93] Young D K, Utkin V I, Ozguner U, *A control engineer's guide to sliding mode control*, Variable Structure Systems 1996 (VSS'96), Proceedings at the IEEE International Workshop (1996)

[94] Zhan M, Wei G W and Lai C H, *Transition from intermittency to periodicity in lag synchronization in coupled Rössler oscillators*, Phys. Rev. E, Vol.65, 036202-05 (2002)

[95] Zhang X and Zhu H, *Anti-synchronization of two different hyperchaotic systems via active and adaptive control*, International Journal Nonlinear Science, Vol.6, pp.216-223 (2008)

[96] MATLAB, *http://www.mathworks.com/*, The MathWorks, Inc. (2004).